1-1-2012

Toward the Complete Characterization of Atmospheric Organic Particulate Matter: Derivatization and Two-Dimensional Comprehensive Gas Chromatography/Time of Flight Mass Spectrometry as a Method for the Determination of Carboxylic Acids

Alexandra Jeanne Boris
Portland State University

Toward the Complete Characterization of Atmospheric Organic Particulate Matter: Derivatization and Two-Dimensional Comprehensive Gas Chromatography/Time of Flight Mass Spectrometry as a Method for the Determination of Carboxylic Acids

by

Alexandra Jeanne Boris

A thesis submitted in partial fulfillment of the
requirements for the degree of

Master of Science
in
Chemistry

Thesis Committee:
James F. Pankow, Chair
Dean B. Atkinson
Kelley C. Barsanti
Andrew Rice

Portland State University
2012

ABSTRACT

Understanding the composition of atmospheric organic particulate matter (OPM) is essential for predicting its effects on climate, air quality, and health. However, the polar oxygenated fraction (PO-OPM), which includes a significant mass contribution from carboxylic acids, is difficult to speciate and quantitatively determine by current analytical methods such as gas chromatography-mass spectrometry (GC-MS). The method of chemical derivatization and two-dimensional GC with time of flight MS (GC×GC/TOF-MS) was examined in this study for its efficacy in: 1) quantifying a high percentage of the total organic carbon (TOC) mass of a sample containing PO-OPM; 2) quantitatively determining PO-OPM components including carboxylic acids at atmospherically relevant concentrations; and 3) tentatively identifying PO-OPM components. Two derivatization reagent systems were used in this study: BF_3/butanol for the butylation of carboxylic acids, aldehydes, and acidic ketones, and BSTFA for the trimethylsilylation (TMS) of carboxylic acids and alcohols.

Three α-pinene ozonolysis OPM filter samples and a set of background filter samples were collected by collaborators in a University of California, Riverside environmental chamber. Derivatization/GC×GC TOF-MS was used to tentatively identify some previously unidentified α-pinene ozonolysis products, and also to show the characteristics of all oxidation products determined. Derivatization efficiencies as measured were 40-70% for most butyl derivatives, and 50-58% for most trimethylsilyl derivatives. A thermal optical method was used to measure the TOC on each filter, and a value of the

quantifiable TOC mass using a gas chromatograph was calculated for each sample using GC×GC separation and the mass-sensitive response of a flame ionization detector (FID). The TOC quantified using TMS and GC×GC-FID ($TMS/TOC_{GC\times GC\ FID}$) accounted for 15-23% of the TOC measured by the thermal-optical method. Using TMS and GC×GC/TOF-MS, 8.85% of the thermal optical TOC was measured and 48.2% of the $TMS/TOC_{GC\times GC\text{-}FID}$ was semi-quantified using a surrogate standard. The carboxylic acids tentatively identified using TMS and GC×GC/TOF-MS accounted for 8.28% of the TOC measured by thermal optical means.

GC×GC TOF-MS chromatograms of derivatized analytes showed reduced peak tailing due in part to the lesser interactions of the derivatized analytes with the stationary phase of the chromatography column as compared to the chromatograms of underivatized samples. The improved peak shape made possible the greater separation, quantification, and identification of high polarity analytes. Limits of detection using derivatization and GC×GC/TOF-MS were <1 ng per μL injected for a series of C_2-C_6 di-acids, *cis*-pinonic acid, and dodecanoic acid using both butylation and TMS. Derivatization with GC×GC/TOF-MS was therefore effective for determining polar oxygenated compounds at low concentrations, for determining specific oxidation products not previously identified in OPM, and also for characterizing the probable functional groups and structures of α-pinene ozonolysis products.

ACKNOWLEDGEMENTS

Funding for this project was provided by the Electrical Power Research Institute (EPRI) and the National Science Foundation (NSF).

I would like to thank Dr. David Cocker, Shunsuke Nakao, and the Cocker research group at the University of California, Riverside, for the filter samples they graciously supplied for this project, without which this study could not have been done.

Thank you to my advisor Dr. James F. Pankow for his guidance and support on this project. Also thank you to the excellent scientists in the James Pankow research group Lorne Isabelle, Dr. Wentai Luo, and Dr. Cai Chen and the committee of atmospheric scientists, especially Drs. Kelley Barsanti and Dean Atkinson, for their willingness to contribute their endless amounts of knowledge and experience to my education, their patience as I took all of it in, and their support as I applied it to my own studies, schoolwork, and teaching.

Thank you finally to my colleagues, family, and friends who have supported me through this process and allowed me to think openly and excitedly about chemistry.

TABLE OF CONTENTS

LIST OF TABLES

LIST OF FIGURES

LIST OF REACTION SCHEMES

LIST OF ABBREVIATIONS AND SYMBOLS

$[i]$	concentration of the compound *i*
ΔHC	amount of hydrocarbon precursor reacted, ppb
ΔM_0	concentration of measured organic matter in air, μg m^{-3}
1D-GC	one-dimensional gas chromatography
${}^1t_R$	primary retention time, seconds
${}^2t_R$	secondary retention time, seconds
A_i	concentration of the compound *i* in the gas phase, ng m^{-3}
A_{is}	concentration of the compound
AMS	aerosol mass spectrometry
APCI	atmospheric pressure chemical ionization
BF_3	boron trifluoride
BF_3/butanol	boron trifluoride and *n*-butanol
BF_3/methanol	boron trifluoride and methanol
BSTFA	*N,O*-bis(trimethylsilyl)trifluoroacetamide
C_i	concentration of the compound *i*, ng μL^{-1}
C_{is}	concentration of an internal standard, ng μL^{-1}
CE	capillary electrophoresis
CI	chemical ionization
CNC	condensation nucleus counter
DCM	dichloromethane
DE_i	derivatization efficiency of the compound *i*
DESI-MS	desorption electrospray ionization mass spectrometry
ECD	electron capture detector
ECN	effective carbon number
ECN_i	effective carbon number of the compound *i*
ECN_{calc}	theoretical calculation of the effective carbon number of compound *i*
ECN_{ref}	effective carbon number of a reference compound
EI	electron impact (ionization)
ESI	electrospray ionization
f	fraction of the total particulate matter that is in the particle phase
F_i	fraction of the compound *i* found in the particle phase, ng m^{-3}
FID	flame ionization detection
GC	gas chromatography
GC×GC	two-dimensional, comprehensive gas chromatography
GC×GC-FID	two-dimensional, comprehensive gas chromatography with flame ionization detection
GC×GC/TOF-MS	two-dimensional, comprehensive gas chromatography with time-of-flight mass spectrometric detection
GC-MS	gas chromatography/mass spectrometry
HMW	high molecular weight

HPLC	high performance liquid chromatography
IC	ion chromatography
ICP-MS	inductively coupled plasma mass spectrometry
k	gas chromatography retention factor
LC/MS	liquid chromatography
LMW	low molecular weight
LOD	limit of detection
MΩ	megaohms (measure of resistance)
m43/OA	ratio of the m/z 43 fragment to total organic mass (AMS)
m44/OA	ratio of the m/z 44 fragment to total organic mass (AMS)
MS	mass spectrometry
MS/MS	tandem mass spectrometry
MSD	mass spectrometric detector
MSTFA	*N*-methyl-*N*-trimethylsilyltrifluoroacetamide
MTBSTFA	*N*-*tert*-butyldimethylsilyl-*N*-methyltrifluoroacetamide
$\overline{MW}$	average molecular weight of the organic material
MW_{ref}	molecular weight of a reference compound
MS	mass spectrometry
$n_{c,GC}$	
nano-DESI	nanospray desorption electospray ionization
NIST	National Institute of Standards and Technology
NO_x	nitrogen oxides (NO_2 and NO)
$O(^3P)$	triplet (ground state) oxygen
OPM	organic particulate matter
$p°_{L,i}(T$	Vapor pressure of the pure component *i*, atm (sub-cooled if necessary, at the specified temperature)
PAH	polycyclic aromatic hydrocarbon
PFBHA	2,3,4,5,6-pentafluorobenzyl hydroxylamine
PFBBr	2,3,4,5,6-pentafluorobenzyl bromide
PM	particulate matter
$PM_{2.5}$	particulate matter with diameter ≤ 2.5 μm
PO-OPM	polar oxygenated organic particulate matter
PTFE	polytetrafluoroethylene
PDHID	pulsed discharge helium ionization detector
R	ideal gas constant, $8.314 m^3$ atm K^{-1} mol^{-1}
r^2	linear correlation coefficient
RSD	relative standard deviation
S/N	signal to noise (ratio)
SEMS	scanning electrical mobility sizer
SMPS	scanning mobility particle sizer
S_N2	bimolecular nucleophilic substitution
SOA	secondary organic aerosol
SV-OPM	semi-volatile organic particulate matter

t'_R	difference in retention time between the mobile phase and the analyte
t_0	retention time of the mobile phase
TBDMS	*tert*-butyldimethylsilyl (derivatives)
TMCS	trimethylchlorosilane
TMPP	2,4,6-trimethoxyphenyl)phosphonium propylamine
TMS	trimethylsilylation
$TMS/TOC_{GC\times GC\text{-}FID}$	total organic carbon mass quantified using trimethylsilylation and GC×GC-FID
TOC	total organic carbon (mass)
$TOC_{GC\times GC\text{-}FID}$	total organic carbon mass quantified using GC×GC-FID
TOC_{TOA}	total organic carbon mass measured using a thermal-optical analysis technique
TOF	time of flight
TOF-MS	time of flight mass spectrometry
UV	ultraviolet
VOC	volatile organic compound
WSOC	water-soluble organic carbon
Y	aerosol yield (percentage)

LIST OF EQUATIONS

1 Introduction

1. Understanding the Composition of Atmospheric Organic Particulate Matter

The temperature of Earth's troposphere is affected by its chemical components, many of which have not yet been identified or quantified (Goldstein & Galbally, 2007; Kleindienst, *et al.,* 2007; Xu, *et al.,* 2003). The magnitude of the effect on the net irradiance to the troposphere (the radiative forcing) caused by these components is uncertain; it is least certain for the components that exist in solid or liquid phase under ambient conditions (Forster, *et al.,* 2007). This particulate matter (PM) is approximately 20-50% organic by mass (Brock, *et al.,* 2008; Morgan, *et al.,* 2010), and this organic particulate matter (OPM) is composed of more than 10,000 individual chemical species (Hamilton, *et al.,* 2004).

Field measurements and satellite data (Heald, *et al.,* 2010) show global OPM production at three times that modeled using currently understood atmospheric mechanisms and pathways. Many of the effects of OPM on climate, air quality, and health cannot be predicted because the reaction precursors, products, mechanisms and rates needed for models are still unknown (Forstner, *et al.,* 2007; Karl & Trenberth, 2003). Although potentially thousands of compounds are present in OPM (Hamilton, *et al.,* 2004), many of their identities have not been elucidated. Zhang, *et al.,* (2007) showed that 64-95% of OPM is oxygenated, making this fraction difficult to separate using current analytical methods. Improvements of these methods are therefore needed to speciate OPM and accurately predict its role in air quality and climate change.

The physical characteristics of oxygenated OPM make its components difficult to detect. Polar interactions cause the compounds to interact strongly with polar surfaces in the atmosphere, and also within the analytical methods used to detect the compounds. The partitioning between gaseous and particulate, aqueous and organic, and acidic and salt phases is due to polar interactions of oxygenated functional groups. These functional groups, including carboxylic acids, alcohols, aldehydes, and ketones, are generated during the breakdown of gaseous hydrocarbon molecules in the atmosphere by oxidation. The partitioning of newly formed, oxygenated compounds into the particle phase occurs because of the attraction of the polar sites, and thus lowered vapor pressures, of the molecules. The resulting particle phase constituents are referred to collectively as secondary organic aerosol[1] (SOA) because the particles were formed by reactions in the atmosphere rather than through direct emission as particles.

The mechanism by which polar interactions cause a compound to have lower vapor pressure can also explain the major challenge in speciating oxygenated OPM. Traditional methods of analytical separation such as gas and liquid chromatography rely on the intensity of the interaction between the analyte and the stationary phase in the separation

---

[1] The distinction between atmospheric particulate matter and aerosol is that the former refers to the compounds as solids or liquids, while the latter refers to those solids or liquids as they are suspended in the atmosphere. This thesis focuses on the identification of polar, oxygenated compounds, so the term OPM will be more often used.

column. If these interactions are too intense, however, an analyte signal will be broadened and decreased in intensity, and the retention of the analyte in the instrument will be increased, which may cause the analyte to not be detectable.

Other instruments have allowed "bulk" analyses (measurements of the total elemental and functional composition of SOA) of OPM samples to give functional group and structural information about particle composition. The use of aerosol mass spectrometry (AMS) has allowed the evaluation of the extent of oxidation of single particles by associating the high abundance of particular signals with high concentrations of fragments from polar, oxygenated OPM (PO-OPM). Such fragments include m/z 44, which indicates a loss of CO_2^+, and m/z 43 indicating a loss of $C_2H_3O^+$. As the compositions of particles are analyzed further from an urban site, increased ratios of these particular masses to the total organic mass (m44/OA and m43/OA) are observed, indicating that oxidation parallels the aging of the air mass (Sato, *et al.,* 2010).

There is a general discrepancy between estimates of the organic fraction mass by bulk analysis approaches such as AMS and molecular speciation approaches. Bulk analyses show that the contribution of oxygenated species to OPM is much higher (Zhang, *et al.,* 2007) than that accounted for by identified components in molecular speciation studies of SOA. Additional oxidation products and reaction pathways must be understood in order to close these gaps in the current OPM mass balance.

Reactions leading to changes in oxidation state will be through one of three mechanisms: addition of an oxidized functional group, cleavage of C-C bonds via oxidation, or accretion to join oxidized molecules. Thus, an increase in the average carbon oxidation state of a molecule observed through an atmospheric oxidation reaction can be explained by the formation of products via these mechanisms (Kroll, *et al.,* 2011). The oxidation state can also be measured to compare the overall character of products from similar oxidation studies. Despite the utility of a metric such as this for experimental comparisons, however, the rates and mechanisms of atmospheric reactions involving OPM are still dependent on the molecular composition of the particle phase. Environmental and health concerns associated with OPM can only be sufficiently and completely addressed if the identities of the compounds are known.

A direct effect of OPM on incoming solar radiation has been characterized based on the size of the particles formed: the diameter of particles (mostly < 2.5 μm, $PM_{2.5}$, containing 20-90% organic species; Kanakidou, *et al.,* 2005) is similar to the wavelengths of the incoming sunlight. Walser, *et al.* (2007) confirmed that the far UV and visible light absorption of air containing hydrocarbons is increased by oxidation. An indirect effect on cloud formation and characteristics has been hypothesized involving mono-, di-, and poly-carboxylic acids in OPM, through the lowering of surface tension of suspended water droplets (Facchini, *et al.,* 2000). This is suggested to cause a larger number of smaller cloud droplets to form, and increase the albedo (reflectivity) of the cloud. The formation of smaller droplets could also lead to fewer precipitation events and increased

cloud lifetime. Without knowledge of the chemical species in the cloud droplets, however, these phenomena cannot be well understood (Facchini, *et al.,* 1999).

Carboxylic acids, as well as other oxygenated compounds in the gas phase, may allow additional OPM to form by taking part in accretion reactions, i.e. the joining of two or more oxygenated molecules. The vapor pressure of the larger product will be low compared to that of the reactants and thus the product may partition into the particle phase (Barsanti & Pankow, 2006). High acidity in aerosol may also catalyze accretion reactions (Jang, *et al.,* 2002) as well as carboxylic acids, which are in general weakly acidic (Gao, *et al.,* 2004, Hoffmann, *et al.,* 1998). The relative contribution of accretion to SOA may depend on the precursor: a larger fraction of biogenic oxidation products have been identified as "oligomers" than in anthropogenic aromatic oxidation products (Gao, *et al.,* 2004).

The analytical preparatory technique of chemical derivatization and the instrumental technique of GC×GC will be used together in this study to detect and determine carboxylic acids in atmospheric OPM samples. The use of these techniques together may allow a more complete detection of compounds in OPM as well as their quantitative determination. Standard solutions of carboxylic acids and samples from atmospheric oxidation reactions will be analyzed to show the efficacy of the method and its potential for identifying compounds in complex OPM samples, respectively.

2. Oxidation Mechanisms and Pathways of Anthropogenic and Biogenic Hydrocarbons

PO-OPM is generated from the atmospheric oxidation of volatile anthropogenic and biogenic hydrocarbon precursors. The oxidation of these precursors can be isolated for study within a Teflon reaction chamber to avoid the complexity of sampled ambient air. One or more precursors is introduced to a chamber along with the oxidant of interest, and allowed to react for a period of time under flowing or static conditions. Relative humidity and temperature are set to either replicate environmental conditions or to produce a sample with particular features (such as high mass loading).

Measurements of gaseous and particulate properties can be made via inlets from the chamber, flowing to instruments for *in-situ* and *ex-situ* study. *In situ* analysis techniques may include AMS or thermal desorption particle beam mass spectrometry (Tobias, *et al.,* 2000) for whole-particle study, or infrared spectrometry for functional group analysis. These techniques can be complementary to chromatographic analysis, but do not allow complete characterization of the chemical species within the sample. Gas chromatography analyses cannot give instantaneous information about an atmospheric sample; the analyses are at least 15 minutes in length (Kuster, *et al.,* 2004), and are also carried out at below atmospheric pressure if a mass spectrometer is used for detection.

The oxidants $OH^{\bullet}$, O_3 and the nitrogen oxides (NO_x) contribute to the formation of SOA (Griffin, *et al.,* 1999) and have been recognized for many years as primary oxidants responsible for hydrocarbon removal from the atmosphere (Atkinson, *et al.,* 1980;

Calvert, *et al.,* 2000) The atmospheric oxidation of anthropogenic, aromatic hydrocarbons such as toluene and *m*-xylene predominantly occurs by reaction with $OH^{\bullet}$, and less so by reaction with O_3 (reactions by photolysis and with triplet oxygen, $O(^3P)$ are less significant than O_3 and are not included here). Biogenic volatile organic compounds (VOCs) react most rapidly with $NO_3^{\bullet}$ in the dark and $OH^{\bullet}$ during the day (Calvert, *et al.,* 2002).

Reaction mechanisms have been proposed for the formation of ring-opening and ring-retaining carboxylic acids from aromatic and biogenic precursors (Figure 1.1). The oxidation pathways of the three major atmospheric oxidants begin with either the addition of the oxidant to the precursor structure or the abstraction of a hydrogen atom to form a radical (Yu, *et al.,* 1999; Calvert, *et al.,* 2002). The well-studied hydrocarbon β-pinene is oxidized readily by O_3 through formation of a molozonide (having three adjacent, singly-bound oxygen atoms within the carbon structure), followed by loss of an oxygen atom to form peroxide intermediates (Figure 1.1). Tautomerization followed by ring opening about a double bond allows the formation of a radical at the carbon atom of a carbonyl, which can be oxidized by O_2 and HO_2 to form various multi-functional carboxylic acids (Yu, *et al.,* 1999).

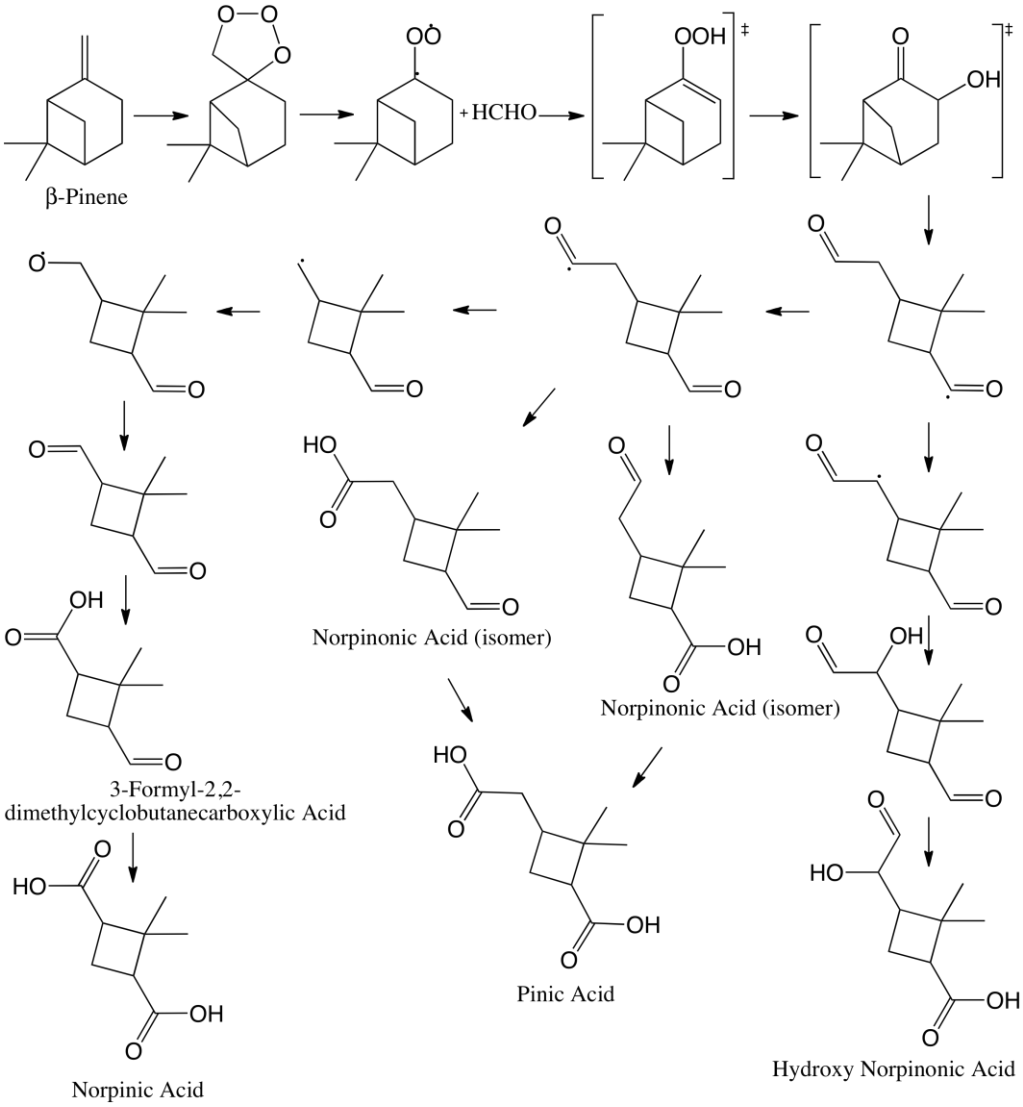

Figure 1.1. Example reaction pathway for the ozonolysis of β-pinene to ring-opening carboxylic acids (adapted form Yu, *et al.,* 1999). Resulting products are multi-functional and vapor pressures are low so that compounds partition readily into the particle phase.

For $OH^{\bullet}$ reaction with methyl-substituted benzene rings, the abstraction of a hydrogen atom from a constituent group (such as the methyl group of toluene) has been hypothesized as a lesser pathway, while electrophilic addition of the radical as an *ortho*- or *para*- substituent (because methyl groups are electron-donating, and thus *ortho*/*para*

directing) may account for approximately 90% of the reaction pathway. The pathways of formation for carboxylic acids can be extrapolated theoretically from the oxidation pathways of biogenic precursors, but the observed products from aromatic compounds contain few carboxylic acids (Forstner, *et al.,* 1997; Jang & Kamens, 2001; Yu, *et al.,* 1997; Calvert, *et al.,* 2002). A large fraction of the particle phase mass has not been speciated, however, and oxidation products are likely to contain highly oxygenated compounds.

Although oxidation mechanisms have been proposed and supported for various precursors and oxidants, the products identified in ambient studies normally account for only 5-10% of the total organic mass. There is an obvious increase in this number when the oxidation of one precursor is isolated in a chamber study (Table 1.1).

Table 1.1. Identified percent mass of OPM by quantitation of ambient and chamber study results.

Sample	Percent Mass Identified	Study
Vehicular emissions	~6%[a]	El Haddad, et al., 2009
Arctic organic carbon	5.1%[b,c]	Fu, et al., 2009
β-Pinene ozonolysis products	13-20% aerosol, 57-71% aerosol and gas[d]	Jaoui & Kamens, 2003a
Brazilian rural water soluble organic carbon	4.5-7.5%[b]	Mayol-Bracero, et al., 2002
Chamber studies of β-pinene oxidation	4-6% aerosol, 34-50% aerosol and gas[d]	Yu, et al., 1999

[a] Total organic mass based on thermal-optical carbon analysis method, assumed OM/OC ratio from other studies
[b] Total organic mass based on thermal-optical carbon analysis method, compared to total carbon identified in sample
[c] Quantity of tracer compounds determined only
[d] Total organic mass based on hydrocarbon precursor carbon mass

The measurement method used to determine total OPM used should be considered as well. Thermal methods (based upon an estimation of the OPM density and extrapolated particle numbers) may be most accurate.

The method used for determining total organic carbon (TOC) mass may also influence the percent mass identified, and assumptions such as that of constant particle density may not be accurate. The common methods used are: (a) thermal-optical determination of TOC mass (such as that of Schauer, *et al.,* 2003), or (b) measurement of the hydrocarbon precursor carbon mass reacted (in a chamber study). Yu, *et al.* (1999) reported identification of 90% and ~100% organic aerosol mass in α-pinene and sabinene oxidation OPM, respectively, with ± 50% uncertainty. This calculation was based on the aerosol yield (not the TOC mass or precursor carbon mass) approximated using the distribution of sizes and number of particles characterized (using a scanning electron particle sizer, SEMS and condensation nucleus counter, CNC). These high identifications have not been reproduced, but similar components have accounted for lower mass contributions in other studies.

3. Theoretical Significance of Oxygenated Compounds including Carboxylic Acids in Atmospheric OPM

Carboxylic acids are in high abundance relative to other organic species in measured air samples: Glasius, *et al.* (2000) found that 20-30% of biogenic oxidation products might be attributable to carboxylic acids, while Mayol-Bracero, *et al.* (2002) found the fraction of Amazonian biomass burning OPM soluble in water to be composed of ~70% carboxylic acids. They are also among the most difficult to detect and determine quantitatively because they exhibit the strongest polar interactions with an instrumental stationary phase.

In aged organic aerosol, the terminal steps of known oxidation mechanisms involve the formation of carboxylic acids that may partition into the particle phase. Because the breakdown of hydrocarbons occurs by oxidation at multiple sites in the precursor molecules, di-carboxylic acids, hydroxy-acids, ω-keto-carboxylic acids, and other multi-functional organic acids are formed. In a well-oxidized air parcel containing many biogenic and anthropogenic hydrocarbon precursors, a high percentage of the total OPM mass can be attributed to these compounds. The concentrations of carboxylic acids are high in OPM samples from many locations, including the poles where the air has been aged and collected after movement across the global circulation cells (Kawamura, *et al.,* 1996), and in the marine boundary layer where aging has occurred during movement away from hydrocarbon sources such as cities and forests (Table 1.2).

Table 1.2. Estimated contributions from previous studies of carboxylic acids in organic aerosol. LMW=low molecular weight.

Study	Method	Samples Studied	Carboxylic Acids in SOA
Mayol-Bracero, et al., 2002	Water extraction, GC-MS and LC/UV	Brazilian rural aerosol	28% by mass
Gao, et al., 2004	ESI-LC/MS	Cycloalkene ozonolysis	3.13-5.49% of total OPM; 78-98% in LMW SOA
Glasius, et al., 2000	GC-MS with BF_3/Methanol, LC/MS	Terpenoid oxidation	20-30% by mass
Kawamura & Ikushima, 1993	GC-MS with BF_3/Butanol	Di-acids in urban aerosol	0.95% on average by mass

The abundance of semi-volatile organic compounds such as carboxylic acids in SOA can be predicted using gas/particle partitioning theory, which relates the phase transition properties of the compounds to the surrounding materials and conditions. This theory is fundamental in the prediction of the formation of PO-OPM, and also serves as a tool to show whether tentatively identified compounds in atmospheric OPM should be present in the particle phase.

Mass yield Y is defined as the ratio of the total mass of OPM formed, ΔM_0 (μg m^{-3}), to the amount of hydrocarbon reacted, ΔHC (μg m^{-3}):

$$Y = \frac{\Delta M_0}{\Delta \mathrm{HC}} \qquad (1.1)$$

Experimental values of Y can be compared to show the relative amounts of OPM generated in chamber studies of individual atmospheric hydrocarbon oxidation. A theoretical calculation of the fraction of a particular oxidation product that will be found in the particle phase, F_i, may also be calculated for a given experiment. This is inversely related to the liquid vapor pressure $p°_{L,i}(T)$ of the pure compound (Pankow, 1994a):

$$F_i = \frac{R\,T\,f\,A_i\,\mathrm{TPM}}{10^6\,\overline{\mathrm{MW}}\,\zeta_i\,p^o_{L,i}} \qquad (1.2)$$

where R is the gas constant, T is the temperature (K), f is the fraction of the total particulate matter that is organic (assumed to be 1 in studies of SOA), A_i is the concentration of compound i in the gas phase (ng m^{-3}), TPM is the total suspended particulate matter (μg m^{-3}), $\overline{\mathrm{MW}}$ is the average molecular weight of the organic matter, and ζ_i is the activity coefficient of the compound i within the organic phase.

The relationship in Equation (1.2) shows that for a given compound in equilibrium between the gas and particle phases, as $p°_{L,i}(T)$ decreases, the fraction of i in the particle phase, F_i, increases. The value of $p°_{L,i}(T)$ has been shown to be well modeled by the presence and positioning of functional groups with respect to the carbon backbone of a compound (Jensen, *et al.*, 1981). The SIMPOL.1 prediction algorithm (Pankow & Asher, 2008) gives a decrease[2] in $\log_{10} p°_{L,i}(T)$ of 3.5 ± 0.4 $\log_{10}$(atm) at 20°C by addition of one carboxylic acid functional group to a carbon backbone. Likewise, a decrease of 2.23 ± 0.22 $\log_{10}$(atm) is observed by addition of a hydroxyl group, 1.35 ± 0.26 $\log_{10}$(atm) by

[2] The absolute error was calculated as the average absolute difference between the predicted and experimentally measured $p°L,i(T)$ for: 13 saturated carboxylic acids, ten saturated hydroxys, five saturated ketones, and five saturated aldehydes. Errors for unsaturated and aromatic compounds as well as for compounds containing other functional groups are given in Table 7 of Pankow & Asher, 2008.

addition of a formyl group, and 0.935 ± 0.24 $\log_{10}$(atm) by addition of a keto group. Thus, compounds containing these oxygenated functionalities will more readily partition into the particle phase in the atmosphere, and the order of the functional groups by which the F_i is increased will be carboxylic acid > hydroxyl > aldehyde > ketone. However, although carboxylic acids are therefore shown to be in high concentrations in OPM by both experimental and theoretical calculation, as mentioned previously, they are difficult to characterize using traditional methods for organic matter analysis.

4. Challenge of Separation of Polar, Oxygenated Compounds including Carboxylic Acids by Gas Chromatography

Gas chromatography (GC) has been an established analytical technique since the 1940s and is now widely used for routine environmental analysis, including the examination of biomarkers in biomass burning particulate matter, and analyses for semi-volatile organic compounds by the U.S. Environmental Protection Agency (Method 8270D; U.S. E.P.A. 2007). Utility of GC lies in its adaptability and range of compounds for which it can be used: GC-MS is used for analyses of metabolites up to 550 a.m.u. (Kind, *et al.,* 2009), GC with inductively coupled plasma mass spectrometry (ICP-MS) and derivatization is used for determination of methylmercury in aquatic systems (Demuth & Heumann, 2001), and GC with a Valco pulsed discharge helium ionization detector (PDHID) is used for measurement of atmospheric trace gases (Steele, *et al.,* 2007). Detection limits at the attogram level have been reported using two-dimensional separation by GC (Patterson, *et al.,* 2005) but typical quantitations are of nanograms to micrograms.

The high resolution, vapor phase separation of GC makes it a common tool for environmental analyses of volatile compounds. Much recent analytical atmospheric chemistry work has focused on the development of GC methods and techniques for determining the complete composition of SOA. For most trace, volatile components in a complex air sample, separation by GC is followed by detection by a method such as mass spectrometry or flame ionization detection, allowing both qualitative and quantitative analysis.

The separation power of components by a GC system can be measured as the distance between adjacent, eluting peaks (the chromatographic resolution), or as the number of peaks resolved within a given unit of separation time (the peak capacity). The separation power can be enhanced by the addition of a second, orthogonal separation stage, which has been accomplished by adding a second column prior to detection. GC×GC can allow increased resolution (or peak capacity) and number of detected analytes within a sample. In a study by Hamilton, *et al.* (2004), GC×GC was used to detect thousands of compounds in the same chromatogram, from high molecular weight, non-polar polycyclic aromatic hydrocarbons to low molecular weight, polar mono-carboxylic acids. A peak capacity of ~500-800 peaks/min (throughout the chromatogram) was achieved for GC×GC[3], compared to ~120 peaks/min measured using a one-dimensional instrument (Wilson, *et al.*, 2011). Mitrevski, *et al.* (2008) also showed that the increased sensitivity of GC×GC allowed the direct identification of compounds that were not identified during a one-dimensional GC analysis using a library search.

The two columns in comprehensive two-dimensional gas chromatograph are separated by a transfer line (generally an inert column) and a modulator so that fractions of the eluant

---

[3] The peak capacity using GC×GC chromatograms was improved by decreasing the transfer time of the eluant into the primary column, and also from the primary to the secondary column using a heated transfer line and high-speed valve injection.

from the primary column are collected and separated through the secondary column. Several designs for a modulator have been built, but the most efficient and durable version is a thermal system using a series of two cold (cryogenic) and two hot jets to trap and release the primary column eluant over a selected time interval. The result of a two-dimensional separation is a figure in three dimensions: the primary and secondary axes correspond to the output of the primary and secondary columns, respectively, and either the tertiary axis or a range of colors represents the abundance (Figure 1.2).

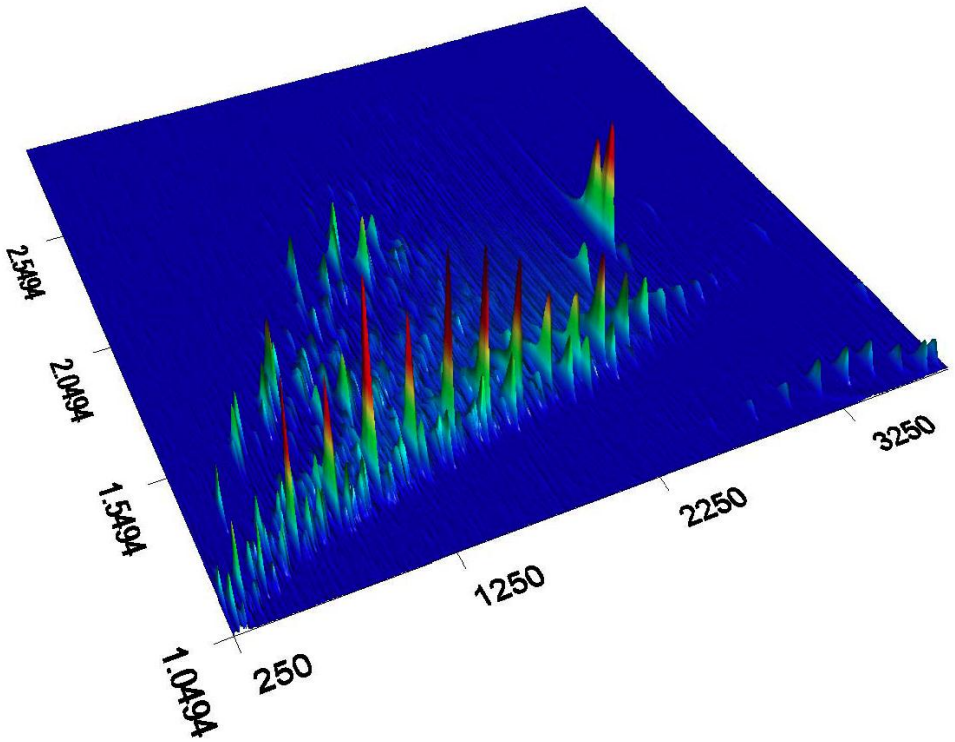

Figure 1.2. GC×GC surface plot showing homologous series of straight-chain alkanes (largest peaks at lowest secondary retention time), as well as branched and some cyclic alkanes in higher secondary dimension times. The primary dimension is represented by the x-axis, and the secondary dimension is

represented by the y-axis. The peaks are shown both as the un-labeled z-axis and variation in color (in grey-scale, the peaks appear grey at the base, lighter in the center, and dark on top; in color, from blue to red from base to peak). Sample is a B-5 biodiesel blend donated by Trimet transportation of Portland, OR.

This three-dimensional visualization is particularly effective for the identification of similar compounds in a sample because homologous series of compounds appear as evenly separated peaks in the primary and secondary dimensions. The separation of each compound is based roughly on volatility in the first dimension (by interaction with a non-polar stationary phase) and polarity in the second dimension (by interaction with a secondary polar stationary phase) when the common "reverse orthogonal" GC×GC column configuration is used. A polar primary and non-polar secondary column configuration may allow decreased peak width for trimethylsilyl sterol ethers (similar to those studied here), but also co-elution (Mitrevski, *et al.,* 2008). When coupled with a mass spectrometer detector (MSD), mass spectra can be gathered for each peak to give separation by a total of four dimensions of data, including the software algorithm for deconvolution (Ramos, 2009).

A high-frequency MS must be applied to the GC×GC system in order to detect the compounds eluting from the secondary column with sufficient resolution (generally 6-10 data points per peak; Ramos, 2009). In contrast to the sampling rates of traditional quadrupole MS detectors, approximately 2.4 Hz, a time of flight (TOF) MS can sample at up to 500 Hz. The unique pulsed spectral data collection in part causes the increase in resolution over scanning mode spectral collection. The development of the latter

instrument therefore allowed the high separation power and high-resolution combination of GC×GC/TOF-MS, first used in 2000 (van Deurson, *et al.*).

Direct separation by GC of semi-volatile compounds, however, results in peak broadening, or a signal to noise ratio (S/N) that is too low for accurate recognition of the compound. This phenomenon is caused by the strong interaction of polar analytes with active silanol sites in the chromatography column, which are formed by breaking of the siloxane bridges that make up the fused silica base of the column (Figure 1.3) (Strazhesko, *et al.,* 1974; Nawrocki, 1997).

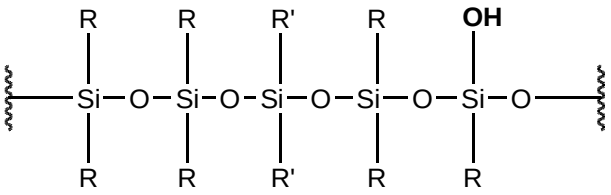

Figure 1.3. Active silanol site within the basic structure of the most common modified silicone polymer, a 5% diphenyl-, 95%-dimethyl-polysiloxane, such as an RTX-5 column (Restek). Siloxane Si-O bridges are within the structure of the phase, and are broken due to wear or high-temperature degradation of the column (some sites exist even prior to use) and thus are made available for interaction with polar analytes. The –OH silanol represents one active silanol site. Stationary phases contain silica backbones with methyl, phenyl or cyanopropyl groups.

Vicinal and geminal active silanol sites can also be formed, and are less reactive because of hydrogen bonding between the adjacent silanol groups. The siloxane bridges are stabilized and unavailable for hydrogen bonding because the lone electron pairs of the O atoms are involved in weak pi-interactions with Si atoms (Nawrocki, 1997; Strazhesko, *et al.,* 1974).

Chemical solutions are available for testing the adsorption of polar analytes in columns, including the Grob test mix (Grob, *et al.,* 1978), which employs a series of polar and non-

polar compounds with similar and reproducible retention characteristics. A chromatogram of the test mix shows increased retention (delayed retention time), decreased response, or distortion from Gaussian peak shape. Grob, *et al.* (1978) showed that changing GC conditions could optimize the peak shape of 1-octanol, as an example, but that the response of the peak could only be increased to approximately 86% of the theoretical peak height. The peak shape of analytes in a PO-OPM sample would not be simple to optimize because of the number of compounds in the sample with differing chromatographic characteristics.

The problems associated with adsorption of polar analytes in a silica base column can be minimized by optimizing the ratio of the time spent by the analyte in the stationary phase relative to that spent in the mobile phase (the retention factor, k):

$$k = \frac{t'_R}{t_0} \qquad (1.3)$$

where t_0 is the retention time of the mobile phase and t'_R is the difference in retention time of the mobile phase and the analyte. The number of peaks eluted within a chromatographic space, or the peak capacity $n_{c,GC,}$, is a measure of the possible separable sample components. The metric $n_{c,GC,}$ can be written to show its dependence on the interactions of the analyte with the stationary phase and the broadening of the peaks, represented by k and w_b, respectively:

$$n_{c,GC} = \frac{k \times t_0}{w_b} \qquad (1.4)$$

These interactions with the stationary phase are the origin of the peak broadening (increased w_b), adjusted retention time t'_R, and diminished peak capacity $n_{c,GC}$ observed for semi-volatile components of PO-OPM. The magnitude of the interactions is related to the number of oxygenated sites in a molecule and the overall oxidation state of the PO-OPM component. If the interactions with the column are great, the peak may be sufficiently broadened, or the analyte retained in the stationary phase, so that the analyte may not be detected in the chromatogram and mass spectrum.

5. Mechanisms and Procedures for Chemical Derivatization

The unfavorably strong interactions of polar, oxygenated analytes with a silica-based GC column can be lessened or avoided by chemically "capping" the active sites on the analyte. This sample preparation process, called chemical derivatization, decreases the analyte retention within the stationary phase (and thus the retention factor *k* in the GC column; Section 1.4) through the transformation of the analyte into an ether, ester, or other, lower polarity functional group. Using derivatization, analytes that otherwise would have poor peak shape or be absent from the chromatogram can be determined. The target functional groups (such as carboxylic or hydroxyl groups) must be reacted with a derivatization reagent that is selective for those groups, or is a broad-spectrum reagent (reacting with most protic sites).

There are well over 50 reagents and procedures available in Blau & Halket's Handbook of Derivatives for Chromatography (1993) for carboxylic acid analysis. Derivatization reactions for carboxylic acids can be categorized as esterifications or silylations, both occurring via bimolecular nucleophilic substitution (S_N2) mechanisms in which an aprotic group from the derivatization reagent displaces the analyte protic group. Esterifications carried out for the purpose of chemical derivatization generally follow the traditional acid-catalyzed mechanism (Reaction Scheme 1.1).

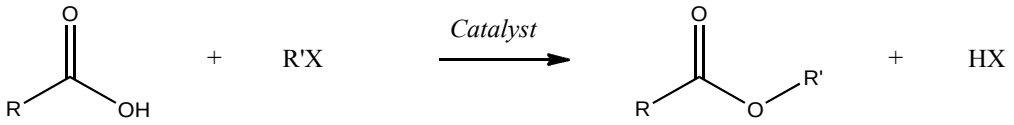

Reaction Scheme 1.1. General derivatization reaction for carboxylic acids. The groups R and R' can be a variety of alkyl or other structures; most often R' is a straight-chain alkyl group. The portion of the derivatization reagent designated as X can be any good leaving group, such as a halogen or hydroxide.

The newly formed ester bond between an analyte and a derivatization reagent moiety can be broken during mass spectral fragmentation. This diagnostic ion is characteristic and effective for recognizing derivatives in mass spectra and can also be composed of a larger fragment lost from the derivative. The derivative must be stable so that the dissociation can only occur during mass spectral analysis, rather than during GC separation or storage.

A primary goal of chemical derivatization is to allow the determination of polar, oxygenated compounds by GC, but there are often characteristics of a derivatization process or derivatives that decrease the potential sensitivity and overall detection of derivatives. Such characteristics include analyte losses during cleanup steps, the absence or low response of diagnostic and molecular ions in the product mass spectrum, various poor chromatographic results due to the improper analyte selectivity of the reagent, degradation of the derivatives, or the generation of byproduct peaks.

Choosing an extraction procedure based on the response of standard compounds in various separation procedures and solvents can lessen losses during cleanup steps. Evaporative losses during concentration and solvent removal steps are problematic when the derivatives are volatile; to avoid this, a derivatization reagent that donates a larger moiety to the analyte can be used. A sufficiently large derivatization moiety can also

allow the derivatives to be easily recognized in a chromatogram because the moiety is usually lost during MS fragmentation, and therefore the corresponding ion can be extracted from the total ion chromatogram to show all or most of the derivatives. The common reagent system boron trifluoride/methanol (BF_3/methanol), for example, adds only m/z 15, which is too low in molecular mass and common throughout any chromatogram to be used as a diagnostic ion.

The selectivity of a reagent refers to the range of functional groups and volatilities over which it can effectively derivatize. A highly selective reagent reacts with only one functional group, such as carboxylic acids, while a low selectivity or broad-spectrum reagent can allow the analysis of nearly all protic functionalities. A reagent with high selectivity will be effective for analyzing a targeted functional group, but only those compounds within a complex sample are analyzed. If several functional groups should be derivatized, several high selectivity reagents can be used in series, or a low selectivity reagent can be used. The chromatogram background generated from a sample derivatized using a low selectivity reagent often contains many reagent byproduct peaks and noise, which can decrease the sensitivity of the technique, and increase the work necessary for data processing. Lower selectivity reagents also are often reactive with water or solvents, so that the derivatives can be degraded during storage, and large byproduct peaks may co-elute with or obscure derivative peaks.

In *Chemical Derivatization in Gas Chromatography*, Drózd (1981) noted that derivatization is synthetic chemistry on a micro-scale and requires a high level of

precision. The complexity of designing and carrying out derivatization makes the technique less desirable for many analyses, although automated derivatization is possible (Nicoll-Griffith, *et al.,* 1993; Frank, *et al.,* 1984) and may help to eliminate some of these challenges. Even the choice of a reagent is not simple: each reagent reacts with particular functional groups, so no specific reagent can be used to detect all polar target compounds in an OPM sample. Even broad-spectrum reagents generally do not react with neutral carbonyl groups. A reagent or combination of reagents may be chosen for a particular sample and/or analytes, however, by matching the goals of the study with the features of available reagents. The advantages and disadvantages of reagents commonly used for the derivatization of carboxylic acids and other polar analytes in OPM samples are summarized in Table 1.3.

Table 1.3. Common derivatization reagent systems used in organic aerosol analysis. Drawbacks and advantages from literature results using each particular reagent system are summarized. *LMW = low molecular weight, HMW = high molecular weight, EI-MS = electron impact ionization mass spectrometry, CI-MS = chemical ionization mass spectrometry, ECD = electron capture detector*

Reagent System/Reaction	Analytes	Advantages	Drawbacks	Studies
BF_3/methanol/Esterification	Carboxylic Acids	Easy and fast reaction, high derivatization efficiencies	Derivatives of LMW acids are volatile, no MS diagnostic ions	Jaoui & Kamens, 2003; combination with BSTFA: El Haddad, et al., 2009
BF_3/*n*-butanol/Esterification	Carboxylic Acids, Aldehydes, Acidic Ketones	Selective for two polar functional groups, reacts well with di-acids and oxo-acids	Requires cleanup step, butanol is high-boiling so that drying step may promote loss of analytes	Kawamura, et al., 1996, 2007; Bao, et al., 2009
Diazomethane/Esterification	Carboxylic Acids	Easy and fast reaction, high derivatization efficiencies, only major byproduct is nitrogen gas (a favorable leaving group)	Not commercially available, explosive with exposure to water or rough glass edges, derivatives of LMW acids are volatile, no MS diagnostic ions	Mazurek, et al., 1987; Primary OA: Lewandowski, et al., 2008
N-(tert-Butyldimethylsilyl)-*N*-methyltrifluoroacetamide (MTBSTFA)/Silylation	All Protic Sites	Larger added moiety than with BSTFA, easy and fast reaction, broad spectrum reagent, MS diagnostic ions for all derivatives and particular derivatized functional groups	Sterically hindered reagent reaction site	Kim, et al., 1989; Schummer, et al., 2009
N-methyl-*N*-trimethylsilyltrifluoroacetamide (MSTFA)/Silylation	All Protic Sites	Lower-boiling reagent so that no co-elution with LMW derivatives; derivatives ECD active	Some LMW mono-acids may not react	Kourtchev, *et al*., 2009; Claeys, *et al.*, 2007

Table 1.3 Continued

Reagent System/Reaction	Analytes	Advantages	Drawbacks	Studies
N,O-bis(trimethylsilyltrifluoroacetamide) (BSTFA)/Silylation	All Protic Sites	Easy and fast reaction, broad spectrum reagent, MS diagnostic ions for all derivatives and particular derivatized functional groups, several optimization studies	Reagent and derivatives react with water, derivatives degrade over time, reagent and byproducts may co-elute with LMW derivatives, may not react with HMW acids	Fu, *et al.*, 2009; Jaoui, *et al.*, 2010; combination with BSTFA: Yu, *et al*., 1998; optimization: Pietrogrande & Bacco, 2011
O-(Pentafluorobenzyl) hydroxylamine (PFBHA)/Oximation	Neutral Carbonyls	Added prior to sample extraction, combined easily with other reagents	Requires 12-36 hours for reaction (depending on analytes), requires cleanup	Combination with BSTFA: Yu, *et al.*, 1998; on-denuder: Healy, *et al*.,
Online BSTFA/Silylation	All Protic Sites	Easy and fast reaction, lower possibility of impurities, less uncertainty from sample preparation steps, broad spectrum reagent, MS diagnostic ions for all derivatives and particular derivatized functional groups	Excess reagent may deposit in GC column leading to degradation, derivatization rates are not easily controlled	Docherty & Ziemann, 2001
Pentafluorobenzyl bromide (PFBBr)/Esterification	Carboxylic Acids	Reaction in aqueous or organic solvent, high responses of most carboxylic acid derivatives, derivatization with phenols can be controlled by pH	Poor molecular ions in EI-MS (use of CI-MS may be required), little documentation of application to GC analysis of carboxylic acids, cleanup needed to remove excess reagent	Chien, *et al.*, 1997, 1998

The reagent systems given in **Error! Reference source not found.** have been used specifically for the analysis of air samples, but there are many more varieties of each type of derivatization reaction. Knapp (1979) provided an excellent source of original procedures for many of these reagents. The conditions needed for optimal reaction have been studied for most common reagents, including the solvent, pH, reaction time and temperature. Optimized procedures are also designed based upon the target analytes because particular procedural steps or conditions such as reaction times may not be suitable for less stable or reactive analytes. The general chemical structures of analytes and objectives of a study should be clearly understood: whether the goal is to qualitatively detect or quantitatively determine the analytes, and whether only tracer compounds or all components of the sample are to be identified. For instance, in a study of PO-OPM, the sample is complex and several reagents may be needed for complete, efficient analysis.

The total organic carbon determined to be on a given filter will differ from that which can be determined using gas chromatography techniques because of interactions of polar analytes with the GC column, low or high volatility of some analytes, or lack of identification by the particular detector in use. The response of a flame ionization detector (FID) is effective for estimating the total mass that can be determined via GC analysis because the response is mass-sensitive and specific to reduced, combustible atoms such as carbon. In a sample containing a large fraction of oxygenated carbon, the carbon will be underestimated; but if the composition of the sample is mostly known, the

oxidized carbon atoms can be adjusted for using the ratio of oxidized to reduced carbon atoms.

The combined method of derivatization with GC×GC analysis for PO-OPM composition determination will be assessed in this study by measuring the total GC-FID quantifiable mass of derivatized oxidation products. The response of GC×GC-FID to extracted, BSTFA derivatized α-pinene ozonolysis products from filter samples will be measured and compared to the response of the same instrument when the same samples are introduced without derivatization. The mass contributed by trimethylsilylation will be estimated using a mass spectral response (that of GC×GC/TOF-MS) and subtracted from the determined FID response. The responses of the TOF-MS and FID are fundamentally different and there will be uncertainty associated with the estimate of mass contributed by trimethylsilylation. However, the values for derivatized and underivatized GC×GC-FID total response will give an estimate of the relatively non-polar total mass that can be determined using a gas chromatographic method without derivatization, and the polar total mass determined using the derivatization/GC×GC method.

It should be noted that derivatization can be used for many analytical methods to form a chemically altered analyte with properties that improve its potential for detection: the addition of a group that fluoresces, that is active in electron-capture detection, or that fragments characteristically for MS detection. Derivatization is also used for analysis by instruments other than GC, as in the improvement of fragmentation for soft ionization by

atmospheric pressure chemical ionization (APCI) and electrospray ionization (ESI) liquid chromatography (LC). The reagents 2-chloro-1-methylpyridinium and (2,4,6-trimethoxyphenyl)phosphonium propylamine (TMPP) have been used to identify fumaric, maleic, sorbic, and salicylic acids at femtomole limits of detection from pharmaceuticals using ESI-LC with tandem mass spectrometry (MS/MS; Cartwright, *et al.,* 2005).

6. Specific Considerations for Choosing a Derivatization Reagent

To select a reagent for use in GC×GC/TOF-MS analysis, the advantages and drawbacks of reagents known to react with carboxylic acids expected in PO-OPM samples were first compared. The testing of reagents and procedures will be based on the formation of relevant derivatives and the best chromatographic characteristics for each derivative. The reagent systems selected for subsequent testing were 2,3,4,5,6-pentafluorobenzyl bromide (PFBBr), boron trifluoride/*n*-butanol (BF_3/butanol), and *N,O*-bis(trimethylsilyl)trifluoroacetamide (BSTFA). The carbonyl-derivatizing reagent 2,3,4,5,6-pentafluorobenzylhydroxylamine (PFBHA) was also considered to accompany the derivatization of carboxylic groups. Methyl alkylation, however, was not used because of unfavorable properties of the derivatives: the lack of diagnostic ions in methyl ester mass spectra, and also the high evaporative losses of the molecular weight methyl esters.

The selection of reagents for testing was based on the applicability to the analysis of α-pinene ozonolysis products, the efficacy and ease of each overall sample preparation procedure, and the ease of data processing. Although PFBBr and PFBHA are more selective, relatively lower selectivity reagents will be advantageous in this study because the objective is to identify as many components of the PO-OPM sample as possible. The sensitivity of the method was prioritized over a faster, simpler procedure because high sensitivity is required for quantifying the analytes. The ease of the procedure was still

considered so that errors and imprecision will be minimal when the method is used in future applications.

1.6.1.1 Pentafluorobenzyl Bromide (PFBBr)

The reagent PFBBr is theoretically an excellent choice for the analysis of carboxylic acids. The reaction is an esterification selective for carboxylic acids (Reaction Scheme 1.2) and the only detected byproducts from the reaction are generated when excess reagent is not removed.

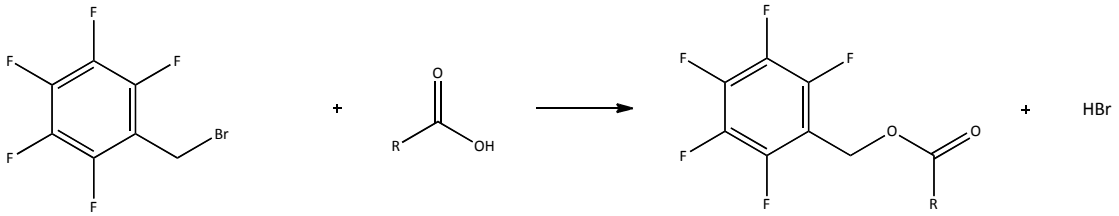

Reaction Scheme 1.2. Esterification reaction of PFBBr, showing that the removal of the proton from the carboxylic acid ROOH is important for the initiation of the reaction because of the increased nucleophilic character of the deprotonated carboxylate. Potassium is often used for deprotonation because in aprotic solvents, the potassium can be transported through the solvent by the phase transfer catalyst 18-crown-6 ether.

For pentafluorobenzyl esterifications, the favorability of a halogen atom leaving group from the reagent increases the rate and efficiency of reaction. The molecular mass of the added moiety is large (Reaction Scheme 1.2) so that the volatilities of small derivatives are optimal for GC separation, and the mass spectra contain a diagnostic ion at *m/z* 181. PFBBr is also advantageous because it is the only derivatization reagent reported to react with carboxylic acids in water (Pan & Pawliszyn, 1997). Reaction in water allows the collection or extraction of a sample into water for the determination of water-soluble organic carbon (WSOC) components without solvent exchange steps in which analytes

could be lost. The WSOC fraction has been shown to account for ~40% of suburban particulate matter with particle diameters of < 2.5 μm ($PM_{2.5}$) (Lewandowski, *et al.,* 2007). Derivatives of many reagents can undergo hydrolysis and some reagents themselves also react with water, so that reagent and reaction solutions are generally kept from water. Most reactions with carboxylic acids occur via nucleophilic attack, and dichloromethane (DCM) or similar, aprotic solvents are used to prevent competition for reaction with the active site on the analyte. It is important to maintain the pH of an aqueous PFBBr reaction solution above the pK_a of target carboxylic acids because the acid groups will be deprotonated at a pH above their particular pK_a values. PFBBr accordingly acts best at a pH just above the pK_a values of the acidic analytes (Pan & Pawliszyn, 1997), so a buffer solution must be prepared and used in aqueous pentafluorobenzyl ester formation. The reaction can also be carried out using an organic solvent, and a phase transfer catalyst (generally 18-crown-6 ether) must be used in organic solvent so that the proton removal catalyst (generally carbonate) is kept in solution.

Aqueous and organic solvated PFBBr derivatizations of standard carboxylic acids were considered for use in this study. The reaction was carried out in reaction solvent rather that water selected, despite the advantages of aqueous reaction. A solvent removal step is required after aqueous derivatization to avoid degrading the chromatographic column and injection liner, and oxidizing the ion source of the MS. These solvent removal steps can

cause significant evaporative losses of the analytes (derivatized or underivatized) under the incident nitrogen gas pressure due to the duration necessary for water removal.

A consistently high response and signal to noise ratio (S/N) are particularly important so that the signal of the target ion(s) can be reliably be distinguished and accurately quantified. The high selectivity of PFBBr should allow less chemical noise and fewer background peaks to be produced, keeping small signals from being obscured. However, large amounts of reagent and byproducts are present in PFBBr derivatized samples, allowing detrimental buildup of the reagent and byproducts in the instrument, and potentially to a very damaging extent in the thinner, secondary GC×GC column. Several methods have been used, and will be tested for post-reaction cleanup. These include solid phase extraction (Saisho, *et al.,* 1997, Ueyama, *et al.,* 2006), solid phase micro-extraction (Pan & Pawliszyn, 1997), evaporation (Galceran, *et al.,* 1995), and liquid-liquid extraction into a non-polar solvent (Hofmann, *et al.,* 1990; Leis, *et al.,* 2003).

It is possible that identifying some PFBBr derivatives will not be possible, particularly without library spectra or authentic standards, because the molecular ions in electron impact (EI) spectra will be absent or in low abundance (Chien, *et al.,* 1997). The softer ionization technique methane chemical ionization (CH_4-CI) has been used for the detection of pentafluorobenzyl derivatives (Chien, *et al.,* 1997, 1998; Jang & Kamens, 1999), but the Leco® Pegasus® 4D GC×GC/TOF-MS is not equipped with a CI source.

1.6.1.2 *N,O*-bis(trimethylsilyl)trifluoroacetamide (BSTFA)

A low selectivity reagent (or combination of reagent) can be used if comprehensive analysis of a sample is the objective to derivatize nearly all protic sites. As a less selective and easier method of derivatization for carboxylic acids, and also to target hydroxy-acids, the reaction of BSTFA was considered. The use of BSTFA has many advantages and has been well studied for a wide variety of analytes. The reaction mechanism of BSTFA with the hydroxy-acid lactic acid is shown in Reaction Scheme 1.3.

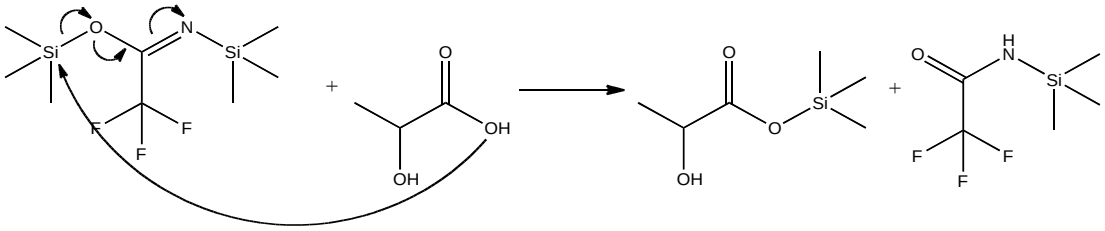

Reaction Scheme 1.3. Mechanism of BSTFA derivatization of lactic acid. Reaction can occur at either trimethylsilyl group of the reagent molecule (reaction at the oxygen site is shown here).

This mechanism is also followed for the reaction of the same reagent with hydroxy groups such as that of lactic acid. Only a few reagent byproducts such as the *N*-trimethylsilyl-trifluoro-acetamide in Reaction Scheme 1.3 are generated, and have been well characterized (Little, 1999). A reaction such as this is simple because no cleanup is necessary; the reaction is therefore easier to replicate precisely, there will likely be a decrease in the number of errors made, and fewer supplies and less time will be required. The reagent BSTFA is an excellent example of a simple reagent, and is well studied and well used because of this. The reaction of BSTFA has been shown to complete in 15 seconds at room temperature for phenols (Li, *et al.,* 2009) and can be used for in-

injection-port derivatization (Docherty & Ziemann, 2001). The reaction with water of trimethylsilyl derivatives and the reagent itself is a major disadvantage of the use of BSTFA. The derivatives will hydrolyze if care is not taken to keep water out of the reaction or sampling vials, or samples are not analyzed soon after derivatization. Quenching the excess reagent with water may increase the stability of the derivatives (Charles & Spaulding, 2002).

Many derivatization reactions with carboxylic acids are carried out in aprotic solvent because of their S_N2 character, so catalysts are used to initiate removal of the acidic proton in the reaction. An aprotic, basic solvent can catalyze the reaction of a weak carboxylic acid by removing the acidic proton. Pyridine is one such basic solvent, used in many procedures for the reaction of BSTFA (Yu, *et al.,* 1998; Clements & Seinfeld, 2006; Docherty & Ziemann, 2001). Trimethylchlorosilane (TMCS), a trimethylsilylation reagent that reacts more strongly with analytes than BSTFA, can also be used as an additive to initiate the reaction of BSTFA (Ding & Chiang, 2003).

Silylation reagents including BSTFA will react with *all* protic sites on an analyte molecule, in the following reactivity order: alcohol > phenol > carboxylic acid > amine > amide (Evershed, 1993). There are several variations of BSTFA that are less common, but suited generally to react with particular shapes of carboxylic acids or alcohols (Evershed, 1993), including *N*-methyl-*N*-(*tert*-butyl-dimethylsilyl)trifluoroacetamide (MTBSTFA) and *N*-methyl-*N*-trimethylsilyltrifluoroacetamide (MSTFA). The larger size of the added moiety of MTBSTFA is favorable because the volatility of low

molecular weight (LMW) acid and alcohol derivatives is lower than trimethylsilyl derivatives. However, this larger reagent reacts at non-sterically hindered carboxylic or hydroxyl sites, and may not react when two or more sites for reaction are adjacent (Ding & Chiang, 2003). Reactions with MSTFA generate fewer byproducts that co-elute with LMW derivatives such as trimethylsilyl acetate. Derivatization efficiencies, however, may be lower for LMW carboxylic acids with MSTFA (Stávová, *et al.,* 2011). BSTFA was selected for testing as a possible derivatization reagent in this study: it is a more readily available and well-studied reagent, LMW acids such as formic and acetic acid that may be more readily detected using MSTFA re not target analytes for this study, and sterically hindered acid sites of oxidation products that may not be derivatized using *tert*-butyl-dimethylsilylation are possible analytes.

Data processing of GC×GC-TOF-MS analysis can be as time-consuming as performing the derivatization reaction itself. Analytes and byproducts must be identified and quantified easily so that the resources needed for each analysis are decreased. The accuracy and precision of the method are also increased, especially at low concentrations. The properties of derivatives that decrease the number of background versus target peaks in the chromatogram can specifically be helpful for processing chromatographic and mass spectral results. Data processing for silylated standard solutions should be simple relative to results of reagents with higher boiling points and those with less characteristic diagnostic ions (such as BF_3-catalyzed alkylations).

Data processing for a derivatized sample can be strenuous because the derivatives may not be listed in mass spectral libraries. For many reagents, even if the spectra are not listed, the ion due to loss of the added reagent portion from the analyte structure can be viewed specifically to identify analytes in the chromatogram (Table 1.4).

Table 1.4. Ions characteristic of common derivatives. Each fragment in particular was used during data processing to show the presence of derivatives in general, or of derivatives of particular functionalities.

Characteristic Ion (m/z)	Reagent	Fragment	Analyte
73	BSTFA	$[Si(CH_3)_3]^{\cdot+}$	All protic sites
117	BSTFA	$[COOSi(CH_3)_3]^{\cdot+}$	Mono-acids
147	BSTFA	$[(CH_3)_2Si{=}OSi(CH_3)_3]^{\cdot+}$	Multi-functional or di-acids
57	BF_3/butanol	$[(CH_2)_3CH_3]^{\cdot+}$	All protic sites
61	BF_3/butanol	$[CH_3C(OH)_2]^{\cdot+}$	Acidic ketones
117	BF_3/butanol	$[CH_3C(OC_4H_9)OH]^{\cdot+}$	Acidic ketones
173	BF_3/butanol	$[CH_3C(OC_4H_9)_2]^{\cdot+}$	Acidic ketones
159	BF_3/butanol	$[CH(OC_4H_9)_2]^{\cdot+}$	Aldehydes
103	BF_3/butanol	$[CH(OC_4H_9)OH]^{\cdot+}$	Aldehydes
181	PFBBr; PFBHA	$[CH_2PhF_5]^{\bullet+}$	Carboxylic acids; neutral carbonyls

The ions *m/z* 73, *m/z* 117, and *m/z* 147 can be extracted from the total ion chromatogram, corresponding respectively to all derivatives of BSTFA, specific derivatives of mono-, and of multi-functional or di-acid derivatives. The large number of background derivatives showing the diagnostic ion m/z 73 complicates this extracted analysis; background carboxylic acids that might be expected as ring-opening products of atmospheric oxidation can be present due to contamination of the reagent or sample. Confusion of these peaks, which may be derivatized solvent and plastic breakdown products, with actual analytes can be avoided by the analysis of extensive derivatized blanks. Contamination can also result from exposure of the reagent to volatile polar, protic compounds during storage or use. Reagent byproduct peaks of BSTFA elute at low

retention times relative to many standard derivatives; thus, the solvent delay can be set to include the retention times of these peaks to avoid confusion with analyte or standard derivatives.

1.6.1.3 Boron Trifluoride/*n*-Butanol (BF_3/Butanol)

Alkylation via reaction with an aliphatic alcohol is another frequently used derivatization technique for GC analysis of carboxylic acids because of its high selectivity and easy reaction. Methanol may be the most commonly utilized alcohol for alkylation, but the vapor pressures of LMW methyl esters such as methyl oxalate and methyl malonate are high and the derivatives may be lost by evaporation after derivatization. The formation of butyl esters is more favorable for LMW acid analysis, although the reagent is also higher boiling and thus produces high chemical noise throughout chromatograms of the derivatized samples. Kawamura and colleagues (1987, 1993a, 1993b, 1993, 1996, 2007) have used butyl esters extensively for the analysis of ω-oxo-acids (terminating in an aldehyde group) and di-acids, which are highly oxidized and found in atmospheric OPM. Limits of detection of 0.7-3.0 ng/m^3 for C_3-C_9 di-carboxylic acids have also been reported using BF_3/butanol and GC-MS (Pietrogrande, et al., 2010).

The proposed mechanism for butylation is driven by the availability of the electrophilic carbonyl site of the carboxylic acid analyte, and by the reactivity of the nucleophile, C_4H_9–OH. For alkyl esterifications (alkylations), the leaving group from the reagent is often a molecule of water, as in butylation (Reaction Scheme 1.4).

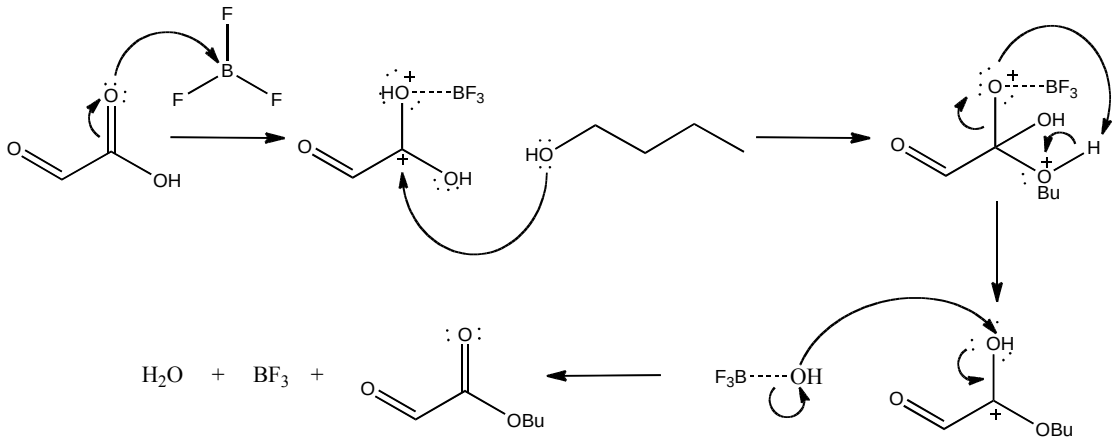

Reaction Scheme 1.4. Proposed mechanism for the reaction of BF_3/butanol with the carboxylic group of glyoxylic acid. Boron trifluoride acts as a catalyst to increase the electrophilicity of the aldehyde carbonyl carbon.

The constituents of a carboxylic acid structure affect its reactivity toward butanol. Electron-donating groups such as added alkyl groups onto the carbon backbone should have an inductive effect on the carboxylic site, increasing the electronegativity of the oxygen atoms in the group and decreasing the acidity. Electron withdrawing groups such as carbonyls and alcohols, conversely, should cause an increase in acidity. Therefore, while mono-acids are derivatized by reaction with BF_3/butanol, the procedure is anticipated to be most effective for di- or oxo-acids. For an adjacent functional group, the effect should be much greater than for a functional group located at the γ- or δ- position from the carboxylic acid (Tiwari & Sharma, 1970). The polarity of the carbonyl is enhanced by the formation of the catalyst-analyte adduct, RHO---BF_3. The catalyst BF_3 is a Lewis acid and is effective in particular because of its lack of free protons and vigorous reactivity Solutions of *n*-butanol with 10-20 w/v% BF_3 catalyst are available commercially.

Unlike the lower alcohols, butanol also reacts with aldehydes and ketones, with which it forms dibutyl acetals (Reaction Scheme 1.5) and ketals.

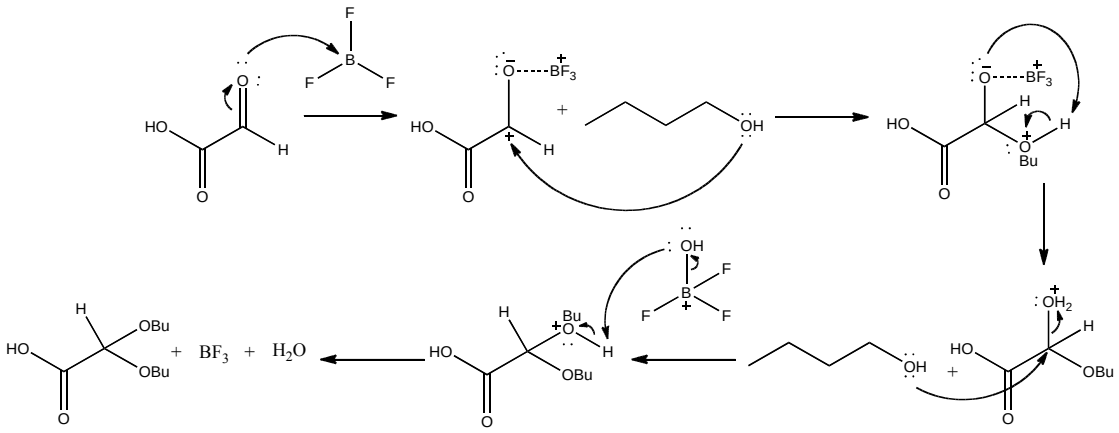

Reaction Scheme 1.5. Proposed mechanism for the reaction of BF_3/*n*-butanol with glyoxylic acid to form a dibutyl acetal. The BF_3 catalyst is used to effect increased electrophilicity of the C-O bond of the aldehyde.

The mechanism proposed for the formation of dibutyl acetals and ketals is based on the general acid-catalyzed formation of acetals (Solomons & Fryhle, 2000). Oxo-acids such as glyoxylic acid Reaction Scheme 1.5) can be identified in a chromatogram by m/z 159 and 103, corresponding to losses from the dibutyl acetal formed, and all derivatives can be identified by the fragment m/z 57, from loss of the butyl group. Similarly, mass spectra of dibutyl ketals contain the diagnostic series of peaks m/z 173, 117, and 61 (Kawamura, 1993). These three, distinguishable derivatization product structures are effective in combination for analyzing atmospheric PO-OPM, in which all three derivatized functional groups are found (Li & Yu, 2005).

Significant drawbacks of the derivatization technique of BF_3/butanol, however, arise primarily from the high boiling point of butanol. Like the chromatograms of derivatives

of PFBBr, elongated tailing portions of large byproduct peaks from BF_3/butanol derivatization can co-elute with analytes. Byproduct peaks cause decreased chromatographic resolution and co-elute with target compounds; co-elution is especially problematic because the reagent and byproducts share characteristic ions with the derivatives (Reaction Scheme 1.4). Chemical noise can also cause decreased resolution; a low background signal is best offered by reagents that are low boiling, and that produce only a few, low boiling byproducts. Removing byproducts and reagent from a sample thoroughly after the reaction is complete can eliminate corresponding peaks and noise from the chromatogram, and are necessary also to avoid degrading sensitive parts of the instrument from deposited reagents or byproducts in large concentrations. The extraction of these byproducts, however, increases the risk of losing derivatives. Cleanup steps. Post-derivatization cleanup steps for derivatization techniques such as BF_3/butanol require time and supplies, and evaporative losses of LMW acid derivatives can be increased, causing lowered sensitivity or a lack of detection of some compounds. Lowered recoveries of analytes can be accounted for (with some uncertainty) using an internal recovery standard (see Section 2.4.c), but only if the compounds are detected (some may not be detected at all if preparation losses are high).

High efficiencies for butylation and other derivatization reactions are best when the reagent and procedure are carefully selected to fit the analytes expected in the study. The stereochemistry of a carboxylic acid with multiple functionalities is important: if a compound is oriented *cis* so that intra-molecular hydrogen bonding may occur between

functional groups, the conjugate base is stabilized and the strength of the acid is increased (Tiwari & Sharma, 1970). Carboxylic acids with *cis* and *trans* isomers may also isomerize during sample preparation, so that the derivatization efficiency may depend on the extent of isomerization to the less reactive *cis* isomer (Bender, 1959 also provides a good discussion of the kinetic and mechanistic considerations). Some carboxylic acid analyte structures also contain ketones, which can tautomerize to the enolate form, and be misidentified if the resulting hydroxyl group is derivatized. These ketone sites are not derivatized using BF_3/butanol unless they have particularly acidic character; instead, there are specific reagents for the analysis of ketones.

1.6.1.4 2,3,4,5,6-Pentafluorobenzylhydroxylamine (PFBHA)

Despite the potentially high evaporative losses of semi-volatile analytes when water is used for extraction of filter samples (the cohesive forces of water necessitate long evaporation steps for water removal), some of the highest percentages of identified OPM mass have been shown by derivatizing ketones in aqueous solution using PFBHA prior to the reaction of carboxylic groups (Yu, *et al.,* 1998; PFBHA/BSTFA). Because this combination with BSTFA has been so effective for identification of the total organic mass (Yu, *et al.,* 1998), its use will also be tested using GC×GC. A large reagent byproduct peak has been shown, similar to the byproducts in PFBBr analyses, however, which must be successfully removed for application to GC×GC analysis. The addition of hydrochloric acid after derivatization may disallow the formation of these byproducts (La Lacheur, *et al.,* 1993).

7. Alternatives to Derivatization and GC-MS

Some monocarboxylic and large acids such as pinic acid can be separated after direct injection. However, better detection limits of these compounds can be reached using derivatization techniques (Joaui & Kamens, 2001), and compounds that are more polar must be chemically altered for analysis by GC. The difficulty and uncertainty involved in derivatization procedures provide motivation for designing alternative analysis methods for compounds not amenable to direct injection. Complex analyses often require extraction steps, and derivatized analytes can be challenging to identify in chromatograms showing many derivatized peaks with similar mass spectra. While techniques elucidating bulk properties of a sample such as functionality (infrared spectrometry, aerosol mass spectrometry) show the significance of carboxylic and other moieties in aerosol, reaction pathways necessary for modeling inputs and predictions of environmental behavior can only be discovered if the absolute composition of the sample is known.

Many instrumental techniques can also be used without derivatization to acquire compound-specific separation. The separation power and range of carboxylic acids detected in each technique is limiting, however. Capillary electrophoresis (CE; van Pinxteren & Herrmann, 2007) analysis has allowed detection of mid-sized di-acids including pentanedioic through decanedioic acids, although the separation power is lower than that reached using GC. By comparison, Yu, *et al.* (1998) externally calibrated using C_2-C_{10} standard acid compounds with formyl, keto, alcohol, and multiple carboxylic

groups using derivatization (PFBHA/BSTFA and GC-MS. For polar, low molecular weight acids (having structures as large as phthalic acid), ion chromatography (IC; Yang & Yu, 2008; Cecinato, *et al.,* 1999) or desorption electrospray ionization MS (DESI-MS; Li, *et al.,* 2009) can be used. Desorption electrospray ionization mass spectrometry (DESI-MS) shows promising limits of detection (about 1 pg mm^{-2} sample for polar, LMW di-acids) and requires little sample preparation. Nanospray DESI (nano-DESI) has also been used, allowing thermally labile components to be better analyzed (Roach, *et al.,* 2010). For higher carbon number acids (up to *n*-octacosanoic acid) liquid chromatography (LC; Antilla, *et al.,* 2008; Glasius, *et al.,* 2000) can be used with various detectors. Use of LC-TOF-MS for targeted carboxylic acids was also successful to 0.9-150 pg/μL for C_{12}-C_{28} mono-acids (Mirivel, *et al.,* 2009) and ESI-LC-MS/MS for C_{12}-C_{28} mono-acids gave limits of detection between 8 and 54 pg/μL (Ŝt'ávová, *et al.,* 2011).

8. Objective Statement

Derivatization and GC×GC will be assessed as an analytical method for detecting and quantitatively determining carboxylic acids in standard solutions and atmospherically relevant OPM samples. A quantitative study of α–pinene ozonolysis OPM samples will be used to show the detection and quantitative determination efficacy of derivatization/GC×GC/TOF-MS for carboxylic acids. The outcomes of the study will be evaluated based on the contrast of total organic mass speciated, any potential newly identified carboxylic acid species, and the limit of detection of the method with previously published determinations, underivatized GC×GC/TOF-MS results, and one-dimensional GC-MS results. Oxidation products will be extracted from filters, then derivatized using BSTFA and BF_3/butanol. An internal recovery standard will be monitored to adjust for losses during sample preparation. The efficiency of the derivatization will be measured using an FID response and the calculated effective carbon number (ECN; see Section 2.X), then used to adjust the measured concentrations of oxidation products. TOC mass, as a proxy for organic mass, will be thermally analyzed and also estimated using particle numbers and sizes to show any divergence between the results of these methods. The response of the FID will also be contrasted with the TOC mass estimation for each underivatized sample to show the total GC×GC-FID quantifiable TOC mass in each filter sample. The results of the study will demonstrate the utility of derivatization with GC×GC/TOF-MS for the detection and determination of carboxylic acids in atmospheric OPM samples.

2 Experimental Methods

1. Materials and Reagents

2.1.1 Supplies for Sample Preparation including Derivatization

A sonication bath and 40 ml amber vials with septa and plastic caps were used for the extraction of filters and storage of filter extracts. Extracts in vials were wrapped with paraffin film and kept at ~-4°C until use. Clean 1 ml syringes were used to deliver each extract to 3 ml conical Reacti-vials for concentration prior to derivatization. A liquid nitrogen cryogenic trap and two activated charcoal traps were used to clean the nitrogen introduced to the samples for concentration. The surfaces coming into contact with the nitrogen prior to introduction to the samples included polytetrafluoroethylene (PTFE) tubing, stainless steel valves, cryogenic trap, and tubing extending from the main nitrogen line to each vial.

The derivatization reagents boron trifluoride/*n*-butanol (BF_3/butanol; 15.4% v/v BF_3) and *N,O*-bis(trimethylsilyltrifluoroacetamide (BSTFA; 1% TMCS) were purchased from Tokyo Chemical Industry, Inc. (Portland, OR) and Thermo Fischer Scientific (Rockford, IL), respectively. The BF_3/butanol facilitated the detection of carboxylic acids (especially di-acids), aldehydes, and acidic ketones, while carboxylic acids and alcohols were reacted with BSTFA. BF_3/butanol was purchased in separate 1 ml aliquots; BSTFA was purchased in one 10 ml bottle and was delivered in 1 ml aliquots to 2 ml auto-sampling vials with septa and crimp-top caps for storage and subsequent use. Reagents were kept at ~4°C. The solvents dichloromethane (DCM; Optima® grade), methanol

(HPLC grade), and hexanes (Optima® grade) were purchased from Fischer Scientific and stored at room temperature. Reagents and solvents were used as delivered, without further purification. Solvents were kept in 40 ml amber vials for extraction and derivatization procedures, and were delivered with clean syringes. These vials were periodically emptied, rinsed, and refilled, or replaced. The septum caps of all reagents and standards were kept in 2 ml auto-sampling vials and were replaced after being punctured by a syringe.

A set of carboxylic acids with various functional characteristics was used for external calibration of the method. These compounds were 2-hydroxy-3-methyl-butyric acid, *cis*-pinonic acid (98%), glyoxal (38-42% w/w solution in water), methyl-malonic acid (99%) (Aldrich, St. Louis, MO), adipic acid, glutaric acid, glyoxylic acid, lactic acid, dodecanoic acid (>99%), malonic acid, oxalic acid, salicylic acid (99%) (all >98%, ChemService, West Chester, PA), *(1S)-(+)*-Ketopinic acid (99%) (Aldrich) and succinic-d_4 acid (98 atom %D; Isotec, St. Louis, MO). Ketopinic acid and succinic-d_4 acids were also used as surrogate recovery standards, *n*-eicosane-d_{42} (98 atom %D; MSD Isotopes, Montreal Canada) was used as the internal recovery standard to adjust for extraction losses, and the internal standards for quantitation were toluene-d_8 (99 atom %D), naphthalane-d_8 (99 atom %D), phenanthrene-d_{10} (98 atom %D), and pyrene-d_{10} (98 atom %D) (Cambridge Isotope Laboratories, Andover, MA). A butylated derivative of adipic acid was also purchased (Aldrich, 96%) to determine the derivatization efficiency (via comparison with in-laboratory esterification). A Fischer Scientific accu-124D Dual

Range balance accurate to ±0.01 mg (at a maximum mass of 60 g) was used to measure each solid compound to a fresh weighing paper. A small flask of water (18 MΩ) was kept in the balance at all times to eliminate static effects on the measurement.

Sodium chloride used during cleanup of the butyl derivatives was purchased from Sigma. Water used for this solution and all other steps of sample preparation was >18 MΩ resistance and was stored high-density polyethylene plastic bottles. Sodium sulfate (J.T. Baker, Inc., Philipsburg, NJ) to remove water after quenching excess BF_3 was dried in a clean container overnight in an oven at 180-300°C and then capped after cooling in the oven and kept in a clean dessicator until use. A clean spatula was used to deliver the sodium sulfate to the reaction vials.

2.1.2 Cleaning of Glassware and Syringes

All glassware (with the exception of syringes and volumetric equipment and/or pieces specifically marked with a lower stability for heat) was cleaned using the following procedure. Each piece of glassware was washed and scrubbed with water (1>8 MΩ resistance purity) using a small tubular brush. Glassware was then sonicated in an aqueous Alkonox detergent solution for 5-10 minutes and rinsed using tap water. The glassware was then sonicated twice for 5-10 minutes in 18 MΩ water and dried in an annealing oven at 400-500°C for 3-5 hrs. Caps for Reacti-vials and 40 ml amber vials were cleaned with the glassware and dried at low (~50°C) heat on foil. Septa were not re-used and data processing vials were also disposed of after the first use.

Prior to use, syringes were rinsed with a series of solvents of varying polarities. The solvents were drawn from 2 ml auto-sampling vials so that larger solvent containers were not contaminated. Syringes were then sonicated in aqueous Alkonox detergent solution once and 18 MΩ water twice for 5-10 minutes each. The plungers were then removed and all pieces were dried at *low* heat (50°C) on foil. Syringes were kept in a foil-lined cardboard box in a clean space in the lab after cleaning.

After each use, syringes were cleaned using flushes of solvent. For syringes 500 µL or larger in volume, flushes used were be approximately 1/5 of the total syringe volume. For syringes less than 500 µL in volume, the flush volumes were the full volume of the syringe. The solvent used for cleaning depended on the type of solution delivered; for polar or water-reactive compounds, water was used, followed by methanol and DCM. If the delivered solution was less polar, only DCM and methanol were used. For less concentrated solutions, 5-10 flushes of each solvent were used. If the solutions were of high concentration (or neat), the plunger was removed from the syringe and both pieces were soaked in water for > 1 hour before regular cleaning.

2.1.3 Analytical Instruments Used

For procedural tests, 1D external calibration, and calculation of limit of detection, an Agilent Technologies 789A GC System equipped with an Agilent Technologies 5975C inert XL EI MSD was used for all one-dimensional separations. An Agilent Technologies 7693 Auto-sampler introduced samples into the GC. The column used was an Agilent J&W DB-5MS UI stationary phase with dimensions as follows: 30 m x 0.250 mm i.d., 0.25 mm film thickness.

Two-dimensional separations for mass spectral detection were analyzed using an Agilent 6890 GC equipped with a quad-stage dual jet modulator (Leco Corporation, Saint Joseph, Michigan, USA), which allowed separation by the secondary chromatography column. The second column was housed in a small oven within the primary oven, and connected to a Leco Pegasus TOF-MS detector. Samples were sent first through a 30m x 0.25mm i.d. x 0.25µm film thickness Rxi-5MS (Restek, non-polar) column, then modulated to a secondary 1.29m x 0.1mm i.d. x 0.1µm BPX-50 (SGE, polar) column. The transfer line to the detector was a 0.210m x 0.1mm x 0.1µm BPX-50 (SGE, polar) column.

The same model Agilent 6890 GC with installed modulator and secondary oven (Leco) equipped with a flame ionization detector (FID), the use of which is referred to hereafter as GC×GC-FID, was used for analysis of the derivatization efficiency and GC×GC-FID quantifiable total organic carbon (TOC) mass. The second column was connected by a transfer line to a hydrogen/compressed air flame FID. The cold and hot jets of the modulator were run using nitrogen gas and compressed air, respectively. The column

stationary phases were chosen to be non-polar (primary dimension) and polar (secondary dimension). For the analysis of butylated calibration standards, a 10 m × 180 μm × 0.20 μm Rxi-17 primary column and a 1.0 m × 100 μm × 0.10 μm RXi-17 secondary column were used. The transfer line between the second dimension output and the detector was a 0.30 m × 100 μm column with no stationary phase (fused silica). For the analysis of BSTFA derivatized calibration standards, a 30 m × 250 μm × 0.25 μm Rxi-5ms primary column and a 1.5 m × 100 μm × 0.10 μm BPx-50 secondary column were used. The transfer line between the second dimension output and the detector was a 0.30 m × 100 μm column with no stationary phase. This configuration was also used for the collection of GC×GC-FID quantifiable TOC mass values.

2. Collection of Samples

2.2.1 Collection of α-Pinene Ozonolysis Products for Quantitative Analysis

To test derivatization with analysis by GC×GC/TOF-MS, samples of particulate phase α–pinene ozonolysis products were collected. A 12 m^3 environmental chamber at the University of California Riverside fitted with a polytetrafluoroethylene (PTFE) bag was used in static mode operation as the reaction vessel (a detailed description of the chamber was provided in Nakao, *et al.,* 2011). Sample filters were collected at ~27°C and ~0% relative humidity (approximately room temperature, at close to zero water conditions so that aqueous phase particulate matter did not form and interactions with water did not occur). The precursor α–pinene (Sigma-Aldrich, >98%) was injected through a glass injection manifold system flushed with purified air (Aadco 737 series air purification system). The small reactive species 1-propanol (Sigma-Aldrich, >99.5%) was introduced in the same way to scavenge $OH^{\bullet}$ radical so that oxidation was isolated to ozone-initiated reactions. 1-Propanol was chosen to avoid possible aerosol mass generated through oxidation of a larger scavenger (Docherty & Ziemann, 2003). The oxidant ozone was introduced through an ozone generator supplied with 20 p.s.i. of purified air. A custom-built scanning mobility particle sizer (SMPS) was used to monitor the particle size distribution between 27 and 685 nm (Nakao, *et al.,* 2011). An estimated value of the organic particulate matter (OPM) concentration in measured air (ΔM_0, μg/m^3) was calculated using the data collected by the SMPS, an average particle density of 1.2 g/cm^3, and the total volume of air collected onto each filter. Wall losses were accounted for in this calculation.

Method blank filters were sampled by pumping clean air (a "clean air blank") or clean air after exposure to the hydrocarbon precursor and scavenger from the chamber (a "no oxidant blank") through a clean filter (Table 2.1).

Table 2.1. Oxidation studies of α-Pinene carried out at the University of California, Riverside environmental chamber. Temperature during each study was kept at ~27°C and 30% relative humidity.

Sample	$[HC]_o$ (ppb)	Δ[HC] (ppb)	[1-Propanol] (ppm)	[Ozone] (ppm)[1]	Collection Volume (L)	OPM Conc., ΔM_0 (μg/m^3)	Aerosol Yield, Y[2]
No Oxidant Blank, 062311-1	461	0	95.6	~1	1530	0	0
Clean Air Blank, 062311-2	0	0	0	0	1550	0	0
α-Pinene SOA, 062311-3	461	461	95.6	~1	1500	1720	0.675
α-Pinene SOA, 062611-3	319	317	69.5	~1	1300	920	0.521
α-Pinene SOA, 062311-4	319	317	69.5	~1	1380	920	0.521
No Oxidant Blank, 062611-2	319	0	69.5	0	1650	0	0
Clean Air Blank, 062611-1	0	0	0	0	1550	0	0

[1] Ozone concentration reported is the introduced value because the ozone analyzer attached the environmental chamber was not in operation.
[2] Aerosol yield was calculated assuming an average molecular weight of 136.23 a.m.u.

Pallflex QA-Ultra Pure 47 mm quartz fiber filters were used to collect all samples and blanks. The filters were pre-fired at 700°C in a muffle furnace for several hours (Sunset Laboratories, Inc., Forest Grove, OR) and packaged in Petri dishes and zipped plastic bags for transport to the University of California Riverside. After collection, the filters were returned to the Petri dishes and bags, and transported back to Sunset Laboratories for TOC mass analysis by a thermal-optical method (see Section 2.8). All filters (samples and blanks) were stored prior to and after collection in plastic Petri dishes and surrounded by zip-sealed plastic bags. The bags containing the filters were then kept at -

4°C until analysis, and transported on dry ice for long distances, or ice packs for short distances.

Reactions conditions were chosen to generate high particulate matter masses for analytical purposes, and thus are not intended to replicate atmospherically relevant conditions. Seed particles were not used (for example, particles of $(NH_4)_2SO_4$, for example, can be used to induce condensation of semi- and low-volatility compounds in chamber studies).

Three α-pinene/ozone reactions were carried out in the dark for 2-3 hours total; collection of aerosol particles was begun after one hour. Collections of "clean air" and air containing only the precursor and scavenger ("no oxidant") blanks were made prior to two of the reactions. One "travel blank" filter was also used in the analyses.

2.2.2 Collection of Anthropogenic Aromatic Hydrocarbon Oxidation Products for Qualitative Analysis

Although the analysis of the anthropogenic aromatic hydrocarbon atmospheric oxidation products is only briefly discussed in this document, the details of the collection procedure are given here. A 90 m^3 environmental chamber at the University of California Riverside lined with PTFE film was used in the collection of oxidation products of anthropogenic aromatic hydrocarbons (Table 2.2). This chamber and all installed monitoring equipment is described in detail in Carter, *et al.,* 2005.

Table 2.2. Chamber samples collected at the University of California Riverside of anthropogenic aromatic hydrocarbon oxidation products. Qualitative analyses were made using the method of combined derivatization and GC×GC-TOF-MS analysis.

Sample	$[HC]_o$ (ppb)	Δ[HC] (ppbv)	[Oxidant] (ppm)	Volume of Collection (L)	[OPM], ΔM_0 (μg/m^3)	Aerosol Yield, Y
Benzene/NO_x, 1236A	938	135	144	4400	203	0.039
Phenol/NO_x, 1273B	106	65.9	53	1400	36	0.062
Toluene/NO_x (+ methylnitrite), 1262B	80	<80	MN 90; NO 90	1100	8	0.018
m-Xylene/H_2O_2, 1244AL	53	<53	1000	3600	117	~0.40
2,4-Xylenol/H_2O_2, 1238AL	84	78	1000	4100	519	1.1

Aerosol yields were calculated as the ratio of the mass of OPM collected in the sample to the amount of precursor reacted over the course of the experiment (Equation 1.1). Precursor and oxidant injected to the chamber was irradiated using 115 W Sylvania 350BL black lamps (350 nm, ultraviolet (UV) range, peak intensity). The samples were collected onto 47 mm PTFE PALL Life Sciences (Teflo, 2.0 μm) filters. Precursors were reacted with either O_3 in the presence of NO_x (NO was added to the chamber in the presence of UV light) or $OH^{\bullet}$ (H_2O_2 was introduced to the chamber in the presence of UV light). In the reaction of toluene with NO_x, methyl nitrite was added to stimulate the formation of $OH^{\bullet}$ radical. The concentration of O_3 was monitored using a Dasibi model 1003-AH ozone analyzer and the concentration of NO was monitored using a Teco model 42C external converter and chemiluminescence analysis. After collection, the filters were placed in Petri dishes, wrapped with paraffin film, and sent on ice packs from the University of California Riverside. The samples were stored at ~-4°C for several months until extraction. The final organic mass collected was calculated by assuming a flow rate

of 25 l.p.m. and a density of 1.4 $\mu g/m^3$, and the measurement of average particle diameter and total particle number was monitored by the same custom-built SMPS (a total organic carbon (TOC) analysis was not done). Reaction chamber temperature was kept at 27 ± 1°C, and relative humidity was approximately zero. Occasional background samples collected from the chamber using irradiation of pure air showed particulate formation <1 $\mu g/m^3$.

3. Methods of Analysis

2.3.1 Filter Extraction Procedure

Filter samples were extracted ultrasonically twice for 45 minutes on ice and washed to produce a total of 22 ml extract in 1:1 v/v dichloromethane/methanol. Extracts were stored at ~4°C until further preparation.

2.3.2 Selection of Derivatization Reagent

To select a reagent for use in GC×GC/TOF-MS of PO-OPM samples, the reactions of three reagents with carboxylic acids expected to be in atmospheric samples were compared. The reagents and procedures were chosen by testing for the formation of all derivatives and the best chromatographic characteristics for GC-MS with a set of mono-, di-, and multi-functional carboxylic acid standards. One-dimensional GC-MS was used for these analyses because its operation was less resource-intensive and time-consuming. The sample preparation methods were then applied to the well-studied α–pinene/ozone system and analyzed using GC×GC/TOF-MS. The reagents tested by GC-MS were pentafluorobenzyl bromide (PFBBr), boron trifluoride/*n*-butanol (BF_3/butanol), and *N*,*O*-bis(trimethylsilyl)trifluoroacetamide (BSTFA). The carbonyl-derivatizing reagent pentafluorobenzylhydroxylamine (PFBHA) was also tested to accompany the derivatization of carboxylic groups. After testing, BSTFA and BF_3/butanol were selected for use. More information about this selection is given in Section 1.5.

2.3.3 Derivatization Procedures

A total of 5 ml of each extract was concentrated in 2 ml conical reaction vials under a

stream of cleaned gaseous nitrogen until near dryness, then either butylated using boron trifluoride/n-butanol (BF_3/butanol) or trimethysilylated using bis-(trimethylsilyl)trifluoroacetamide (BSTFA).

Derivatization by BF_3/butanol allows reaction of carboxylic acids to form butyl esters and of aldehydes to form dibutyl acetals. The concentrated extracts were mixed with 150 µL BF_3/butanol and 100 µL hexanes, and the reaction was allowed to proceed 1 hour at 65°C. The products were extracted into 500 µL hexane by vortexing 20 sec with 1.5 ml sodium chloride saturated water, then again with 1 ml de-ionized water. The remaining organic solution was dried over ~0.5 g sodium sulfate and washed into a total of 1 ml hexane. The solvent was removed under a stream of cleaned gaseous nitrogen and the products reconstituted into 300 µL 1:1 v/v dichloromethane/hexane. A more detailed procedure can be found in the Standard Operating Procedures (Appendix A).

Derivatization with BSTFA allows reaction of carboxylic acids to form trimethylsilyl esters and of alcohols to form trimethylsilyl ethers. The concentrated extracts were reacted with 500 µL dichloromethane and 20 µL BSTFA for 1 hour at 65°C. Products were dried under a stream of cleaned gaseous nitrogen, and reconstituted into 300 µL dichloromethane.

2.3.3.1 Temperature Stability Tests of Derivatives

The injection and analysis by GC-MS of many samples by an auto-sampler requires that the sample vials be allowed to wait in the auto-sampler for several hours (without cooling

unless a coolant is used in the autosampler). The temperature stability of butyl and TMS esters was tested after the solutions were allowed to sit for 18 hours on ice (the ice pack was determined to change from -9°C to 7°C over seven hours). If water was added for reaction of excess BSTFA, the TMS esters were preserved over 18 hours. However, in a later experiment neglecting the quenching step (this step is likely to degrade the derivatives somewhat), the TMS esters were observed to degrade after only ~eight hours. The quenching step was not used to perform the reactions for which the results are shown here, so care was taken to minimize the time that reacted standards or samples were allowed to sit in the auto-sampler before and after analysis.

2.3.4 GC×GC/TOF-MS and GC-MS Methods

The GC-MS methods used for butylated and BSTFA derivatized samples were the same, with the exception of the temperature programs. Each program was tailored to provide a slower rate of temperature increase for the period of time within the chromatogram in which the derivatives eluted. The temperature programs used for 1D and GC×GC separations of butylated solutions are shown in Table 2.3.

Table 2.3. Temperature program used for 1D-GC-MS and GC×GC/TOF-MS for the analysis of butylated α–pinene ozonolysis products. For the second dimension, the temperature program was identical, but ten degrees higher throughout.

Rate (°C/min)	Temperature (°C)	Hold Time (min)
---	45	4
10	120	0
6	204	0
10	300	0

Only a slight change was made from the temperature program used for 1D-GC and GC×GC analyses of butylated α–pinene ozonolysis products to those of BSTFA

derivatized products. The BSTFA derivatized calibration standards showed generally lower primary retention times, so that the slower temperature rate of increase was begun at a lower temperature to allow the best separation of all trimethylsilyl derivatives (Table 2.4).

Table 2.4. Temperature program used for 1D-GC-MS and GC×GC/TOF-MS for BSTFA derivatized and underivatized α–pinene ozonolysis product analysis. For the second dimension, the temperature program was identical, but ten degrees higher throughout. This program was also used to collect two-dimensional data from the GC×GC-FID, including derivatization efficiency and GCxGC-FID quantifiable TOC mass analyses.

Rate (°C/min)	Temperature (°C)	Hold Time (min)
---	45	4
10	90	0
6	204	0
10	299	0

The temperature programs used for the analyses of derivatized anthropogenic aromatic hydrocarbon oxidation products are given below; the programs are slightly different from those used for α–pinene ozonolysis product analyses. The temperature program for BSTFA derivatized anthropogenic aromatic hydrocarbon oxidation product analysis was set to reach a final temperature 10°C higher than the program for butylated products (Table 2.5 and 2.6).

Table 2.5. Temperature program used for butylated anthropogenic, aromatic oxidation product analysis 1D-GC-MS and GC×GC/TOF-MS). For the second dimension, the temperature program was identical, but ten degrees higher throughout.

Rate (°C/min)	Temperature (°C)	Hold Time (min)
---	45	4
5	140	0
10	300	1

Table 2.6. Temperature program used for BSTFA derivatized anthropogenic, aromatic oxidation product analysis (1D-GC-MS and GC×GC/TOF-MS). For the second dimension, the temperature program was identical, but ten degrees higher throughout.

Rate (°C/min)	Temperature (°C)	Hold Time (min)
---	45	4
5	150	0
10	310	1

Other parameters of the GC and MS methods were chosen to optimize the signal of the derivatived α-pinene ozonolysis product calibration standards. Similar methods were used in the 1D-GC and GC×GC and MS systems, but parameters specific to the GC×GC system such as modulation, spectral collection frequency, are listed separately here.

Instrumental Method Parameters of GC and MS used for 1D GC-MS analyses:
Injection Volume: 1 µL
Mode: Splitless
Purge Flow to Split Vent: 50 mL/minute at 1.00 minute
Injector Temperature: 220°C
Column Flow: 0.93162 mL/minute
Carrier Gas: Helium
Solvent Delay: 300 sec
Electron Multiplier Voltage: 1294 V (absolute)
Electron Energy: 69.92 eV
Mass Scanning Range: 34.0 – 500.0 m/z
Mass Spectrometer Source Temperature: 230°C
Mass Spectrometer Quadrupole Temperature: 150°C

Most parameters were designed to replicate successful published derivatization procedures. Larger volume injections and programmed injection temperatures have been used in other studies, but were not needed here because a higher mass was collected onto the filter samples analyzed, and the derivatives were anticipated to be of high enough volatilities to be sufficiently volatilized from the injection liner at 220°C and thermally stable enough to avoid pyrolysis. Splitless injections were made in order to show low concentration compounds in the samples; some low split ratios (7:1 and 10:1) were initially tested.

Prior to analysis using GC×GC/TOF-MS, one-dimensional trial analyses of derivatized calibration standards were made to show the retention times, separation, and peak shapes of the α-pinene ozonolysis product calibration standards. Based on the responses of these compounds, the temperature programs and parameters of the GC and MS methods were set.

Instrumental Method Parameters of GC and MS used for Derivatized and Underivatized GC×GC/TOF-MS analyses:
Injection Volume: 1 µL
Mode: Splitless
Purge Flow to Split Vent: 100 mL/min at 60 sec
Injector Temperature: 220°C
Column Flow: 1.20 mL/min (constant flow)
Gas saver: 15 mL/min at 5 min
Carrier Gas: Helium
Solvent Delay: 484 sec
Transfer Line Temperature: 260°C
Modulator Temperature Offset (°C, relative to the GC oven temperature): +20°C
Modulation period: 4.00 sec
Hot Pulse Time: 0.90 sec
Cool Time Between Stages: 1.10 sec
Electron Multiplier Voltage: 1500 V
Electron Energy: -70 eV
Acquisition Rate: 150 spectra/second
Mass Scanning Range: 34-500 a.m.u.
Mass Spectrometer Source Temperature: 200°C

Parameters chosen for GC×GC/TOF-MS analyses were based on prior methods used on the instrument for other studies. The modulation period provided a sufficient number of data points per peak (2-5 points per peak were found) and the collection of 150 spectra/second allowed the recognition of several calibration standards that were close in retention time or co-eluting.

The effective carbon number (ECN) measurements to find derivatization efficiency and GC×GC-FID quantifiable total organic carbon mass in underivatized extracts were analyzed using GC×GC FID. Initially, both measurements were made using a one-dimensional method in which the sample was passed through the second column, but the modulator was not used. The separation was too low, however, for sufficient calculation of the peak area of many calibration standards. A two dimensional separation was then attempted with a shorter temperature program; this temperature program was used in the

determination of derivatization efficiency of butylated calibration standards (**Error! Reference source not found.**).

Table 2.7. Original GC×GC-FID first dimension (primary oven) temperature program used in the analysis of total GC-detectable organic carbon and derivatization efficiencies. The temperature program of the second dimension was identical, but ten degrees higher throughout. This program was used in the determination of derivatization efficiency of butylated calibration standards.

Rate (°C/min)	Temperature (°C)	Hold Time (min)
---	45	2
15	295	5

The separation is both dimensions, however, was insufficient to determine the derivatization efficiencies of the BSTFA derivatized calibration standards (degradation of the derivatives was also noted), and an improved temperature program was used (Table 2.8).

Table 2.8. Improved GC×GC-FID first dimension (primary oven) temperature program used in the analysis of total GC-detectable organic carbon of α–pinene ozonolysis products and derivatization efficiencies for BSTFA derivatized calibration standards. For the second dimension, the temperature program was identical, but ten degrees higher throughout. This program was also used to collect two-dimensional data from the GCxGC FID, including derivatization efficiency and GCxGC-FID quantifiable TOC mass analyses.

Rate (°C/min)	Temperature (°C)	Hold Time (min)
---	45	4
10	90	0
6	204	0
10	299	0

This temperature program was identical to that used for the GC×GC/TOF-MS analyses, and allowed the direct correlation of GC×GC/TOF-MS retention times to those of GC×GC-FID. This was of particular utility because the recognition of each peak of interest can be difficult using FID, and in particular when many peaks are present in a chromatogram (which is true for derivatized spectra in which reagent and byproduct peaks are present). The column set was also changed to the set used for GC×GC/TOF-

MS analyses, which also allowed increased separation (the column used in the original FID setup was only 10 m in length). The parameters of all methods are shown below. Details of the columns used are given in Section 2.1c.

Instrumental Method Parameters for GC×GC-FID for BSTFA derivatized Samples:
Injection Volume: 2 µL
Mode: Split
Split Ratio: 5:1
Injector Temperature: 250°C
Column Flow: 1.20 mL/minute
Carrier Gas: Helium
Solvent Delay: 484 seconds
Modulator Temperature Offset: 15°C
Modulation Period: 5 seconds
Hot Pulse Time: 1.10 seconds
Cool Time Between Stages: 1.40 seconds
Data Collection Rate: 180 Hz
FID Temperature: 250°C
Makeup Gas: Nitrogen, 10 mL/minute
Hydrogen Flow: 40 mL/minute
Air Flow: 450 mL/minute

The underivatized samples were analyzed using the BSTFA derivatized GCxGC FID method shown above, but using a solvent delay of 180 seconds. The longer solvent delay used for BSTFA derivatized sample eliminated high concentration reagent and byproducts from the chromatogram. Note that a 2µL injection volume was used because this decreased the effect of possible variations introduced during manual injections.

4. Calibration and Quantitation

2.4.1 Standard Solutions

Stock solutions were prepared at high concentrations (500-1000 ng/μL) by delivering neat solid and liquid standards to volumetric flasks using a clean microspatula and syringes, respectively. All stock solutions were stored in volumetric flasks wrapped with paraffin film at ~-4°C. Diluted solutions (5-500 ng/μL) were prepared and stored in crimp-top 2 ml amber vials at ~4°C. Caps were replaced after being punctured by a syringe.

2.4.2 Calibration Standards

For external calibration, thirteen standards were chosen because they were anticipated to be present in, or structurally similar to, the oxidation products of α-pinene. The characteristics of the gas chromatograph and mass spectrometer signals for the trimethylsilyl derivatives of these standard compounds are tabulated in Table 2.9.

Table 2.9. Trimethylsilyl derivatives of calibration standards used in quantitative and semi-quantitative external calibration of oxidation products. Retention times listed are averaged over all calibration points. Internal standards were chosen based upon proximity in retention time. The target ion or sum or ions used in quantitation in the 2D results is listed first under characteristic ions for each standard.

Common Name/Systematic Name	Approximate Retention Times (2D primary, secondary; 1D, min)	Characteristic Ions (m/z): Target; Qualifiers; Molecular Ion	Internal Standard Compound Used
Lactic Acid/2-hydroxy-Propanoic Acid	831.9,1.00,12.93	147+73; 117, 45; 234	Naphthalene-d_8
2-hydroxy-3-methyl-Butyric Acid	979.9,1.33,12.72	145+73; 147, 75; 262	Naphthalene-d_8
Malonic Acid/Propanedioic Acid	1023.9, 1.12,13.57	147; 73; 248	Naphthalene-d_8
methyl-Malonic Acid/methyl-Propanedioic Acid	1023.9, 1.12,13.80	147; 73, 148, 75; 262	Naphthalene-d_8
Glutaric Acid/Pentanedioic Acid	1439.9, 0.78,19.85	147, 73, 75, 55; 276	Naphthalene-d_8

Common Name/Systematic Name	Approximate Retention Times (2D primary, secondary; 1D, min)	Characteristic Ions (m/z): Target; Qualifiers; Molecular Ion	Internal Standard Compound Used
Adipic Acid/Hexanedioic Acid	1399.9, 1.23, 20.01	111, 75, 73, 147; 290	Naphthalene-d_8
Salicylic Acid/2-hydroxy-Benzoic Acid	1423.9, 1.4, 20.10	267+135; 73, 268; 282	Naphthalene-d_8
cis-Pinonic Acid/ [(1R,3R)-3-acetyl-2,2-dimethylcyclobutyl]acetic acid	1439.9, 1.53, 20.38	73+121+83; 75, 171; 290	Naphthalene-d_8
Lauric Acid/Dodecanoic Acid	1575.9,1.27, 23.008	257+73; 75, 117; 272	Phenanthrene-d_{10}

While the derivatization reagents (BF_3/butanol and BSTFA) were introduced to solutions of all standard compounds, only some calibration standards were detected because of the selectivity of the reagents. For example, the hydroxy-acid lactic acid was only derivatized using trimethylsilylation by BSTFA. The derivative products of the calibration standards used in the BF_3/*n*-butanol butyl reactions are tabulated in Table 2.10.

Table 2.10. Butyl derivatives of calibration standards used in quantitative and semi-quantitative external calibration of oxidation products. Retention times listed are averaged over all calibration points. Internal standards were chosen based upon proximity in retention time. The target ion used in quantitation in the 1D results is listed first as a characteristic ion for each standard.

Common Name/Systematic Name	Approximate Retention Times (2D primary, secondary; 1D, min)	Characteristic Ions (m/z): Target; Qualifier(s); Molecular Ion	Internal Standard Compound Used
Oxalic Acid/Ethanedioic Acid	1131.9, 1.37,15.39	147; 103, 57; 202	Naphthalene-d_8
Malonic Acid/Propanedioic Acid	1227.9, 1.34, 16.82	105; 87, 143, 161 216	Naphthalene-d_8
methyl-Malonic Acid/methyl-Propanedioic Acid	1247.9, 1.3, 17.20	101; 74, 119, 157; 230	Naphthalene-d_8
Salicylic Acid/2-hydroxy-Benzoic Acid	1279.9, 1.43, 18.28	120; 92, 138, 194; 194	Naphthalene-d_8
Glyoxylic Acid/2-oxo-Ethanoic Acid	1403.9, 1.21, 19.87	159; 91, 103, 117; 260	Naphthalene-d_8
Glutaric Acid/Pentanedioic Acid	1471.9, 1.41, 22.045	115; 87, 142, 189; 244	Naphthalene-d_8

Common Name/Systematic Name	Approximate Retention Times (2D primary, secondary; 1D, min)	Characteristic Ions (m/z): Target; Qualifier(s); Molecular Ion	Internal Standard Compound Used
cis-Pinonic Acid/ [(1*R*,3*R*)-3-acetyl-2,2-dimethylcyclobutyl]acetic acid	1479.9, 1.5, 22.26	125; 83, 98, 167; 226	Naphthalene-d_8
Adipic Acid/Hexanedioic Acid	1583.9, 1.47, 23.44	185; 129, 111, 87; 258	Phenanthrene-d_{10}
Lauric Acid/Dodecanoic Acid	1603.9, 1.45, 25.13	201; 57, 105, 73; 256	Phenanthrene-d_{10}
Glyoxal/Ethanedial	1603.9, 1.25, 25.36	159; 57, 103, 133; 318	Phenanthrene-d_{10}

In some cases, the underivatized compounds were also observed in derivatized standard solutions. The retention times and characteristic ions used for quantification and identification of these underivatized compounds are given in

Table **2.11**.

Table 2.11. Underivatized calibration standards used in quantitative and semi-quantitative external calibration of oxidation products (compounds identified in underivatized samples were not quantified). Retention times listed are averaged over all calibration points.

Common Name/Systematic Name	Approximate Retention Times (2D primary, secondary; 1D, min)	Characteristic Ions (m/z): Target, Qualifier Ion; Molecular Ion
Lactic Acid/2-hydroxy-Propanoic Acid	*Not found*	*Not found*
2-hydroxy-3-methyl-Butyric Acid	*Not found*	*Not found*
Malonic Acid/Propanedioic Acid	*Not found*	*Not found*
methyl-Malonic Acid/methyl-Propanedioic Acid	*Not found*	*Not found*
Glutaric Acid/Pentanedioic Acid	*Not found*	*Not found*
Adipic Acid/Hexanedioic Acid	*Not found*	*Not found*
Salicylic Acid/2-hydroxy-Benzoic Acid	*Not found*	*Not found*
cis-Pinonic Acid/ [(1R,3R)-3-acetyl-2,2-dimethylcyclobutyl]acetic acid	1341, 2.02; 8.22	83; 125; 166

Common Name/Systematic Name	Approximate Retention Times (2D primary, secondary; 1D, min)	Characteristic Ions (m/z): Target, Qualifier Ion; Molecular Ion
Lauric Acid/Dodecanoic Acid	1463.9, 1.47; *not Found*	60; 73, 129; 200

Stock solutions containing 1-5 calibration standards at 1000 ng/μL were prepared in dichloromethane (DCM), methanol, or methyl-*tert*-butyl-ether (MTBE), depending upon solubilities (Table 2.12). In particular, the solubility of succinic-d_4 acid was low in DCM, acetonitrile, and MTBE. The latter solvent was used, however, in large quantity to dissolve this acid (Table 2.12).

Table 2.12. The stock solutions of calibration standards are shown. The ratio of solvents used was based upon solubility of compounds in solution.

Calibration Standard Stock Solution	Standard Compounds	Solvent(s) Used	Final Volume, Concentration
Di-acid Solution	Adipic acid, glutaric acid, malonic acid, oxalic acid	3:7 MTBE:DCM	50 ml, 1000 ng/μL
Multi-acid Solution A	Lauric acid, methylmalonic acid, salicylic acid, *cis*-pinonic acid, lactic acid, citric acid	17:8 MTBE:DCM	25 ml, 2000 ng/μL
Multi-acid Solution B	Glyoxylic acid, 2-hydroxy-3-methyl-butyric acid	DCM	10 ml, 1000 ng/μL
Recovery Solution	Succinic-d_4 acid, ketopinic acid	4:1 MTBE:DCM	50 ml, 1000 ng/μL
Glyoxal	Glyoxal	Methanol	10 ml, 1000 ng/μL

One solution containing all calibration standards was diluted from each stock solution into dichloromethane. The concentration of this diluted solution was such that <1 ml of the solution could be delivered to each reaction vial in order to generate the highest and lowest concentrations in the calibration curve (0.5 ng/μL and 20 ng/μL). Standard concentrations in all stock solutions were within +/-10% of the value shown (Table 2.13).

Table 2.13. Actual concentrations of calibration standards used in external calibration. Values are given as calculated from actual masses or volumes of standard compounds diluted to each calibration level. See Table 3 for information about each calibration solution.

Common Name/Systematic Name	Actual Conc. in 0.5 ng/µL Solution	Actual Conc. in 1.0 ng/µL Solution	Actual Conc. in 5.0 ng/µL Solution	Actual Conc. in 10.0 ng/µL Solution	Actual Conc. in 20.0 ng/µL Solution
Oxalic Acid/Ethanedioic Acid	0.505	1.01	5.05	10.1	20.2
Malonic Acid/Propanedioic Acid	0.503	1.01	5.03	10.1	20.1
methyl-Malonic Acid/methyl-Propanedioic Acid	0.502	1.00	5.02	10.0	20.1
Lactic Acid/2-hydroxy-Propanoic Acid	0.498	0.996	4.98	9.96	19.9
2-hydroxy-3-methyl-Butyric Acid	0.489	0.978	4.89	9.78	19.6
Salicylic Acid/2-hydroxy-Benzoic Acid	0.499	0.998	4.99	9.98	20.0
Glyoxylic Acid/2-oxo-Ethanoic Acid	0.485	0.969	4.85	9.69	19.4
Glutaric Acid/Pentanedioic Acid	0.502	1.00	5.02	10.0	20.1
cis-Pinonic Acid/ [(1*R*,3*R*)-3-acetyl-2,2-dimethylcyclobutyl]acetic acid	0.501	1.00	5.01	10.0	20.1
Adipic Acid/Hexanedioic Acid	0.506	1.01	5.06	10.1	20.2
Lauric Acid/Dodecanoic Acid	0.506	1.01	5.06	10.1	20.2
Glyoxal/Ethanedial	0.506	1.01	5.06	10.1	20.3

The concentration range used was designed to be just above the potential limit of detection and also above the concentration expected for oxidation products in the

atmospheric samples. Citric acid was originally included in the list of standard compounds, but was not observed using either derivatization reaction, and a literature observation of the TBDMS derivative of citric acid (Kim, *et al.,* 1989, using MTBSTFA) detailed a procedure quite dissimilar to that used, including a reaction time of up to eight hours (in contrast to the one hour reaction time used here).

2.4.3 Recovery Standard and Surrogate Recovery Standards for Extraction Efficiency

In order to assess the efficiency of each α-pinene ozonolysis sample filter extraction, a recovery standard and two surrogate recovery standards were used. A 1000 ng/μL stock solution of eicosane-d_{42} was prepared in DCM and a 5 ng/μL secondary dilution was prepared in order to externally calibration the compound. The final concentration of 7.64 ng/μL in each sample was delivered to each filter by spiking with 10 μL of the 1000 ng/μL solution. Because the concentration of the eicosane-d_{42} in each sample chromatogram was needed to adjust for any losses during the procedure, the compound was externally calibrated along with the calibration standards. The retention time was estimated to be 30.865 minutes in the primary dimension and 1.19 seconds in the second dimension. The target ion used for quantitation was m/z 66, and the qualifier ions used for identification were m/z 50, 82, and 98.

Two carboxylic acid compounds, *(1S)-(+)*-ketopinic acid (ketopinic acid) and succinic-d_4 acid, can be assumed to be absent from atmospheric aerosol samples and so were used as surrogate compounds to assess extraction recovery of carboxylic acids. A standard

solution at 500 ng/μL was prepared in 4:1 MTBE:DCM and diluted to 5 ng/μL for external calibration. The final concentration of 9.87 ng/μL for succinic-d_4 acid and for 9.46 ng/μL for ketopinic acid in each sample was reached by spiking each filter sample with 25 μL of the 500 ng/μL solution. This solution was not spiked onto all blank filters so that any breakdown could be observed of these compounds or byproducts formed by the reaction.

The mass spectral properties of the surrogate recovery compounds were compiled so that they could be easily identified in each chromatogram. The derivatized and underivatized signals are tabulated below (Table 2.14).

Table 2.14. Characteristics of BSTFA derivatized, butylated, and underivatized surrogate recovery standards. Ions are listed in the following order: target (used in quantification); qualifiers; and molecular ion. Underivatized succinic-d_4 acid was not found in the chromatograms without derivatization; ions from the spectrum in the NIST library are listed in this table.

Common Name/Systematic Name	Approximate Retention Times (GC×GC primary, secondary; 1D-GC, min)	Characteristic Ions (m/z): Target; Qualifiers, Molecular Ion	Internal Standard Compound Used
Trimethylsilyl Derivatives			
Succinic-d_4 Acid/Butanedioic-d_4 Acid	1151.9, 1.02; 15.84	147; 73, 76, 148; 266	Naphthalene-d_8
(1S)-(+)-Ketopinic Acid/7,7-dimethyl-2-oxo-Bicyclo[2,2,1]heptane-1-Carboxylic Acid	1419.9, 1.68; 19.85	95; 73, 197, 239; 254	Phenanthrene-d_{10}
Butyl Derivatives			
Succinic-d_4 Acid/Butanedioic-d_4 Acid	1363.9, 1.36; 19.92	105; 161, 123, 179; 234	Naphthalene-d_8
(1S)-(+)-Ketopinic Acid/7,7-dimethyl-2-oxo-Bicyclo[2,2,1]heptane-1-Carboxylic Acid	1491.9, 1.62; 22.14	165; 67, 109, 165; 238	Phenanthrene-d_{10}
Underivatized			
Succinic-d_4 Acid/Butanedioic-d_4 Acid	*Not found*	100; 55, 74; 118	Naphthalene-d_8

Common Name/Systematic Name	**Approximate Retention Times (GC×GC primary, secondary; 1D-GC, min)**	**Characteristic Ions (m/z): Target; Qualifiers, Molecular Ion**	**Internal Standard Compound Used**
(1S)-(+)-Ketopinic Acid/7,7-dimethyl-2-oxo-Bicyclo[2,2,1]heptane-1-Carboxylic Acid	1379.9, 2.17; 19.13	95; 67, 112, 138, 154; 182	Phenanthrene-d_{10}

Only one instance of these surrogate standards was not located in the chromatograms: succinic-d_4 acid was not located without derivatization, which is expected because of its high polarity and therefore interaction with active silanol sites within the GC column. All derivatives were identified using predicted ions, shown here (Table 2.14), and the underivatized *(1S)-(+)*-ketopinic acid was identified by a library mass spectrum.

2.4.4 Internal Standards

Four polycyclic aromatic hydrocarbons were used to assess the efficiency of the injection and GC analysis: toluene-d_8, naphthalene-d_{10}, phenanthrene-d_{10}, and pyrene-d_{10} (Figure 2.1).

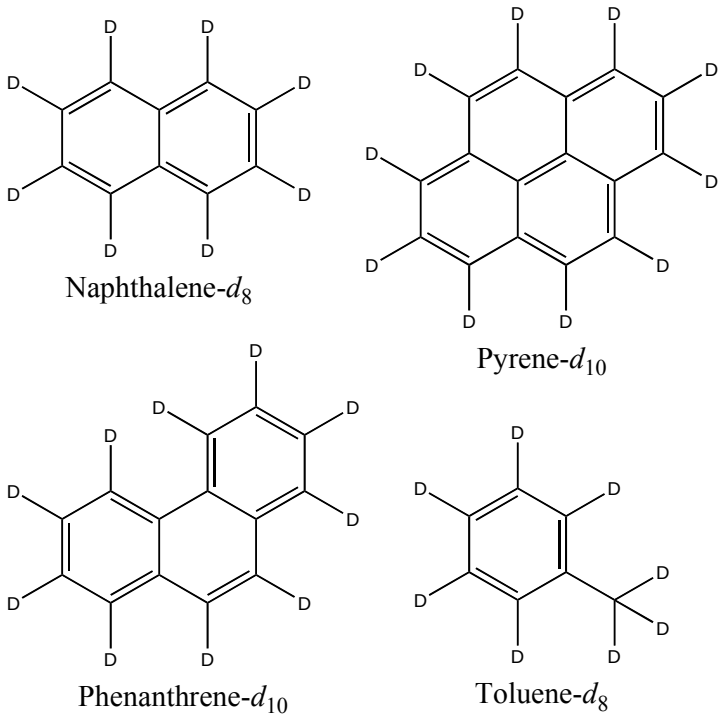

Figure 2.1. Perdeuterated polycyclic aromatic hydrocarbons (PAHs) used for internal calibration. The elution order was: toluene-d_8, naphthalene-d_8, phenanthrene-d_{10}, and pyrene-d_{10}.

A stock solution of 300 ng/μL PAH internal standards was made in DCM. A 3 μL aliquot of this solution was added to each sample just before capping of the auto-sampling vial, giving a final concentration of 3 ng/μL (this was used for 1D-GC-MS, GC×GC/TOF-MS and GC×GC-FID analyses). Note that toluene-d_8 eluted before the end of the solvent delay (when no signal was collected, in order to avoid damaging the mass spectrometer ion source) or during the solvent front (the large band of solvent peaks observed at the

beginning of the chromatogram) in most analyses. It was not used for calibration, and its retention time and response varied more greatly than did those of the other three PAH internal standards. Similarly, pyrene-d_{10} was not used in calibration because the peak areas of phenanthrene-d_{10} were more reproducible and the retention time of phenanthrene-d_{10} was close to late eluting standard compounds (derivatized). The retention times and ions used for quantitation and identification within the chromatogram are listed in Table 2.15.

Table 2.15. Characteristics used to identify each of the internal standards within the chromatograms and mass spectra. Toluene-d_8 was not found in some chromatograms due to the volatility of the compound and the overlap of the retention time with the solvent delay.

Common Name	**Actual Concentration (ng/µL)**	**Approximate Retention Times (GC×GC Primary, Secondary; 1D-GC, min)**	**Characteristic Ions (m/z): Target, Qualifier**
Toluene-d_8	3.016	479.9, 1.10, *not found*	98, 99, 70
Naphthalene-d_8	3.048	1011.9, 1.82,12.93	136, 108, 137
Phenanthrene-d_{10}	2.968	1739.9, 2.73, 25.17	188, 189, 184, 187
Pyrene-d_{10}	3.036	2035.8, 2.34, 31.766	212, 75

5. Quantitation

2.5.1 Calibration and Response Factor Calculation to Characterize α–Pinene Ozonolysis Products

Five external calibration points were produced using two solutions at concentrations of 0.5 ng/μL, 1.0 ng/μL, 5.0 ng/μL, 10 ng/μL, and 20 ng/μL. Two to three quantitation ions were identified in each mass spectrum and used to identify the peaks of each calibration standard. For quantitation, the peak areas of one or more high-abundance target ion(s) was tabulated for each standard at increasing concentration, and plotted relative to the peak areas of the nearest internal standard (see Section 2.4.d). The target ions used and their relative abundances are listed in Table 2.15.

The linearity of each calibration curve was checked using the value of the correlation coefficient, r^2. Response factors were calculated for each calibration standard relative to the internal standard nearest in retention time using the following equation:

$$\mathrm{RF} = \frac{A_i \times C_{\mathrm{is}}}{A_{\mathrm{is}} \times C_i} \qquad (2.1)$$

The RF was used to quantify the response of analytes in the sample chromatograms using Eqn. (2.2):

$$C_i = \frac{A_i \times C_{\mathrm{is}}}{A_{is} \times \mathrm{RF}} \qquad (2.2)$$

Each compound was adjusted for extraction efficiency using the recovery of the internal recovery standard, derivatization efficiency using the average derivatization efficiency

measurement (see Section 2.5.b) for the standard compound or a calibration standard with a similar structure, the volume of extract used (see Section 2.3), and the proportional amount of the compound that was removed during total organic carbon analysis.

It should be noted that the uncertainty is high for concentrations estimated using the response of surrogate standards (rather than directly calculated using an authentic standard of the compound itself). This uncertainty is primarily from the differential response of the surrogate standard in external calibration (due to losses and differential instrumental response) and unknown differential derivatization efficiency.

2.5.2 Derivatization Efficiency

In order to show the efficiency with which chemical derivatizations could be carried out using the procedures followed, the efficiency of the derivatization reactions (DE_i) were measured for the standards used in external calibration. The effective carbon number (ECN) method for DE_i determination reported in Scanlon & Willis, 1985 and more recently used by Docherty & Ziemann, 2001, was used. This method utilizes mass-sensitive detection of "active" carbon atoms by GC×GC-FID; DE_i is subsequently calculated as the ratio between the theoretical response, ECN_{calc}, and that measured in practice, ECN_i (Eqns. 2.3 and 2.4).

$$\mathrm{ECN}_i = \frac{\mathrm{ECN}_{\mathrm{ref}} \times A_i \times m_{\mathrm{ref}} \times \mathrm{MW}_i}{A_{\mathrm{ref}} \times m_i \times \mathrm{MW}_{\mathrm{ref}}} \qquad (2.3)$$

$$\mathrm{DE}_i = \frac{\mathrm{ECN}_i}{\mathrm{ECN}_{\mathrm{calc}}} \qquad (2.4)$$

The subscripts ref and *i* represent the reference and target compounds, respectively, ECN_{ref} is the calculated ECN of a reference *n*-alkane, *A* is the peak area (FID response), *m* is the mass (g) of the compound injected, and MW is the molecular weight (g mol^{-1}).

Derivatization efficiency calculations were made using a series of alkanes as reference compounds (to find ECN_{ref}) that were introduced as the DRO Mix (Tennessee/Mississippi; Restek, Bellefont, PA). The effective carbon numbers of these compounds are tabulated in Table 2.16 (Scanlon & Willis, 1985).

Table 2.16. Reference hydrocarbons used in the calculation of the derivatization efficiency using the effective carbon number method.

Standard Name	ECN_{ref}	MW_{ref} (a.m.u.)
n-Decane	10	142.3
n-Undecane	11	156.3
n-Dodecane	12	170.3
n-Tridecane	13	184.4
n-Tetradecane	14	198.4
n-Pentadecane	15	212.4
n-Hexadecane	16	226.4
n-Heptadecane	17	240.5
n-Octadecane	18	254.5
n-Nonadecane	19	268.5
n-Eicosane	20	282.6
n-Heneicosane	21	296.6
n-Docosane	22	310.6
n-Tricosane	23	324.6
n-Tetracosane	24	338.7
n-Pentacosane	25	352.7

The value of ECN_{calc} for each calibration standard was calculated by summing the contributions of the carbon atoms in the target compound and functional groups added by derivatization (Appendix D, Table A; an extensive list is given in Sternberg, *et al.*, 1962). The response of phenanthrene-d_{10} was used to calculate the ECN_i for each reference *n*-alkane. Holm (1999) showed that the ECN_i of non-methane hydrocarbons are equivalent

for non-deuterated and per-deuterated versions. Simplified values contributing to ECN_{calc}, were used in this work to calculate ECN_{calc} for butyl and trimethylsilyl derivatives of the calibration standards. The values of ECN_{calc} and molecular weights (MW_i) of all calibration standards are tabulated in Table C, Appendix D.

GC×GC-FID (see Section 2.1.c) was used to find the mass-sensitive response peak areas so that the ECN_i could be calculated for each calibration standard. The derivatization efficiencies were measured at each concentration used in the external calibration for analysis of GC×GC/TOF-MS data (see Section 2.1.c) to show any variation of the derivatization efficiency with standard concentration. The alkanes used as reference compounds were identified in chromatograms containing the calibration standards by comparing a GC×GC-FID chromatogram of only the alkane mixture.

GC×GC-FID analyses to find all measured butyl DE_i values were carried out on a short primary column (Section 2.3.4) and using a rapid temperature program (Table 2.3) to allow the most efficient use of liquid nitrogen. The integration of distinct peaks was possible, but the separation afforded by this temperature program was not ideal. This low separation was exemplified by the butyl derivatives of cis-pinonic, ketopinic, and glutaric acids (Figure 2.2).

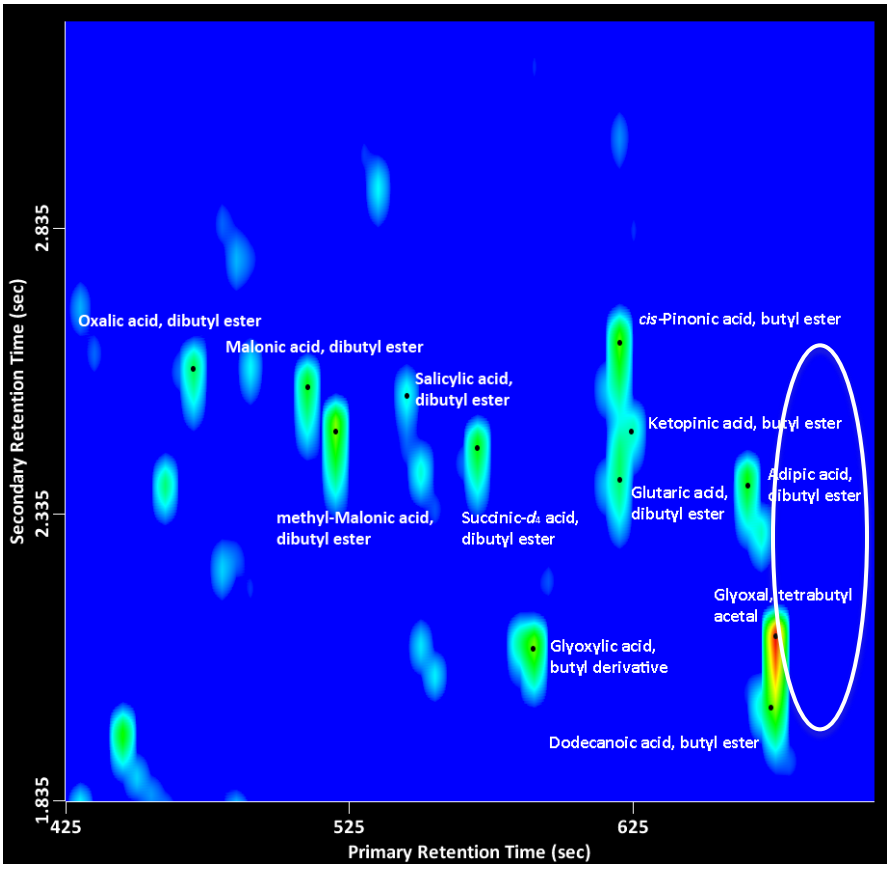

Figure 2.2. The GC×GC-FID quantifications of derivatized acids were challenging using the shorter secondary column and faster temperature program (used in butyl analyses) because the separation between peaks was low. This was shown for several groupings of derivatives, but in particular the butyl derivatives of *cis*-pinonic, ketopinic, and glutaric acids. This chromatogram (zoomed) shows the highest concentration (20 ng/µL) used in these analyses and the external calibration on GC×GC/TOF-MS.

Analysis using the short secondary column and fast temperature program caused the separation between several derivatized acid standards to be low; however, peak area integrations were made for butyl derivatives based on visual inspection of the peaks.

Trimethylsilyl DE_i values could not be accurately determined using the GC conditions used for analysis of butyl DE_i (Figure 2.3).

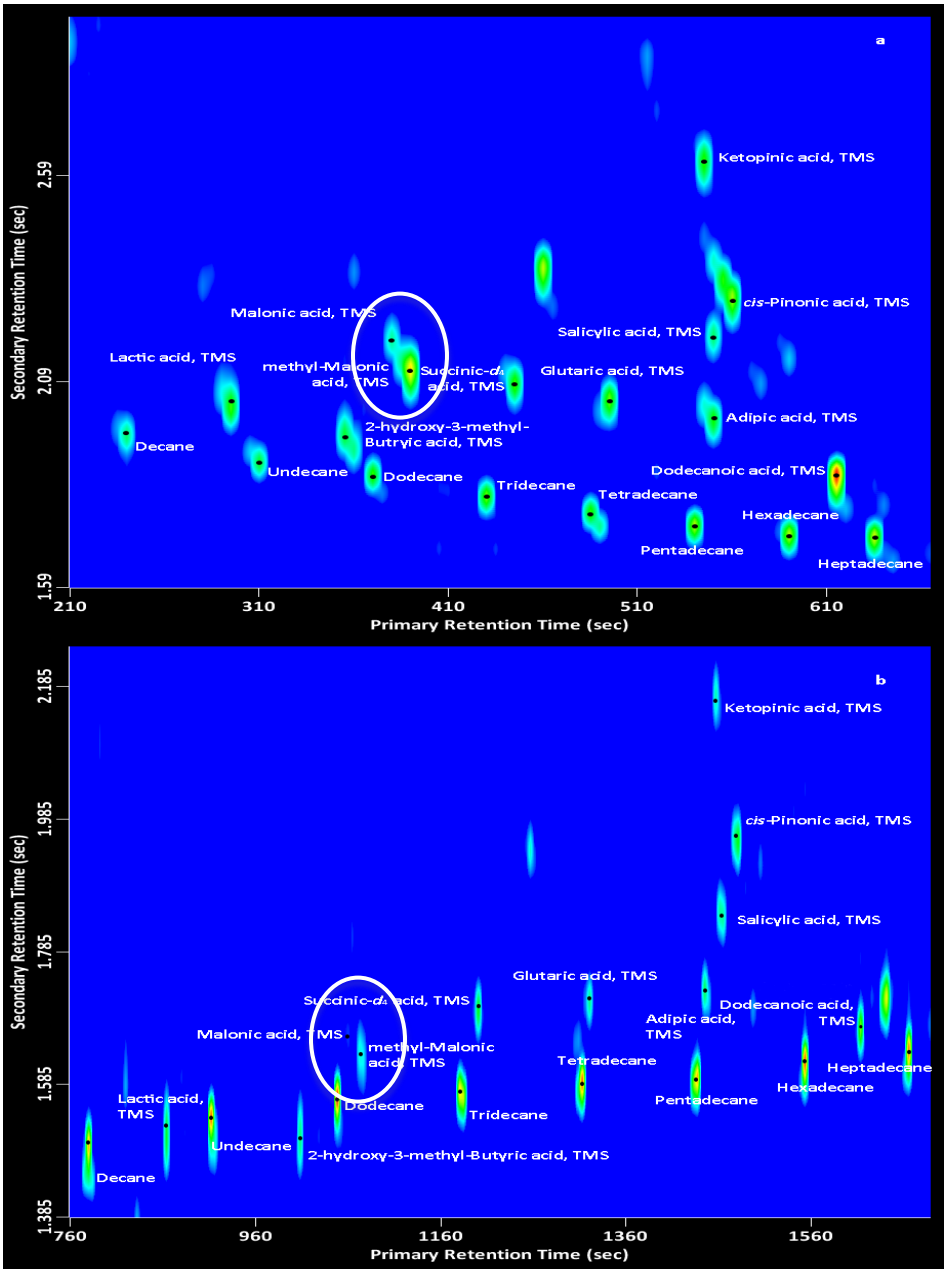

Figure 2.3. Separations of BSTFA derivatized standards by GC×GC-FID using the original, rapid temperature program [chromatogram (a)]; malonic and methyl malonic derivatives are circled to show in particular the low separation of these two standards. The distinction of many peaks in chromatogram (a) as concurrent slices of one eluting component versus as several different components could not be made. The temperature program used in chromatogram (b) was slower and the secondary column was longer to allow complete separation (malonic and methyl-malonic derivatives are again circled).

The separation between trimethylsilyl malonic and methyl-malonic esters was particularly poor. Lower abundance and clearer peaks for methyl-malonic and malonic acids were present in chromatograms collected using a new secondary column and temperature program. The conditions used to collect the data for the trimethylsilyl DE_i values were chosen to be similar to those used for GC×GC/TOF-MS analysis (Table 2.8).

The results of four of five initial GC×GC-FID analyses for the calculation of trimethylsilyl DE_i showed degradation of the trimethylsilyl derivatives, despite re-capping and refrigeration at ~-4°C in sealed plastic bags within three hours of injection to the gas chromatograph. Freshly derivatized calibration standards were prepared and analyzed using the new gas chromatograph settings (Section 2.1.c, Table 2.8).

6. Blank Analyses

2.6.1 Method Blanks

Method blanks with and without derivatization (using both derivatization reagents) were analyzed prior to calibration and sample analyses. All compounds in these chromatograms were tabulated as byproducts or impurities and eliminated from sample chromatogram analyte lists. In order to minimize the presence of these compounds, glassware and syringes were cleaned well prior to use (Appendix A, Section 1) and septa used in reaction vials and crimp caps used to top the auto-sampling vials were not re-used.

2.6.2 Solvent Blanks

To eliminate the filters or extraction process as the source of any impurities in the sample, solvent blanks without extraction were analyzed. These consisted of derivatized or underivatized concentrated solvent (5 ml). The 1D-GC analysis of a solvent blank prior to derivatization of actual samples was also used to show whether any contaminants were present in the solvent or reagent.

2.6.3 Travel Blanks

During the collection of the oxidation products of α-pinene, one filter was allowed to travel, but not used for sampling. An analysis of the total organic carbon was done, and the filter was extracted into 22 ml total 1/1 v/v dichloromethane/methanol. One 5 ml aliquot was analyzed using BF_3/butanol derivatization, one using BSTFA, and one was left underivatized.

2.6.4 Collection Blanks

Clean air was introduced into the environmental chamber prior to the ozonolysis of α–pinene, and pumped through clean filters. Any background particle-phase compounds identified by the analytical method (derivatization/GC×GC/TOF-MS) to be present in the "clean" chamber were therefore omitted from the results of the oxidation experiment by subtracting the impurities from the list of results for the samples.

2.6.5 No-Oxidant Blanks

Prior to the introduction of ozone into the α-pinene oxidation reaction vessel, a comparable volume of total air was pumped through a filter in order to collect any particulate matter that had formed in the chamber prior to oxidation. This could arise from any reactions of the precursor or scavenger (1-propanol), or from any background compounds in the environmental chamber. These blanks were analyzed in the same manner as the samples, including extraction, derivatization, and analysis by GC×GC/TOF-MS.

7. Data Processing Methods

The data processing was also different for each of the instruments because each system was equipped with a different application for data collection and analysis. For the Agilent 1D instrument, data was collected and processed using the Enhanced ChemStation E.02.00.493 with Enhanced Data Analysis and a library search (probability-based method) of the NIST and Wiley libraries. The RTE Integrator was used because there are additional parameters in this integrator that can be set for the particular use (the ChemStation Integrator could also be used). The parameters of the integration were as follows:

Data Processing Method Parameters for 1D-GC-MS:
Data point sampling: 1
Smoothing: on
Detection filtering: 5 point
Start threshold: 0.300
Stop threshold: 0.300
Minimum peak area: 50.0 area counts
Peak location: top
Maximum number of peaks: 250 (max)
Baseline reset (# point): > 5
If leading or trailing edge < 100.0%: baseline drop else tangent

For the calibration of standard compounds, the EasyID feature was used to adjust the retention times between derivatization methods. Calibration was performed using the Quantitation Database and Calibrate menu in Enhanced Data Analysis. The data was fit using a linear regression.

For the Leco/Agilent 2D TOF system, ChromaTOF^{TM} (Version 4.22) software was used

for data processing. A similar library search was made using the NIST library of mass spectra. The automated search was followed by a manual verification of the identifications based upon positive matches with the library spectra, as well as spectra from previous analyses and anticipated ions. All two-dimensional chromatograms were shown as either contour plots, in which a color scale from dark blue to red shows low to high abundance in the chromatogram, or surface plots, in which the abundance is viewed as a third dimension (the same color scale is also used in surface plots).

Because data processing is arguably the major limitation to use of GC×GC use (Vogt, *et al.,* 2007), several methods for data processing were used in tandem for the most complete and accurate identification of all compounds based upon mass spectral results. In order to eliminate any peaks that were obviously not of interest, peaks below the solvent line (which appears at <1 minute as a long string of peaks along approximately a static secondary retention time, and corresponds to the elution of solvent and column bleed) were eliminated. Peaks that were < 0.0001 times the peak area of the highest peak or <50 S/N ratio were also eliminated. The first method was a reverse library search, specified within the data processing method in the ChromaTOF™ software:

Data Processing Method Parameters for GC×GC/TOF-MS:
Baseline: computed (beginning to end of data collection)
Peak find: found above the baseline
Match required to combine
Baseline offset below: 0.5
Number of data points averaged for smoothing below: Auto
1st Dimension peak width: 5 seconds
Match required to combine: 700
Secondary retention time allowed for override of retention time shift for combine: 0.020 min early, 0.000 min late
2nd Dimension peak width: 0.1 seconds

Subpeak minimum S/N ratio: 20
Integration: Traditional
Classifications: TMS solvent exclusion area (to remove solvent front and column bleed)
S/N Ratio: 1000.0
Library search: Identified all peaks found
Library search mode: Normal
Mass to library search: All masses collected
Molecular weight range allowed: 50-500 a.m.u.
Minimum similarity match before name is assigned: 500
Mass to use for area/height calculation: Total ion signal
Calculate area/height: Computed without a calibration
Common masses in derivatized products: Not specified

This automated process was followed by a manual verification of the identifications based on positive matches with the NIST spectra (Wiley was not included on the computer system used for GC×GC analysis). An extracted ion analysis was then carried out by searching for ions and ionic ratios of known or anticipated oxidation.

A script method based primarily on extracted ion analysis was also used for data processing of the anthropogenic aromatic hydrocarbons to both show its efficacy in contrast to the other methods (those used regularly in 1D-GC) and to increase the number of identified compounds in the chromatograms. This method has been published previously as effective for non-derivatized analysis using GC×GC/TOF-MS (Groger, *et al.,* 2008; Vogt, *et al.,* 2007). The method of Welthagen, *et al.,* (2003) was used to positively locate seven underivatized carboxylic acids (noted to be in blank analyses as well) in one aromatic hydrocarbon oxidation product sample as a preliminary test for the utility of the script data processing method. The use of script for di-acids, however, was not successful because the algorithm written for this type of compound also selected mono- and multi-functional acids. Welthagen, *et al.* also used the relatively high

secondary retention time of polar compounds to differentiate, which was not written into these scripts for use with derivatized analytes, but could potentially be effective in the future.

The scripts used in this study were written in Microsoft VBScript using ChromaTOF™ (Version 4.22). Each script contained an algorithm to select for characteristic ions of all derivatives of a reagent or particular derivatized functionality. For example, the script used to find all butyl derivatives was as follows:

```
Function BuOH_Match()
        If Abundance(41)>400 AND Abundance(57)>400 then
            BuOH_Match = TRUE
        End If
    End Function
```

The result of the use of the script was a visual as well as column tabulated classification of all compounds fitting the parameters. The visual representation was in the form of colored bubbles mapped onto the chromatogram, as set by the Script™ capability within ChromaTOF™.

Using the results of the script and classified chromatogram, a comparison was made of the number of peaks identified as derivatives by the script versus the results of the more intensive spectral-based data processing method. A comparison was also shown for particular functionalities derivatized by each reagent used: carboxylic acids by BSTFA, and aldehydes and acidic ketones by BF_3/butanol.

The processing of GC×GC-FID data was done using Leco® ChromaTOF® Optimized for GC×GC-FID (Version 4.41) software and Microsoft Excel 2007. An initial data

processing method was run to delineate each peak in the chromatogram. The retention times of calibration standards were recognized by comparing GC×GC-FID results to those from the analysis by GC×GC/TOF-MS.

Data processing method parameters of GC×GC-FID used for total GC-detectable carbon mass and derivatization efficiency measurements

Baseline – computes baseline
Peak find: Find peaks above the baseline
Calculate Area/Height: Compute without calibration
Baseline offset: 0.8
Smoothing: Auto
1st Dimension expected peak width: 30 seconds
2nd Dimension R. T. shift override: Do not combine
2nd Dimension expected peak width: 0.15 seconds
Subpeak minimum S/N Ratio: 6
Maximum number unknown peaks: 1000
Integration approach: Traditional
S/N Ratio: 10.0

8. Total Organic Carbon Analysis

A thermal-optical method was used for quantitation of the total organic carbon (TOC) mass collected onto the filters (Sunset Laboratory, Tigard, OR). This measure of the TOC mass was referred to throughout Section 3 as TOC_{TOA}. The analysis of TOC_{TOA} was carried out by heating a portion of the samples at a programmed rate, and subsequently converting the evolved carbon gases to methane for analysis by GC-FID. The punch-size of 1.5 cm^2 was combined with the known flow rate to calculate the final concentrations of each analyte.

A blank filter (labeled the "travel blank" because it was allowed to travel, unopened, to and from Sunset Laboratory to the University of California Riverside) was analyzed for TOC_{TOA} and shown to contain a minimal amount of carbonaceous matter (0.57 ± 0.23 $\mu g/cm^2$ total carbon; Table 2.17).

Table 2.17. Thermal-optical carbon analysis results (Sunset Laboratory, Tigard, OR) showing the minimal carbon collected by pumping clean air through the filter, the precursor and 1-propanol without oxidant, and without collection. The "travel blank" was transported to and from the University of California, Riverside, but was not opened until carbon analysis.

Sample	Organic Carbon ($\mu g/cm^2$)	Elemental Carbon ($\mu g/cm^2$)	Total Carbon on Filter (μg)
Travel Blank	0.57 ± 0.13	0.00 ± 0.10	6.13 ± 0.23
062311-2 No Oxidant Blank	0.89 ± 0.14	0.00 ± 0.10	9.57 ± 0.24
Clean Air Blank, 062311-2	0.97 ± 0.15	0.00 ± 0.10	10.43 ± 0.25
α-Pinene SOA, 062611-3	38.28 ± 2.01	0.00 ± 0.10	412.6 ± 2.11
α-Pinene SOA, 062611-4	50.35 ± 2.62	0.00 ± 0.10	541.3 ± 2.72
α-Pinene SOA, 062311-3	105.2 ± 5.36	0.00 ± 0.10	1131 ± 5.46
Clean air blank, 062611-1	1.34 ± 0.17	0.00 ± 0.10	14.41 ± 0.27
No-Oxidant Blank, 062611-2	1.59 ± 0.18	0.00 ± 0.10	17.09 ± 0.28

The values of TOC_{TOA} were contrasted with values from the scanning mobility particle sizer used during filter sample collection and also with values of the GC×GC-FID quantifiable TOC mass.

2.8.1 GC×GC-FID Quantifiable TOC Mass

Extracts of the α-pinene ozonolysis filter samples were concentrated to dryness under a gentle stream of clean nitrogen gas and reconstituted to 300 μL in 1.5 ml autosampler vials with 300 μL glass inserts. Internal standards (3 μL) were added and the vials were capped to an appropriate tightness. Each underivatized sample was then analyzed using GC×GC-FID and integrated to find the total organic carbon mass in each sample. The same α-pinene ozonolysis filter sample extracts were derivatized and then prepared and analyzed using GC×GC-FID in the same way. The oxygenated carbon atoms were adjusted for (because the response of the FID is sensitive to reduced, combustible carbon atoms) using the organic carbon/organic mass ratio estimated from the α-pinene

ozonolysis products tabulated in Yu, *et al.* (1999). The trimethylsilylation contributions to the total estimated masses in derivatized samples were estimated using the response factors of BSTFA derivatized calibration standards in the calibration standard solutions quantified using GC×GC-FID. These values were subtracted from the total GC×GC-FID response to find the GC×GC-FID quantifiable TOC mass, which was then compared to the values of total organic mass using a scanning mobility particle sizer (SMPS) and total organic carbon measured using thermal-optical analysis.

9. Demonstration of the Quantitative Efficacy of the Method: Validation Parameters

In order to show the efficacy of the method of derivatization with GC×GC/TOF-MS for oxidation products of atmospherically relevant hydrocarbons, tests of the following parameters of a quantitative method were made. Some contrasts were also made using these parameters between the two derivatization methods, as well as the two instrumental methods (1D-GC and GC×GC).

2.9.1 Limit of Detection

In order to measure the limit of detection (LOD) with respect to the sensitivity of the method, the standard deviation of five to seven replicates at low concentration (1.0 ng/μL) was measured for each derivatization method, and each method of GC (one and two dimensional). The standard deviation of the signal was calculated and multiplied by three in order to find the value of the signal above which there was a 95% certainty that the signal was different from the blank value, assuming a blank value of zero. The LOD was calculated using the equation of the linear regression corresponding to each calibration curve. Values were compared to those of other, similar studies.

2.9.1.1 Precision

Several measurements can be made that show that the responses of the calibration and internal standards do not vary significantly, and that demonstrate the difference between the instrumental responses of the one and two-dimensional methods. The precision of retention times and signals were measured for the calibration standards, which were

analyzed in replicate at low concentration (1 ng/µL). Acceptable values for the retention time variation are < 0.5 minutes (based on the integration parameters) and for the response variation, ≤ 20%.

2.9.2 Linearity of Response

The assumption that the response of the method is linear was verified using the linear correlation coefficient, r^2. The value of was r^2 expected be within 20% of 1.00, showing that the calibration as linear with a certainty of 80%.

3 Results and Discussion

1. Synopsis

The method of coupled chemical derivatization and two-dimensional gas chromatography/time-of-flight mass spectrometry (derivatization/GC×GC/TOF-MS) was evaluated for its suitability in speciating polar oxygenated secondary organic aerosol (SOA) components, and in particular, carboxylic acids. This was examined by identifying and characterizing structures and functionalities of chamber-generated particle phase products of α-pinene ozonolysis. Butylation (from the reaction of BF_3/butanol) and trimethylsilylation (TMS, from the reaction of BSTFA) were compared as derivatization methods. Standard compounds were determined to evaluate the method and sample components were analyzed to allow comparison of the method results with those of previously published methods.

The efficiencies of derivatization for polar oxygenated standards were measured; the values were used to discuss the potential derivatization yields for secondary organic aerosol (SOA) sample components, based on structural and functional group similarities. For each of the derivatized standard compounds determined using GC×GC/TOF-MS, the linearity and precision of the responses as well as the limits of detection are presented. The measured values of these metrics show that the method is applicable to the quantitative determination of polar oxygenated SOA components such as carboxylic acids.

Particle phase α-pinene ozonolysis products that could be identified tentatively or characterized by functional group and structure were quantified using derivatization/GC×GC/TOF-MS. Separation along the second GC×GC chromatographic dimension allowed high peak resolution and therefore recognition of a large number of oxidation product peaks. Mass spectra collected showing fragmentation patterns used to identify products are included in Section 3, as are diagnostic ions used to assign structures and functional groups of many oxidation products. A large percentage of the quantified sample mass was attributed to previously published high abundance products of α-pinene ozonolysis. Some previously unidentified α-pinene ozonolysis products were detected using derivatization/GC×GC/TOF-MS. Tentative identifications were made for a small number of these compounds; others were designated as previously unidentified oxidation porducts because predicted or published mass spectral characteristics of known α-pinene ozonolysis products did not match those collected. The volatility and polarity of compounds were also characterized according to GC×GC/TOF-MS retention time to support identifications.

The total organic carbon (TOC) mass is used to evaluate the mass fraction of SOA sample quantified using the derivatization/GC×GC/TOF-MS method (Section 28) and to compare the mass fractions quantified and identified with the results of other studies. TOC mass of the collected α-pinene organic particulate matter (OPM) was quantified as the carbon mass (μg) on each filter sample using four methods: analysis using a thermal-optical technique (TOC_{TOA}), analysis by GC×GC with flame ionization detection

($TOC_{GC\times GC\text{-}FID}$), with and without derivatization, and estimation using a scanning electrical mobility sizer (SEMS). The $TOC_{GC\times GC\text{-}FID}$ mass was measured as a proxy for the TOC mass that could be quantified using a GC technique. Percentages of the organic carbon mass quantified using derivatization/GC×GC/TOF-MS were compared with each of the TOC mass values (those measured using TOC_{TOA}, $TOC_{GC\times GC\text{-}FID}$, TMS/$TOC_{GC\times GC\text{-}FID}$ or SEMS).

The results of the method evaluation, application to SOA samples, and percentage of the TOC quantified using the method of derivatization/GC×GC/TOF-MS are discussed in the following sections.

2. Method Evaluation

3.2.1 Derivatization Efficiencies

The derivatization efficiency (DE_i) was measured for polar oxygenated standard compounds similar in functionality to expected particle phase products of α-pinene ozonolysis: di-acids, hydroxy-acids, keto-acids, one aldehydic acid, and one aldehyde (Section 2.4.2). DE_i was measured by comparing the actual mass-sensitive GC×GC-FID response of each BSTFA derivatized (using BSTFA) or butylated (using BF_3/butanol) calibration standard with the expected response for that compound, called the effective carbon number (ECN) method.

A complete description of the ECN method as used in this study is included in Section 2.5.2. Briefly, butylation and TMS values of DE_i for calibration standards were measured and the accuracy of the ECN method of DE_i approximation was evaluated. The relationship between DE_i and concentration was investigated for butylated standards, and the deviation between values of DE_i found using replicate analyses at the same concentration was investigated for BSTFA derivatized standards. Derivatization reaction yields depend on the structure and functionality of the analyte; therefore, the trends of DE_i with respect to structure and functionality of the standards were examined.

Docherty & Ziemann (2001) monitored the values of DE_i during the optimization of their derivatization procedure. The values of DE_i were not measured prior to development of the DE_i method used in this study; instead, the efficiency was assumed to be high in GC-MS analysis when a significant and approximately Gaussian response was observed. The

derivatization efficiency should be monitored while the procedure is further developed to improve the efficiency of derivatization prior to future derivatization/GC×GC analyses.

3.2.1.1 Evaluation of the Effective Carbon Number Method for Derivatization Efficiency Measurement

Reproducibility of the integration and of the method response was investigated using precision of the ECN_i values of *n*-alkane and BSTFA derivatized standards between replicate analyses (Appendix D, Table J). The accuracy of the method was shown by comparing the ECN method values of DE_i for butylated adipic acid to those found using the ratio of the responses of butylated adipic acid and an authentic standard of dibutyl adipate.

The average response of the authentic standard dibutyl adipate was used to calculate the DE_i as the ratio of the laboratory derivatization and the standard compound (Appendix D, Table H), for comparison to the DE_i value calculated using the ECN method.

The butyl derivatization efficiency of adipic acid was 84% (mass response of the butylated adipic acid as a percentage of the average mass response of the dibutyl adipate authentic standard). The average butylation efficiency of adipic acid measurement using the ECN method, by comparison, was 51% at a concentration of 0.5 ng/μL and 55% at a concentration of 5.0 ng/μL. These values show some agreement between the methods for DE_i measurement.

The low (<10%) RSD of the ECN_i values for the series of C_{10}-C_{25} *n*-alkane reference compounds showed the reproducibility of the ECN method of derivatization efficiency measurement (Appedix D, Table I). The calculated *n*-alkane ECN_i values were consistently higher than expected values (the ECN_i should be equivalent to the number of carbon atoms for each *n*-alkane). Noting the equation for calculation of ECN_i (Equation 3.1), such a systematic error could have been caused by variation of the perdeuderated internal standard peak areas. Deviation of all ECN_i values could also be explained by integrated peak area values: integration of the peaks in GC×GC-FID analyzed samples was not straightforward (some evaluation of the distinction between peaks and the extent of the area associated with each peak was necessary). However, the ratios of the mass sensitive peak area responses expected for the C_{10}, C_{14}, and C_{16} perdeuterated ineternal standards were observed.

3.2.1.2 Results of the Effective Carbon Number Method

Method blanks were analyzed to show the influence of background compounds on standard compound responses and therefore DE_i values and trends. A GC×GC-FID analyzed method blank, butylated, showed compounds at a concentration over 0.5 ng/μL (using the response of naphthalene-d_8) present at the same retention times as the butylated calibration standards of oxalic acid, succinic-d_4 acid, and glyoxylic acid. However, the background compounds did not appear to affect the values of DE_i measured: the expected decreasing trend with analyte concentration was not observed for any butyl derivatives. Background signals were present at the retention times of the

BSTFA derivatized calibration standards lactic acid, glutaric acid, and ketopinic acid, but not at the retention time of *cis*-pinonic acid; again, the values of DE_i were apparently unaffected.

The high molar ratio of derivatization reagent to carboxylic acid analyte reaction sites was shown to be an important factor in obtaining high values of DE_i by Docherty & Ziemann (2001). A butyl DE_i for each calibration standard was calculated at 0.5, 5.0, and 20.0 ng/μL, corresponding to molar ratios of reagent to analyte reaction sites of 1.3:1, 13:1, and 53:1, respectively (Table 3.1).

Table 3.1. Values of DE_i at three reagent to analyte molar ratios, as well as the average and standard deviation of DE_i for each **BF_3/butanol** derivatized calibration. Internal standards used as reference compounds were the series of *n*-alkanes C_{10}-C_{25}. The DE_i was not related in this study to the molar ratio of reagent to analyte.

Standard Name	DE_i (%) at 3:1 Molar Ratio	DE_i, (%) at 13:1 Molar Ratio	DE_i, (%) at 53:1 Molar Ratio	Avg. DE_i	RSD (%) DE_i
Adipic acid	51.0	54.9	38.0	48.0	18.4
Dodecanoic acid	69.3	67.8	45.6	60.9	21.8
Glutaric acid	53.5	52.1	28.8	44.8	31.0
Glyoxal	38.5	28.9	79.8	49.1	55.1
Glyoxylic acid	21.7	15.0	30.0	22.2	33.6
2-Hydroxy-3-methyl-Butyric acid	---	---	---	---	---
Ketopinic acid	15.1	10.2	3.5	9.6	61.1
Lactic acid	---	---	---	---	---
Malonic acid	57.0	43.8	55.9	52.2	14.0
Methyl-malonic acid	79.8	91.7	48.3	73.3	30.6
Oxalic acid	43.5	36.9	38.5	39.6	8.7
cis-Pinonic acid	92.3	76.8	73.1	80.7	12.6
Salicylic acid	48.8	58.8	26.8	44.8	36.6
Succinic-d_4 acid	51.6	55.5	33.1	46.7	25.6

All standards were sufficiently derivatized for detection, and the DE_i values of the standards were somewhat reproducible (average RSD = 30%). Average DE_i values were similar for most (eight of 12) measured calibration standards (40-61%); average DE_i values were lower for glyoxylic acid and ketopinic acid. The average DE_i of dodecanoic acid, the only straight-chain acid analyzed, was higher than most values (60.9%). The average DE_i of *cis*-pinonic acid was also higher than for other standards (80.7%); this was especially important because it is an α-pinene ozonolysis product, and is similar in structure to other α-pinene ozonolysis products. Malonic acid is a low MW compound and therefore likely to be lost by evaporation, but its DE_i was high (52.2% on average). Even oxalic acid was derivatized using BF_3/butanol with a similar efficiency (39.6% on average) as were other carboxylic acids. The average butylation efficiency of the di-acid

calibration standards was 50%; only the DE_i values for malonic and methyl-malonic acids were higher. The low separation between the two compounds and therefore inaccurate integration may have caused the calculated DE_i values to be high.

DE_i values measured by Docherty and Ziemann (2001) were higher overall than those measured here. Using a ~1:1 molar ratio of reagent to analyte reaction site, values of DE_i were > 90% for all C_5-C_{18} mono- and C_2-C_{11} di-carboxylic acids with the exceptions of pentanoic, heptadecanoic, octadecanoic, oxalic, malonic, and undecanedioic acids (these were 70-80%).

Dissimilarly also to the finding of Docherty & Ziemann (2001), no trend of DE_i was observed with respect to the reagent to analyte active site molar ratio. Neither were there appartent trends of butylation efficiencies with functionality or structure. The responses of the two derivatized keto-acid standards were quite different, and the butyl derivative of only one hydroxy-acid was detected. A low butyl DE_i was observed for ketopinic acid; this observed impeded derivatization is potentially due to the stabilizing influence of the nearby keto group, or steric effects of the bi-cylic structure. Previous variations of the butylation procedure gave no measurable response using GC-MS or GC×GC/TOF-MS for the ketopinic butyl ester. Values of glyoxylic acid DE_i were also low, which was anticipated after low responses were measured during testing of the butylation procedure. However, the electron withdrawing effect by the vicinal carbonyl groups should have allowed increased acidity and therefore high DE_i. The DE_i values for oxalic acid and glyoxal, which also contain vicinal carbonyl groups at which butylation occurs, were

higher than those reached for glyoxylic acid. Butylation efficiency did not vary with carbon number, including between the series of di-acids included in the calibration standards.

Five replicate solutions of the BSTFA derivatized calibration standards at 1 ng/μL were analyzed using the ECN method to find the derivatization efficiencies and standard deviations of each derivatization (Table 3.2).

Table 3.2. Derivatization efficiencies of **BSTFA derivatized** calibration standards. Efficiencies were low throughout the analyses, as calculated by the effective carbon number method (Docherty & Ziemann, 2001). Mass-sensitive responses were measured using GC×GC-FID. All standards solutions were 1 ng/μL.

	Derivatization Efficiency						
	Replicate 1	**Replicate 2**	**Replicate 3**	**Replicate 4**	**Replicate 5**	**Average**	**RSD (%)**
Lactic acid	95.6	162	108	142	61.8	114	34.5
2-Hydroxy-3-methyl-butyric acid	72.2	107	90.4	83.9	42.5	79.2	30.4
Malonic acid	18.2	6.74	3.36	25.5	26.8	16.1	66.3
Methyl-malonic acid	81.1	22.9	26.4	51.2	100	56.4	60.0
Succinic-d_4 acid	96.7	23.9	87.3	67.3	118	78.7	45.4
Glutaric acid	61.4	13.3	40.9	52.0	90.7	51.4	55.1
Adipic acid	73.2	29.0	89.9	62.3	98.7	70.6	38.6
Salicylic acid	74.0	31.2	63.6	42.7	115	65.3	49.9
Ketopinic acid	39.6	68.4	62.6	62.1	78.9	62.3	23.1
cis-Pinonic acid	138	170	160	152	152	155	7.6
Dodecanoic acid	129	104	127	120	99.5	116	11.6

BSTFA DE_i values greater than 50% were achieved for all compounds with the exceptions of malonic acid and dodecanoic acid; average values of DE_i for five of the eleven compounds reacted were between 60 and 100%. The DE_i of BSTFA derivatized *cis*-pinonic acid was greater than 100%. Background signal at this retention time does not explain this anomaly: no compounds were detected at the retention time of BSTFA derivatized *cis*-pinonic acid in blank analyses. The DE_i of dodecanoic acid was also high, showing a trend of increased DE_i with retention time as calculated by the ECN method. The efficiency of the BSTFA reaction at a low concentration (1 ng μL^{-1} was used) was not reproducible: the RSDs achieved for nearly all of the calibration standards were high (>30%; excluding ketopinic acid, for which RSD was only ~8%).

No trend was observed between the derivatization efficiencies of those calibration standards with similar functional groups or structures. The DE_i of adipic acid was consistently higher than that of glutaric acid, however, possibly showing the effects of evaporative losses. The response of BSTFA derivatized malonic acid was noted to be low throughout all analyses, likely due to evaporative losses of the derivatized product. Calculated DE_i values were much higher for malonic acid, showing the utility of BF_3/butanol for low molecular weight carboxylic acid analysis (the evaporative losses of dibutyl malonate were likely lower than those of bis(trimethylsilyl) malonate). Oxalic and malonic acid trimethylsilyl derivatives were mentioned in Docherty & Ziemann (2001) to have been below 90% derivatization efficiency, as also measured here. The volatilities of these resulting TMS esters are likely sufficiently high to cause evaporative losses to decrease the sensitivity of the method.

3.2.1.3 Expected Derivatization Efficiencies of α-Pinene Ozonolysis Products

The yields of derivatives from the reaction of each external calibration standard were used to determine the expected extent of derivative formation for each component identified in samples. The carbon structure of most α-pinene ozonolyis products was the same 2,2-dimethyl-cyclobutyl structure as in *cis*-pinonic acid (an authentic standard of this α-pinene ozonolysis product was available). The average DE_i for butanol reaction with this compound was 81±10% (one standard deviation, 1σ), much higher than other values of DE_i measured using either derivatization method. Although the average BSTFA DE_i of *cis*-pinonic acid was well over 100%, the RSD of the response was low

(~8%). No major trends of DE_i were observed with structure and functional groups for derivatized calibration standards, but average DE_i values of standards with particular functional groups showed whether high responses of similar sample component derivatives were expected.

The functionalities of α-pinene ozonolysis products include carboxylic acids: di-acids, hydroxy-acids, keto-acids, and aldehydic acids. The acid standards most closely related in structure and functionality to the 2,2-dimethyl-cyclobutyl ozonolysis products (those with the above-mentioned functionalities, $>C_4$ carbon chains, and no ring structure with $>C_4$) were sufficiently derivatized: values of DE_i were >50% using BSTFA derivatization and >45% using BF_3/butanol. Variation between analyses was generally high (>40%), and highest when BSTFA reaction was used. Because the overall values of DE_i were lower for BF_3/butanol derivatization, the expected yields of α-pinene ozonolysis product derivatives were lower; this was accounted for, however, by using the measured RF of *cis*-pinonic acid to calculate concentrations of α-pinene ozonolysis products. Thus, the formation of derivatized ozonolysis products was expected for both derivatization methods; however, it should be noted that uncertainty in the calculated concentrations of the ozonolysis products is high because of the high variation in most values of DE_i.

Hydroxy-acids were best measured using the reagent system that allowed derivatization of both alcohol and carboxylic acid sites, BSTFA. Hydroxy-acid DE_i values as shown by the reactions of BSTFA with lactic, 2-hydroxy-3-methyl-butyric, and salicylic acids were >60%, but with high variation (RSD ≥ 30%). The response of ring-retaining ozonolysis

products as measured by the DE_i of the keto-acid ketopinic acid was lower for butylation: 4-15%; the trimethylsilyl DE_i was 62 ± 14% (1σ). The DE_i values of the aldehydic acid glyxoylic acid were low: ~22% on average (note that no standard deviations are given for butyl esters because butyl responses were measured at three differing concentrations, and response was dependent on concentration).

3.2.2 Linearity and Precision of the External Calibration

Polar, oxygenated standards were externally calibrated using derivatization/GC×GC/TOF-MS (the same set of standards was used in determination of DE_i). The total ion and quantitation ion signals of each derivatized standard at several concentrations were measured to show the linearity of the method responses. The same calibrations were used to quantify the compounds in α-pinene SOA samples (this was only done when the authentic standard of the compound was available).

The externally calibrated BSTFA derivatized and butylated standards showed high linearity with standard concentration (r^2 >0.90) for nearly all total ion and quantitation ion signals. Correlation coefficients for total ion signal calibrations were high for all standards (r^2=0.9070 to 0.9999). The quantitation ion responses of salicylic and succinic-d_4 acids showed significantly lower linearity than the other calibration standards (r^2=0.581 and 0.0985, respectively); this was likely because of co-elution of these standards with background compounds; the quantitation ions were m/z 120 and 105, respectively, corresponding to major ions in a background product identified in the retention time window of these standards. The quantitation ion response of BSTFA

derivatized malonic acid was also less linear; the DE_i of this compound was much lower than other compounds and the low response in both DE_i measurement and calibration may be attributed to evaporative losses of this low MW derivative.

The RSDs of the RF values obtained for the calibration standards were ≤35% for all standards except BSTFA derivatized malonic and salicylic acids (noted as above to show evaporative losses and co-elution of background compounds, respectively). The RSDs of the total ion response factors calculated were much higher than those of quantitation ion signals for almost all compounds, as might be expected due to the generally less accurate total ion response measurement: butyl total ion RSDs were 17-125%, and trimethylsilyl total ion RSDs were16-108%. The response factor used to quantify the SOA sample components was calculated from the total ion response of *cis*-pinonic acid, butyl ester RF= 5.09 ± 2.49 (one standard deviation, 1σ) and trimethylsilyl RF=5.375 ± 3.21 (1σ). At minimum, three of the five responses at measured concentration levels (0.5 – 20.0 ng/μL) were used in the calibration of each calibration and recovery standard. All metrics of the calibrations discussed in this section are shown in Appendix D, Tables K-N.

The total ion signals at each calibration concentration of recovery standard eicosane-d_{42} were also less linear (r^2 = 0.87), which can be explained by the presence of background components obscuring the accurate integration of the total ion signal (many high molecular weight acids and acid derivatives such as hexadecanoic acid and butyl hexadecanoate were noted in the background at approximately the same retention time).

All values of the retention time and area RSDs were sufficiently low (<20%) for accurate calculation of the responses of the standards used in external calibration, and for semi-quantitation of α-pinene SOA components. The variations of the peak areas of the internal standards used for quantifying SOA sample components in butyl and trimethylsilyl GC×GC/TOF-MS analyses were <20% for phenanthrene-d_{10} and naphthalene-d_8 (pyrene-d_{10} was not used as an internal standard because the variations in its retention time and response were too high and the two other perdeuterated PAHs were sufficiently spread in retention time for use). Primary and secondary retention time RSDs of internal standards used were <1% in butyl samples and <2% in trimethylsilyl samples. Retention time RSDs for butylated calibration standards were low: <5% for all calibration standards throughout the external calibration (higher RSDs were noted for succinic-d_4, glyoxylic, and dodecanoic acids in the secondary dimension, and for glyoxylic acid in the primary dimension). The primary retention times (^1t_R) of many of the calibration standards did not vary from the four second modulation period. BSTFA derivatized calibration standards showed a higher retention time variation: all ^1t_R RSDs were <5% except that of methyl-malonic acid (^2t_R RSD was 10.27%). All other BSTFA derivatized ^2t_R RSDs were <10%. The precisions of the responses of the internal and calibration standards with respect to retention time and peak area are shown in Appendix D, Tables O and P.

3.2.3 Limit of Detection

The limit of detection (LOD) is an effective metric for establishing the low-end concentration measurable for an analyte using a technique of interest. The LODs were calculated and contrasted for polar oxygenated standards analyzed by TMS/GC×GC/TOF-MS and butylation/GC×GC/TOF-MS. The LODs from several studies in which similar carboxylic acids as those used in this study were compared to the LODs calculated here (Table 3.3).

Table 3.3. Limits of detection calculated for similar analyte compounds as those used in the external calibration in this study: carboxylic acids with multiple functional groups and low to mid-range MW. Derivatization methods were used in all three studies shown here; values are given as a mass injected to the gas chromatograph.

Study	Analytical Method	LOD Estimation Method	LODs
Pietrogrande, *et al.*, 2010	BSTFA; BF_3/butanol	LOD = 6 σ_b/ slope	1.1-1.5 ng C_5-c_9 di-acids BSTFA;1.6- 2.7 ng BF_3/butanol
Stávová, *et al.*, 2011	BSTFA, MSTFA, BF_3/butanol	LOD = 3.3 σ_b/ slope	C_2-C_{14} di-acids: 2-216 pg BSTFA; 2.4-38 pg BF_3/butanol
Beiner, *et al.*, 2009	CPP(TMAAc)-GC-MS[4]	LOD = b + 3 σ_b	Adipic: 2.3 ng; Pinonic: 1.4 ng

[4] CPP: Curie point pyrolyser; TMAAc: tetramethylammonium acetate (thermally assisted methylation)

Limits of detection found in this study were lower than those found in two of three studies shown in Table 3.3, but were up to three orders of magnitude greater than those reported using TMS and butylation in Stávová, *et al.* (2011) (Table 3.4 and Table 3.5).

Table 3.4. Limits of detection (LODs) of calibration standards using butylation/GC×GC/TOF-MS. Values were calculated as 3σ of the response of seven replicate analyses at 1 ng/µL. The responses used to calculate the LODs are also shown as reference. The deviation of all responses at 1 ng/ µL was >35% (relative standard deviation, RSD) for tetrabutyl glyoxal, butyl glyoxylate, dibutyl hexanedioate, and butyl ketopinate. Values are given as mass injected to the instrument.

Name	Average	Std. Dev.	RSD (%)	LOD = 3σ (ng)
cis-Pinonic acid, butyl ester	0.660	0.085	12.9	0.255
Eicosane-d_{42}	0.811	0.167	20.6	0.501
Oxalic acid, dibutyl ester	0.861	0.188	21.8	0.563
Glutaric acid, dibutyl ester	0.692	0.114	16.5	0.343
Glyoxal, tetrabutyl acetal	0.922	0.408	44.2	1.22
Glyoxylic acid, butyl derivative	0.261	0.317	122	0.951
Adipic acid, dibutyl ester	0.601	0.295	49.1	0.885
Ketopinic acid, butyl ester	0.721	0.496	68.7	1.49
Malonic acid, dibutyl ester	0.960	0.100	10.5	0.301
Dodecanoic acid, butyl ester	0.828	0.139	16.8	0.417
Malonic acid, methyl-, dibutyl ester	0.838	0.128	15.3	0.384
Salicylic acid, butyl ester	2.14	0.692	32.4	2.08
Succinic-d_4 acid, dibutyl ester	0.926	0.100	10.8	0.300

Table 3.5. Limits of detection (LODs) as the mass injected of calibration standards using TMS/GC×GC/TOF-MS. Values were calculated as 3σ of the response of three replicate analyses at 1 ng per µL injected. The responses used to calculate the LODs are also shown as reference. The deviation of all responses at 1 ng per µL injected was <35% (relative standard deviation, RSD). Values were adjusted to reflect the mass per unit volume sampled. Values are given as mass injected to the instrument.

Name	Average	Std. Dev.	RSD (%)	LOD = 3σ (ng)
Lactic acid, TMS	0.911	0.175	19.2	0.524
2-hydroxy-3-methyl-butyric acid, TMS	1.85	0.515	27.8	1.55
Malonic acid, TMS	0.890	0.298	33.5	0.894
Methyl-Malonic acid, TMS	1.42	0.139	9.81	0.417
Succinic-d_4 acid, TMS	1.60	0.317	19.8	0.951
Glutaric acid, TMS	0.933	0.221	23.7	0.663
Adipic acid, TMS	1.10	0.211	19.2	0.634
Ketopinic acid, TMS	0.393	0.109	27.7	0.327
Salicylic acid, TMS	1.35	0.161	12.0	0.483
cis-Pinonic acid, TMS	0.732	0.127	17.4	0.381
Dodecanoic acid, TMS	1.31	0.221	16.9	0.662
Eicosane-d_{42}	0.682	0.231	33.9	0.692

Values of LOD found using TMS were approximately twice those found using butylation for all calibration standards measured in both derivatization methods except adipic, ketopinic, and salicylic acids. Values of LOD for butylated ketopinic and salicylic acids and glyoxal were noted to be much higher than those of other butylated calibration standards; lower butyl DE_i values were also measured for ketopinic acid. The responses of salicylic acid and glyoxal, butyl derivatives, varied highly, leading to higher measured LODs. Variation in the response of the calibration standards was much higher for butylated standards; however, seven replicates were made for the calculation of butyl LOD, while only three replicates were made for trimethylsilyl LOD calculation.

3. Composition of α-Pinene Ozonolysis Secondary Organic Aerosol

3.3.1 Quantitation and Semi-Quantitation of α-Pinene Ozonolysis Products: Butylated Products

Particle phase products of α-pinene ozonolysis collected onto filters that could be tentatively identified or characterized (by functional group or structure) by derivatization/GC×GC/TOF-MS analysis were quantified. Sample SOA 26-3 (Table 2.1) was used to express the total mass of aerosol compounds quantified as a fraction of TOC_{TOA} and $TOC_{GC\times GC\text{-}FID}$. This allowed comparison of the total quantifiable and identifiable masses using derivatization/GC×GC/TOF-MS with those of previous methods.

The results of separately quantified butylated and BSTFA derivatized products showed the utility of each reagent system in detection and identification of the polar oxygenated OPM (PO-OPM) components, and in particular for the carboxylic acid products. Carboxylic acids, as discussed in Section 1.3, are of particular importance in OPM because their high polarities cause their particle phase concentrations to be high; they are also important to consider from an analytical perspective because their high polarities relative to other known OPM components make them difficult to analyze. The total mass attributable to carboxylic acids was thus by derivatization/GC×GC/TOF-MS and is shown below as a percentage of the total organic mass quantified by derivatization/GC×GC/TOF-MS and of the $TOC_{GC\times GC\text{-}FID}$.

The quantitative ion RF (Section 2.4.2) was used in quantitation of sample components for which the response of an authentic standard was measured. Aerosol compounds without authentic standards were quantified using the total ion response of a surrogate standard (*cis*-pinonic acid). Using the response of derivatized *cis*-pinonic acid for semi-quantitation of sampled SOA components, each semi-quantified component was adjusted for derivatization efficiency, assuming the same derivatization efficiency as the surrogate standard was obtained (near 100% for both derivatization schemes). The recovery from the extraction and sample preparation processes was also estimated for each derivatized sample using the recovery standard eicosane-d_{42} (response ≥100%). Background signals were quantified using the travel blank.

The components quantified in the butylated extract of SOA sample 3 collected on 6/26/11 are tabulated in 3.6.

Table 3.6. Recognized oxidation products (ox. products) and quantified butyl derivatives (butyl ders.) identified in SOA sample 3 collected on 6/26/11 and analyzed by GC×GC/TOF-MS. Unless a separate quant mass was specified (quant masses are listed), the total ion response factor for *cis*-pinonic acid was used in quantitation. The mass of each compound was divided into the volume of air pulled through the filter to give the mixing ratio. Compounds are organized by primary retention time in seconds (^1t_R) and secondary retention time in seconds (^2t_R). Standards and internal standards (int. std.) are noted in the first column. Mjnor products (contributing > 1 µg mass) are in bold.

Peak	Name	Quant Masses	^1t_R (sec)	^2t_R (sec)	Peak Area	Mass (µg)	Mass Quantified (%)
2	Int. Std: Naphthalene-d_8	136	947.9	1.51	82937445		
5	Ox. product	t	1027.9	1.37	2765707		
6	Pinonaldehyde, underivatized	t	1047.9	1.47	7382185		
7	Ox. Product	t	1051.9	1.33	66020946		
9	Ox. Product	t	1059.9	1.36	21992193		
10	Ox. Product	t	1063.9	1.43	37070486		
12	Pinalic-4-acid,underivatized	t	1079.9	1.38	8089072		
13	Ox. Product	t	1079.9	1.21	3252352		
14	Ox. Product	t	1095.9	1.39	2040802		
17	Oxalic acid, dibutyl ester	147	1131.9	1.35	36559	0.18	0.54
22	4-oxo-Pinonic acid, underivatized	t	1175.9	1.46	109867178		
24	Ox. Product	t	1179.9	1.37	1641887		
25	Dimethyl pinate	t	1191.9	1.28	1808704	0.02	0.05
29	Butyl der.	t	1219.9	1.37	10808144	0.11	0.32
30	Malonic acid, dibutyl ester	105	1223.9	1.35	1013716	0.09	0.25
18	Butyl der.	t	1227.9	1.25	2086914	0.02	0.06
33	Ox. product	t	1239.9	1.70	11028635		
35	Ox. product	t	1247.9	1.51	9689833		
37	Ox. product	t	1255.9	1.54	17437494		
41	Butyl der.	t	1299.9	1.25	8991655	0.09	0.27
43	Ox. Product	t	1335.9	1.37	80121046		
45	Ox. Product	t	1351.9	1.36	36785348		
46	Ox. Product	t	1351.9	1.68	5100990		
49	Unknown butyl derivative	t	1359.9	1.56	16417168	0.17	0.49
48	Standard: succinic-d_4 acid, dibutyl ester	105	1359.9	1.38	37883357		
50	Pinalic-4-acid, butyl derivative	t	1371.9	1.44	51397444	0.53	1.55
54	Ox. Product	t	1379.9	1.39	10890057		
55	Butyl der.	t	1387.9	1.36	54146609	0.55	1.63
56	Butyl der.	t	1395.9	1.41	13188345	0.14	0.40
58	Butyl der.	t	1399.9	1.31	69451911	0.71	2.09
59	Glyoxylic acid, butyl derivative	159	1399.9	1.21	229250	0.27	0.79

Peak	Name	Quant Masses	^1t_R (sec)	^2t_R (sec)	Peak Area	Mass (µg)	Mass Quantified (%)
67	Butyl der.	t	1443.9	1.52	9284494	0.10	0.28
68	Butyl der.	t	1443.9	1.23	6519487	0.07	0.20
70	Ox. Product	t	1463.9	1.46	32430212		
73	Pinonic acid, butyl ester	t	1479.9	1.47	192656029	1.97	5.79
75	Hydroxy pinonic acid, butyl ester	t	1487.9	1.47	663785494	6.80	19.96
76	Pinic acid, dibutyl ester	t	1495.9	1.49	695716456	7.13	20.92
77	Standard: ketopinic acid, butyl ester	t	1495.9	1.64	22337654		
85	Butyl der.	t	1539.9	1.70	195102748	2.00	5.87
86	Ox. Product	t	1547.9	1.54	31739921		
88	Butyl der.	t	1559.9	1.41	13103728	0.13	0.39
89	Ox. Product	t	1559.9	1.74	3305609		
90	Butyl der.	t	1563.9	1.27	3320249	0.03	0.10
91	Butyl der.	t	1575.9	1.39	4758893	0.05	0.14
93	Ox. product	t	1575.9	1.74	5596064		
94	Butyl der.	t	1579.9	1.28	4986467	0.05	0.15
96	Butyl der.	t	1599.9	1.31	62787888	0.64	1.89
97	Butyl der.	t	1599.9	1.45	17216980	0.18	0.52
98	Glyoxal, tetrabutyl acetal	159	1599.9	1.21	58655	0.01	0.02
105	Butyl der.	t	1619.9	1.38	18700870	0.19	0.56
106	Int. Std.: Phenanthrene-d_{10}	188	1627.9	1.99	24532902		
107	Butyl der.	t	1635.9	1.29	25792535	0.26	0.78
108	Butyl der.	t	1635.9	1.38	12473932	0.13	0.38
109	Butyl der.	t	1655.9	1.39	5483249	0.06	0.16
111	Butyl der.	t	1667.9	1.40	15512719	0.16	0.47
112	Butyl der.	t	1675.9	1.33	34786288	0.36	1.05
114	Butyl der.	t	1691.9	1.44	51843290	0.53	1.56
116	Butyl der.	t	1703.9	1.50	10446312	0.11	0.31
117	Butyl norpinonaldehyde	t	1739.9	1.45	7297609	0.07	0.22
122	Butyl der.	t	1763.9	1.47	454172588	4.65	13.66
123	Butyl der.	t	1771.9	1.39	18147472	0.19	0.55
128	Butyl der.	t	1779.9	1.37	250339139	2.57	7.53
127	Standard: Eicosane-d_{42}	66	1779.9	1.18	4668678		
129	Butyl der.	t	1827.9	1.29	41376681	0.42	1.24
134	Butyl der.	t	1887.9	1.55	3443826	0.04	0.10
136	Int. Std.: Pyrene-d_{10}	212	1947.9	2.40	16427423		
138	Butyl pinonaldehyde	t	1963.8	1.34	189266614	1.94	5.69
140	Butyl der.	t	2139.8	1.41	31664448	0.32	0.95
					Sum	34.09	100.00

Seven components of the butylated SOA sample were determined to make up ~ 80% of the butylation/GC×GC/TOF-MS quantified organic mass: pinic acid (20.9%; #76), a hydroxy pinonic acid (20.0%; #75), butyl derivative #122 (1763.9 sec, 1.47 sec, 13.7%), butyl derivative #128 (1779.9 sec, 1.39 sec, 7.5%), butyl derivative #85 (1539.9, 1.70 sec, 5.9%), pinonic acid (5.8%; #73), and pinonaldehyde (5.7%; #138). Each of these components contributed >1 μg mass to the sample. Pinic acid was the most abundant compound measured (~7 μg); dimethyl pinate (peak #25) is almost certainly a product of methylation of pinic acid present in the SOA sample, and its contribution to the SOA mass was estimated as a dibutyl ester (0.02 μg, 0.05% of the GC×GC/TOF-MS semi-quantified mass).

The butyl derivatives of oxalic and malonic acids, glyoxylic acid, and glyoxal were previously unidentified as oxidation products of α-pinene. Although these compounds were used in the external calibration and so could have been introduced during sample preparation, the concentrations found here were significantly higher than those identified in the blank. The compounds were found in the blank at the following concentrations: 0.072 μg dibutyl oxalate, 0.0055 μg dibutyl malonate, 0.010 μg butyl glyoxylate, and 0.00051 μg tetrabutyl glyoxal (note that these blank concentrations have already been subtracted from those values listed in Table 3.6). Although these compounds were determined using BF_3/butanol but not BSTFA derivatization, it is possible that these compounds were not detectable using TMS/GC×GC/TOF-MS: only malonic acid was

successfully BSTFA derivatized during standard analyses, and the derivatization efficiencies for malonic acid were consistently lower than 25%.

Several underivatized SOA sample components were of similar peak areas as the abundant butyl derivatives, showing that the use of derivatization did not preclude the analysis of underivatized compounds (those with functional groups that do not react with BF_3/butanol or BSTFA) in a sample extract. Assuming that the response factors of these underivatized compounds would be similar to that of butyl pinonate, it is possible that a large portion of the mass in this sample was contributed by underivatized compounds. The underivatized portion can be visualized by comparing the total ion and m/z 57 extracted ion chromatograms (Figure 3.1).

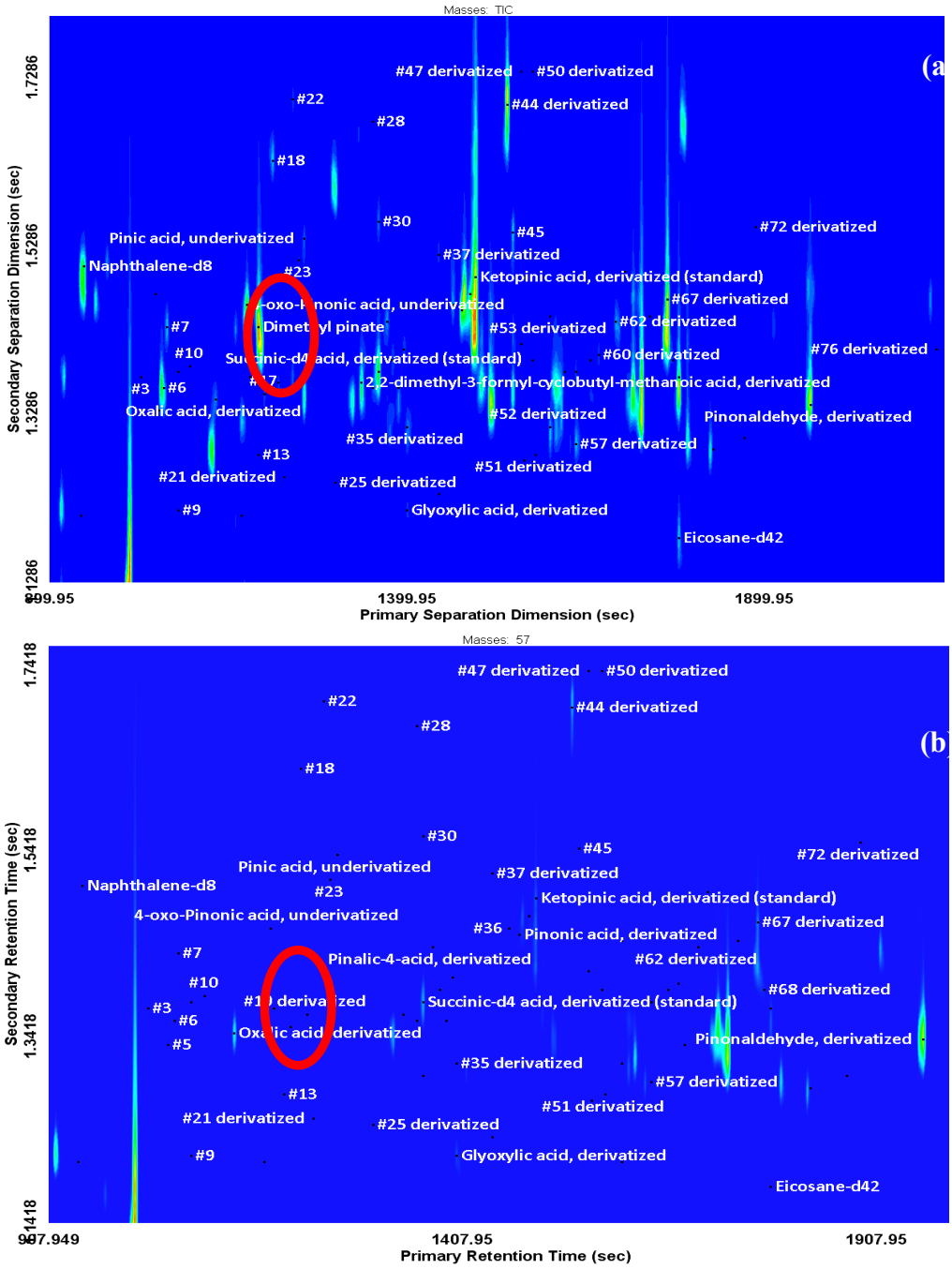

Figure 3.1. Total ion (a) and m/z 57 extracted ion (b) chromatograms of butylated components showing all components and derivatized components, respectively. The red circles surround the peaks of underivatized 4-oxo-pinonic acid and methylated pinic acid in chromatogram (a) and the lack of peaks in (b). The relative abundance of m/z 57 in mass spectra of butyl derivatives is often low so the abundances of derivatized peaks appear lower in the extracted ion chromatogram. Note also that chromatogram (a) is zoomed to show the major components.

The highest abundance peaks in the butylated SOA sample chromatogram appear above 1350 seconds in the primary dimension, because of the addition of the butyl moiety, and thus lowered volatility, of these compounds. However, several abundant peaks are present in the total ion chromatogram below 1350 seconds in the primary dimension, corresponding to underivatized oxidation products. These underivatized components are lower polarity (lower ^2t_R values) than the di-acids observed in underivatized samples.

3.3.2 Quantitation and Semi-Quantitation of α-Pinene Ozonolysis Products: BSTFA Derivatized Products

Fewer α-pinene ozonolysis products were identified and quantified in the BSTFA derivatized SOA 26-3 sample than in the butylated sample, but the derivatization process and data analysis were simpler for TMS, allowing characterization by functional groups for a large percentage of the mass quantified by TMS/GC×GC/TOF-MS (Table 3.7).

Table 3.7. SOA sample 26-3 components quantified using GC×GC/TOF-MS. Concentrations were calculated based on the total ion response factor of *cis*-pinonic acid, trimethylsilyl derivative, unless a separate quant mass is specified ("t" indicates total ion). Major oxidation products (≥1 µg mass) are in bold.

Peak	Name	Quant Masses	^1t_R (sec)	^2t_R (sec)	Area	Mass (µg)	Percent of Quantified Derivatized Mass
1	Ox. product	t	848.0	1.76	10227033		
2	Ox. Product	t	991.9	1.62	113133099		
3	Norpinonaldehyde, underivatized	t	1008.0	1.93	12551320		
4	Int. Std. Naphthalene-d_8	136	1012.0	1.81	22082869		
5	Ox. product	t	1032.0	1.83	4498042		
6	Ox. Product	t	1079.9	1.48	8346496		
7	Pinonaldehyde, underivatized	t	1127.9	1.84	114625142		

Peak	Name	Quant Masses	^1t_R (sec)	^2t_R (sec)	Area	Mass (µg)	Percent of Quantified Derivatized Mass
5	Ox. Product	t	1127.9	2.28	2214832		
9	Pinalic-4-acid, underivatized	t	1147.9	1.72	10907302		
10	TMS der.	t	1151.9	1.60	11632112	0.39	0.64
11	Ox. Product	t	1155.9	2.15	12795854		
	Std. Succinic-d_4 acid, TMS	147	1167.9	1.27	35679		
12	TMS der.	t	1183.9	1.64	17850047	0.59	0.99
13	Ox. product	t	1195.9	1.89	3417707		
14	TMS der.	t	1199.9	1.58	14615693	0.48	0.81
15	TMS der.	t	1207.9	1.33	5143037	0.17	0.28
16	TMS der.	t	1215.9	1.47	23130496	0.77	1.28
17	Norpinic acid, underivatized	t	1231.9	1.97	48940167		
18	TMS der.	t	1231.9	1.47	6563904	0.22	0.36
19	TMS der.	t	1243.9	1.59	7519850	0.25	0.42
20	Pinonic acid, underivatized	t	1331.9	1.89	11741090		
21	Ox. Product	t	1339.9	2.07	5289437		
	TMS der.	t	1351.9	1.51	22868970	0.76	1.26
23	Std. Ketopinic acid, underivatized	t	1379.9	2.21	24785908		
24	Std. Ketopinic acid, TMS	95	1419.9	1.70	1394612		
25	Pinic acid, underivatized	t	1423.9	2.03	17900471		
26	TMS der.	t	1427.9	1.41	14070008	0.47	0.78
28	Ox. product	t	1439.9	2.33	9863663		
27	Pinonic acid, TMS	73+171 +83	1439.9	1.53	78503653	9.38	15.62
29	TMS der.	t	1459.9	1.27	5362448	0.18	0.30
30	Ox. Product	t	1471.9	2.05	8794309		
31	Norpinic acid, TMS	t	1507.9	1.79	638834297	19.66	32.74
32	oxo-Pinonic acid, underivatized	t	1527.9	2.34	16981976		
33	Hydroxy pinonaldehyde, TMS	t	1535.9	1.60	92486667	2.85	4.74
34	Pinic acid, TMS	t	1603.9	1.44	666905357	20.52	34.18
35	TMS der.	t	1703.9	1.80	12083963	0.37	0.62
36	TMS der.	t	1711.9	1.58	91731121	2.82	4.70
37	Int. Std. Phenanthrene-d_{10}	188	1739.9	2.65	22637342		
38	Std. Eicosane-d_{42}	66	1895.9	1.21	8975552		
39	Int. Std. Pyrene-d_{10}	212	2035.8	2.32	16314104		

Peak	Name	Quant Masses	$^{1}t_{R}$ (sec)	$^{2}t_{R}$ (sec)	Area	Mass (µg)	Percent of Quantified Derivatized Mass
					Sum	59.87	100.00

The components of the BSTFA derivatized SOA sample were determined to make up ~75% of the TMS/GC×GC/TOF-MS quntified organic mass: pinic acid (34.1%; peak #34), norpinic acid (32.7%; peak #31), pinonic acid (15.6%; peak #27), a hydroxy pinonaldehyde (4.7%; peak #33), and trimethylsilyl derivative #36 (1711.9 sec, 1.58 min; 4.7%). No dimethyl pinate was detected in the BSTFA derivatized sample, supporting the hypothesis that the dimethyl pinate quantified in the butylated SOA sample was due to methylation of pinic acid.

The clear recognition of each BSTFA derivatized peak area was possible using GC×GC separation (Figure 3.2) and diagnostic ions were again used to recognize derivatives of BSTFA.

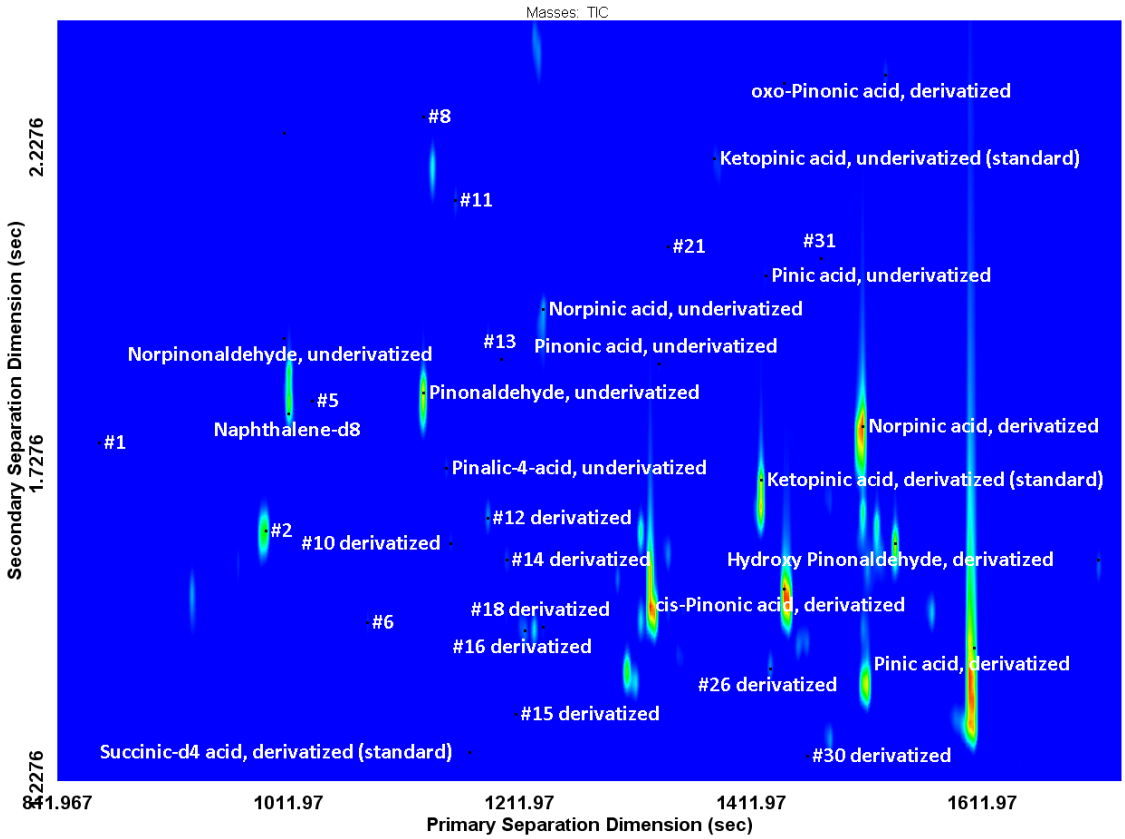

Figure 3.2. Total ion chromatogram of the response of the method of GC×GC/TOF-MS BSTFA derivatized SOA sample 26-3. Components were separated in both dimensions, allowing clear peaks for each sample component, and therefore clear mass spectra and peak areas to be recognized.

Sample components of highest abundance were eluted after 1450 seconds (^1t_R) and mostly before 1.80 seconds (^2t_R), demonstrating the lower polarity and volatility of the derivatives. Underivatized oxidation products of only slightly smaller peak areas appeared at lower primary and higher secondary retention times. Compounds were identified in association with many of the major peaks in the SOA sample 26-3 chromatograms, but some peaks could not be associated with oxidation products based on the mass spectra collected. The details of the tentative identifications and lack of identification for many peaks is explained in Section 3.3.3.1.

3.3.3 Compound Identifications: BSTFA Derivatized α-Pinene Ozonolysis Products

The α-pinene ozonolysis reaction has been well studied because it contributes a large mass of organic matter to the global secondary organic aerosol (SOA) budget (Fehsenfeld, 1992). It was used in this study because the identities of major oxidation products have been established, and also because new products of a well-known and important system could potentially be characterized. Previous characterizations of the α-pinene/ozone oxidation products have been made using LC-MS and APCI-MS (Hoffmann, *et al.,* 1998; qualitative; Glasius, *et al.,* 1999; quantitative), GC-EI-MS with BSTFA derivatization (Presto, *et al.,* 2005a), GC-CI-MS with PFBHA and PFBBr derivatization (Jang & Kamens, 1999; qualitative), FT-IR (Jang & Kamens, 1999), GC-EI-MS and GC-CI-MS with PFBHA/BSTFA derivatization (Yu, *et al.,* 1999; Fick, *et al.,* 2003; quantitative). Particle formation in this oxidation reaction system was also studied under high and low relative humidity conditions and with and without aerosol seed (Cocker, *et al.,* 2001a). Major products identified in the studies mentioned for α-pinene ozonolysis include norpinonic acid, pinonic acid, 2,2-dimethyl-cyclobutane-1,3-dicarboxylic acid, pinic acid, norpinonaldehyde, and pinonaldehyde. Two di-carbonyls (Fick, *et al.,* 2003) and many other functionalized compounds containing a 2,2-dimethyl-cyclobutyl center have also been identified.

3.3.3.1 Methods for Identifying α-Pinene Ozonolysis Products using Mass Spectra

The α-pinene ozonolysis products that were identified in this study using derivatization/GC×GC/TOF-MS results from extracted chamber study filter sample

analyses were tabulated. Identifications were based on the fragmentation patterns of spectra found in the NIST and Wiley mass spectral libraries, as well as in published studies (Jaoui & Kamens, 2001; Yu, *et al.,* 1999; Jang, *et al.,* 2003; Li & Yu, 2005). The spectra collected using GC×GC/TOF-MS were slightly different from those tabulated in the library and publications used as reference, which can be attributed in part to the use of a TOF-MS rather than a quadrupole or ion trap (ITMS) instrument, and electron impact (EI) rather than chemical ionization (CI) mass spectrometer source. The primary differences between TOF-MS and quadrupole or ITMS spectra were the change in abundance ratio of low m/z ions (<100 a.m.u.), and the lack of a molecular ion and other high m/z characteristic ions. These differences made identification challenging, but did not preclude matching of previously collected mass spectra with spectra collected in this study.

In the analysis of oxidation products in the SOA sample, the mass spectra of each derivatized or underivatized compound was tabulated as a positively identified compound, a tentatively identified compound, an unknown derivative, or an unknown oxidation product. Positive identification was limited to a small number of compounds for which authentic standards were available. If no identification could be made, but a molecular ion could be recognized, a molecular mass was associated with the component.

Characteristic ions previously noted in mass spectra of α-pinene oxidation products, in particular those containing the backbone 2,2-dimethyl-cyclobutyl structure, were used to recognize peaks corresponding to oxidation products in sample chromatograms. These

ions were also used in assigning a structure for interesting mass spectra. Figure 3.3 shows the structure of pinic acid with the common ring-opening structure and thus common characteristic ions of most α-pinene ozonolysis products.

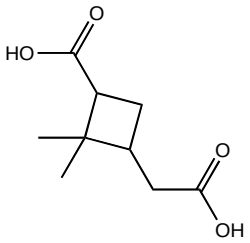

Figure 3.3. Chemical structure of an α-pinene ozonolysis product, pinic acid, displaying the 2,2-dimethyl-cyclobutyl backbone and functionalization at carbon atoms 1 and 3 of the cyclobutyl ring.

The 2,2-dimethyl-cyclobutyl centers of ring-opening α- and β-pinene oxidation products are most often functionalized at carbon atoms 1 and 3 of the ring; characteristic fragments used in compound identification arise mostly from fragmentation around these functional groups (Yu, *et al.,* 1998; Jaoui & Kamens, 2001). Radical-site initiation, also referred to as α-cleavage (McLafferty & Tureček, 1993), is a primary fragmentation process for functionalities containing carbonyl groups. For example, the ion with m/z 111 in α-pinene ozonolysis product mass spectra often corresponds to the fragment 2,2-dimethyl-cyclobutyl-formaldehyde (with one radical at the site of a removed hydrogen atom, likely located on the cyclobutyl ring). The ion with m/z 111 therefore appeared almost exclusively in aldehyde mass spectra among α-pinene oxidation products (Table 3.8).

Table 3.8. Characteristic ions of alpha-pinene oxidation products with the central structure 2,2-dimethyl-cyclobutane. Not all ions could be associated with only one characteristic fragment, so multiple ions were necessary for the identification of a component based on a mass spectrum.

Mass to Charge Ratio	Identified Group(s)
69, 83	Underivatized mono-acids, alcohols, ketones
82, 100	Underivatized di-acids
83, 71 (strong)	Underivatized mono-acids
111	Aldehydes
114	Carboxylic acids
124	Carboxylic acids, aldehydes, ketones
125	CH_2-aldehydes
126	Acids, ketones
141	CH_2-acids

Despite the large number of characteristic ions that have been documented and recognized here, some mass spectra generated from derivatization/GC×GC/TOF-MS analysis of α-pinene ozonolysis products did not contain sufficient unambiguous characteristic ions for tentative identification of the parent compound or its functional groups. For example, although strong peaks at m/z 71 and 83 were associated by Jaoui & Kamens (2001) with mono-acids, the presence of these ions (in ~40 and 100% abundance) were observed in the norpinonaldehyde mass spectrum (having no acid groups) in the same publication.

There was uncertainty in particular, in the identification of di-acids because both di-acids and ring-retaining products in previously published mass spectra displayed a peak at m/z 82. Ring-retaining products were also noted to fragment characteristically to produce an ion with m/z 95, but this ion was observed in the mass spectra of pentafluorobenzyl hydroxylamine (PFBHA)/BSTFA derivatized pinonaldehyde and hydroxy

pinonaldehyde, ring-retaining oxidation products were therefore particularly difficult to identify. Despite these discrepancies, some identifications were tentatively made in this study based on the presence of multiple characterstic ions. The continued use and examination of these similarly structured α-pinene ozonolysis products will allow for more certainty in the identification of functional groups and oxidation products using mass spectral patterns.

3.3.3.2 Mass Spectra of BSTFA Derivatized α-Pinene Ozonolysis Products

The presence of characteristic ions from derivatized 2,2-dimethyl-cyclobutyl groups showed whether the mass spectrum of an α-pinene ozonolysis product pertained to a compound functionalized by a BSTFA reactive group (Table 3.9).

Table 3.9. Characteristic ions of α-pinene oxidation products noted in prior studies or discovered by examination of published and analyzed spectra. Jaoui & Kamens, 2001, and Yu, *et al.,* 1999.

Mass to Charge Ratio	Fragment or Identified Group(s)
73	All TMS; $[Si(CH_3)_3]^{\cdot+}$
89	All TMS; $[OSi(CH_3)_3]^{\cdot+}$
117	TMS esters; $[COOSi(CH_3)_3]^{\cdot+}$
123	TMS CH_2-esters, 2,2-dimethyl-cyclobutyl
129	TMS esters, ethers, 2,2-dimethyl-cyclobutyl
131	TMS CH_2-esters, 2,2-dimethyl-cyclobutyl
143	TMS CH_2-esters, 2,2-dimethyl-cyclobutyl
147	bis(TMS) esters; $[(CH_3)_2Si{=}OSi(CH_3)_3]^{\cdot+}$

The most common of the characteristic ions in BSTFA derivatized mass spectra were: m/z 131, hypothesized to correspond to a β-cleavage from the carboxylic site and a McLafferty rearrangement to protonate the carbonyl carbon of the carboxylic group, and m/z 143, corresponding to cleavage of the 2,2-dimethyl-cyclobutyl group at β and δ sites

from the carboxylic acid carbonyl (Figure 3.4).

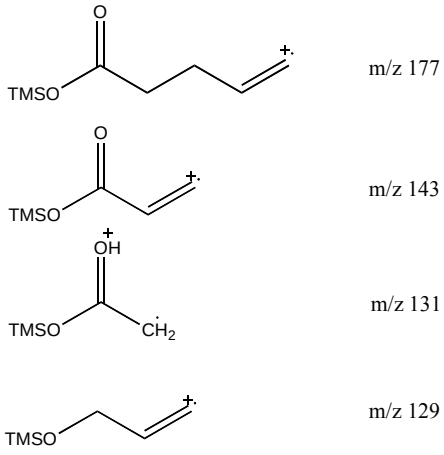

Figure 3.4. Hypothesized BSTFA derivatized fragments appearing in the mass spectra of BSTFA derivatized α-pinene ozonolysis products.

Although BSTFA derivatized α-pinene ozonolysis product mass spectra generally showed a high abundance characteristic ion at m/z 73 (expected for trimethylsilyl derivatives), this was not true of all BSTFA derivative mass spectra.

The molecular ions in most collected mass spectra were not identifiable; however, many spectra of BSTFA derivatized compounds tabulated in the NIST mass spectral library showed a $[M-15]^+$ ion; the ion corresponding to this loss could be used in some mass spectra to identify the molecular weight of a compound. Tentative identifications were only made when multiple ions shown in the mass spectrum could be associated with predicted fragments, and the molecular ion was present or characteristic losses (such as $[M-73]^+$ or $[M-15]^+$) were present.

All spectra from the BSTFA derivatized SOA sample 26-3 are tabulated in Appendix F, Table R; the spectra of the most abundant peaks and associated identifications are given in Table 3.10.

Table 3.10. Selected mass spectra of α-pinene ozonolysis products detected using TMS/GC×GC/TOF-MS in SOA sample 26-3 (all spectra are in Appendix F, Table B). Only some molecular ions were present; the value of the MW is listed ("Deriv. M.W." is the derivatized molecular weight; "Un. M.W." is the underivatized MW of each compound). Mass spectra are shown with horizontal axis as m/z ratio, and vertical axis as relative abundance.

Peak	Identification	^1t_R (sec)	^2t_R (sec)	Mass Spectrum and Closest NIST Library Match (m/z Ratio Horizontal Axis: Rel. Abund. Vertical Axis)
1	Unknown oxidation product M.W. 128 $C_7H_{12}O_2$ e.g. 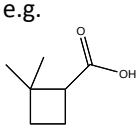	848.0	1.76	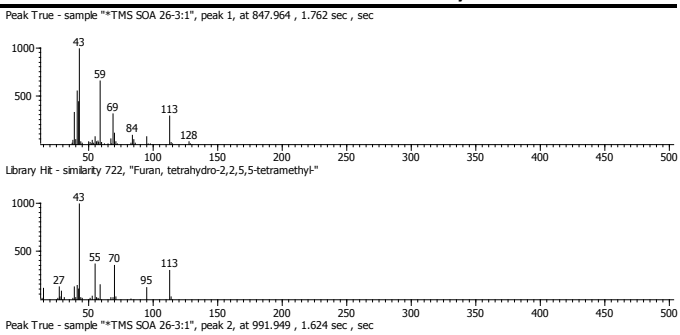
2	Unknown oxidation product Carboxylic acid	992.0	1.62	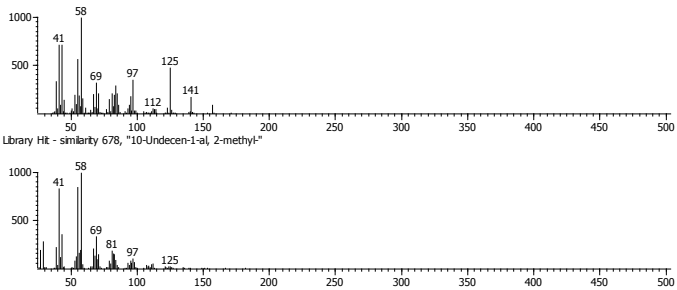
3	Norpinonaldehyde, underivatized M.W. 154 Aldehyde 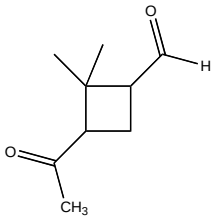	1008.0	1.93	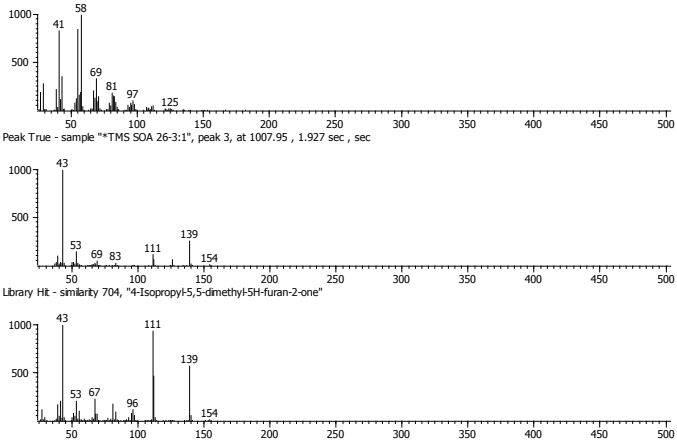

Peak	Identification	^1t_R (sec)	^2t_R (sec)	Mass Spectrum and Closest NIST Library Match (m/z Ratio Horizontal Axis: Rel. Abund. Vertical Axis)
9	Pinalic-4- acid, underivatized M.W. 170 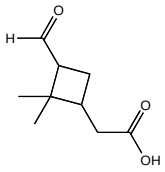	1147.9	1.72	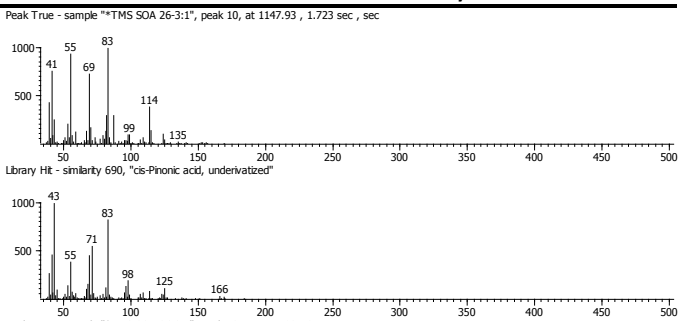
11	Unknown oxidation product M.W. 198 Methylene carboxylic acid e.g. 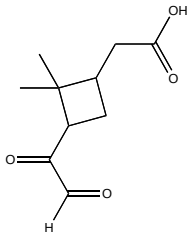	1155.93	2.145	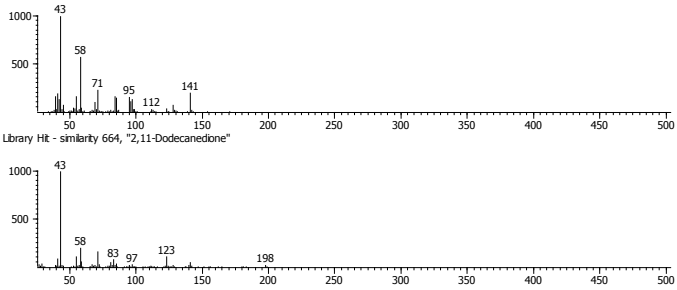
16	Unknown TMS derivative Alcohol or carboxylic acid	1215.9	1.47	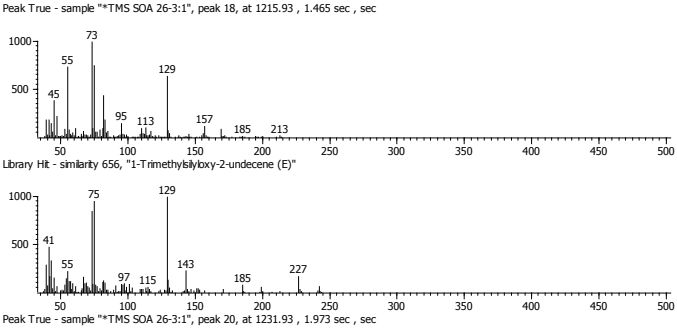
17	Norpinic acid, underivatized M.W. 186 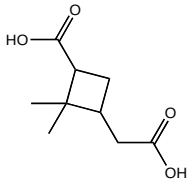	1231.9	1.97	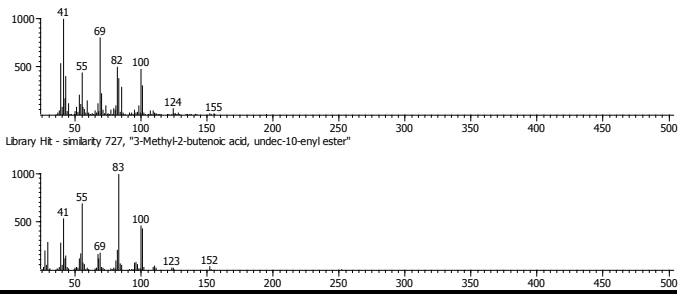

Peak	Identification	^1t_R (sec)	^2t_R (sec)	Mass Spectrum and Closest NIST Library Match (m/z Ratio Horizontal Axis: Rel. Abund. Vertical Axis)
20	Pinonic acid, underivatized M.W. 184 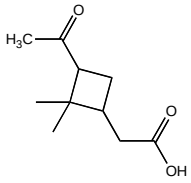	1331.9	1.88	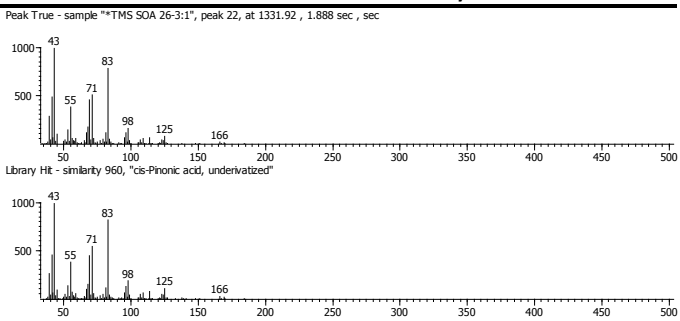
25	Pinic acid, underivatized M.W. 186 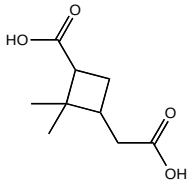	1423.9	2.03	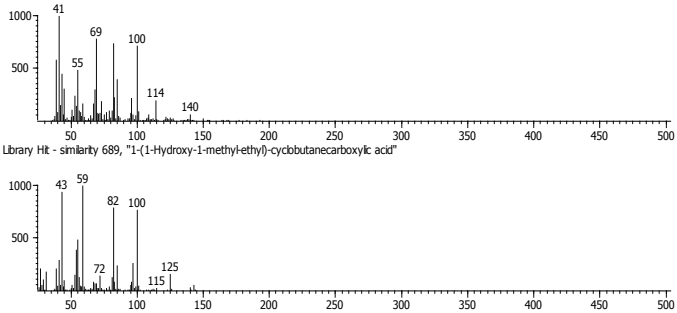
27	Pinonic acid, TMS derivative Deriv. M.W. 256 Un. M.W. 184 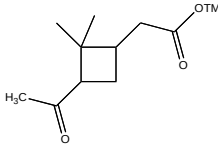	1439.9	1.53	See calibration standard spectrum
28	Unknown oxidation product M.W. 154 Aldehyde	1439.9	2.33	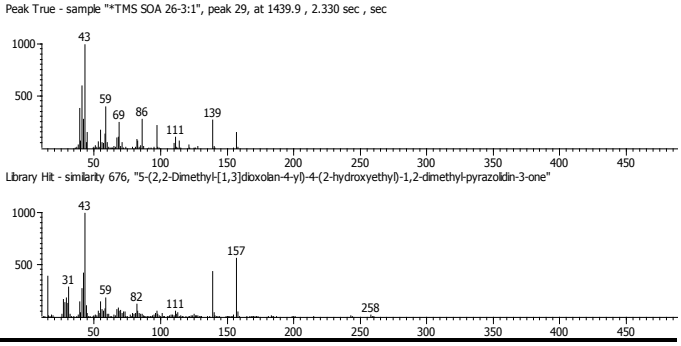

Peak	Identification	^1t_R (sec)	^2t_R (sec)	Mass Spectrum and Closest NIST Library Match (m/z Ratio Horizontal Axis: Rel. Abund. Vertical Axis)
30	Unknown TMS derivative Deriv. M.W. 318 Un. M.W. 174 Carboxylic acid	1459.9	1.27	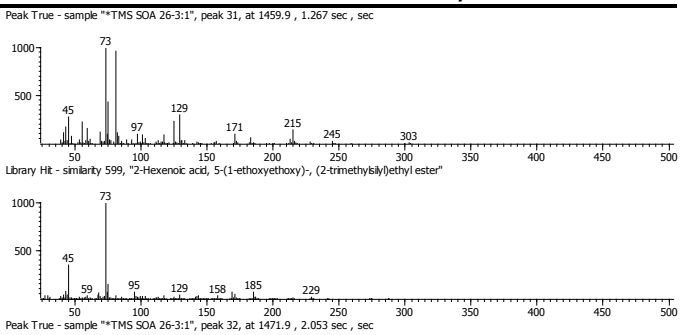
31	Unknown oxidation product Alcohol, carboxylic acid, or ketone	1471.9	2.05	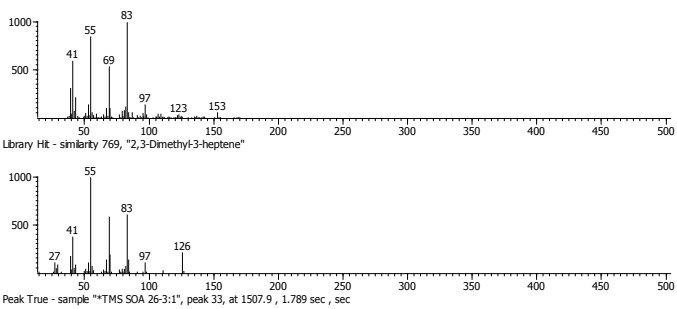
32	Norpinic acid, TMS ester Deriv. M.W. 316 Un. M.W. 172 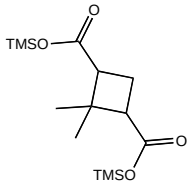	1507.9	1.79	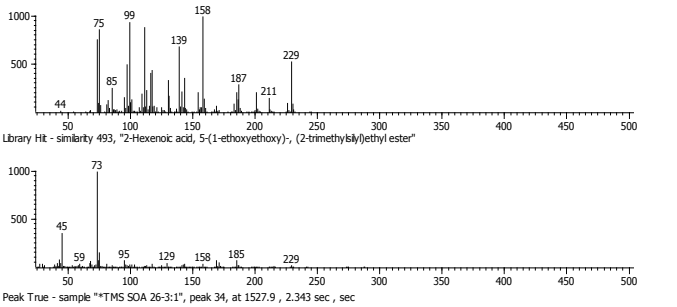
33	Oxo-Pinonic acid M.W. 198 e.g. 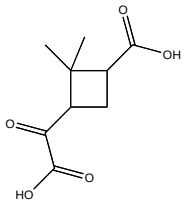	1527.9	2.34	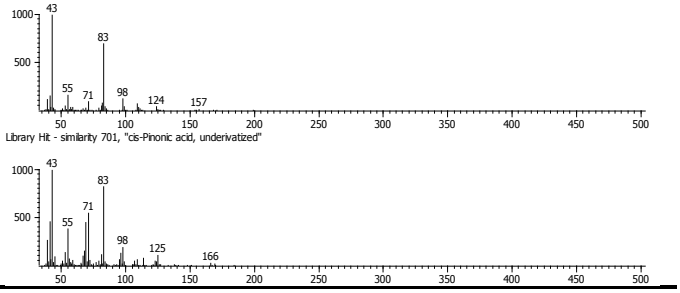

Peak	Identification	^1t_R (sec)	^2t_R (sec)	Mass Spectrum and Closest NIST Library Match (m/z Ratio Horizontal Axis: Rel. Abund. Vertical Axis)
34	Hydroxy pinonaldehyde Deriv. M.W. 256 Un. M.W. 184 e.g. 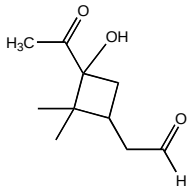	1535.9	1.60	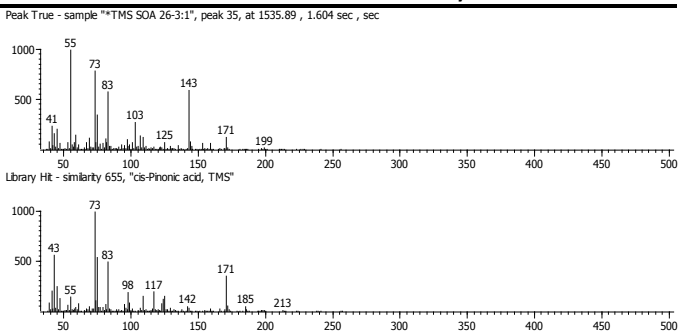
35	Pinic acid, TMS di-ester Deriv. M.W. 330 Un. M.W. 186 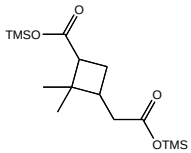	1603.9	1.44	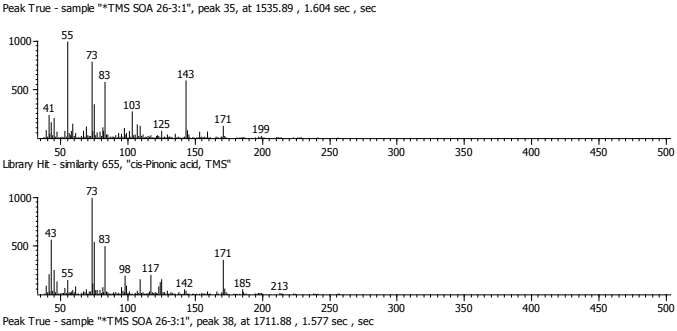
37	Unknown TMS derivative Carboxylic acid	1711.9	1.58	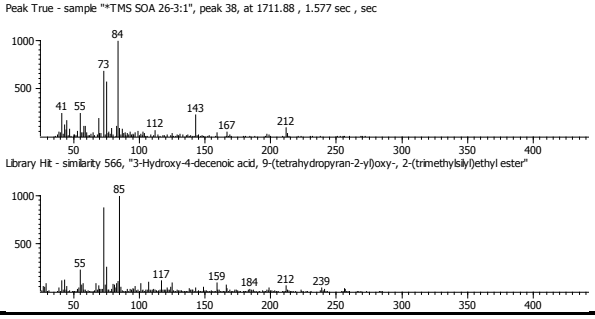

While no explicit identifications of previously unidentified α-pinene ozonolysis products were made using TMS/GC×GC/TOF-MS, several mass spectra did not match with previously identified α-pinene oxidation product spectra. Of the 33 components detected using TMS/GC×GC/TOF-MS, 11 components could be positively identified and some functional group identification was possible for 17 unidentified components. The molecular weights, however, of 20 components could not be recognized. The

identifications tentatively and positively made for other mass spectra in Table 3.10 are explained below.

The fragments at m/z 82 and 100 in mass spectra were reliable ions for unambiguous identification of di-acid α-pinene oxidation products, but in the spectra of both BSTFA derivatized pinic and norpinic acids (peaks #17 and 25), the ions with m/z 82 and 100 were not present; the spectra for these two di-esters in fact did not show any significant common fragments (in agreement with the spectra of PFBHA/BSTFA derivatized pinic and norpinic acids from Yu, *et al.*, 1999). The ion with m/z 147 found in BSTFA derivatized di-acids was not observed in di-acid α-pinene oxidation products with a 2,2-dimethyl-cyclobutyl central structure. The peak at m/z 117, however, which is normally associated with all TMS esters, was observed in mono-acid esters.

A handful of ozonolysis products were tentatively identified; pinonic acid was the only compound positively identified because an authentic standard was available. A molecular ion as well as an $[M-15]^+$ ion were present in the spectrum at 1147.9 sec, 1.72 sec, associated with the compound pinalic-4-acid. The sequence of ions m/z 55, 69, and 83, as well as the diagnostic ion at m/z 114 were used to identify the presence of a mono-acid. The mass spectrum of the authentic standard of *cis*-pinonic acid was used in identifying not only pinonic acid within α-pinene ozonolysis products, but also similar compounds. Oxo-pinonic acid was identified (1527.9 sec, 2.34 sec; #33) as being structurally similar to pinonic acid by its mass spectrum, but the higher MW of #33 versus pinonic acid indicated that some part of the structure was different. The molecular

ion at m/z 198 allowed the identification of this compound as an oxo-pinonic acid. A further identification as to the placement of the additional carbonyl group could not be made because no mass spectra of previously identified oxo-pinonic acids were available for comparison, and no characteristic fragments particular to the carbonyl position could be recognized.The identification of norpinonaldehyde at 1008.0 sec, 1.93 sec was made based on the detection of the ion with m/z 111 as well as the presence of a strong $[M-15]^+$ and molecular ion at m/z 139 and 154, respectively. The mass spectrum presented in Jaoui & Kamens (2001) was significantly different from this spectrum; the much lower abundance of the ions at m/z 55, 69, and 83 in the observed mass spectrum was in particular different; this could be explained by the often higher abundances of low molecular weight fragments in TOF mass spectra.

The mass spectra of α-pinene oxidation products that did not appear to match the few published spectra or predicted fragmentation patterns of oxidation products were recognized only as *potential* unidentified products. The unknown oxidation product at peak #1, for example, was given a possible structure, 2,2-dimethyl-cyclobutyl-methanoic acid. This identification has not previously been reported in α-pinene oxidation samples, but not all fragments predicted for this product were shown in the mass spectrum at 848.0 sec, 1.76 sec. A component similar to norpinonaldehyde was tabulated as peak #7 (1439.9 sec, 2.33 sec): the molecular weight was 154, and an aldehyde was indicated by the presence of a peak at m/z 111. However, other ions in the mass spectrum did not match those of the published spectrum for norpinonaldehyde, including the series m/z 55,

69, and 83. Unknown oxidation product #8 appeared to be an underivatized carboxylic acid with a molecular weight of 130 a.m.u.; a MW of 142 a.m.u. was found for unknown TMS derivative at #19. Neither of these molecular weights could be associated with previously identified α-pinene oxidation products. The presence of peaks at and just below m/z 170, and at m/z 155, in the mass spectrum of unknown oxidation product #31 (1471.9 sec, 2.05 sec) indicate that the MW of this underivatized compound is likely 170 a.m.u. This MW has been reported for the α-pinene oxidation products pinalic-4-acid and norpinonic acid, neither of which are predicted to give fragments shown in the mass spectrum of peak #31 (other characteristic ions are expected for both compounds, and pinalic-4-acid was associated with a separate mass spectrum). Abundant peaks at m/z 55, 69, and 83 are indicative of either an alcohol, mono-acid, or ketone within the structure of the compound.

Some compounds could be identified only by functional groups and in some cases MW. Unknown oxidation product at #11, with a recognizable methylene carboxylic acid and M.W. 198 a.m.u. (1155.9 sec, 2.15 sec), was similar to component A_{14} in Yu, *et al.*, 1999, but could not be positively identified as the same component without comparison to the mass spectrum of A_{14}. The MW of unknown TMS derivative #30 (1459.9 sec, 1.27 sec) was 174 a.m.u. (based on the presence of peaks corresponding to [M-73] and [M-15] losses), which does not correspond to a known α-pinene oxidation product. The ions at m/z 117 and 129 additionally indicated that the compound is a carboxylic acid and that the chemical formula was either $C_9H_{16}O_3$ or $C_8H_{14}O_4$.The presence of a carboxylic acid

was recognized, for example, in the structure corresponding to unknown oxidation product #2 (992.0 sec, 1.62 sec) by the fragments at m/z 125 and 141. The spectrum of unknown TMS derivative #29 did not allow distinction between an alcohol or carboxylic acid (m/z 129). No molecular ion was obvious, however, so that losses such as $[M-15]^+$ and $[M-73]^+$ could not be easily recognized.

3.3.4 Compound Identifications: BF_3/Butanol α-Pinene Ozonolysis Products

Butylated sample components gave mass spectra with common characteristic ions, allowing quick distinction between the derivatized acid, aldehyde and ketone groups in a given α-pinene ozonolysis sample chromatogram and product mass spectrum (Table 3.11).

Table 3.11. Characteristic ions of butylated pinene oxidation products noted in prior studies or discovered by examination of published and analyzed spectra.

Mass to Charge Ratio	Fragment or Identified Group(s)
57	All butyl; $[(CH_2)_3CH_3]^{\cdot+}$
61	Dibutyl ketals; $[CH_3C(OH)_2]^{\cdot+}$
103	Dibutyl acetals; $[CH(OC_4H_9)OH]^{\cdot+}$
117	Dibutyl ketals; $[CH_3C(OC_4H_9)OH]^{\cdot+}$
159	Dibutyl acetals; $[CH(OC_4H_9)_2]^{\cdot+}$

The characteristic ions of butylated ozonolysis products appeared in groupings: m/z 57/103/159 in mass spectra of butylated aldehydes (dibutyl acetals), and m/z 61/117 in mass spectra of butylated ketones (dibutyl ketals). The butyl group (m/z 57) appeared in all butylated mass spectra including those of carboxylic acids (butyl esters).

The extracted ion chromatograms (Figure 3.1a and b; Appendix F, Table Q) show the diagnostic utility of butylation: the presence of functional groups can be identified immediately upon inspection of these characteristic ions. The appearance of peaks in multiple extracted ion chromatograms for characteristic ions (excluding m/z 57) indicates that the compounds were multifunctional, and derivatized at multiple sites. The presence of these ions in individual mass spectra was also effective for the functional group identification of most chromatographic peaks.

3.3.4.1 Mass Spectra of BF_3/Butanol α-Pinene Ozonolysis Products

Similar to the mass spectra of BSTFA derivatized compounds, the molecular ions in butylated spectra were very low abundance or not present. In most cases, an ion appeared at either $[M-73]^+$ or $[M-74]^+$, corresponding to whether or not, respectively, a fragment was observed at m/z 73. However, the $[M-73]^+$ and $[M-74]^+$ fragments were not easily identifiable in most spectra. While $[M-15]^+$ ions were common in BSTFA derivatized mass spectra, the fragment corresponding to this loss was not often present in butylation/GC×GC/TOF-MS spectra.

Identifications of the butylated ozonolysis products were made based on the molecular ion if present, as well as the ions characteristic of α-pinene ozonolysis products (Table 3.7) and butylated compounds. Some authentic standards for identified sample components were available: oxalic acid, malonic acid, glyoxylic acid, glyoxal, and pinonic acid. The spectra corresponding to a large percentage of the mass in the

butylation/GC×GC/TOF-MS results as well as any spectra that are particularly interesting for discussion are presented in Table 3.12.

Table 3.12. Selected mass spectra of α-pinene ozonolysis products identified using butylation/GC×GC/TOF-MS in SOA sample 26-3 (all spectra are in Appendix F, Table A). Only some molecular ions were present; the value of the MW is listed ("Deriv. M.W." is the derivatized molecular weight; "Un. M.W." is the underivatized MW of each compound). Mass spectra are shown with horizontal axis as m/z ratio, and vertical axis as relative abundance.

Peak	Identification	^1t_R (sec)	^2t_R (sec)	Mass Spectrum and Closest NIST Library Match (m/z Ratio Horizontal Axis: Rel. Abund. Vertical Axis)
5	Oxidation product Possible M.W. 202 Ring opening product with possible aldehyde	1051.9	1.33	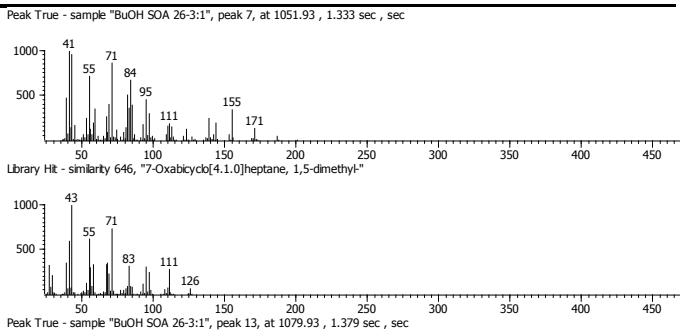
8	Pinalic-4-acid M.W. 170	1079.9	1.38	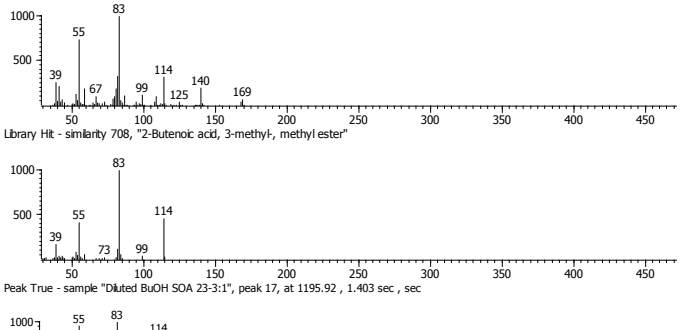
16	Dimethyl pinate M.W. 214	1191.9	1.28	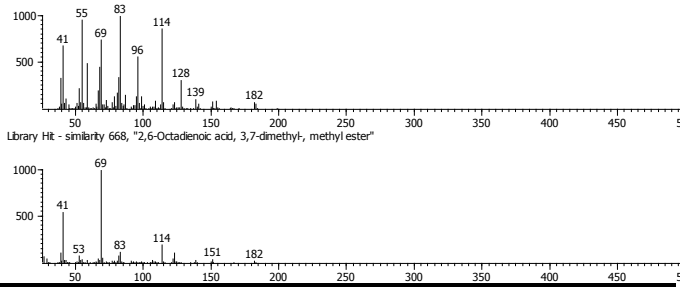

Peak	Identification	^1t_R (sec)	^2t_R (sec)	Mass Spectrum and Closest NIST Library Match (m/z Ratio Horizontal Axis: Rel. Abund. Vertical Axis)
22	4-oxo-Pinonic acid, underivatized M.W. 198 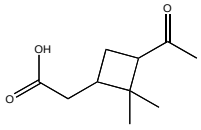	1175.9	1.46	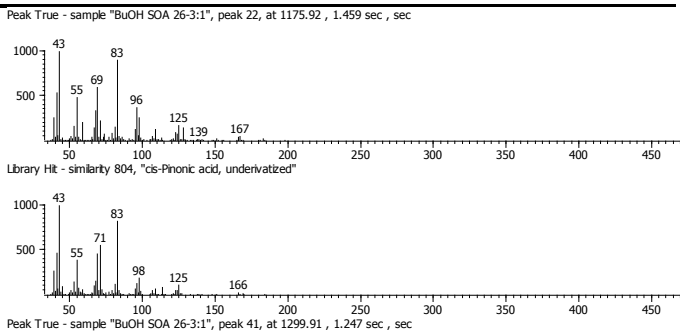
25	Butyl derivative Deriv. M.W. 236 Un. M.W. 180 Ring-retaining carboxylic acid	1299.9	1.25	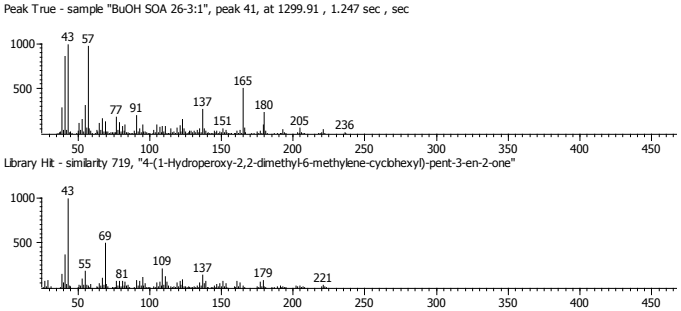
26	Oxidation product	1335.9	1.37	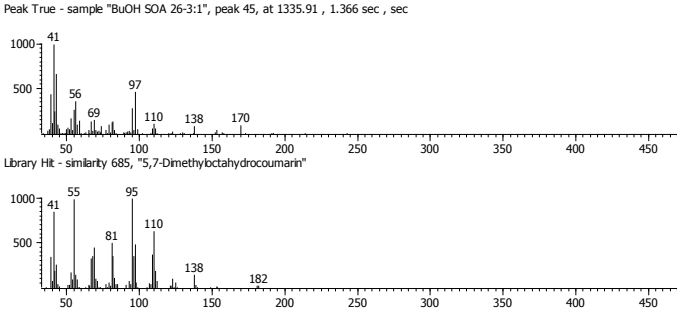
31	Pinalic-4-acid, butyl derivative Deriva M.W. 338 Un. M.W. 170 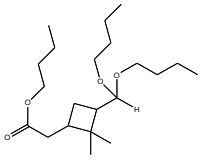	1371.9	1.44	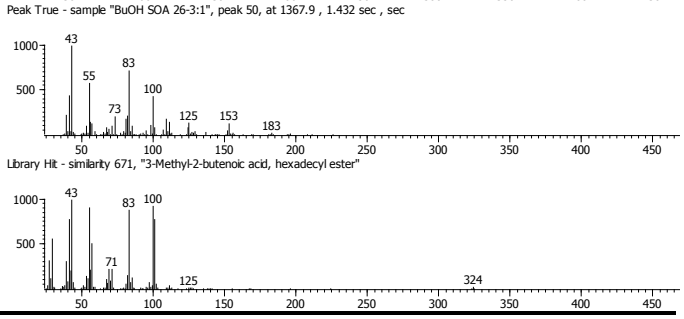

Peak	Identification	^1t_R (sec)	^2t_R (sec)	Mass Spectrum and Closest NIST Library Match (m/z Ratio Horizontal Axis: Rel. Abund. Vertical Axis)
40	Pinonic acid, butyl ester Deriv. M.W. 240 Un. M.W. 184 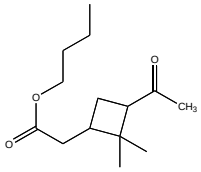	1479.9	1.47	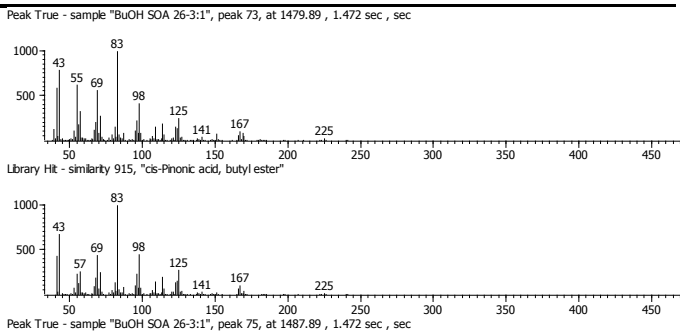
41	Hydroxy pinonic acid, butyl ester Deriv. M.W. 256 Un. M.W. 200 e.g. 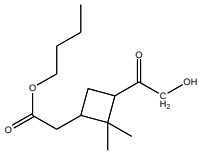	1487.9	1.47	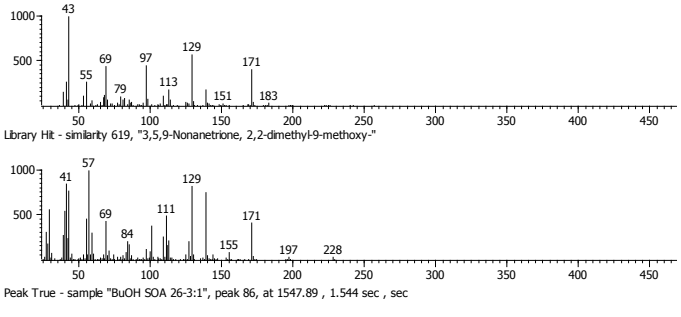
45	Oxidation product Deriv. M.W. 224 Un. M.W. 168 Carboxylic acid	1547.9	1.54	
54	Glyoxal, tetrabutyl acetal Deriv. M.W. 318 Un. M.W. 58 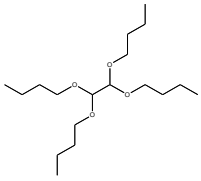	1599.9	1.21	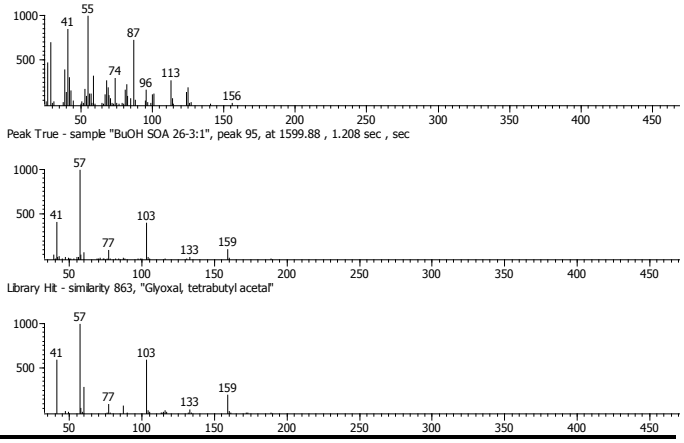

Peak	Identification	^1t_R (sec)	^2t_R (sec)	Mass Spectrum and Closest NIST Library Match (m/z Ratio Horizontal Axis: Rel. Abund. Vertical Axis)
64	Norpinonaldehyde, butyl derivative M.W. 284 Un. M.W. 154	1739.9	1.45	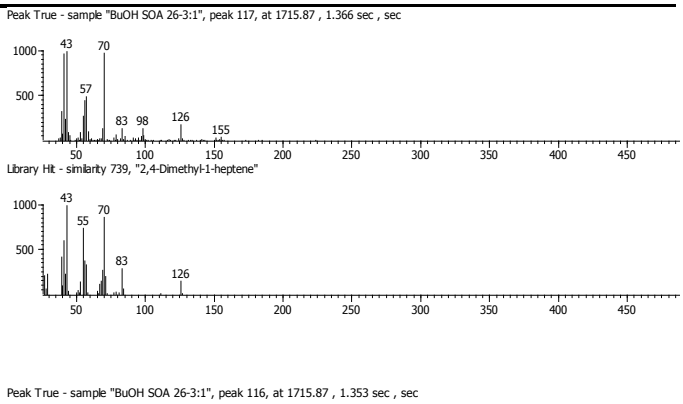
65	Norpinonaldehyde, butyl derivative (2)	1739.9	1.45	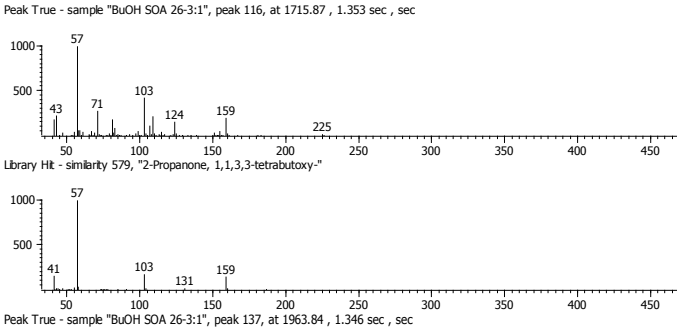
74	Pinonaldehyde, dibutyl acetal Deriv. M.W. 298 Un. M.W. 168	1963.8	1.35	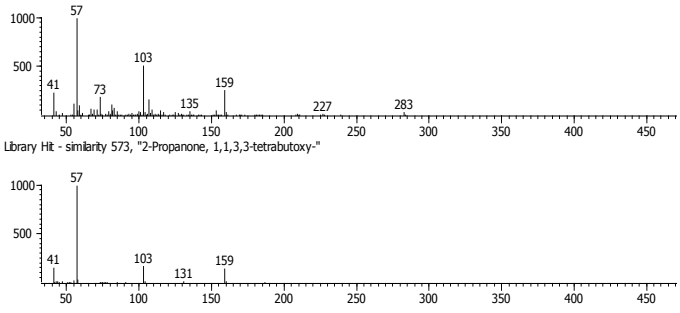
75	Pinonaldehyde, dibutyl acetal (2)	1963.8	1.35	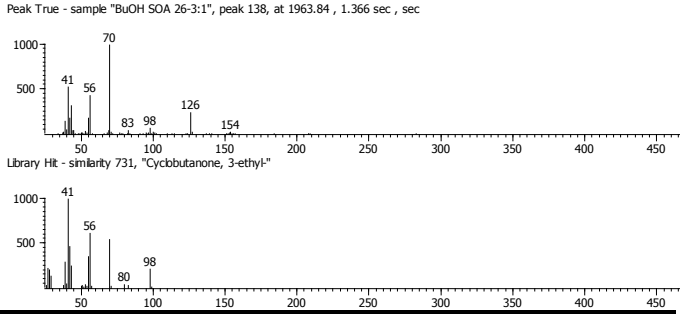

Several mass spectra corresponded to previously unidentified α-pinene ozonolysis products: glyoxylic acid and three LMW straight-chain di-acids were positively identified as butyl derivatives. These compounds were determined to be in the SOA sample at concentrations above those in the blank (the travel blank was used). Only pinonic acid was positively identified and not found in blank extracts. Explanations for the tentative identifications made of α-pinene ozonolysis an SOA sample 26-3 using butylation/GC×GC/TOF-MS presented in Table 3.12 are given below.

Butyl derivative #8 (1367.9 sec, 1.43 sec; #8) was determined to be pinalic-4-acid by noting the molecular ion at m/z 226, giving an underivatized MW of 170 a.m.u. The [M-56] loss was likely associated with a McLafferty rearrangement, protonating the carboxylic acid carbonyl oxygen, and subsequent loss of the remaining butyl group. A carboxylic acid was therefore identified in this oxidation product. The presence of a peak at m/z 111 indicated that the compound was pinalic-4-acid and not norpinonic acid (which has the same underivatized MW). This identification was confirmed by comparison of the methylated derivative (Ma, *et al.*, 2008 Supporting Info). Note that the fragments associated with the dibutyl acetal portion of the derivatized compound were of too low intensity to be detected. One ozonolysis product mass spectrum was availble in the Wiley library in addition to pinonic acid: the dimethyl pinate spectrum was used to positively identify the compound at 1191.9 sec, 1.43 sec (#16). The diagnostic series at m/z 55, 69, and 83 were present in this spectrum, as was a very strong ion at m/z 114, indicating the presence of a carboxylic acid. There is some evidence from previous

analyses of standard carboxylic acids that methyl esters form because of the presence of methanol in solution. As noted previously. it is probable that the dimethyl pinate was a product of methylation of pinic acid, and was not actually present in the original sample. 4-oxo-pinonic acid was identified (1175.9 sec, 1.46 sec; #22) by comparison to the mass spectrum for the authentic standard of *cis*-pinonic acid. The greater MW than pinonic acid indicated that a third functional group was present and the lack of m/z 111 peak indicated that the group was not an aldehyde. Oxidation product #4 (1487.9 sec, 1.47 sec; #41) was identified as hydroxy pinonic acid, butyl ester, in a similar way, using the mass spectrum of pinonic acid, butyl ester, and the higher MW of product #41. The two mass spectra shown in Table 3.12 tentatively associated with norpinonaldehyde (peaks #64 and 65) display the m/z 57, 103, and 159 ions expected for a dibutyl acetal, as well as m/z 71 and 83 found in the norpinonaldehyde underivatized spectrum (Jaoui & Kamens, 2001). No molecular ion was apparent; the molecular ions for high MW butyl derivatives, however, were not present throughout the sample chromatograms. The butyl derivative of pinonaldehyde (peaks #74 and 75) was tentatively identified at 1963.8 sec, 1.35 sec using similar ions to those found in the mass spectra of norpinonaldehyde.

Compounds that did not match previously identified α-pinene ozonolysis product mass spectra or predicted fragments were detected using butylation/GC×GC/TOF-MS. The mass spectrum of unknown butyl derivative #26 (1335.9 sec, 1.36 sec) displayed a relatively strong $[M-15]^+$ peak at the high m/z 22. In agreement with the loss [M-56] to give m/z 186, this showed that the MW of the derivatized compound was 242 a.m.u. No

previously identified α-pinene oxidation products have to an underivatized MW of 156 a.m.u., but this assignment was uncertain because no molecular ion was present. The strong peak at m/z 111 indicated the presence of an aldehyde in the structure of this component, as noted earlier. The unknown butyl derivative eluting at 1547.9 sec, 1.54 sec (peak #45) was also recognized as a potentially previously unidentified ozonolysis product: the MW only corresponded to the known product pinonaldehyde, which was tentatively identified elsewhere in the chromatogram, and 2-hydroxy-3-pinanone (Jaoui & Kamens, 2001), which does not have a carboxylic acid in its structure. Although m/z 114 displated within the mass spectrum of peak #45 was assumed to correspond to a carboxylic acid, it is possible that some rearrangement fragments could give m/z 114 (a loss of [M-54] from the underivatized structure); no tentative identification was made for this sample component.

Some α-pinene ozonolysis products were detected but could not be identified or associated with known ozonolysis products. A loss of [M-56] was used to recognize many butylated carboxylic acids such as butyl derivative #25, eluted at 1299.9 sec, 1.25 sec. As in the mass spectra of BSTFA derivatized ozonolysis products, identifications were very challenging without the recognition of a molecular ion. Unknown oxidation product #5 (1051.9 sec, 1.33 sec) could not be tentatively identified because ions in the mass spectrum for this component were dissimilar from those in published α-pinene oxidation product spectra. It is probable that this component is a ring-opening product because of the ion at m/z 95, as well as the presence of multiple ion series in the low

mass range of the spectrum (typically seen in mass spectra both alkanes and cyclic structures).

3.3.5 Compound Identifications: Underivatized α-Pinene Ozonolysis Products

To show the advantage of derivatization for GC×GC/TOF-MS analysis, underivatized α-pinene ozonolysis product mass spectra were also tabulated. The components identified did not necessarily have the same retention times when analyzed within derivatized versus underivatized solutions because of the matrix effects of the derivatization reagent and derivatives themselves. However, the mass spectra of underivatized compounds were generally reproducible between derivatization methods.

A large number of component identifications were possible using derivatization, and the chromatographic characteristics of polar, oxygenated components were improved by derivatization. The components identified tentatively in chromatograms of underivatized filter extracts as carboxylic acids, and particularly those with multiple carboxylic acid groups, showed significant peak tailing in both dimensions. This was likely due in part to overconcentration of sample components, but also to interaction of the polar oxygenated components with the stationary phase of the column. Despite the gas chromatograph settings optimized for oxygenated compounds, including a slow temperature program, the peak tailing was sufficient to cause ambiguity between the presence of multiple components versus simply peak "slices" within the underivatized sample chromatogram (Figure 3.5).

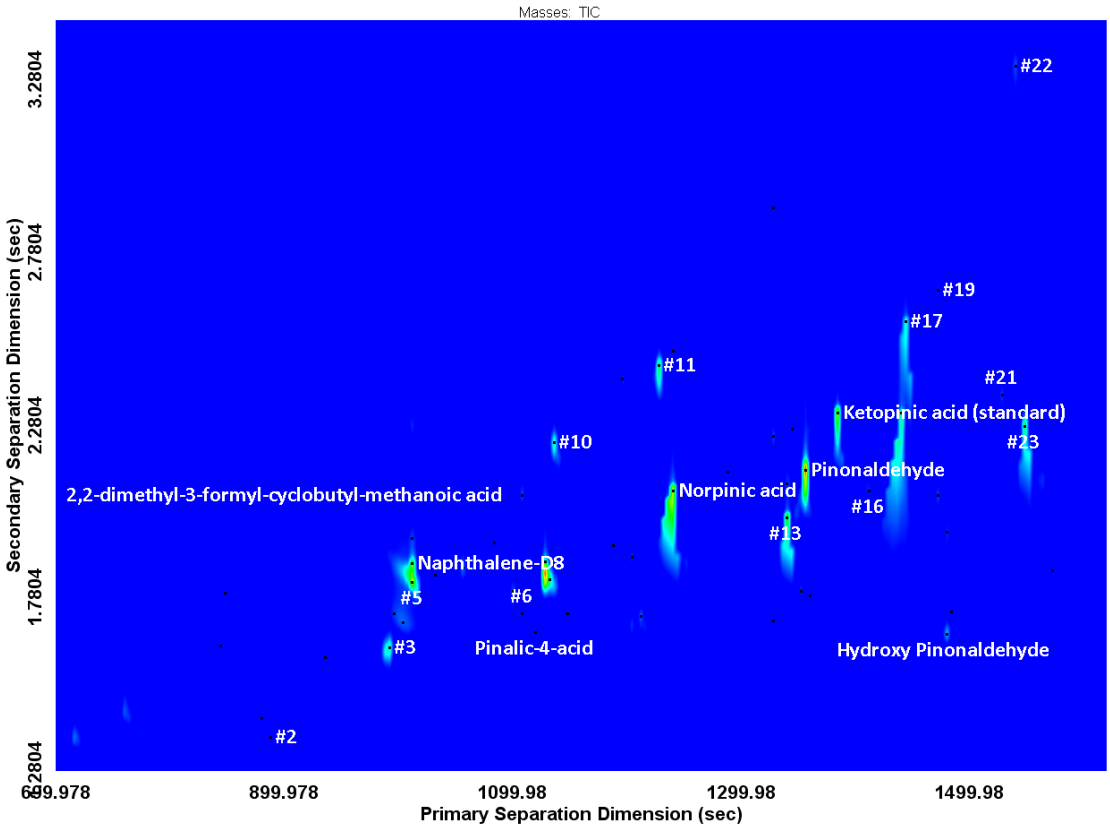

Figure 3.5. GC×GC/TOF-MS extracted ion chromatogram of underivatized SOA sample 6/26/11-3 showing the sum of the masses 82 and 100, which correspond to di-acid α-pinene oxidation products. High peak tailing is noted for the two large peaks (norpinic and pinic acids) because of a high degree of interaction

Peak tailing was observed for pinic acid (1455.9 sec, 2.30 sec) and norpinic acid (1247.9 sec, 2.12 sec). A 1:3 dilution was made of BSTFA derivatized SOA components when over-saturation was discovered; however, the dilution caused several compounds initially detected in the un-diluted sample to go un-detected and a dilution was therefore not made of the underivatized components.

Results obtained after initial, automated data processing for GC×GC/TOF-MS chromatograms were more challenging to finish analyzing when ambiguous tailing, as seen in underivatized sample chromatograms, was present. This was because the mass

spectral abundance ratios and fragments varied throughout the area of these tailing peaks. These tailing peaks were particularly problematic for analysis of complex samples in which components were likely to co-elute with tailing peaks. Derivatization in general decreased this tailing effect (particularly in the second dimension) and increased the range of retention times between derivatized and underivatized components (this allowed better separation between components).

3.3.5.1 Mass Spectra of Underivatized α-Pinene Ozonolysis Products

The GC×GC/TOF-MS mass spectra of the underivatized components of SOA 26-3 are tabulated below (Table 3.13). As with the derivatized mass spectra, tentative identifications were made based on comparisons to available spectra from publications and the NIST and Wiley mass spectral libraries, or from predicted fragmentation pathways of known α-pinene oxidation products. The peak areas of underivatized components can be used as a rough estimate (assuming equal sensitivity of the method to each component) of the amounts of the underivatized components in the sample.

Table 3.13. Mass spectra of α-pinene ozonolysis products identified using GC×GC/TOF-MS without derivatization in SOA sample 23-3. No calibration was made for underivatized compounds, so no quantitation is presented. Instead, the absolute peak area values are given here so that the relative component amounts can be estimated by assuming similar sensitivities of the method to each component. Only some molecular ions were present; the value of the MW is listed ("Deriv. M.W." is the derivatized molecular weight; "Un. M.W." is the underivatized MW of each compound). Mass spectra are shown with horizontal axis as m/z ratio, and vertical axis as relative abundance.

Peak	Name	^1t_R (sec)	^2t_R (sec)	Peak Area	Mass Spectrum and Closest NIST Library Match (m/z Ratio Horizontal Axis: Rel. Abund. Vertical Axis)
1	2,2-dimethyl-cyclobutyl-methanoic acid Un. M.W. 140 Carboxylic acid	840.0	1.68	10866097	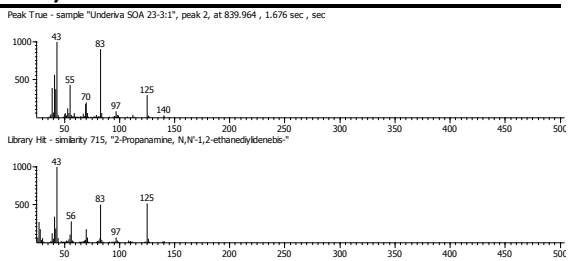
2	Unknown Oxidation Product	888.0	1.42	31523954	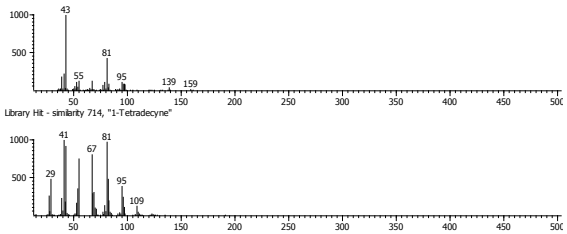
3	Unknown Oxidation Product	992.0	1.63	82015902	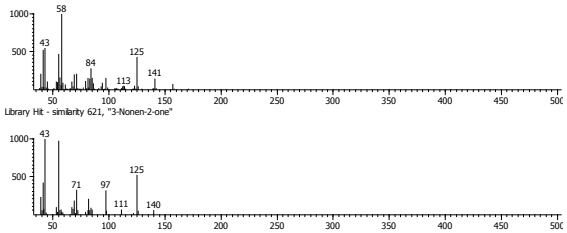
4	Unknown Oxidation Product	1004.0	1.71	61692326	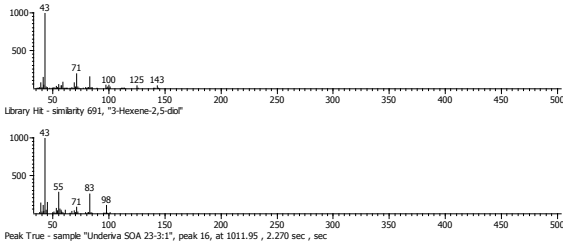
5	Unknown Oxidation Product	1012.0	1.88	114742457	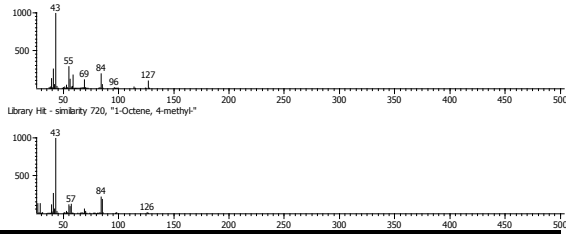

Peak	Name	$^{1}t_R$ (sec)	$^{2}t_R$ (sec)	Peak Area	Mass Spectrum and Closest NIST Library Match (m/z Ratio Horizontal Axis: Rel. Abund. Vertical Axis)
6	Unknown Oxidation Product	1107.9	1.73	55215546	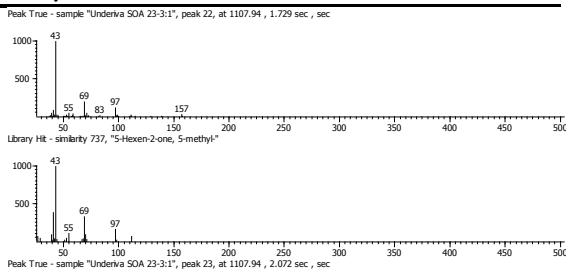
7	2,2-dimethyl-3-formyl-cyclobutyl-methanoic acid Un. M.W. 156 Aldehyde, carboxylic acid	1107.9	2.07	11239558	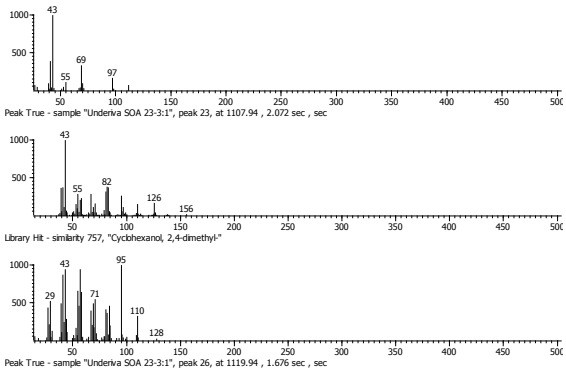
8	Pinalic-4-acid Un. M.W. 170 Aldehyde, carboxylic acid	1119.9	1.68	13159623	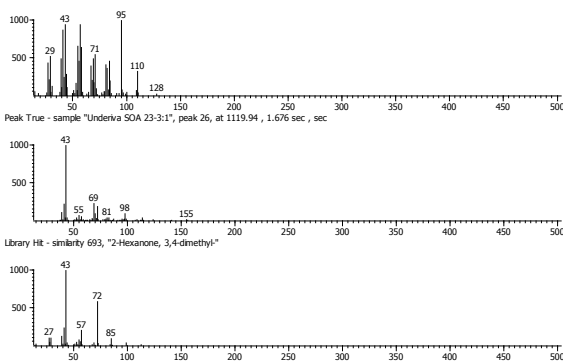
9	Unknown Oxidation Product	1127.9	1.89	28827281	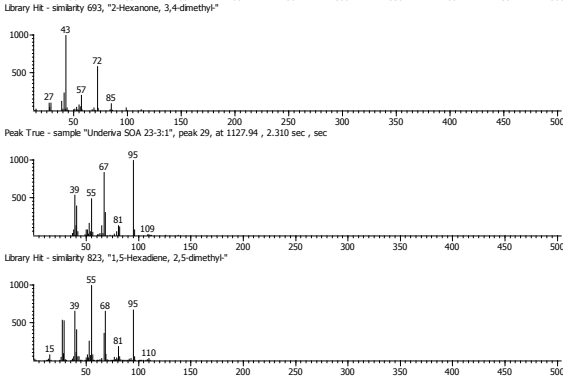
10	Unknown Oxidation Product	1135.9	2.24	106082900	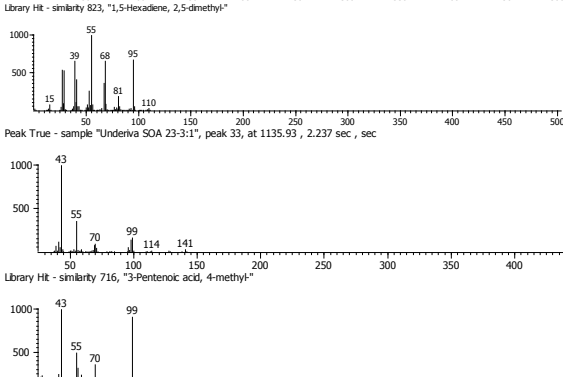
11	Unknown Oxidation Product	1227.9	2.48	74238246	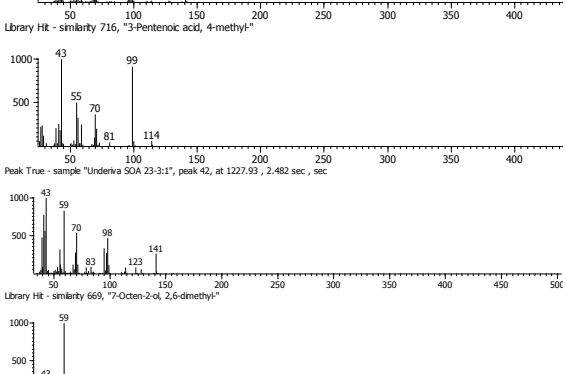

Peak	Name	^1t_R (sec)	^2t_R (sec)	Peak Area	Mass Spectrum and Closest NIST Library Match (m/z Ratio Horizontal Axis: Rel. Abund. Vertical Axis)
12	Norpinic acid Un. M.W. 172 Carboxylic acid (2)	1247.9	2.12	613975928	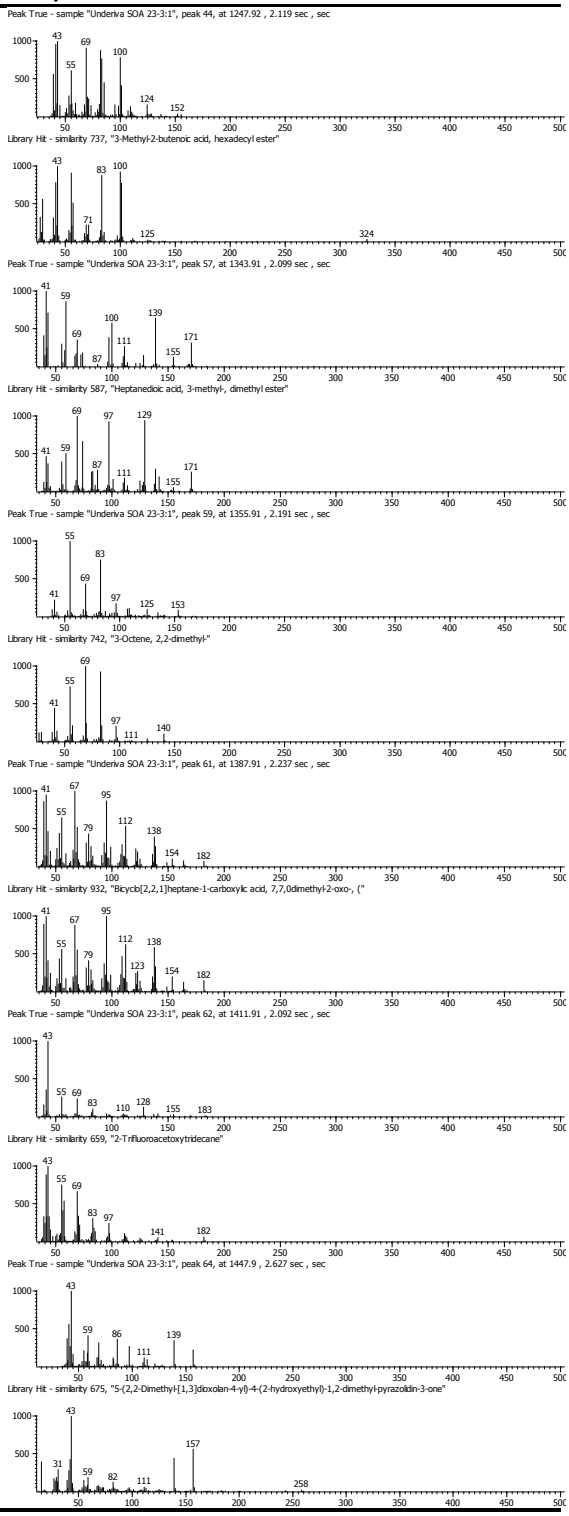
13	Unknown Oxidation Product Aldehyde, carboxylic acid	1343.9	2.05	438923813	
14	Pinonaldehyde Un. M.W. 158	1355.9	2.19	311102981	
15	Ketopinic acid, underivatized (standard) Un. M.W. 182	1387.9	2.24	67560442	
16	Unknown Oxidation Product	1411.9	2.09	12532403	
17	Unknown Oxidation Product Aldehyde	1447.9	2.63	116306186	

Peak	Name	$^{1}t_R$ (sec)	$^{2}t_R$ (sec)	Peak Area	Mass Spectrum and Closest NIST Library Match (m/z Ratio Horizontal Axis: Rel. Abund. Vertical Axis)
18	Pinic acid Un. M.W. 186 Carboxylic acid (2)	1455.9	2.30	829098952	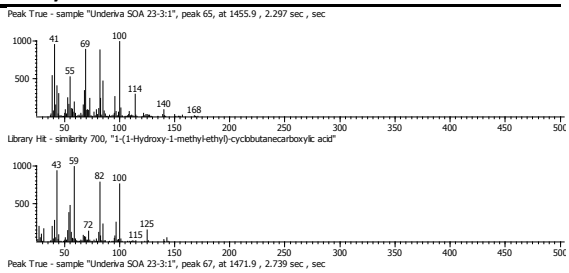
19	Unknown Oxidation Product	1471.9	2.08	10019927	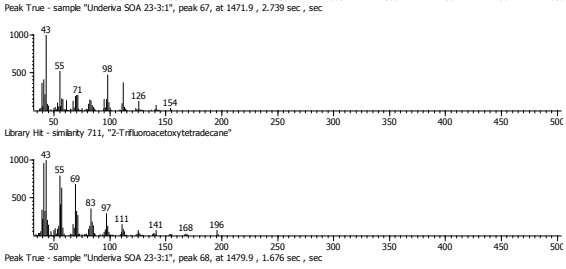
20	Hydroxy pinonaldehyde Un. M.W. 184 Alcohol, aldehyde, and ketone	1479.9	1.68	40593837	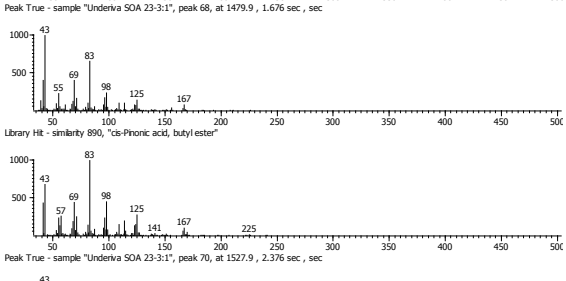
21	Unknown Oxidation Product	1527.9	2.38	11252417	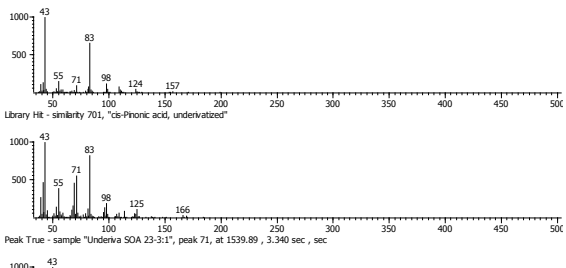
22	Unknown Oxidation Product	1539.9	3.34	15878143	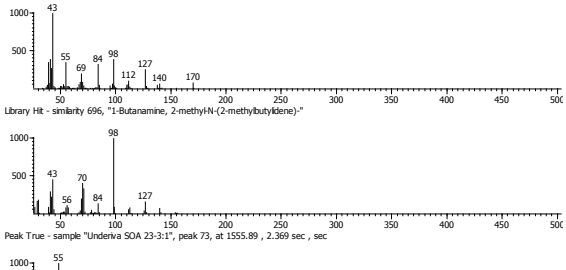
23	Unknown Oxidation Product	1555.9	2.37	271291693	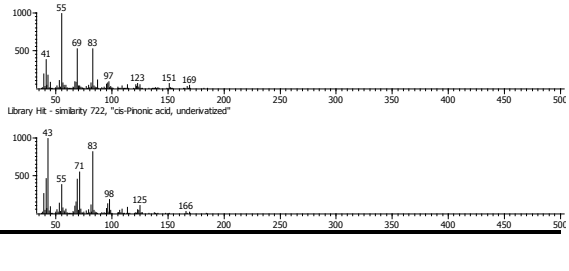

The underivatized α-pinene ozonolysis product mass spectra collected using GC×GC/TOF-MS were significantly different in some cases from published GC-MS spectra. For example, the spectrum of norpinic acid at 1247.9 sec, 2.12 sec (peak #12) differed from the spectrum presented in Joaui & Kamens, 2001 in that the LMW fragments (m/z 43, 55, and 69) were higher abundance peaks in the spectrum collected here. The high abundance ion at m/z 126 was also not present. Despite the apparently poor match with the one available published mass spectrum, the high peak area, $[M-15]^+$ ion at m/z 155, and di-acid characteristic ions were used in identifying norpinic acid.

Other tentatively identified compounds were 2,2-dimethyl-3-formyl-cyclobutyl-methanoic acid(1107.9 sec, 2.07 sec; #6); pinalic-4-acid (1119.9 sec, 1.68 sec; #8); pinonaldehyde (1355.9 sec, 2.19sec #14); pinic acid (1455.9 sec, 2.30 sec; #18); and hydroxy pinonaldehyde (1479.9 sec, 1.68 sec; #20). Pinic acid and pinonaldehyde were identified by comparison to published spectra (Joaui & Kamens, 2001); predicted fragments of the previously identified structures were used to identify hydroxy pinonaldehyde and 2,2-dimethyl-3-formyl-cyclobutyl-methanoic acid. The electron impact mass spectrum of pinalic-4-acid, methyl ester was published in Ma, *et al.*, 2008, and was used to confirm the identification of this compound.

3.3.6 Trends and Observations of Mass Spectra and Chromatograms

A comprable percentage of the TOC mass was identified using derivatization/GC×GC/TOF-MS relative to the identified products in other

characterization studies of α-pinene ozonolysis products (Section 3.4). However, the properties of the unidentified compounds can also be examined using the information gathered by GC×GC separation: the volatility and polarity of the sample components can be described relative to an internal standard based on the primary and secondary separations of GC×GC, respectively. The standard succinic-d_4 acid, eluting approximately in the center of each sample chromatogram, was used as a reference.

The volatilities of most butyl derivatives (as approximated by ^1t_R) were lower than the volatility of succinate-d_4 acid, butyl derivative; there was no clear trend in polarity amongst butyl derivatives (as approximated by ^2t_R). For most trimethylsilyl esters and ethers, the volatility was lower, and polarity higher than for bis(trimethylsilyl) succinate-d_4. The difference between the observed volatility and polarity trends of the derivative products found using the different derivatization schemes may reflect the higher percentage mass contributed by carboxylic acids in the BSTFA derivatized sample extract (based on TMS/GC×GC/TOF-MS results).

Trends in ^1t_R and ^2t_R with respect to derivatized analyte structures have also been previously shown: the ^2t_R in a GC×GC chromatogram does not increase due to the addition of a trimethylsilylated alcohol to a compound, while a compound with an added unprotected keto group will have an increased ^2t_R value (Mitrevski, *et al.,* 2008; multi-functional sterol identification). Values of the GC×GC/TOF-MS retention times of α-pinene ozonolysis products were compared between underivatized and derivatized

compounds with differing functional groups to show possible retention time trends (Table 3.14).

Table 3.14. Values of ^1t_R and ^2t_R of compounds identified in multiple derivatization schemes of GC×GC/TOF-MS chromatograms. BSTFA derivatized samples are designated by "TMS"; those compounds identified as underivatized with samples that had been treated with derivatization reagent are designated by "Un.". Compounds not derivatizable by a particular derivatization technique were denoted as "—" and those compounds not detected are denoted, "N.D."

Compound Name	^1t_R Un. Butyl	^2t_R Un. Butyl	^1t_R Un. TMS	^2t_R Un. TMS	^1t_R Butyl	^2t_R Butyl	^1t_R TMS	^2t_R TMS
Pinonic acid	N.D.	N.D.	1331.9	1.88	1479.9	1.47	1351.9	1.51
Pinic acid	1231.9	1.97	1423.9	2.03	1495.9	1.49	1603.9	1.44
Norpinic acid	N.D.	N.D.	1231.9	2.03	1379.9	1.39	1507.9	1.79
Pinalic-4-acid	1079.9	1.38	1008	2.25	1371.9	1.44	N.D.	N.D.
Norpinonaldehyde	N.D.	N.D.	1008	1.93	1739.9	1.45	--	--
Pinonaldehyde	1047.9	1.47	1127.9	2.28	1963.8	1.34	--	--

Unfortunately, no major trends could be identified between the underivatized and derivatized compounds, or between the BSTFA derivatized and butylated compounds. The presence of retention time trends may have been recognizable if a larger number of compounds had been identified in common between derivatization methods.

No trends between retention times of derivatized calibration standards were recognized. However, the homologous series of di-acids used as calibration standards (malonic, succinic-d_4, glutaric, and adipic acids) could be identified as a series in chromatograms by visual inspection. The use of derivatized compound structures for retention time prediction may be possible in other samples. These trends have been explored for many years (Clayton, 1961a,b; Langer & Pantages, 1961), and previously published information may be applicable to derivatization/GC×GC/TOF-MS.

TMS and butylation provided different advantages toward the characterization of the compounds in the analyzed SOA samples. Many characteristic ions available for both

general BSTFA esters and BSTFA derivatized α-pinene oxidation products were mostly unambiguous and allowed a large portion of the TMS/ GC×GC/TOF-MS quantified mass of SOA sample 26-3 to be attributed to carboxylic acids.

The identification of components within butylated SOA samples was more challenging than within BSTFA derivatized samples, but also provided information about the three functional groups derivatizable using BF_3/butanol. While BSTFA ethers could not be easily differentiated from BSTFA esters, dibutyl acetals and ketals could easily be distinguished from butyl esters by the presence of the high abundance and otherwise uncommon characteristic ions. Although no particular ions could be associated specifically with α-pinene oxidation product butyl derivatives, losses and fragments characteristic to all α-pinene ozonolysis products in many of the mass spectra allowed the identification of functional groups within the BF_3/butanol derivatized analytes.

Although SOA sample 26-3 was used to determine and identify α-pinene ozonolysis products using derivatization/GC×GC/TOF-MS, sample SOA 23-3 was much higher in mass loading (Section 2.2), and a greater number of oxidation products may have been collected onto that filter. Peaks identified in sample 23-3, however, did not include a much larger number of components; similar spectra were collected at retention times of high abundance peaks of all SOA filter sample chromatograms.

4. Quantifiable TOC Mass Measurement using GC×GC-FID

The TOC mass is a measurement used to quantify the mass of OPM collected onto a

filter sample, and the fraction of an OPM sample that can be identified or quantified. The TOC mass is used to compare the mass of oxidation products collected onto filter samples from different experimental systems or studies of atmospherically relevant oxidation reactions. However, the TOC mass determined to be on a filter sample using a thermal-optical (TOC_{TOA}) or other common TOC analysis technique may be greater than the mass that can be quantified by an analytical method such as GC-MS. Polar oxygenated compounds known to be present in OPM may not be completely separated using GC, so that the total mass of OPM quantified using GC will not be equivalent to TOC_{TOA}. A mass sensitive detector such as an FID can be used to quantify the TOC mass separated using a GC, allowing an estimation of TOC mass that can be identified using a GC technique.

GC×GC has been shown to allow the recognition of a much greater number of components of OPM than one-dimensional GC, including some oxygenated components (Hamilton, *et al.,* 2004). Derivatization can be used to allow the quantitative separation of PO-OPM using GC, and was examined in this study as a method of sample preparation both for the analysis of PO-OPM using GC×GC/TOF-MS and for quantification of TOC mass by GC×GC-FID ($TOC_{GC\times GC\text{-}FID}$). The TOC mass of α-pinene ozonolysis products was quantified using GC×GC with and without derivatization. The TOC_{TOA} mass was also measured (Sunset Laboratories, Beaverton, OR) so that the fraction of the OPM mass quantified using derivatization/GC×GC/TOF-MS could be calculated relative to a more inclusive TOC

measurement.

3.4.1 Measurement of $TOC_{GC\times GC\text{-}FID}$

To find the $TOC_{GC\times GC\text{-}FID}$ mass for each α-pinene ozonolysis SOA sample, all peaks associated with siloxane column bleed were first eliminated from the chromatograms, as were all high abundance solvent peaks and internal standards. All peaks in the remaining chromatogram were then integrated and summed. Measured $TOC_{GC\times GC\text{-}FID}$ masses on "blank" filter samples were low compared to values from SOA filter samples. Although small, some mass on the "blank" filters was measured using the GC×GC-FID quantitation method, suggesting the presence of background from solvent and plastics breakdown.

$TOC_{GC\times GC\text{-}FID}$ was measured using underivatized and BSTFA derivatized SOA samples. Some corrections were necessary in the quantification of BSTFA derivatized $TOC_{GC\times GC\text{-}FID}$ ($TMS/TOC_{GC\times GC\text{-}FID}$). The $TMS/TOC_{GC\times GC\text{-}FID}$ masses were found by subtracting the trimethylsilyl group masses from the total mass of all derivatized components (Eqn. 3.3).

$$TMS/TOC_{GCxGC\text{-}FID} = [TOC_{GCxGC\text{-}FID} \times (1 - 0.06719)] \times (1 - 0.3231) + (TOC_{GCxGC\text{-}FID} \times 0.06719) \quad (3.3)$$

Where each numerical value is a factor calculated from results of previousl studies to adjust $TOC_{GC\times GC\text{-}FID}$. The total mass attributed to trimethylsilyl groups was estimated using the average of the GC×GC-FID RF values of adipic, *cis*-pinonic, and ketopinic

trimethylsilyl esters at 1 ng/μL, calculated to be the unitless value 0.3231. This factor also accounted for DE_i and the lesser FID response of oxygenated carbon atoms. To account for the mass of "underivatizable" compounds (such as an aldehyde in the case of a BSTFA derivatized solution), the ratio of the "underivatizable" to total mass was estimated (α-pinene ozonolysis products from Yu, *et al.*, 1999 were used to calculated this value). This fraction, weighted by percent mass of each identified oxidation product, was calculated to be the unitless value 0.06719.

To show the reproducibility of $TOC_{GC\times GC\text{-}FID}$, three replicate injections of underivatized SOA sample 23-3 were made. The use of the underivatized sample in replicate analyses eliminated the need for mathematical corrections used for $TMS/TOC_{GC\times GC\text{-}FID}$ calculations (such as that for "underivatizable" mass). The tabulated responses and values of $TOC_{GC\times GC\text{-}FID}$ for the three replicate injections of SOA sample 23-3 are shown in Table 3.15.

Table 3.15. α-Pinene ozonolysis SOA sample 23-3 was analyzed using GC×GC-FID three times (the injection was repeated) to show the reproducibility of the method for SOA samples. The RSD was <10% between injections.

Sample Name	Total Area	Phenanthrene-d_{10} Area	$TOC_{GC\times GC\text{-}FID}$ (μg/m^3)	$TOC_{GC\times GC\text{-}FID}$ (μg)
SOA 6/23/11-3 Underivatized 2D-1	255139893	5376991	111.9	167.9
SOA 6/23/11-3 Underivatized 2D-2	280216609	4982458	132.6	199.0
SOA 6/23/11-3 Underivatized 2D-3	294416615	5166984	134.4	201.6
	Average		126.3	189.5
	Standard Deviation		12.50	18.75
	RSD (%)		9.90	9.90

The RSD between the three replicate $TOC_{GC\times GC\text{-}FID}$ injections was <10%. Some uncertainty may have been introduced into the values of $TOC_{GC\times GC\text{-}FID}$ during the removal of solvent and siloxane peaks from the chromatograms, or during integration.

3.4.2 Calculated $TOC_{GC\times GC\text{-}FID}$ Values with and without TMS

The TMS/$TOC_{GC\times GC\text{-}FID}$ measured was contrasted with that measured without derivatization to show the difference in mass that could be identified when derivatization was used. Underivatized and BSTFA derivatized SOA sample solutions were analyzed by GC×GC-FID and the results tabulated (Table 3.16).

Table 3.16. $TOC_{GC\times GC\text{-}FID}$ values measured for collected α-pinene ozonolysis samples with and without derivatization. Phenanthrene-d_{10} was used as an internal standard; the peak areas of the total response of each sample and the internal standard are shown for reference. Note that the sample SOA 6/23/11-3 Underivatized 2D is an averaged value of three replicate analyses shown in Table 3.15.

Sample Name	Total Peak Area	Phenanthrene-d_{10} Peak Area	GC×GC-FID Quantifiable TOC Mass (μg/m^3)	GC×GC-FID Quantifiable TOC Mass (μg)
SOA 6/23/11-3 Underivatized 2D (Average)	'---	'---	126.3	189.5
SOA 6/26/11-3 Underivatized 2D	120414182	3651298	58.87	76.54
SOA 6/26/11-4 Underivatized 2D	161738729	4119981	71.28	98.36
SOA 6/23/11-3 TMS 2D[a,b]	213066555	2026538	173.2	259.8
Travel Blank Underivatized 2D[c]	38695090	4550965	8.89	8.89
Clean Air Blank 6/23/11-2 Underivatized 2D	28267447	2422349	14.51	22.50
Clean Air Blank 6/26/11-1 Underivatized 2D	27002561	1020472	31.13	47.63
No Oxidant Blank 6/26/11-2 Underivatized 2D	27684388	2426706	9.36	15.45

[a]Values were adjusted to account for the BSTFA derivatized mass of each derivatized component using the factor 0.323092518 corresponding to the average GC×GC-FID response factor at 1 ng/μL of the BSTFA derivatized acids: adipic, cis-pinonic and ketopinic.
[b]Values were adjusted to account for the underivatized components in each BSTFA derivatized sample using the ratio of underivatized to derivatized components (weighted by percent mass) in α-pinene ozonolysis samples characterized by Yu, et al., 1999. The value of this factor was found to be 0.06719.
[c]No sample collection was made onto the travel blank sample; measurement is given in μg total (no adjustment for total volume sampled).

Values of $TOC_{GC\times GC\text{-}FID}$ mass (without TMS) for SOA samples 26-3 and 26-4 (from the same α-pinene/ozone reaction) were 76.54 and 98.36 μg total, respectively. Values of $TOC_{GC\times GC\text{-}FID}$ were highest for SOA sample 23-3; the average $TOC_{GC\times GC\text{-}FID}$ was 189.5 μg, and TMS/$TOC_{GC\times GC\text{-}FID}$ 259.8 μg total. Derivatization prior to GC×GC separation was expected to allow a portion of the organic carbon to be quantified that was not otherwise amenable to gas chromatographic separation. The analysis of this

additional fraction was confirmed by the lower calculated the value of SOA sample $TOC_{GC\times GC\text{-}FID}$ without derivatization. This difference was more apparent in the values of mass measured without mathematical correction in the BSTFA derivatized samples: a total quantified "active" carbon mass of 371.93 µg was measured with BSTFA derivatization, and 189.5 µg was measured without derivatization.

Distinct peaks in an SOA sample chromatogram after a two-dimensional separation as compared to a one-dimensional separation are clearly shown in Figure 3.6.

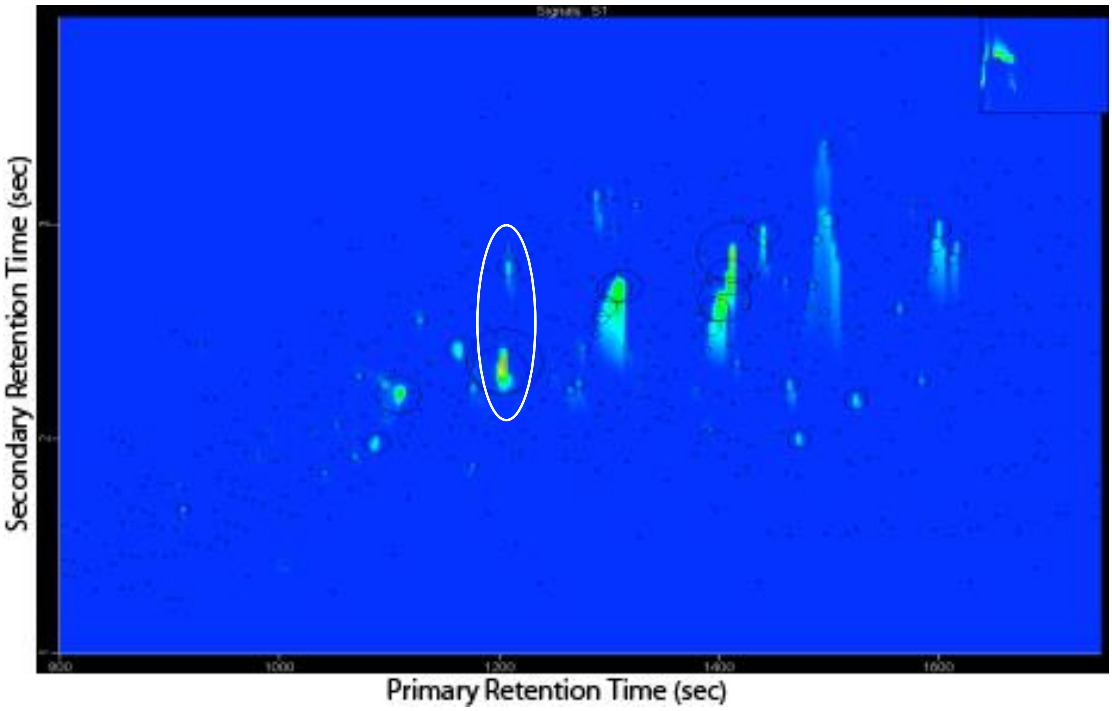

Figure 3.6. A two-dimensional GC×GC-FID chromatogram of the underivatized extract of SOA sample 23-3 Several components are well resolved in the second dimension, including the two peaks eluting just before 1200 seconds in the primary dimension (outlined).

Peaks with overlapping primary retention times in the analysis of the SOA sample were resolved in the second dimension. For example, two high abundance peaks

eluting just before 1200 sec (^1t_R) are separated only in the second dimension. Images of the one-dimensional and two-dimensional chromatograms of the GC×GC-FID separation BSTFA derivatized SOA components are shown in Figure 3.7a and b, respectively.

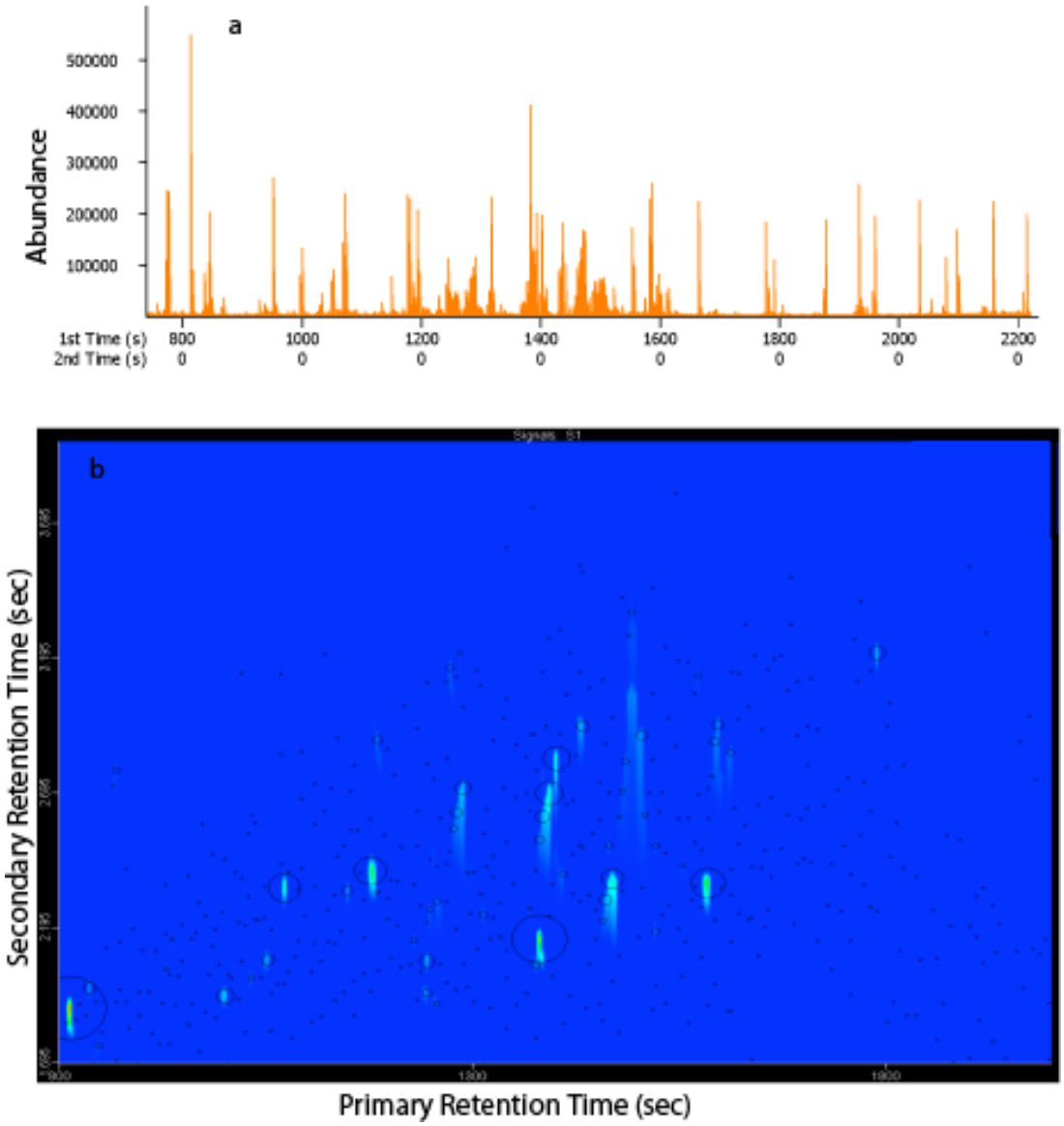

Figure 3.7. Total ion chromatograms of BSTFA derivatized SOA sample 23-3. Several sample component peaks that overlap in a one-dimensional separation (a) are well resolved in two-dimensional separation (b). Note that the modulation periods of a two-dimensional separation cause peak shape to differ in the one-dimensional chromatogram shown from those in a true one-dimensional chromatogram.

Some peaks corresponding to SOA sample components in the GC×GC/TOF-MS derivatized sample chromatogram were separated in the secondary dimension, showing the utility of using GC×GC separation for the analysis of polar oxygenated SOA components. High abundance BSTFA derivatized compounds with low ${}^{2}t_{R}$ values relative to other peaks in the GC×GC chromatogram appear only in the derivatized sample chromatogram. Because the second dimension GC column used contained a polar stationary phase, the decreased polarity of the derivatized components relative to the underivatized components is shown by a decrease in the secondary retention time. This is due in part to decreased interaction between analytes and the stationary phase. The tailing peaks in the underivatized chromatogram corresponding to carboxylic acids and other polar oxygenated compounds that interacted strongly within the chromatographic column and were better chromatographed using BSTFA derivatization. Note that peak tailing is also due to the high concentration of the sample components corresponding to those peaks, and the respective amounts of this tailing due to each effect could not be estimated.

After mathematical corrections were made, the total TMS/$TOC_{GC\times GC\text{-}FID}$ mass on SOA sample 23-3 was estimated to account for almost 40% greater $TOC_{GC\times GC\text{-}FID}$ than the mass without derivatization. The TOC_{TOA} mass and TOC mass measured using a scanning electron mobility sizer (SEMS)[5] were contrasted with values of $TOC_{GC\times GC\text{-}FID}$ mass to show discrepancies between frequently used TOC mass estimation methods and $TOC_{GC\times GC\text{-}FID}$ (Table 3.17).

Table 3.17. Two TOC mass values of α-pinene ozonolysis SOA samples were measured for comparison with GC×GC-FID determination: TOC measured using SEMS and TOC_{TOA}. Values of TMS/$TOC_{GC\times GC\text{-}FID}$ are shown in column four, and are lower for samples than either the TOC measured using SEMS or TOC_{TOA} values. Uncertainties were not estimated for TOC_{TOA} and TOC measured using SEMS.

Sample	TOC Measured using SEMS (μg)[a]	TOC_{TOA} (μg)	$TOC_{GC\times GC\text{-}FID}$ (μg)	$TOC_{GC\times GC\text{-}FID}$/ TOC_{TOA} (%)
Travel Blank	---	6.13 ± 0.45	8.89	145.0
No Oxidant Blank, 23-1	0	9.57 ± 0.48	---	---
Clean Air Blank, 23-2	0	10.4 ± 0.86	22.5	216
TMS α-Pinene SOA,23-3[b]	1570	1130 ± 18.24	260	23.0
TMS α-Pinene SOA, 26-3[b]	725	412 ± 6.88	75.6	18.4
TMS α-Pinene SOA, 26-4[b]	725	541 ± 8.97	78.9	14.6
No-Oxidant Blank, 26-2	0	14.4 ± 0.58	15.5	107
Clean air blank, 26-1	0	17.1 ± 0.61	47.6	279

[a]The value of the total organic mass estimated using SEMS was adjusted to reflect the TOC mass using the estimated fraction of carbon to total mass in the positively identified α-pinene ozonolysis products of Yu, *et al.*, 1999 (the value was 0.6067).
[a]Values were adjusted to account for the BSTFA derivatized mass of each derivatized component using the factor 0.323 corresponding to the average GC×GC-FID response factor at 1 ng/μL of the

[5] The value of the total organic mass estimated using an SEMS was adjusted to reflect the TOC mass using the estimated fraction of carbon mass to total mass in the positively identified α-pinene ozonolysis products from Yu, et al., 1999 (the value was 0.6067).

BSTFA derivatized acids: adipic, pinonic and ketopinic.
[b]Values were adjusted to account for the underivatized components in each BSTFA derivatized sample using the ratio of underivatized to derivatized components (weighted by percent mass) in α-pinene ozonolysis samples characterized by Yu, et al., 1999. The value of this factor was found to be 0.06719.

The values of $TOC_{GC\times GC\text{-}FID}$ (with and without derivatization) were smaller than those values of TOC_{TOA}, as expected. The $TMS/TOC_{GC\times GC\text{-}FID}$ in α-pinene ozonolysis SOA samples (no derivatization was used for "blank" analyses) accounted for approximately 15-23% of the TOC_{TOA}. Using GC×GC-FID, less than one third of the organic carbon mass collected in α-pinene ozonolysis SOA was quantified, reflecting the possible quantity of TOC mass measurable using a GC technique. The values of TOC measured using SEMS were much higher than values of TOC_{TOA}: a possible discrepancy of 5-8% of TOC mass collected was shown between these two methods for TOC mass analysis.

All four methods of TOC mass analysis (including GC×GC-FID with and without derivatization) showed that the sample of highest mass was SOA sample 23-3. Similar values between the two SOA samples collected on 6/26/11 (filter samples 3 and 4) were also measured, showing agreement between all TOC mass analytical methods used.

3.4.3 Characterization of a High Percentage of TOC Mass

The characterization of a high percentage of OPM mass generated by oxidation of atmospheric hydrocarbons is an important benchmark for understanding and predicting the chemistry of atmospheric OPM. Information about the composition and properties of

atmospherically relevant secondary organic aerosol (SOA) can be used in understanding and predicting changes in air quality and climate. It was therefore an objective in this study to evaluate the TOC mass in atmospherically relevant OPM samples that could be quantified or identified using derivatization/GC×GC/TOF-MS.

Previous studies have separated and identified 4-18% of ambient OPM, and 34-71% of oxidation product organic carbon produced in environmental chamber studies (Table 3.18).

Table 3.18. Organic mass identified in published studies of atmospherically relevant OPM samples.

Method	Sample	Organic Mass Measurement Method	Percent Organic Mass Identified	Study
BF_3/methanol, BSTFA (separate fractions)	Vehicular emissions (polar OPM)	Thermal analysis	4% OC	El Haddad, et al., 2009
BSTFA	Arctic aerosol	Thermal analysis	5.05% (SOA tracers) OC	Fu, et al., 2009
BF_3/methanol, direct injection	β-Pinene SOA	Precursor organic carbon mass	13-20% aerosol, 57-71% total OC	Jaoui & Kamens, 2003a
Water extraction, methoxyamine, BSTFA	Brazilian rural aerosol	Thermal analysis	4.5-7.5% WSOC	Mayol-Bracero, et al., 2002
BSTFA/PFBHA	Chamber studies of terpenoid oxidation	Precursor organic carbon mass	4-6% aerosol, 34-50% total OC	Yu, et al., 1999

Despite the use of chemical derivatization with GC-MS, a large percentage of SOA mass is un-identified in most studied OPM samples. The most widely used TOC mass estimation method for determining this identified percentage of SOA was a thermal-optical analysis method. Values of TOC_{TOA} mass were shown in Section 3.2 to vary directly with $TOC_{GCGC\text{-}FID}$ and SEMS quantified TOC.

The percentages of the mass α-pinene ozonolysis SOA quantified relative to $TOC_{GC\times GC\text{-}FID}$ and TOC_{TOA} are shown in Table 3.19.

Table 3.19. Percentages of organic carbon mass on SOA sample 26-3 quantified using butylation or TMS with GC×GC/TOF-MS analysis, normalized to TOC mass values measured using four methods of TOC analysis. The organic mass (unadjusted for carbon/organic mass) was used in calculating the aerosol yield, which is normalized to the precursor mass.

	TOC Mass Quantified by GC×GC/TOF-MS (μg)	**Percent Quantified TOC Measured using SEMS**	**Percent Quantified TOC_{TOA}**	**Percent Quantified $TMS/TOC_{GC\times GC\text{-}FID}$**	**Percent Identified Aerosol Yield (Precursor Mass)**
SOA Sample 26-3, Butylated	20.7	2.85%	5.02%	---	4%
Carboxylic Acids in Sample 26-3, Butylated	12.8	1.47%	3.11%	---	---
SOA Sample 26-3, TMS	36.4	5.03%	8.9%	48.2%	3%
Carboxylic Acids in Sample 26-3, TMS	34.1	4.70%	8.3%	45.1%	---

A total of 34.1 μg of derivatized organic mass was determined quantitatively in the sample (SOA 6/26/11-3) by butylation/GC×GC/TOF-MS. Using the same carbon to total organic mass ratio used in Section 3.1, an estimated 20.7 μg derivatized organic carbon mass was quantified using butylation/GC×GC/TOF-MS in SOA sample 26-3. Normalizing to TOC_{TOA}, the total derivatizable organic carbon mass determined using butylation and GC×GC/TOF-MS accounted for 5.02% of the TOC. This is comparable to that found in other studies (4-6% TOC mass in aerosl, Yu *et al.,* 1999; 13-20% TOC mass in aerosol, Jaoui & Kamens, 2003a β-pinene oxidation; Table 3.18), but only includes derivatized sample components. The sum of quantified (using functional group diagnostic ions) carboxylic acids within the butyl derivative mass was 12.8 μg, or 61.9% of the GC×GC/TOF-MS semi-quantified sample TOC mass. An estimated 3.13% of the

carbon sample mass found using butylation/GC×GC/TOF-MS was potentially composed of carboxylic acids relative to TOC_{TOA} mass.

A greater derivatized organic mass was determined in SOA sample 26-3 using TMS/GC×GC/TOF-MS versus using butylation/GC×GC/TOF-MS (59.9 µg). Using the same carbon to total organic mass ratio used in Section 3.1, an estimated 36.4 µg derivatized organic carbon mass can be quantified using TMS/GC×GC/TOF-MS in SOA sample 26-3. By comparison, the $TMS/TOC_{GC\times GC\text{-}FID}$ was 75.6 µg. As a function of $TMS/TOC_{GC\times GC\text{-}FID}$, the percentage determined organic carbon mass was 48.2%. As a function of TOC_{TOA}, the percentage organic carbon mass determined using TMS/GC×GC/TOF-MS was 8.9%. The sum of the quantified mass attributed to carboxylic acids was 34.1 µg; this was 93.6% of the TMS/GC×GC/TOF-MS quantified sample mass. An estimated 45.1% of the $TOC_{GC\times GC\text{-}FID}$ mass and 8.3% of the TOC_{TOA} mass was likely carboxylic acid-containing.

The studies of Yu, *et al.,* 1999 and Jaoui & Kamens, 2003a used the summed aerosol yield (Section 1.3) of identified oxidation product to characterize the total mass of the sample identified. The aerosol yield, *Y*, uses the precursor carbon mass, rather than TOC, to normalize the mass of collected and identified products. Values of *Y* for β-pinene oxidation products were 4-6% and 13-20%, respectively, for the studies done by Yu, *et al.,* and Joaui & Kamens (Table 3.4). Values of *Y* found in this study of α-pinene ozonolysis products were 4% using butylation/GC×GC/TOF-MS and 3% using TMS/GC×GC/TOF-MS. Values of *Y* of products explicitly identified (by product name)

using TMS/GC×GC/TOF-MS and butylation/GC×GC/TOF-MS were 2% and 0.09%, respectivel. Yu, *et al.,* also calculated the organic aerosol mass by further normalizing the sum of the aerosol yields of each product to the total aerosol yield approximated using values measured by an SEMS and condensation nucleus counter (CNC); the values of *Y* for identified β-pinene oxidation products accounted for 83% and 98% of the SEMS/CNC estimated mass in two replicate reactions. In this study, the *Y* values of identified oxidation products for α-pinene oxidation accounted for 5.03% by TMS and 2.85% by butylation of the SEMS/CNC estimated mass. These values are much lower than those accounted for by Yu, *et al.,* but underivatized oxidation products, again, were not quantified, and many products were quantified using this method but not identified. It should be noted that not all products identified using the two reagent systems were identical; therefore, values of *Y* were between 5 and 8% of the TOC measured using SEMS was identified.

Values of *Y* of high abundance oxidation products were of a similar order of magnitude to those found in Jaoui & Kamens, 2001, but higher, in part because only derivatized components were quantified. Pinic and norpinic acids were found to account for 5.6-12.1% and <0.1%, respectively, in Jaoui & Kamens, 2001; values of *Y* for pinic and norpinic acids in this study were 0.889% and 0.851, respectively, using TMS/GC×GC/TOF-MS. The lower ratio of norpinic to pinic acid mass yields was also observed in Yu, *et al.,* 1999; this could be from the much higher mass of OPM collected onto the sample filters in this study, allowing more norpinic acid to partition into the

particle phase (between 14 and 24 times more mass was collected onto filter sample 26-3 than was collected in the three analyses of α-pinene oxidation from Yu, *et al.,* 1999). Pinonic acid, similarly, was 16% of the mass in SOA sample 26-3 using TMS/GC×GC/TOF-MS, but only 2.0-3.1% of the mass in the publication by Jaoui & Kamens (2001).

5. Conclusions and Future Work

Based on the results of this study, the method of derivatization/GC×GC/TOF-MS has potential for allowing increased atmospherically relevant SOA mass closure and advancing interpretation of the functional groups and structures present in SOA sample components. Peaks co-eluting at equal primary retention times (e.g., that would co-elute in a one-dimensional GC analysis) were separated in the second dimension using GC×GC. Derivatization allowed for better separations, more accurate identifications, and better peak shape for quantification of high polarity analytes. Additionally, the higher ${}^{i}t_{R}$ values observed for derivatized analytes allowed better separation between derivatized and un-reacted oxidation products.

The values of the derivatization efficiency (DE_i) measured in this study were lower than measured in previous studies for similar polar oxygenated standards; analyses prior to the measurement of DE_i showed strong responses from most derivatized standard compounds. The DE_i values measured in this study were 50-58% for most trimethylsilyl derivatives, and 40-70% for most butyl derivatives, with high variation (average RSD values were 29% and 44%, respectively). The DE_i of BSTFA reactions could potentially be improved by changing the procedure: as an example, pyridine could be used as a catalyst for active site proton removal in BSTFA procedures (Yu, *et al.,* 1998 and 1999).

Separations by GC×GC allow trends to be formed in retention time for analytes with similar structures. A clear visual trend was noted for the series of homologous di-acid standards used in calibration, but no visual or mathematical relationships were noted

between the retention times in derivatized GC×GC chromatograms of α-pinene ozonolysis products. The retention time of the calibration standard methyl-malonic acid was noted to be slightly higher in the primary dimension (*i.e.,* less volatile) and lower in the secondary dimension (*i.e.,* less polar) than that of malonic acid (using both derivatization schemes); retention time trends could therefore be used in future studies to identify multiple, similar analyte structures with differing substituents such as added hydroxyl or methyl groups.

Most derivatives were distinguishable in each sample or standard chromatogram by their higher primary retention times; this was more easily observed in the BSTFA derivatized chromatograms for which the diagnostic ion m/z 73 could be extracted. The primary and secondary retention times of the derivatives in BSTFA derivatized and butylated SOA sample extracts were further used to estimate the volatilities and polarities, respectively, of the analytes with resepect to the standard succinic-d_4 acid (included in all samples to show recovery of carboxylic acid compounds through the sample preparation process). Most butyl derivatives were of lower volatilities than succinic-d_4 acid, butyl ester; polarities were both higher and lower than for succinic-d_4 acid, butyl ester. BSTFA derivatives were also lower in volatility, but mostly higher in polarity than succinic-d_4 acid, BSTFA derivative, potentially showing that derivatives not positively or tentatively identified were highly oxygenated.

The following previously unidentified compounds were identified as α-pinene oxidation products (above background concentrations) using butylation/GC×GC/TOF-MS: oxalic,

malonic, glyoxylic acids, and glyoxal. No previously unidentified components could be identified in BSTFA SOA samples, but many known and unknown oxidation products were determined quantitavely (using a surrogate standard) in the BSTFA derivatized sample. Unknown oxidation products were detected by the lack of matching the mass spectra published in previous α-pinene oxidation studies or predicted for known oxidation products.

Many studies attempting to increase mass closure of atmospherically relevant SOA have used combinations of soft and hard ionization techniques to allow fragments and molecular ions to be detected; pairing derivatization/GC×GC/TOF-MS with chemical ionization MS would likely allow a greater number of sample components to be identified, including some high abundance oxidation products. Three unidentified derivatives along with pinic acid (largest), hydroxy pinonic acid, pinonaldehyde, and pinonic acid accounted for over 80% of the butylated organic mass semi-quantified using GC×GC/TOF-MS. One unidentified trimethylsilyl derivative, pinic acid, pinonic acid, norpinic acid, and a hydroxy pinonaldehyde accounted for >75% of the TMS and GC×GC/TOF-MS analyzed organic mass.

Further changes to data processing methods may allow simpler, less time-consuming analyses of GC×GC/TOF-MS data, and in particular, for complex samples such as ambient SOA. Data processing could also be simplified by pre-derivatization fractionation of samples. The use of different derivatization reagents should also be examined; in particular, the PFBHA/BSTFA combination (Yu, *et al.,* 1998, 1999). This

combination was not used here because large reagent byproduct peaks associated with PFBHA could not be removed, and therefore the derivatives could not be analyzed from the reaction solutions without significantly damaging the GC×GC/TOF-MS instrument and/or secondary GC column. Derivatization using this combination would allow for the analysis of all oxo-acids in one sample (rather than the analysis of simultaneous samples derivatized by BF_3/butanol and BSTFA). It would also prevent extraction losses of any neutral carbonyl-containing compounds.

The use of improved ChromaTOF® Scripts could be used to easily show the different functional groups and derivatized compounds within a sample. Additions of TOF mass spectral data to mass spectral libraries would allow simpler and faster characterization of unknown derivatives. Mitrevski, *et al.* (2008) also suggested after processing TMS derivatized sterols that a new TOF-MS spectral library should be generated because of the dissimilarities from quadrupole and ITMS spectra and increased frequency of TOF-MS use. The primary differences observed in TOF-MS spectra in this study were the increased abundance or change in abundance ratio of low m/z ions (generally less than 100 a.m.u.), as well as a lack of molecular ions and other higher high m/z characteristic ions. A significant number of analytes were not positively or tentatively identified due to these mass spectral characteristics.

Diagnostic ions could be used, but were more frequently recognized for BSTFA derivatized oxidation products than for butylated products. Mass spectra of butyl esters of oxidation products were sometimes indistinguishable from underivatized components

because the butyl diagnostic ion m/z 57 was of relatively low abundance compared to other ions in the derivative spectra, and is common to most alkanes.

A larger mass of organic carbon was quantified for α-pinene ozonolysis products using TMS/GC×GC/FID in sample extracts than in underivatized extracts, based on values of $TOC_{GC\times GC\text{-}FID}$ (values were 15-23% of TMS/$TOC_{GC\times GC\text{-}FID}$). The TOC_{TOA} accounted for by butylation/GC×GC/TOF-MS was slightly lower than that by TMS: 5%, and it was estimated (by comparing peak areas of underivatized compounds to those of high abundance derivatives) that a large portion of mass was additionally underivatized. This portion remained in the sample after derivatization, and would be quantifiable in the derivatized sample extracts if an underivatized calibration were made. A greater number of trace analytes may therefore be detectable by further altering the derivatization procedure. The method of TMS/GC×GC/TOF-MS allowed 48.2% of the $TOC_{GC\times GC\text{-}FID}$ and 8.85% of the TOC_{TOA} to be quantified. The method of TMS/GC×GC/TOF-MS was particularly effective for analysis of carboxylic acids: identified or potentially identified carboxylic acids made up 45.1% of TMS/$TOC_{GC\times GC\text{-}FID}$ and 8.28% of TOC_{TOA}.

The combined successful results of this study support the continued analysis of chamber and ambient OPM samples by derivatization/GC×GC/TOF-MS. Future applications should include analyses of other biogenic hydrocarbon systems and oxidation products of anthropogenic, aromatic hydrocarbons. The presence of unidentified carboxylic acids in the atmospheric oxidation products of anthropogenic aromatic hydrocarbons is likely: aerosol mass spectrometer data shows high m/z 44 peaks, corresponding to carboxylic

acids or other polar, oxygenated compounds that have not yet been detected (correspondence with Dr. David Cocker, U.C. Riverside). This coupled analytical technique has been shown here to allow the speciation and characterization of polar oxygenated OPM, and has potential to become an effective tool for simultaneously analyzing the detailed composition of an organic sample and also characterizing the present functional groups and structures.

LITERATURE CITED

Antilla, P., Hyötyläinen, T., Heikkilä, A., Jussila, M., Finell., J., Kulmala, M., Riekkola, M.-L., 2004. Determination of organic acids in aerosol particles from a coniferous forest by liquid chromatography-mass spectrometry. Journal of Separation Science 28, 337-346.

Atkinson, R., Carter, W.P.L., Darnall, K.R., Winer, A.M., Pitts, J.N., 1980. A smog chamber and modeling study of the gas phase NOx–air photooxidation of toluene and the cresols. International Journal of Chemical Kinetics 12, 779-836.

Bao, L., Matsumoto, M., Kubota, T., Kazuhiko, S., Wang, Q., Sakamoto, K., 2009. Gas/particle partitioning of low-molecular-weight dicarboxylic acids at a suburban site in Saitama, Japan. Atmospheric Environment In Press.

Barsanti, K.C., Pankow, J.F., 2006. Thermodynamics of the formation of atmospheric organic particulate matter by accretion reactions--Part 3: Carboxylic and dicarboxylic acids. Atmospheric Environment 40, 6676-6686.

Beiner, K., Plweka, A., Haferkorn, S., Iinuma, Y., Engewald, W., Herrmann, H., 2009. Quantification of organic acids in particulate matter by coupling of thermally assisted hydrolysis and methylation with thermodesorption-gas chromatography-mass spectrometry. Journal of Chromatography A 1216, 6642-6650.

Blau, K., & Halket, J. M., 1993. Handbook of Derivatives for Chromatography. John Wiley & Sons.

Brock, C.A., Sullivan, A.P., Peltier, R.E., Weber, R.J., Wollny, A., de Guow, J.A., Middlebrook, A.M., Atlas, E.L., Stohl, A., Trainer, M.K., Cooper, O.R., Fehsenfeld, F.C., Frost, G.J., Holloway, J.S., Hübler, G., Neuman, J.A., Ryerson, T.B., Wrneke, C., Wilson, J.C., 2008. Sources of particulate matter in the northeastern United States in summer: 2. Evolution of chemical and microphysical properties. Journal of Geophysical Research 113, 1-16.

Calvert, J.G., 2002. The Mechanisms of Atmospheric Oxidation of Aromatic Hydrocarbons. Oxford University Press, New York.

Cartwright, A.J., Jones, P., Wolff, J.-C., Evans, H., 2005. Derivatisation of carboxylic acid groups in pharmaceuticals for enhanced detection using liquid chromatography with electrospray ionisation tandem mass spectrometry. Rapid Communications in Mass Spectrometry 19, 1058-1062.

Cecinato, A., Amati, B., Di Palo, V., Marino, F., Possanzini, M., 1999. Determination of short-chain organic acids in airborne aerosols by Ion Chromatography. Chromatographia 50, 670-672.

Chien, C.-J., Charles, M.J., Sexton, K.G., Jeffries, J.E., 1998. Analysis of airborne carboxylic acids and phenols as their pentafluorobenzyl derivatives: gas

chromatography/ion trap mass spectrometry with a novel chemical ionization reagent, PFBOH. Environmental Science and Technology 32, 299-309.

Chien, C.-J., Jeffries, H.J., Charles, M.H., Sexton, K.G., 1997. Analysis of airborne carboxylic acids and phenols as their pentafluorobenzyl derivatives in the oxidation products of isoprene and toluene, in: Laboratory, A.a.W.M.A.U.S.E.P.A.s.N.E.R. (Ed.), Measurement of Toxic and Related Air Pollutants. Air & Waste Management Association, Research Triangle Park, NC, pp. 803-816.

Claeys, M., Szmigielski, R., Kourtchev, I., Van der Veken, P., Vermeylen, R., Maenhaut, W., Jaoui, M., Kleindienst, T.E., Lewandowski, M., Offenberg, J.H., Clements, A.L., Seinfeld, J.H., 2007. Hydroxydicarboxylic acids: markers for secondary organic aerosol from

the photooxidation of α-pinene. Atmospheric Environment 41, 1628-1634.

Clayton, R.B., 1961. Gas-liquid chromatography of sterol methyl esters. Nature 190, 1071-1072.

Clayton, R.B., 1961. Group retention factors in the gas-liquid chromatography of steroids. Nature 192, 524-526.

Clements, A.L., Seinfeld, J.H., 2006. Detection and quantification of 2-methyltetrols in ambient aerosol in the southeastern United States. Atmospheric Environment 41, 1825-1830.

Cocker Iii, D.R., Clegg, S.L., Flagan, R.C., Seinfeld, J.H., 2001. The effect of water on gas‚Äìparticle partitioning of secondary organic aerosol. Part I: Œ±-pinene/ozone system. Atmospheric Environment 35, 6049-6072.

Demuth, N., Heumann, K.G., 2001. Validation of methylmercury determinations in aquatic systems by alkyl derivatization methods for GC analysis using ICP-IDMS. Analytical Chemistry 73, 4020-4027.

Ding, L.C., Ke, F., Wang, D.K.W., Dann, T., Austin, C.C., 2009. A new direct thermal desorption-GC-MS method: Organic speciation of ambient particulate matter collected in Golden, B.C. Atmospheric Environment 43, 4894-4902.

Docherty, K.S., Ziemann, P.J., 2001. On-line, onlet-based trimethylsilyl derivatization for gas chromatography of mono- and dicarboxylic acids. Journal of Chromatography A 921, 265-275.

Drózd, J., 1981. Chemical Derivatization in Gas Chromatography. Elsevier Scientific Pub. Co., New York.

El Haddad, I., Marchand, N., Dron, J., Temime-Roussel, B., Quivet, E., Wortham, H., Jaffrezo, J.L., Baduel, C., Voisin, D., Besombes, J.L., Gille, G., 2009. Comprehensive primary particulate organic characterization of vehicular exhaust emissions in France. Atmospheric Environment 43, 6190-6198.

Evershed, R.P., 1993. Advances in Silylation, in: Blau, K., & Halket, J. M. (Ed.), Handbook for Derivatives for Chromatography, 2nd ed. John Wiley & Sons, Chichester.

Facchini, M.C., Decesari, S., Mircea, M., Fuzzi, S., Loglio, G., 2000. Surface tension of atmospheric wet aerosol and cloud/fog droplets in relation to their organic carbon content and chemical composition. Atmospheric Environment 34, 4853-4857.

Facchini, M.C., Mircea, M., Fuzzi, S., Charlson, R.J., 1999. Cloud albedo enhancement by surface-active organic solutes in growing droplets. Nature 401, 257-259.

Fehsenfeld, F., Calvert, J., Fall, R., Goldan, P., Guenther, A.B., Hewitt, C.N., Lamb, B., Liu, S., Trainer, M., Westberg, H., Zimmerman, P., 1992. Emissions of volatile organic compounds from vegetation and the implications for atmospheric chemistry. Global Biogeochem. Cycles 6, 389-430.

Fick, J., Pommer, L., Nilsson, C., Barbro, A., 2003. Effect of OH radicals, relative humidity, and time on the composition of the products formed in the ozonolysis of α-pinene. Atmospheric Environment 37, 4087-4096.

Forster, P., Ramaswamy, V., Artaxo, T., Betts, R., Fahey, D.W., Haywood, J., Lean, J., Lowe, D.C., Myhre, G., Nganga, J., Prinn, R., Raga, G., Schulz, R., Van Dorland, R., 2007. Changes in atmospheric constituents and in radiative forcing, in: Solomon, S., Qin, D., Manning, M., Chen, Z., Marquis, M., Averyt, K. B., Tignor, M., and Miller, H. L. (Ed.), Climate Change 2007: The Physical Science Basis. Contribution of Working Group I to the Fourth Assessment Report of the Intergovernmental Panel on Climate Change. Cambridge University Press, Cambridge.

Forstner, H.J.L., Flagan, R., Seinfeld, J.H., 1997. Secondary organic aerosol from the photooxidation of aromatic hydrcarbons: Molecular composition. Environmental Science & Technology 31, 1345-1358.

Frank, M.P., Powers, R.W., 2007. Simple and rapid quantitative high-performance liquid chromatographic analysis of plasma amino acids. Journal of Chromatography B 852, 646-649.

Fu, P., Kawamura, K., Chen, J., Barrie, L.A., 2009. Isoprene, monoterpene, and sesquiterpene oxidation products in the high arctic aerosols during late winter to early summer. Environmental Science & Technology 43, 4022-4028.

Galceran, M.T., Moyano, E., Poza, J.M., 1995. Pentafluorobenzyl derivatives for the gas chromatographic determination of hydroxy-polycyclic aromatic hydrocarbons in urban aerosols. Journal of Chromatography A 710, 139-147.

Gao, S., Keywood, M., Ng, N.L., Surratt, J., Varutbangkul, V., Bahreini, R., Flagan, R.C., Seinfeld, J.H., 2004. Low-molecular-weight and oligomeric components in secondary organic aerosol from the ozonolysis of cycloalkenes and α-pinene. Journal of Physical Chemistry A 108, 10147-10164.

Glasius, M., Duane, M., Larsen, B.R., 1999. Determination of polar terpene oxidation

products in aerosols by liquid chromatography‚Äìion trap mass spectrometry. Journal of Chromatography A 833, 121-135.

Glasius, M., Lahaniati, M., Calogirou, A., Di Bella, D., Jensen, N.R., Hjorth, J., Kotzias, D., Larson, B.R., 2000. Carboxylic acids in secondary aerosols from oxidation of cyclic monoterpenes by ozone. Environmental Science & Technology 34, 1001-1010.

Goldstein, A.H., Galbally, I.E., 2007. Known and unexplored organic constituents in the Earth's atmosphere. Environmental Science & Technology 41, 1514.

Grob, K., Jr., Grob, G., Grob, K., 1978. Comprehensive, standardized quality test for glass capillary columns. Journal of Chromatography 156, 1-20.

Gröger, T., Welthagen, W., Mitschke, S., Schäffer, M., Zimmerman, R., 2008. Application of comprehensive two-dimensional gas chromatography mass spectrometry and different types of data analysis for the investigation of cigarette particulate matter. Journal of Separation Sciences 31, 3366-3374.

Hamilton, J.F., Webb, P.J., Lewis, A.C., Hopkins, J.R., Smith, S., Davy, P., 2004. Partially oxidized organic components in urban aerosol using GCxGC-TOF/MS. Atmospheric Chemistry and Physics 4, 1279-1290.

Heald, C.L., Ridley, D.A., Kreidenweis, S.M., Drury, E.E., 2010. Satellite observations cap the atmospheric organic aerosol budget. Geophysical Research Letters 37.

Healy, R.M., Temime, B., Kuprovskyte, K., Wenger, J.C., 2009. Effects of radiative humidity on gas/particle partitioning and aerosol mass yield in the photooxidation of *p*-xylene. Environmental Science & Technology 43, 1884-1889.

Healy, R.M., Wenger, J.C., Metzger, A., Duplissy, J., Kalberer, M., Dommen, J., 2008. Gas/particle partitioning of carbonyls in the photooxidation of isoprene and 1,3,4,5-trimethylbenzene. Atmospheric Chemistry & PHysics 8, 3215-3230.

Hoffmann, T., Bandur, R., Marggraf, U., Linscheid, M., 1998. Molecular composition of organic aerosols formed in the α-pinene/O_3 reaction: Implications for new particle formation processes. Journal of Geophysical Research 103, 25569-25578.

Hofmann, U., Holzer, S., Meese, C.O., 1990. Pentafluorophenyldiazoalkanes as novel derivatization reagents for the determination of sensitive carboxylic acids by gas chromatography-negative-ion mass spectrometry. Journal of Chromatography 508, 349-356.

Holm, T., 1999. Aspects of the mechanism of the flame ionization detector. Journal of Chromatography A 842, 221-227.

Hoyle, C.R., Myhre, G., Berntsen, T.K., Isaksen, I.S.A., 2009. Anthropogenic influence on SOA and the resulting radiative forcing. Atmospheric Chemistry and Physics 9, 2715-2728.

Jang, M., Carroll, B., Chandramouli, B., Kamens, R.M., 2003. Particle growth by acid-

catalyzed heterogeneous reactions of organic carbonyls on preexisting aerosols. Environmental Science and Technology 37, 3828-3837.

Jang, M., Czoschke, N.M., Lee, S., Kamens, R.M., 2002. Heterogeneous atmospheric aerosol production by acid-catalyzed particle-phase reactions. Science 298, 814-817.

Jang, M., Kamens, R.M., 1999. Newly characterized products and composition of secondary aerosols from the reaction of α-pinene with ozone. Atmospheric Environment 33, 459-474.

Jaoui, M., Docherty, K., Gerald, T., Corse, E., Kleindienst, T.E., Offenberg, J.H., Lewandowski, M., 2010. SOA Formation from the Reaction of Isoprene with NO_3 Radicals, American Association for Aerosol Research Annual Conference, Portland, OR.

Jaoui, M., Kamens, R.M., 2001. Mass balance of gaseous and particulate products analysis from α-pinene/NO_x/air in the presence of natural sunlight. Journal of Geophysical Research 106, 12541-12558.

Jaoui, M., Kamens, R.M., 2003. Mass balance of gaseous and particulate products from β-pinene/O_3/air in the absence of light and β-pinene/NO_x/air in the presence of natural sunlight. Journal of Atmospheric Chemistry 43, 101-141.

Jensen, T., Fredenslund, A., Rasmussen, P., 1981. Pure-component vapor pressures using UNIFAC group contribution. Industrial & Engineering Chemistry Fundamentals 20, 239-246.

Kanakidou, M., Seinfeld, J.H., Pandis, S.N., Barnes, I., Dentener, F.J., Facchini, M.C., Can Dingenen, R., Ervens, B., Nenes, A., Nielsen, C.J., Swietlicki, E., Putaud, J.P., Balkanski, Y., Fuzzi, S., Horth, J., Moortgat, G.K., Winterhalter, R., Myhre, C.E.L., Tsigaridis, K., Vignati, E., Stephanou, E.G., Wilson, J., 2005. Organic aerosol and global climate modelling: a review. Atmospheric Chemistry & Physics 5, 1053-1123.

Karl, T.R., Trenberth, K.E., 2003. Modern Global Climate Change. Science 302, 1719-1723.

Kawamura, K., Ikushima, K., 1993. Seasonal changes in the distribution of dicarboxylic acids in the urban atmosphere. Environmental Science & Technology 27, 2227-2235.

Kawamura, K., Kasukabe, H., Barrie, L., 1996. Source and reaction pathways of dicarboxylic acids, ketoacids and dicarbonyls in Arctic aerosols: One year of observations. Atmospheric Environment 30, 1709-1722.

Kim, K.R., Hahn, M.K., Zlatkis, A., Horning, E.C., Middleditch, B.S., 1989. Simultaneous gas chromatography of volatile and non-volatile carboxylic acids as *tert*-butyldimethylsilyl derivatives. Journal of Chromatography 468, 289-301.

Kind, T., Wohlgemuth, G., Yup Lee, D., Lu, Y., Palazoglu, M., Shahbaz, S., Fiehn, O., 2009. FiehnLib: Mass spectral and retention index libraries for metabolomics based on quadrupole and time-of-flight gas chromatography/mass spectrometry. Analytical Chemistry 81, 10039-10048.

Kleindienst, T.E., Jaoui, M., Lewandowski, M., Offenberg, J.H., Lewis, C.W., Bhave, P.V., Edney, E.O., 2007. Estimates of the contributions of biogenic and anthropogenic hydrocarbons to secondary organic aerosol at a southeastern US location. Atmospheric Environment 41, 8288-8300.

Knapp, D.R., 1979. Handbook of Analytical Derivatization Regents. John Wiley & Sons, New York.

Kourtchev, I., Copolovici, L., Claeys, M., Maenhaut, W., 2009. Characterization of atmospheric aerosols at a forest site in central Europe. Environmental Science & Technology 43, 4665-4671.

Kroll, J.H., Donahue, N.M., Jimenez, J.L., Kessler, S.H., Canagaratna, M.R., Wilson, K.R., Altieri, K.E., Mazzoleni, L.R., Wozniak, A.S., Bluhm, H., Mysak, E.R., Smith, J.D., Kolb, C.E., Worsnop, D.R., Carbon oxidation state as a metric for describing the chemistry of atmospheric organic aerosol. Nat Chem 3, 133-139.

Kroll, J.H., Donahue, N.M., Jimenez, J.L., Kessler, S.H., Canagaratna, M.R., Wilson, K.R., Altieri, K.E., Mazzoleni, L.R., Wozniak, A.S., Bluhm, H., Mysak, E.R., Smith, J.D., Kolb, C.E., Worsnop, D.R., Carbon oxidation state as a metric for describing the chemistry of atmospheric organic aerosol. Nat Chem 3, 133-139.

Kuster, W.C., Jobson, B.T., Karl, T., Riemer, D., Apel, E., Goldan, P.D., Fehsenfeld, F.C., 2003. Intercomparison of Volatile Organic Carbon Measurement Techniques and Data at La Porte during the TexAQS2000 Air Quality Study. Environmental Science & Technology 38, 221-228.

La Lacheur, R.M., Sonnenberg, L.C., Singer, P.C., Christman, R.F., Charles, M.J., 1993. Identification of carbonyl compounds in environmental samples. Environmental Science & Technology 27, 2745-2753.

Langer, S.H., Pantages, P., 1961. Peak-shift technique in gas-liquid chromatography: Trimethylsilyl ether derivatives of alcohols. Nature 191, 141-142.

Leis, J.H., Fauler, G., Rchberger, G.N., Windischhofer, W., 2003. Q uantitative trace analysis of estriol in human plasma by negative ion chemical ionization gas chromatography–mass spectrometry using a deuterated internal standard. Journal of Chromatography, B 794, 205-213.

Lewandowski, M., Jaoui, M., Offenberg, J. H., Kleindienst, T. E., Edney, E. O., Sheesley, R. J., & Schauer, J. J., 2008. Primary and secondary contributions to ambient PM in the midwestern United States. Environmental Science & Technology 42, 3303-3309.

Lewandowski, M., Jaoui, M., Kleindienst, T.E., Offenberg, J.H., Edney, E.O., 2007. Composition of PM2.5 during the summer of 2003 in Research Triangle Park, North Carolina. Atmospheric Environment 41, 4073-4083.

Li, M., Chen, H., Yang, X., Chen, J., Li, C., 2009. Direct quantification of organic acids

in aerosols by desorption electrospray ionization mass spectrometry. Atmospheric Environment 43, 2717-2720.

Li, Y.-C., Yu, J.Z., 2005. Simultaneous determination of mono- and dicarboxylic acids, ω-oxo-carboxylic acids, and aldehydes in atmospheric aerosol samples. Environmental Science & Technology 39, 7616-7624.

Li, Y.C., Yu, J.Z., 2005. Simultaneous determination of mono- and dicarboxylic acids, ω-oxo-carboxylic aicds, midchain ketocarboxylic acids, and aldehydes in atmospheric aerosol samples. Environmental Science & Technology 39, 7616-7624.

Little, J.L., 1999. Artifacts in trimethylsilyl derivatization reactions and ways to avoid them. Journal of Chromatography A 844, 1-22.

Ma, Y., Russell, A.T., Marston, G., 2008. Mechanisms for the formation of secondary organic aerosol components from the gas-phase ozonolysis of α-pinene. Physical Chemistry Chemical Physics 10, 4292-4312.

Mayol-Bracero, O.L., Graham, B., Roberts, G., Andreae, M.O., Decesari, S., Facchini, M.C., Fuzzi, S., Artaxo, P., 2002. Water-soluble organic compounds in biomass burning aerosols over Amazonia 2. Apportionment of the chemical composition and importance of the polyacidic fraction. Journal of Geophysical Research 107.

Mazurek, M.A., Simoneit, B.R.T., Cass, G.R., Gray, A., 1987. Quantitative High-Resolution Gas Chromatography and High-Resolution Gas Chromatography/Mass Spectrometry analyses of carbonaceous fine aerosol particles. International Journal of Environmental Analytical Chemistry 29, 119-139.

McLafferty, F.W., Tureček, F., 1993. Interpretation of Mass Spectra, Fourth ed. University Science Books, Mill Valley, CA.

Mirivel, G., Riffault, V., Galloo, J.-C., 2009. Development and validation of an ultra-high-performance liquid chromatography coupled to time-of-flight mass spectrometry method to quantify benzoic acid and long-chain monocarboxylic acids (C_{12}-C_{28}) in atmospheric aerosols. Journal of Chromatography A 1216, 6481-6489.

Mitrevski, B.S., Brenna, J.T., Zhang, Y., Marriott, P.J., 2008. Application of comprehensive two-dimensional gas chromatography to sterols analysis. Journal of Chromatography A 1214, 134-142.

Morgan, W.T., Allan, J.D., Bower, K.N., Highwood, E.J., Liu, D., McMeeking, G.R., Northway, M.J., Williams, P.I., Krejci, R., Coe, H., 2010. Airborne measurements of the spatial distribution of aerosol chemical composiion across Europe and evolution of the organic fraction. Atmospheric Chemistry and Physics 10, 4065-4083.

Nawrocki, J., 1997. The silanol group and its role in liquid chromatography. Journal of Chromatography A 779, 29-71.

Nicoll-Griffith, D., Scartozzi, M., Chiem, N., 1993. Automated derivatization and high-performance liquid chromatographic analysis of ibuprofen enantiomers. Journal of

Chromatography A 653, 253-259.

Pan, L., Pawliszyn, J., 1997. Derivatization/Solid-Phase Microextraction: New approach to polar analytes. Analytical Chemistry 69, 196-205.

Pankow, J.F., 1994. An absorption model of the gas/aerosol partitioning involved in the formation of secondary organic aerosol. Atmospheric Environment 28, 189-193.

Pankow, J.F., 1994. An absorption model of gas/particle partitioning of organic compounds in the atmosphere. Atmospheric Environment 28, 185-188.

Pankow, J.F., Asher, W.E., 2008. SIMPOL 1: A simple group contribution method for predicting vapor pressures and enthalpies of vaporization of multifunctional organic compounds. Atmospheric Chemistry and Physics 8, 2773-2796.

Patterson, D.G., Jr., Welch, S.M., Turner, W., Focant, J.-F., 2005. The use of cryogenic zone compression for the measurement of POPs in human serum at attogram levls by GCxGC/ID-HRMS. Organohalogen Compounds 67, 107-109.

Pietrogrande, M.C., Bacco, D., & Mercuriali, M., 2010. GC-MS analysis of low-molecular-weight dicarboxylic acids in atmospheric aerosol: comparison between silylation and esterification derivatization procedures. Analytical Bioanalytical Chemistry 396, 877-885.

Pietrogrande, M.C., & Bacco, D., 2011. GC-MS analysis of water-soluble organics in atmospheric aerosol: Response surface methodology for optimizing silyl-derivatization for simultaneous analysis of carboxylic acids and sugars. Analytica Chimica Acta 689, 257-264.

Presto, A.A., Huff Hartz, K.E., Donahue, N.M., 2005. Secondary organic aerosol production from terpene ozonolysis. 1. Effect of UV radiation. Environmental Science & Technology 39, 7036-7045.

Roach, P.J., Laskin, J., Laskin, A., 2010. Molecular characterization of organic aerosols using nanospray desorption/electrospray ionization-mass spectrometry. Analytical Chemistry.

Saisho, Y., Kuroda, T., Umeda, T., 1997. A sensitive and selective method for the determination of mevalonic acid in dog plasma by gas chromatography/negative ion chemical ionization-mass spectrometry. Journal of Pharmaceutical and Biomedical Analysis 15, 1223-1230.

Sato, K., Takami, A., Isozaki, T., Hikida, T., Shimono, A., Imamura, T., 2010. Mass spectrometric study of secondary organic aerosol formed from the photo-oxidation of aromatic hydrocarbons. Atmospheric Environment 44, 1080-1087.

Scanlon, J.T., WIllis, D.E., 1985. Calculation of flame ionization detector relative response factors using the effective carbon number concept. Journal of Chromatographic Science 23, 333-340.

Schauer, J.J., Mader, B.T., DeMinter, J.T., Heidemann, G., Bae, M.S., Seinfeld, J.H., Flagan, R.C., Cary, R.A., Smith, D., Huebert, B.J., Bertram, T., Howell, S., Kline, J.T., Quinn, P., Bates, T., Turpin, B., Lim, H.J., Yu, J.Z., Yang, H., Keywood, M.D., 2003. ACE-Asia Intercomparison of a Thermal-Optical Method for the Determination of Particle-Phase Organic and Elemental Carbon. Environmental Science & Technology 37, 993-1001.

Schreiner, M., Hulan, H.W., 2004. Determination of the carbon deficiency in the flame ionization detector response of long-chain fatty acid methyl esters and dicarboxylic dimethyl esters. Journal of Chromatography A 1045, 197-202.

Schummer, C., Delhomme, O., Appenzeller, B.M.R., Wennig, R., Millet, M., 2009. Comparison of MTBSTFA and BSTFA in derivatization reactions of polar compounds prior to GC-MS analysis. Talanta 77, 1473-1482.

Solomons, T.W.G., Fryhle, C., 2003. Organic Chemistry. Wiley.

Spaulding, R.S., Charles, M.J., 2002. Comparison of methods for extraction, storage, and silylation of pentafluorobenzyl derivatives of carbonyl compounds and multi-functional carbonyl compounds. Analytical Bioanalytical Chemistry 372, 808-816.

Ŝtávová, J., Beránek, J., Neson, E.P., Diep, B.A., Kubátová, A., 2011. Limits of detection for the determinatino of mono- and dicarboxylic acids using gas and liquid chromatographic methods coupled with mass spectrometry. Journal of Chromatography B 879, 1429-1438.

Steele, L.P., Porter, L.W., van der Schoot, M.V., Langerfelds, R.L., 2007. Measuring selected atmospheric trace gases using gas chromatography and Valco pulsed discharge ionisation detector, in: Laurila, T. (Ed.), World Meteorological Organization Global Atmospheric Watch: 14th WMO/IAEA Meeting of Experts on Carbon Dioxide, Other Greenhouse Gases and Related Tracers Measurement Techniques. World Meteorological Organization, Helsinki, Finland.

Sternberg, J.C., Gallaway, W.S., Jones, D.T.L., 1962. The mechanism of response of flame ionization detectors, in: Brenner, N., Callen, J.E., Weiss, M.D. (Eds.), Gas Chromatography. Academic Press, New York, pp. 231-267.

Strazhesko, D.N., Strelko, V.B., Belyakov, V.N., Rubanik, S.C., 1974. Mechanism of cation exchange on silica gels. Journal of Chromatography 102, 191-195.

Tiwari, R.D., Sharma, J.P., 1970. The determination of carboxylic functional groups. Pergamon Press, Oxford; New York.

Tobias, H.J., Ziemann, P.J., 2000. Thermal Desorption Mass Spectrometric Analysis of Organic Aerosol Formed from Reactions of 1-Tetradecene and O3 in the Presence of Alcohols and Carboxylic Acids. Environmental Science & Technology 34, 2105-2115.

U.S.E.P.A., 2007. Method 8270D: Semivolatile Organic Compounds by Gas Chromatography/Mass Spectrometry (GC-MS), in: U.S.E.P.A. (Ed.).

Ueyama, J., Saito, I., Kamijima, M., Nakajima, T., Gotoh, M., Suzuki, T., Shibata, E., Kondo, T., Takagi, K., Miyamoto, K., Takamatsu, J., Hasegawa, T., Takagi, K., 2006. Simultaneous determination of urinary dialkylphosphate metabolites of organophosphorus pesticides using gas chromatography–mass spectrometry. Journal of Chromatography, B 832, 58-66.

van Deursen, M.M., Beens, J., Janssen, H.G., Leclercq, P.A., Cramers, C.A., 2000. Evaluation of time-of-flight mass spectrometric detection for fast gas chromatography. Journal of Chromatography A 878, 205-213.

van Pinxteren, D., Herrmann, H., 2007. Determination of functionalised carboxylic acids in atmospheric particles and cloud water usping capillary electrophoresis/mass spectrometry. Journal of Chromatography A 1171, 112-123.

Vogt, L., Gr√∂ger, T., Zimmermann, R., 2007. Automated compound classification for ambient aerosol sample separations using comprehensive two-dimensional gas chromatography‚Äìtime-of-flight mass spectrometry. Journal of Chromatography A 1150, 2-12.

Walser, M.L., Park, J., Gomez, A.L., Russell, A.R., Nizkorodov, S.A., 2007. Photochemical aging of secondary organic aerosol particles generated from the oxidation of d-limonene. Journal of Physical Chemistry A 111, 1907-1913.

Welthagen, W., Schnelle-Kreis, J., Zimmerman, R., 2003. Search criteria and rules for comprehensive two-dimensional gas chromatography-time-of-flight mass spectometry analysis of airborne particulate matter. Journal of Chromatography A 1019, 233-249.

Wilson, R.B., Siegler, W.C., Hoggard, J.C., Fitz, B.D., Nadeau, J.S., Synovec, R.E., 2011. Achieving high peak capacity production for gas chromatography and comprehensive two-dimensional gas chromatography by minimizing off-column peak broadening. Journal of Chromatography A 1218, 3130-3139.

Xu, X., van Stee, L.L.P., Williams, J., Beens, J., Adahchour, M., Vreuls, R.J.J., Brinkman, U.A.T., Lelieveld, J., 2003. Comprehensive two-dimensional gas chromatography (GC×GC) measurements of volatile organic compounds in the atmosphere. Atmospheric Chemistry & Physics 3, 665-682.

Yang, L., & Yu, L. E., 2008. Measurements of oxalic acid, oxalates, malonic acid, and malonates in atmospheric particulates. Environmental Science & Technology 42, 9268-9275.

Yu, J., Cocker, D.R., III, Griffin, R.J., Flagan, R.C., Seinfeld, J.H., 1999. Gas-Phase Ozone Oxidation of Monoterpenes: Gaseous and Particulate Products. Journal of Atmospheric Chemistry 34, 207-258.

Yu, J., Flagan, R.C., Seinfeld, J.H., 1998. Identification of products containing -COOH, -OH, and -C=O in atmospheric oxidation of hydrocarbons. Environmental Science & Technology 32, 2357-2370.

Zhang, Q., Jimenez, J.L., Canagaratna, M.R., Allan, J.D., Coe, H., Ulbrich, I., Alfarra, M.R., Takami, A., Middlebrook, A.M., Sun, Y.L., Dzepina, K., Dunlea, E., Docherty, K., DeCarlo, P.F., Salcedo, D., Onasch, T., Jayne, J.T., Miyoshi, T., Shimono, A., Hatakeyama, S., Takegawa, N., Kondo, Y., Schneider, J., Drewnick, F., Bormann, S., Weimer, S., Demerjian, K., Williams, P., Bower, K., Bahreini, R., Cottrell, L., Griffin, R.J., Rautiainen, J., Sun, J.Y., Zhang, Y.M., Worsnop, D.R., 2007. Ubiquity and dominance of oxygenated species in organic aerosols in anthropogenically-influenced Northern Hemisphere midlatitudes. Geophysical Research Letters 34.

APPENDICES

APPENDIX A: Standard Operating Procedure for Derivatization of Polar, Organic Compounds Prior to Analysis in GCxGC TOF-MS

Contents

1. Cleaning of Glassware and Syringes

1.1 Glassware and Syringe Handling

Syringes should be soaked in solvent and sonicated in detergent, then distilled water 2x before use (and dried at *low* heat, 50°C) for derivatizations requiring use of water-reactive solvents (this includes trimethylsilylation reagents and those catalyzed by boron trifluoride (BF_3)). All other glassware should be washed by the protocol below. Glassware, including syringes, should be kept clean between cleaning and use.

1.2 Glassware Cleaning Procedure:

All glassware with the exception of syringes and all volumetric equipment (or pieces specifically marked with a lower stability for heat) should be cleaned using the following procedures (procedure one is best):

1.2.a Glassware Cleaning Procedure One:

- Rinse and scrub using brush in DI water
- Make solution of detergent (use hot water and stir, only add small amount so that no particles are left)
- Submerge all glassware in and allow glassware to sit in detergents solution ~1hr (or sonicate ~10 mins)
- Rinse with deionized/18 MΩ water thoroughly
- After rinsing, sonicate ~10 mins in deionized/18 MΩ water
- Dry in muffle furnace at 400°C for 3-5 hrs

- Remove and keep in clean, dry space (such as in a drawer, covered by aluminum foil) until use

1.2.b Glassware Cleaning Procedure Two:

- Mix detergent solution; pour over glassware in large container.
- Sonicate ~5-10 minutes
- Remove and scrub with both .5cm and 1cm brushes
- Repeat sonication with detergent solution
- Rinse each piece thoroughly with distilled water (from silver tap) or 18 MΩ water
- Rinse each piece with a series of solvents from squeeze bottles, tipping into waste jar after each: DCM, hexane, acetone
- Rinse each piece thoroughly with distilled water (from silver tap)
- Dry in oven overnight at >150°C
- Remove and keep in clean, dry space until use

1.3 Syringe Cleaning Procedure:

Note that some syringes are designed to deliver from the side of the needle, rather than the tip, and care should be taken to put the tip of the syringe into the waste jar to avoid spray.

For syringes 500 µl or larger in volume, flushes used in cleaning should be approximately 1/5 of the total syringe volume. For syringes less than 500 µl in

volume, the flush volumes should be the entire volume of the syringe.

Depending upon the type of solution delivered, different solvents should be used:

- If aqueous:
    - Use 5-10 flushes of 18 MΩ water
    - Use 5-10 flushes of methanol/other solvent miscible with water
    - For smaller than 50-100 ul syringes, follow with several flushes of DCM and other solvents so that 20-30 ~full flushes.
- If non-aqueous solvent:
    - Clean with just that solution, 10-15 flushes.
- If solution used was neat or highly concentrated or of other concern for contamination:
    - Soak or sonicate in 18 MΩ water in clean 40 ml vial >1 hour, inverting after about half the soak time has passed so that both the needle and the body are soaked (less time is needed if sonicated).
    - Use 10 flushes 18 MΩ water
    - Use 10-15 flushes methanol/other solvent miscible with water
    - Use 10-15 flushes DCM and/or less polar solvents
- Preheat oven to ~50C, shut off, add syringes without plungers in (but adjacent so that each syringe and plunger pair is not separated), for about an hour. Make sure to use a volatile solvent and completely depress the syringe to remove excess solvent before heating.

1.4 Syringe Use:

- If any liquid is visible on the outside of the needle, this means that there is either contamination on the outside of the needle or some defect in the needle. Clean the needle and use another needle of the same size.
- Use a laboratory wipe to wipe clean the outside of the needle in one upward motion, making sure the slant of the needle tip is toward you. Make sure that no laboratory wipe fibers are left on the outside of the needle.
- In order to draw up a liquid, pulling out a small amount of the liquid beyond the desired measurement, then tipping the syringe so that the needle is facing upward, push the remaining volume (and any air) out of the needle, holding a laboratory wipe against the needle tip.

1.5 Sodium Sulfate Drying:

Sodium sulfate should be dried in a clean container overnight in an oven at 180-300°C in order to remove all water. The container containing the drying agent should then be capped after cooling in the oven or a clean dessicator and kept in a clean dessicator until use. A clean spatula should be used to deliver the sodium sulfate.

2 Standard Solutions

Much of this section will be based upon EPA Method 8270C, Semi-volatile Organic Compounds by Gas Chromatography/Mass Spectrometry (GC/MS); and EPA Method 8015C, Nonhalogenated Organics by Gas Chromatography.

Each solution should be prepared as a stock solution, at higher concentrations that those anticipated to be used (such as 1 or 0.5 mg/ml). Secondary solutions should then be made by serial dilution prior to addition into the samples or standards for analysis. All solutions should be stored in capped ~2 ml autosampling vials at ~4°C in plastic vial holders or jars. Stock solutions should be remade after a period of six months to one year; secondary solutions should be remade after a period of three to six months. All solutions should be properly labeled with the approximate concentration and date.

Stock solutions should be prepared using the top-loading analytical balance with closing doors, properly balanced. The appropriately sized volumetric flask (larger is preferable so that small errors in addition of the standard solutions are not as effective in the overall concentration within the standard solution) should contain a small volume of solvent prior to addition of the standard compounds so that solubility is observed and compounds cannot be volatilized while the flask is open.

Solid solutions should be massed onto a tared, bi-folded weigh paper using a cleaned microspatula. Masses and volumes added of standards should be recorded to the nearest hundredth of a milligram, and used during quantitation (rather than the

approximate value, such as 50 mg if the solution is intended to be 50 mg/ml). Any excess standard compound should be discarded into the hazardous bin using a lab wipe, and *not returned to the standard container*. Liquid standards can be delivered using a microsyringe of the appropriate size (calculate volume needed using the density of the standard); syringes should be washed thoroughly immediately after use. A small volume of solvent can follow introduction of each standard into the solution flask so that no standard may be volatilized from the neck of the flask during subsequent opening. The flask should be closed tightly and inverted at least twice before the final volume is reached, allowing pressure to be relieved after each inversion by opening the flask briefly. Vortexing or swirling gently may be used in order to cause dissolution, but *heating should not be used because of potential alteration of the calibration of the flask as well as volatilization of the standard compounds.*

2.1 Recovery Standards

2.1.a Purpose: The accuracy (recovery) of each sample or standard prepared and analyzed should be assessed by the use of a standard compound, the concentration of which is assumed to be within 20% of its initial concentration (this needs to be verified prior to use). If the recovery of the compound is not within this limit in a given sample or standard, when this recovery is consistently reached, the final concentrations of analytes/standards may be adjusted using this calculated

recovery. Adjustment is not necessary if the recovery of the recovery standard is determined to be within 90-110% of the injected concentration.

2.1.b Criteria: This compound should be chosen so that it will not be found within the sample (deuterated compounds are useful), and so that its volatility is low so that it can be accurately be assumed to be injected into the sample at the same precise quantity as it will be measured using the resulting chromatogram. Because the recovery must be sufficiently high in each analysis so that the quantities of the analytes can be calculated, the response of recovery standards with similar structure and functionality to the analytes can also be monitored to show that compounds closer in structure and functionality were recovered.

2.1.c Concentration: The concentration of this compound should be the same as the concentration of the standard compounds so that a calibration range is given for this compound (this should be approximately 0.01-50 ng/μL in the final injected sample).

2.1.d To be used: *n*-eicosane-d_{42} (for calculation); succinic-d_4 acid, ketopinic acid

2.1.e Prior to use: Test the recovery of this compound by external calibration relative to the internal standard closest in retention time. The recovery must be consistently within 100% +/-20% of the anticipated concentration. The relative response factor can then be calculated so that the compound can be used during external calibration of calibration and surrogate standards and during sample analysis.

2.2 Surrogate Standards

2.2.a Purpose: In order to assess the extraction efficiency, at least one compound similar in structure and functionality to the analytes should be spiked into each sample and standard prior to extraction (when extraction is used).

2.2.b Criteria: Also use a surrogate standard (only correct with this if it's not within 20% of 100% efficiency): deuterated acid (succinic-*d4*). This way, calibration does not require extraction ----just do with the benchtop method.

2.2.c Concentration: The concentration of this compound should be the same as the concentration of the standard compounds.

2.2.d To be used: succinic-*d4* acid, ketopinic acid

2.2.e Prior to use: Test recovery of these prior to use on actual samples; find RF using calibration procedures

2.3 Internal Standards

2.3.a Purpose: Compounds to be used in relation to the response of the calibration and recovery standards in order to find the response factor, and thus the concentration of the calibration standards.

1.1.a Criteria: These should not be anticipated to volatilize from the solution between injection after the sample preparation procedure and introduction of the sample into the instrument. These compounds likewise should be known to respond well to the particular GC-MS setup (column, temperature program, etc.).

1.1.b Concentration: The concentration should be constant throughout the analyses so that the response factor is not allowed to change between sample/standard analyses; approximately 2-5ng/µl in final injection.

1.1.c To be used: toluene-d_8, naphthalene-d_{10}, phenanthrene-d_{12}, pyrene-d_{12}

1.1.d Prior to use: Test the recovery of these compounds by noting the consistent peak areas between analyses. The recovery must be consistently within 100% +/-20% of the anticipated area.

2.4 Calibration Standards

2.4.a Purpose: This list of compounds should correspond to those anticipated to be in the sample to be analyzed; for example, an urban aerosol sample may contain ring-opening and alkene oxidation products (see Calvert, *et al.,* series).

2.4.b Criteria: For each compound or type of compound anticipated to be in the sample, at least one compound of comparable volatility and functionality should be used.

2.4.c Concentration: The solution should be prepared as a stock solution at a concentration higher than should be found in the sample (the latter is dependent upon the loading of the filter and the extract total volume, but resulting concentrations are generally in the range of 0.01 – 20 ng/µL) so that dilution to low concentration is possible in generating a calibration curve (secondary solutions) and small amounts may be delivered to each standard reaction vial. Consideration of the mass of each standard compound to be delivered to the

volumetric flask should be made prior to making the stock solution. Each solid or liquid standard should not be delivered at masses less than ~10 mg. A large volume of the stock solution may therefore be necessary in order to increase delivered masses.

2.4.d To be used: See Tables T and U below.

Table T. Trimethylsilyl derivatives of calibration standards. Retention times listed are averaged over all calibration points measured during several standard analyses. The target ion or sum or ions used in quantitation in the 2D results is listed first under characteristic ions for each standard.

Common Name/Systematic Name	**Approximate Retention Times (2D primary, secondary; 1D, min)**	**Characteristic Ions (m/z): Target; Qualifiers; Molecular Ion**
Lactic Acid/2-hydroxy-Propanoic Acid	831.9,1.00,12.93	147+73; 117, 45; 234
2-hydroxy-3-methyl-Butyric Acid	979.9,1.33,12.72	145+73; 147, 75; 262
Malonic Acid/Propanedioic Acid	1023.9, 1.12,13.57	147; 73; 248
methyl-Malonic Acid/methyl-Propanedioic Acid	1023.9, 1.12,13.80	147; 73, 148, 75; 262
Glutaric Acid/Pentanedioic Acid	1439.9, 0.78,19.85	147, 73, 75, 55; 276
Adipic Acid/Hexanedioic Acid	1399.9, 1.23, 20.01	111, 75, 73, 147; 290
Salicylic Acid/2-hydroxy-Benzoic Acid	1423.9, 1.4, 20.10	267+135; 73, 268; 282
cis-Pinonic Acid/ [(1R,3R)-3-acetyl-2,2-dimethylcyclobutyl]acetic acid	1439.9, 1.53, 20.38	73+121+83; 75, 171; 290
Lauric Acid/Dodecanoic Acid	1575.9,1.27, 23.008	257+73; 75, 117; 272

Table U. Butyl derivatives of calibration standards. Retention times listed are averaged over several standard analyses. The target ion used in quantitation in the 1D results is listed first as a characteristic ion for each standard.

Common Name/Systematic Name	**Approximate Retention Times (2D primary, secondary; 1D, min)**	**Characteristic Ions (m/z): Target; Qualifier(s); Molecular Ion**
Oxalic Acid/Ethanedioic Acid	1131.9, 1.37,15.39	147; 103, 57; 202
Malonic Acid/Propanedioic Acid	1227.9, 1.34, 16.82	105; 87, 143, 161 216
methyl-Malonic Acid/methyl-Propanedioic Acid	1247.9, 1.3, 17.20	101; 74, 119, 157; 230
Salicylic Acid/2-hydroxy-Benzoic Acid	1279.9, 1.43, 18.28	120; 92, 138, 194; 194
Succinic-d_4 Acid/Butanedioic-d_4 Acid	1359.9, 1.38,19.92	105; 77, 161, 179; 243
Glyoxylic Acid/2-oxo-Ethanoic Acid	1403.9, 1.21, 19.87	159; 91, 103, 117; 260
Glutaric Acid/Pentanedioic Acid	1471.9, 1.41, 22.045	115; 87, 142, 189; 244
cis-Pinonic Acid/ [(1*R*,3*R*)-3-acetyl-2,2-dimethylcyclobutyl]acetic acid	1479.9, 1.5, 22.26	125; 83, 98, 167; 226
Adipic Acid/Hexanedioic Acid	1583.9, 1.47, 23.44	185; 129, 111, 87; 258
Lauric Acid/Dodecanoic Acid	1603.9, 1.45, 25.13	201; 57, 105, 73; 256
Glyoxal/Ethanedial	1603.9, 1.25, 25.36	159; 57, 103, 133; 318

2.4.e Prior to use: Retention times should be measured to prevent co-elution and allow mixing of secondary quantitation standard solutions with that in mind. It may be useful to also find studies characterizing this compound to contrast the relative retention time with other standards for quantitation, so that none of the standards will co-elute.

3 Filter extraction

3.1 Standard and Blank Filter Cleaning Procedure

All filters (quartz) are purchased after cleaning by heating to ~500C, which removes all contaminants to ~8 μg total. Filters should be kept in freezer (~-4°C) in Petri dish, wrapped in foil and zip-closed plastic bag until use. Clean gloves should be used when handling filters (only cleaned tweezers should be used to handle the filters directly) and care should be taken to remove any possible sources of contamination from the hood before Petri dishes are opened (close waste jar, clean syringes used for delivery of anything other than solvents). If the extraction will be of a filter containing sample or blank, the filter should be spiked with only the internal recovery standard prior to extraction; if the extraction will be a standard (calibration) extraction, the standard compounds should additionally be spiked onto the filter prior to extraction.

3.2 Extraction Procedure (Standard and Blanks)

- Equipment and supplies (maximum four extractions):
    - Sonication bath
    - Ice (~0.5 lbs)
    - Syringe of appropriate size to deliver standard(s) to filter
    - Two 1 ml syringes to deliver solvent
    - Two 5 ml volumetric pipets with bulb
    - Lab wipes

  - 50-100 ml dichloromethane (each extraction)
  - 50-100 ml methanol (each extraction)
  - Quartz filter (one per extraction) in Petri dish
  - *Two* clean 40 ml vol-a-vials with septa and caps
  - Vol-a-vial Styrofoam holder
  - Paraffin lab film
  - 40 ml vol-a-vial marked to 22 ml total volume
  - Aluminum foil
  - Refrigerator at ~4°C
  - Glassware to have on hand: 2-3 clean ~250 ml beakers or Erlenmeyer flasks
  - 10-20 autosampling vials for syringe cleaning
  - Scalpel and clean blade (preferably new; soak in DCM/methanol) and wipe carefully with a laboratory wipe.
- Label each 40 ml vol-a-vial (two for each extract) with tape AND on cap with permanent ink
- Set up sonication bath in hood (fill so that vials will float, but melting ice will not cause bath to overflow)
- Use cleaned, dried syringes to add standard mixture and/or recovery standard (7 micrograms) to cleaned filter, replace lid of Petri dish after delivery to dry
- Use clean volumetric pipets to add 5 ml each dichloromethane and methanol; rinse and cover with foil between uses (syringes may also be used, but the final

volume is not greatly affected by the aqueous calibration of the volumetric pipets. If syringes are used, some method of keeping track of the number of injections should be used with a 1 ml syringe).

- Cut filter into quarters using scalpel with clean, dry blade and place into bottom of vol-a-vial (into solvent as much as possible)
- Cap and sonicate 45 mins on ice (ice in sonicator water, vials floating in Styrofoam holder)
- Decant extract using dried Pasteur pipette to clean, labeled Vol-a-vial, wash with 1 ml each dichloromethane and methanol (use clean, dried 1 ml syringes to deliver), decant to same Vol-a-vial
- Use volumetric pipets to deliver 5 ml each dichloromethane and methanol, rinse and cover pipets with foil
- Sonicate again 45 mins on ice
- Decant extract using dried Pasteur pipette to clean, labeled Vol-a-vial, wash with 1 ml each dichloromethane and methanol (use clean, dried 1 ml syringes to deliver), decant to same Vol-a-vial
- Compare volume of extract to Vol-a-vial marked with 22 ml total volume, use dichloromethane or methanol to add any volume lacking
- Cap, wrap lid (with septum) in paraffin film, store at ~4°C (in refrigerator)
- Clean all syringes and equipment used

4 Blank Procedures

Blank procedures should be used at the beginning of each set of samples or before calibration in order to ensure that the background will be low in the following analyses. The procedures outlined here are those run within the sample preparation laboratory; a series of filter collection blanks (consisting of analysis of a filter having had an equivalent volume of environmental chamber or ambient air drawn through) should also be run in order to show that the background from the collection device is low.

4.1 Solvent Blanks without Derivatization

For each series of samples or standards, at least one solvent blank should be run, consisting of the solvents used in the analysis, including internal injection standards and the recovery standard.

Procedure:

- To a clean, dry spring insert in data processing vial:
- Use clean, dry 1ml syringes to add 3 ml of one of the following solvents: DCM, acetonitrile, methanol, hexanes
- Allow to concentrate under gentle stream of nitrogen until volume is less than 1 ml
- Use a clean, dry 1 ml syringe to add 2 ml solvent
- Allow to concentrate under gentle stream of nitrogen until ~dryness

- Reconstitute by using a clean, dry 500 µL syringe to add 300 µL solvent
- Use clean, dry 10 µL syringe to injection 4.5 µL internal std PAHs: (30µl)(300ng/µl)/(2000µl) = 4.5 ng/µL added.
- Analyze using comprehensive GC-MS method with short solvent delay
- Three to four replicates should be made so that a standard deviation can be calculated, and loss of one vial will not necessitate restarting the procedure.

4.2 Solvent Blanks with Derivatization

For all series of analyses in which a method blank is prepared and analyzed, a method blank without extraction should also be made in order to assess the background compounds present and concentrations of those compounds *other than any introduced during the extraction procedure.*

Procedure:

- To a clean, dry 3 ml Reacti-vial:
- Use a clean, dry 1 ml syringe to add 3 ml solvent
- Allow to concentrate under gentle stream of nitrogen until volume is less than 1 ml
- Use a clean, dry 1 ml syringe to add 2 ml solvent
- Allow to concentrate under gentle stream of nitrogen until ~dryness
- Carry out derivatization procedure (both for *n*-butanol/BF_3 and BSTFA) without analytes, add injection std. PAHs (4.5 ng/µL).
- Three to four replicates should be made

4.3 Reagent Blanks

In the case of contamination or unwanted peaks in the other blanks with derivatization, reagent blanks may be used in order to show the background contributed by the reagent, or byproducts of reaction with the reagent. The solvent used should be the same that is in the derivatization procedure, but should not be concentrated.

Procedure:

- To a clean, dry 3 ml Reacti-vial:
- Use a clean, dry 1 ml syringe to add 2 ml solvent
- Use a clean, dry syringe of appropriate size to add derivatization reagent (see derivatization procedures for volume reagent to be added)
- Heat as directed by derivatization procedure
- Allow to cool, transfer 300 µL to 2 ml autosampling vial with 300 µL insert
- Add internal injection standards, cap
- Analyze via one-dimensional GC using a method appropriate from the derivatization procedure (it is especially important in this case that the solvent delay is observed because the reagent excess may be large).

4.4 Filter Blanks

A filter blank (rather than a filter collection blank, through which "clean" sampler air should be passed) should be processed using a filter used in the analysis of the samples, to be extracted and run as the derivatized and underivatized blank. A

compound in the resulting standard or sample chromatograms should have a statistically significant increase from those in the blank chromatograms. For each set of standards or samples with similar derivatization and extraction, three blank filters should be extracted so that a standard deviation may be calculated and there is statistical certainty of whether a compound is in the background, and not in the standards or samples.

Quartz fiber filters are cleaned in a muffle furnace at high temperature prior to use by Sunset Laboratories. After receipt, the filters should be stored within Petri dishes (closed tightly by paraffin film), foil, and a closeable plastic container. The filters should be kept at ~-4°C. Filters should be handled only in clean conditions and using clean, dry tweezers (not with gloves, even if new).

- Using a properly cleaned and kept quartz fiber filter:
- Open the Petri dish and quickly use a clean, dry 1 ml syringe to add internal recovery standard to the filter.
- Use a clean, dry cutting tool to cut the filter into four approximately equal in size pieces. Use the clean, dry tweezers to put the filter pieces into a clean, dry 40 ml vial.
- Use clean, dry 1ml syringes to add 5.00 ml each dichloromethane and methanol
- Place vol-a-vial in larger glassware such as Erlenmeyer flask filled with ice (do not allow to tip over into water of sonicator), extract for 45 minutes

- Maintain ice in Erlenmeyer flask or other large glassware so that side reactions accelerated by heat are not allowed (this is particularly prevalent with dichloromethane)
- Remove from sonicator, transfer extract to clean, labeled Vol-a-vial using clean, dry Pasteur pipette. *Ensure that the Vol-a-vials will not tip over while on benchtop.*
- Rinse using clean, dry 1 ml syringes with 2x 500 µL each DCM and MeOH, decant washes to labeled Vol-a-vial
- Repeat sonication on ice for another 45 minutes, followed by transfer and rinse steps. Total volume will be 22000 µL.
- Store 40 ml vial in refrigerator (4°C) with septum cap covered by paraffin film.
- Use clean, dry 1 ml syringe to transfer 3 ml extract to clean, dry Reacti-vial.
- Carefully place under tube end, into slot in heating block fitting, ensuring that the stream of nitrogen only makes a 1-2 mm dent in the surface of the liquid.
- Allow the liquid to dry until 2 additional ml solvent can be added; remove from heat and use a clean, dry 1 ml syringe to do so.
- Allow liquid to dry *just* until the surface of the extract appears oily.
- Cap and refrigerate any dried extracts until all are dried.
- Reconstitute the dried extract using a clean, dry 500 µL syringe into 150 µl each dichloromethane and hexanes.

- Transfer using Pasteur pipet to 300 µl insert in 2 ml autosampling vial, properly labeled.
- Add injection internal standards (300µl)(5ng/µl)/(300ng/µl) = 3 µl needed (if a 1D chromatograph is used, 5 µL should be delivered).
- Three to four replicates should be made.

4.5 Filter Blanks with Derivatization

For all series of analyses, method blanks (also known as procedural blanks) should be made in order to assess the background compounds present and concentrations of those compounds given the system used (including all aspects of the sample preparation and analysis).

Extraction procedure:

- Fill the ultrasonicating bath approximately half full with tap water and place in the hood.
- Using a clean, dry collection filter:
- Use a clean, dry cutting tool to cut the filter into four approximately equal in size pieces. Use the clean, dry tweezers to put the filter pieces into a clean, dry 40 ml vial.
- Use clean, dry 1ml syringes to add 5.00 ml each dichloromethane and methanol
- Cap and place into Styrofoam vial holder so that the vial fits tightly.

- Add 2-3 cups ice to the water of the ultrasonicating bath.
- Place the vials in the Styrofoam holder into the ultrasonicating bath and turn on. Extract 45 minutes.
- Maintain ice so that side reactions accelerated by heat are not allowed (this is particularly prevalent with dichloromethane)
- Remove from sonicator, transfer extract to clean, labeled Vol-a-vial using clean, dry Pasteur pipette. *Ensure that the Vol-a-vials will not tip over while on benchtop.*
- Rinse using clean, dry 1 ml syringes with 2x 500 µL each DCM and MeOH, decant washes to labeled Vol-a-vial
- Repeat sonication on ice for another 45 minutes, followed by transfer and rinse steps. Total volume will be 22000 µL.
- Store Vol-a-vial in refrigerator (4°C) with septum cap covered by paraffin film until derivatization.

Derivatization procedure:

- Turn on power to heating block and turn dial to 30°C.
- Ensure that nitrogen gas is available and that the nitrogen blowdown system is working (close system, cool using liquid nitrogen bath for five minutes, then allow N_2 to flush forward through the system for at least five minutes with tube ends attached/open). *Note: Do not allow air to flow back through apparatus (attach close cap ends during short*

periods of non-use, but allow to vent for short period of time when finished); flow-back will be slow, so that this should only contaminate the impurity traps if left open for more than a few hours.

- Use clean, dry 1 ml syringe to transfer 3 ml extract to clean, dry Reacti-vial.
- Carefully place under tube end, into slot in heating block fitting, ensuring that the stream of nitrogen only makes a 1-2 mm dent in the surface of the liquid.
- Allow the liquid to dry until 2 additional ml solvent can be added; remove from heat and use a clean, dry 1 ml syringe to do so.
- Allow liquid to dry *just* until the surface of the extract appears oily.
- Cap and refrigerate any dried extracts until all are dried.
- Turn heating block knob to appropriate temperature for particular derivatization procedure.
- Derivatize with *n*-butanol/BF_3 or BSTFA as listed in this document, add injection std PAHs (3 ng/µL for a 2D-GC, 5 ng/µL for a 1D-GC).
- Four replicates should be made so that a standard deviation can be calculated, and loss of one vial will not necessitate restarting the procedure.

5 Derivatization Procedures

5.1 Derivatization Procedures

5.1.a *N,O-bis*-(trimethylsilyl-)-trifluoro-acetamide (BSTFA, trimethylsilylation reagent)

This reagent is to be used to target compounds containing carboxylic acids and hydroxy- groups. The reagent reacts strongly with water so that the reaction system should be kept dry until specified by the reaction procedure for cleanup of the excess reagent. Some tautomerization to the enolate of neutral carbonyl-containing compounds may occur, generating a bis-(trimethylsilyloxy)- group where the carbonyl was located. Care should be taken to prevent misidentification in particular of compounds where the carbonyl may possess acidic character.

Adapted from (Yu, et al., 1999), (Pietrogrande, et al., 2010):

- All filter extracts: to 5 ml extracts in Reacti-vial, dried (in two parts due to size of vial) under a gentle stream of nitrogen *(not heated)* until "oily":
- Standards without extraction: to standards solution(s) in reaction vial:
- Use clean syringes to add 500 µL DCM
- Add 20 µl BSTFA (syringe directly from septum cap of reagent), cap Reacti-vial using septum and cap
- React 60 mins @ 65°C in heat block in hood

- Cool on benchtop ~5 mins
- Dry *just* until "oily" under a gentle stream of nitrogen (no heating)
- Reconstitute into 300 µL DCM
- Transfer using a clean Pastuer pipette to data processing vial containing a 300 µl spring insert
- Add 3 µl internal injection standard solution @ 300 ng/µl
- Cap using crimptop cap and crimper
- Analyze immediately if possible or store at ~4°C (in refrigerator)

5.2 Boron Trifluoride/*n*-Butanol (BF_3/BuOH, butylating reagent)

Target analytes reacted by this compound include carboxylic acids (particularly di-acids), aldehyde groups, and neutral carbonyls with acidic character.

Adapted from (Jaoui, et al., 2004), (Kawamura and Ikushima, 1993):

- All filter extracts: to 5 ml extracts in Reacti-vial, dried (in two parts due to size of vial) under a gentle stream of nitrogen (*not heated*) *just* until "oily":
- Standards without extraction: to standard solution(s) in cleaned Reacti-vial, dried (in two parts due to size of vial) under a gentle stream of nitrogen *just* until "oily" (no need for drying if standard compounds not in methanol):
- Use cleaned syringes to add 150 µL BF_3/BuOH, 100 µL hexanes (if no other solvent), cap Reacti-vial using septum and cap

- React 60 mins @ 65C in heating block in hood
- Cool on benchtop ~5 mins
- Use a clean 500 µL or 1 ml syringe to Add 500 µL hexanes (before adding water)
- Use a clean 1 ml syringe to add 1.5 ml NaCl saturated water (thoroughly clean syringe with water after use; NaCl can be deposited at the tip)
- Cap and vortex 20 sec
- Decant out water layer using clean Pasteur pipette
- Wash with 1 ml deionized/18 MΩ water (use clean 1 ml syringe)
- Cap and vortex 20 sec, decant out water layer
- Dry over ~0.5-1g dry Na_2SO_4 while shaking on shaking block on low about 30 mins (capped; a sufficient amount of drying agent should be added so that the particles are mobile at the bottom of the vial when gently tipped)
- Decant into clean Reacti-vial; do not decant solids
- Wash with 500 µL hexanes, decant again to same Reacti-vial
- Dry *just* until "oily" under a gentle stream of nitrogen (no heating)
- Use a clean syringe to reconstitute to 300 µL 1:1 DCM:hex
- Transfer using a clean Pastuer pipette to data processing vial containing a 300 µl spring insert

- Add 3 µL IS @ 300 ng/µL
- Cap using crimptop cap and crimper
- Store at ~4°C (in refrigerator)

5.3 Pentafluorobenzyl-hydroxylamine (PFBHA, neutral carbonyl oximating reagent)

- To extracts in DCM/MeOH, dried:
- Add 50 uL PFBHA in ACN, 1 ml 1:1 DCM:ACN
- 24 hrs at room temp
- Blow to dryness liquid nitrogen reconstitute
- Add IS, cap, and store as above, or continued with BSTFA procedure

5.4 2,3,4,5-*O-bis*-Pentafluorobenzyl-bromide (PFBBr, esterifying reagent)

- To extracts in DCM/MeOH, dried:
- Add 12 molar equivalents PFBBr
- Add 15 uL 18-cr-6
- Add 10 mg K2CO3
- Add 2 ml DCM
- React 3 hrs @55-60C
- Blow to dryness using gentle stream of liquid nitrogen
- Reconstitute in 200 uL hexanes

6. Calibration

6.1 Calculation of Response Factors from Calibration and Analyte Concentration

The samples will be analyzed in the same method as the blank filters, with the internal standard compound (eicosane-d_{42}) injected prior to extraction All standard compounds should be injected so that the concentrations are between 2 and 10 ng/ul in the chromatogram.

Calibration curve: need one data point for each concentration used.

Response Factors, *RF*, should be calculated for all standard compounds from the four to five concentrations used to form the calibration curve:

$$RF = (A_S \times C_{IS})/(A_{IS} \times C_S) \qquad \text{(A6.1)}$$

Where A_s is the sum of the area of the two quantitation ions for the calibration standard, C_s is the concentration of the calibration standard, A_{is} is the sum of the quantitation ion areas of the internal standard, and C_{is} is the concentration of the internal standard. The quantitation ions (2-3 for most standard compounds; 1 is acceptable where more are not appropriate due to similarity to solvent or coeluting compounds) should be used for find the C_s and C_{IS} rather than simply the peak area.

If the analytical standard was available for a compound identified in a given sample, the relative concentration (relative to the recovery standard) in the sample can be calculated using the *RF* from the external calibration of the corresponding standard compound. Since the *RF* is known, the experimental peak area of the compound *i*, A_i can be used in Equation X, rearranged to find the concentration of compound *i*:

$C_{i,\,rel} = (A_i \text{ x } C_{IS})/(A_{IS} \text{ x } RF)$ (A6.2)

The absolute recovery of the recovery standard (eicosane-d_{42}) can be calculated using this equation (as the relative concentration) because the variation in its concentration between analyses is assumed to be zero. The percent recovery, PR_{rs}, is thus simply the percent difference from the concentration injected, and the absolute concentration of compound *I* can then be calculated by multiplying the relative concentration, $C_{i,\,rel}$, by PR_{rs}.

$C_{i,\,abs} = C_{i,\,rel} \times PR_{rs}$ (A6.3)

Plot the response factor versus the concentration of the standard compound ---- should give slope of 0 (horizontal line), report std. dev. about this with each RF.

6.2 Retention Time Checks

Retention time checks after a few samples have been run to ensure that the integrity of the system is kept, and that the method is accurately measuring the compounds? (EPA method suggests 0.8-1.20 relative retention time to internal standards between chromatograms).

6.3 Derivatization Efficiency

Each target compound concentration should be adjusted for the efficiency of the derivatization. This has been estimated by utilizing the mass-sensitive detection of derivatized compounds with respect to a reference compound and calculated corrections for oxidized carbon sites. The calculations have been generated by (Scanlon and WIllis, 1985)and adapted for TMS derivatization by (Docherty and

Ziemann, 2001). The theoretical response, ECN_{calc} is calculated by finding the sum of the contributions of each carbon atom in a molecule: the number of reduced (saturated) carbon atoms and the contributions of carbon atoms with associated functional groups (Table 2). Note that the responses for deuterated compounds (other than methane) are identical to those of the parent compounds (Holm, 1999).

Table V. Contributions from prior measurements of FID responses to functional groups using the Effective Carbon Number correction scheme (Scanlon and WIllis, 1985); (Docherty and Ziemann, 2001).

Group or Atom	ECN_{calc} Contribution
Trimethylsilyl group (3 C, Si)	3.0
Aliphatic or aromatic carbon atom	1.0
Doubly bound carbon atom	0.95
Triply bound carbon atom	1.30
Neutral carbonyl	0
Carboxylic acid	0
Deuterated aliphatic or aromatic carbon atom	1.0
Ether group	-1.0
Primary alcohol group	-0.5
Secondary alcohol group	-0.75
Tertiary alcohol group	-0.25

The internal injection standard solution containing four PAHs can therefore be used as the reference compound for the measurement of the effective carbon number of compound *i*, ECN_i:

$$ECN_i = \frac{ECN_{ref} \times A_i \times m_{ref} \times MW_{ref}}{A_{ref} \times m_i \times MW_i} \qquad (6.3)$$

where *ref* and *i* represent the reference and target compounds, respectively, RF_{molar} is the molar reference factor of the target compound, ECN_{ref} is the ECN of a reference alkane, known from literature, *A* is the peak area (FID response), *m* is the

mass, in grams, and *MW* is the molecular weight, in grams per mole. The derivatization efficiency, *DE* (Equation 6.2) can be calculated as the ratio of the measured and calculated values of the effective carbon number for the compound:

$$DE = \frac{ECN_i}{ECN_{calc}} \qquad (6.4)$$

The *DE* should be calculated for each derivatization method used (BF_3/*n*-butanol, BSTFA) and each calibration standard. This efficiency calculation can be compared to the ratio of the concentrations of a standard derivatized within the lab, and the concentration of the same standard, purchased as the derivative. The latter should be used in particular if the system by which the GC-MS measurements are made is very different from that on which the *DE* is measured (i.e. if a GC x GC is used for the mass spectral analysis, but a one-dimensional GC is used to separate compounds for the measurement of *DE*).

6.3.1 Derivatization Efficiency Procedure using the ECN Method

- Calculate the ECN_{calc} for all calibration standards, derivatized by all methods used.
- Find within the literature the ECN_{ref} for the reference standard(s) to be used in your analysis (injection internal standard mix is suggested).
- Derivatize all calibration standards by all derivatization methods at two concentrations at two central points within the calibration curve used for external calibration (suggested: 10 ng/l and 1 ng/l). Three replicates of each derivatization method should be made so that a standard deviation can be calculated.

- Analyze by GC-FID using a similar temperature program, column, and other settings as in the mass spectral analysis to be done for identification and quantification. Obtaining a similar response to that of the mass spectral system is important because the approximate retention times of the compounds being measured must be known.
    - GC-FID analysis should be done as soon as possible after derivatization, so that the derivatives do not degrade. For the duration of any storage or transport, the derivatives should be kept within autosampling vials in a clean jar containing dessicant and a cooler with coolant, refrigerator, or freezer.
- Tabulate the responses of each compound and calculate DE_i and the average and standard deviation of ECN_i for each compound. The standard deviation about DE_i
- Report the DE_i as $DE_i \pm t \times s$ where t is the tabulated t-statistic allowing 3 degrees of freedom in a two-tailed test at the 95% confidence level, 3.18 (Anderson, 1987), and s is the standard deviation about DE_i, which can be calculated by dividing ECN_{calc} by the standard deviation about ECN_i.

7 GC-MS Method

The method for analysis on the gas chromatograph and mass spectrometer to be used should be troubleshooted throughout the blank and standard testing procedures.

7.1 GC Method

The method should be designed so that the full set of calibration standards is separated in the chromatogram, signal to noise is high, and analysis time before and after the standard peaks appear in the chromatogram is minimized. The temperature program is the most flexible variable in order to accomplish these goals, but the injection port temperature, and split flow ratio should also be optimized (there are many other variables available for changing, but most other parameters are dependent upon other system characteristics such as the column type).

These three variables should therefore be adjusted to fit the derivatives of whichever reagent(s) will be used, and the method can be set in the data acquisition list (ChromaTOF) or sequence (Agilent). A suggested beginning method to be used is:

Temperature program: 45°C (4 mins) @10°C/min to 120 °C to 300°C @ 5°C/min
Injection port temperature: 220°C
Split flow ratio: 20:1

Because an excess of most derivatization reagents remain in the derivatized solution and generate large byproduct and reagent peaks or noise throughout the chromatogram, it is useful to add “bake” analyses throughout the sequence/data acquisition list. These include injection of a volatile solvent such as DCM or methanol and use of a rapidly ramping, high-temperature GC method. This should be run after each three to four sample analyses in order to avoid buildup in

the column, injection port liner, and ion source. A suggested GC-MS method for a “bake” is as follows:

Temperature program: 45°C (0 mins) @20°C/min to 300 °C

Injection port temperature: 220 °C

Split flow ratio: 20:1

7.2 Mass Spectrometer Method

Important variables available for altering in a mass spectrometer method include the scanning range and solvent delay. These will be dependent upon the molecular mass of the resulting derivatives and the volatility of the reagent and byproducts, respectively, and should be again optimized throughout the testing procedures. The scanning range should be selected so that the value is large enough to capture all potential derivatives, but in tradeoff that the scanning rate is not limiting to the detection. Generally, ranges near 40-400 m/z are used.

Note that during a "bake" method, the solvent delay should last almost the duration of the run (best not to expose the ion source to any contaminants being removed from the system).

8 Metrics of Method

8.1 Limits of Detection and Quantitation:

Several methods of calculation are available for the limit of detection (LOD), based upon sensitivity or noise level limitations of the method. To estimate the limitation of sensitivity, the calculation is based upon the region of high probability generated by drawing a normal distribution from the value of the signal that represents a zero concentration of the analyte. An excellent figure to accompany this idea is given in Keith, *et al.,* 1983. Methods approximating limitation by noise level in the chromatogram use the replication of samples until the concentration at with a 3:1 signal to noise ratio is found.

There are several ways to estimate the blank level and standard deviation of the blank level for sensitivity limited methods of LOD calculation. For the blank level, the y-intercept of the calibration curve may be used; an average of the blank level over several blank replicates (generally, 7 or 10 replicates), or the value zero may be used. The standard deviation may be similarly found using the standard deviation about several blank replicates, or about several low concentration samples.

In order to measure the limit of detection with respect to the sensitivity of the method, the standard deviation of seven replicates at low concentration (1.0 ng/μL) was measured for each derivatization method, and each GC (one and two dimensional). The standard deviation of the signal was calculated and multiplied by 3 in order to find the value of the signal above which there was a 95% certainty that the signal was different from the blank value, assuming a blank value of zero. The MDL (the concentration, rather than the response) was calculated using the equation of the linear regression corresponding to each calibration curve. Values were compared to those of other, similar methods.

According to Keith, *et al.* (Keith, et al.), the LOD and LOQ border the "region of less-certain quantitation", while below the LOD is the "region of high uncertainty" and the region between the total concentration signal S_t and S_b is the "region of reliability". These regions represent the certainty with which results can be presented, and should be reported in some manner.

Additional variations of the LOD that may be useful to report:

- The LOD of the analyte can additionally be calculated, as $C_D = L_D/a$, where a is the slope of the calibration curve regression line.
- The limit of quantitation (for actual measurement, versus the LOD which correlates with detection of the compound of interest) can be calculated as 10*LOD.
- The limit of quantitation of the concentration (rather than the signal) can be calculated as 10 * C_D. Because it is very difficult to actual measure reproducibly at C_D, the limit of quantitation should be reported (Bliesner, 2006).

8.2 Accuracy: Recoveries of internal standards:

The values should be within 90-110% of the actual injected values.

8.3 Precision/Repeatability

The standard deviation of calibration standards, S_y, can be given to represent the variation of each value of the signal with respect to the introduced concentration, over the entire calibration.

Several measurements can be made that show that the responses of the calibration and internal standards do not vary significantly from the expected values, and that demonstrate the difference between the instrumental responses of the 1D and 2D methods.

8.3.1 Standard Deviation about the Concentration of Analyte, S_c

The standard deviation, S_c, about the concentration of an analyte was calculated using the following equation (Skoog, et al., 2007):

$$S_c = \frac{S_r}{m}\sqrt{\frac{1}{M}+\frac{1}{N}+\frac{(\langle y_c\rangle - \langle y\rangle)^2}{m^2 S_{xx}}} \qquad (8.1)$$

where S_r is the standard deviation about the regression, m is the slope of the regression line, M is the number of points in the calibration, N is the number of sample replicates, $<y_c>$ is the average signal of the analyte, $<y>$ is the average signal of calibration points, and S_{xx} is the residual of x. All calculations of the variables in this equation can be found in Skoog, *et al.* (Skoog, et al.); pp. 1075-1076). An acceptable value for S_c is ≤ 10% of the value of the concentration.

8.3.2 Standard Deviation about the y-Intercept, S_b

The standard deviation about the y-intercept, S_b was be calculated and used to estimate the confidence interval about the value of the intercept, b, within which the value of zero should be located (Skoog, et al., 2007).

$$S_b = S_r\sqrt{\frac{1}{N-(\Sigma x_i)^2/\Sigma x_i^2}} \qquad (8.2)$$

The value of $b \pm (1.96\times S_b)$ was calculated to test whether b was significantly (95%) different from zero.

8.3.3 Repeatability of the Signals of the Calibration Standards

The precision of retention times and signals were measured for the calibration standards, which were analyzed in replicate at low concentration (1 ng/μL). Acceptable values for the retention time variation are < 0.5 minutes (based on the integration parameters) and for the response variation, ≤ 20%.

8.4 Linearity of Calibrations: The coefficient of determination, R^2, can be used to show the deviation from linearity of the calibration. This correlates to the percentage of certainty that the calibration is linear. The assumption that the response of the method is linear was checked using the linear correlation coefficient, R^2:

$$R^2 = \frac{\sum_i \left\{ \left(x_i - \hat{x} \right) \left(y_i - \hat{y} \right) \right\}}{\left\{ \left[\sum_i \left(x_i - \hat{x} \right)^2 \right] \left[\sum_i \left(y_i - \hat{y} \right)^2 \right] \right\}^{1/2}} \qquad (8.3)$$

The value of was R^2 expected be within 20% of 1.00, showing that the calibration as linear with a certainty of 80%.

8.5 Peak Capacity (Resolution): The number of peaks resolved in a given unit of area of the chromatogram can be calculated as (Wilson, et al., 2011):

$$n_{c,GC} = \frac{{}^1t_R - {}^1t_M}{{}^1w_b} \qquad (8.4)$$

where ${}^1t_R$ represents the total run time, ${}^1t_M$ is the retention time of the mobile phase, and ${}^1w_b$ is the average width of peaks in the chromatogram. For a two

dimension chromatogram where the second dimension parameters are shown with a prior superscript '*2*':

$$n_{c,GCxGC} = \frac{{}^{1}t_R - {}^{1}t_M}{{}^{1}w_b} \times \frac{{}^{2}t_R}{{}^{2}w_b} \qquad (8.5)$$

The values of $n_{c,GC}$ and $n_{c,GCxGC}$ should be calculated for the highest concentration calibration curve point of each derivatization method (including non-derivatization) to show the difference in resolution for each method combination.

8.6 Analytical Sensitivity: The sensitivity of an analytical method can be determined by the ratio of the response to the amount introduced of a compound to the method. For each calibration standard and each derivatization method, the analytical sensitivity *a* can be calculated as:

$$a = \frac{m\,r}{s_s} \qquad (8.6)$$

where *m* is the slope of the calibration curve, *r* is the relative response of the internal injection standard, and s_s is the standard deviation of *m*.

Standard Operating Procedure: Literature Cited

Bliesner, D.M., 2006. Validating Chromatographic Methods: A Practical Guide. John Wiley & Sons, Inc., Hoboekn, NJ.

Docherty, K.S., Ziemann, P.J., 2001. On-line, onlet-based trimethylsilyl derivatization for gas chromatography of mono- and dicarboxylic acids. Journal of Chromatography A 921, 265-275.

Holm, T., 1999. Aspects of the mechanism of the flame ionization detector. Journal of Chromatography A 842, 221-227.

Jaoui, M., Kleindienst, T.E., Lewandowski, M., Edney, E.O., 2004. Identification and quantification of aerosol polar oxygenated compounds bearing carboxylic or hydroxyl groups. 1. Method development. Analytical Chemistry 76, 4765-4778.

Kawamura, K., Ikushima, K., 1993. Seasonal changes in the distribution of dicarboxylic acids in the urban atmosphere. Environmental Science & Technology 27, 2227-2235.

Keith, L.H., Libby, R.A., Crummett, W., Deegan, J., Jr., Taylor, J.K., Wentler, G., 1983. Principles of Environmental Analysis. Analytical Chemistry 1983, 2210-2218.

Pietrogrande, M.C., Bacco, D., Mercuriali, M., 2010. GC-MS analysis of low-molecular-weight dicarboxylic acids in atmospheric aerosol: comparison between silylation and esterification derivatization procedures. Analytical Bioanalytical Chemistry 396, 877-885.

Scanlon, J.T., WIllis, D.E., 1985. Calculation of flame ionization detector relative response factors using the effective carbon number concept. Journal of Chromatographic Science 23, 333-340.

Skoog, D.A., Holler, F.J., Crouch, S.R., 2007. Principles of Instrumental Analysis, 6th ed. Brooks Cole.

Wilson, R.B., Siegler, W.C., Hoggard, J.C., Fitz, B.D., Nadeau, J.S., Synovec, R.E., 2011. Achieving high peak capacity production for gas chromatography and comprehensive two-dimensional gas chromatography by minimizing off-column peak broadening. Journal of Chromatography A 1218, 3130-3139.

Yu, J., Cocker, D.R., III, Griffin, R.J., Flagan, R.C., Seinfeld, J.H., 1999. Gas-Phase Ozone Oxidation of Monoterpenes: Gaseous and Particulate Products. Journal of Atmospheric Chemistry 34, 207-258.

APPENDIX B: Reaction Mechanisms of Common Derivatization Reagents for Polar Compounds in Atmospheric Organic Particulate Matter

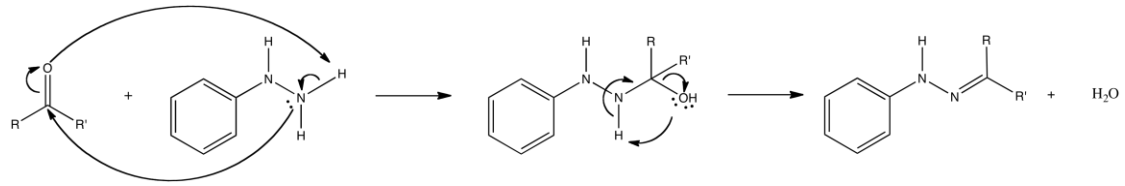

Reaction Scheme 6. Formation of a dinitrophenylhydrazone by derivatization of a ketone with 2,4-dinitrophenylhydrazine (DNPH). Reaction adapted from Dong & Moldoveanu, 2004.

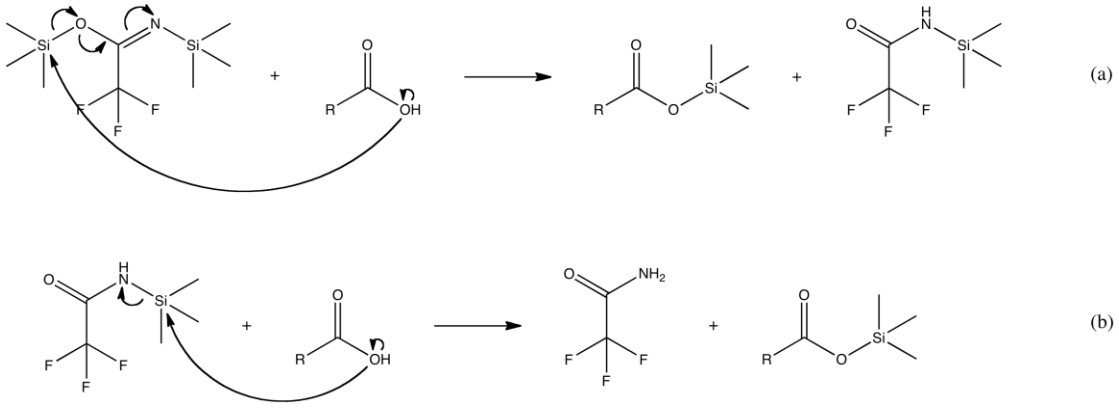

Reaction Scheme 7. Formation of trimethylsilyl esters from reaction of a carboxylic acid with *N,O*-bis-(trimethylsilyl)-trifluoroacetamde. The two parts of the reaction show (a) the formation of one ester via nucleophilic attack at the oxygen-bound silicon atom, and (b) the formation of one ester via nucleophilic attack at the nitrogen-bound silicon atom. Reaction adapted from Yu, *et al.,* 1998.

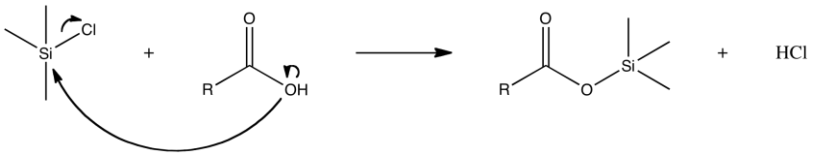

Reaction Scheme 8. Formation of a trimethylsilyl ester from reaction of a carboxylic acid with trimethylchlorosilane (TMCS). This reaction is used in order to induce trimethylsilylation via the less reactive trimethylsilylating reagent BSTFA, and is sold as a 10% v/v solution with BSTFA.

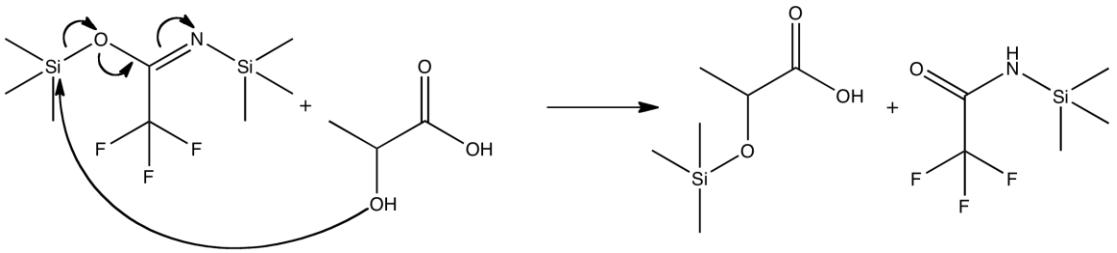

Reaction Scheme 9. Derivatization mechanism of BSTFA with the hydroxyl group in lactic acid. The *O* and *N* trimethylsilyl sites can participate in the reaction (the *O* site is shown here).

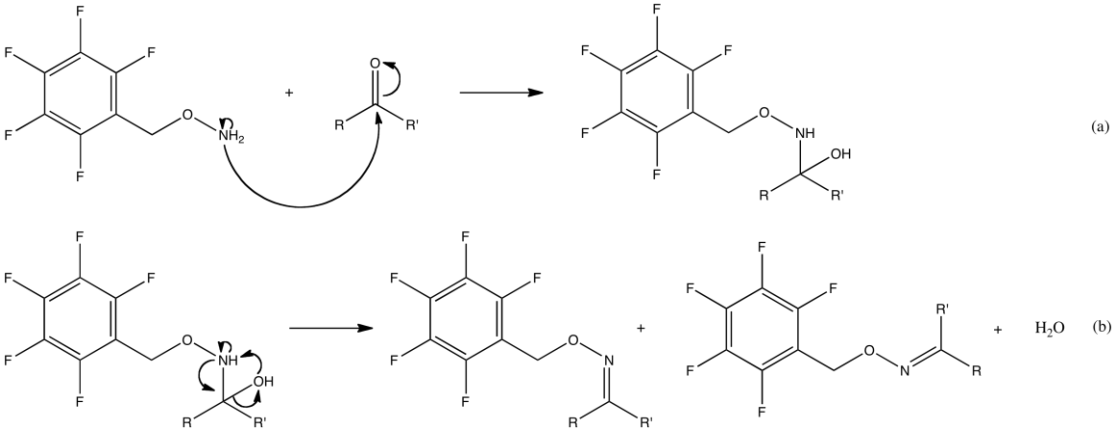

Reaction Scheme 10. Formation of pentafluorobenzyl oxime isomers from reaction of a neutral carbonyl with *2,3,4,5,6*-pentafluorobenzyl hydroxylamisne (PFBHA).

APPENDIX C: Tabulated GCxGC TOF-MS Chromatograms

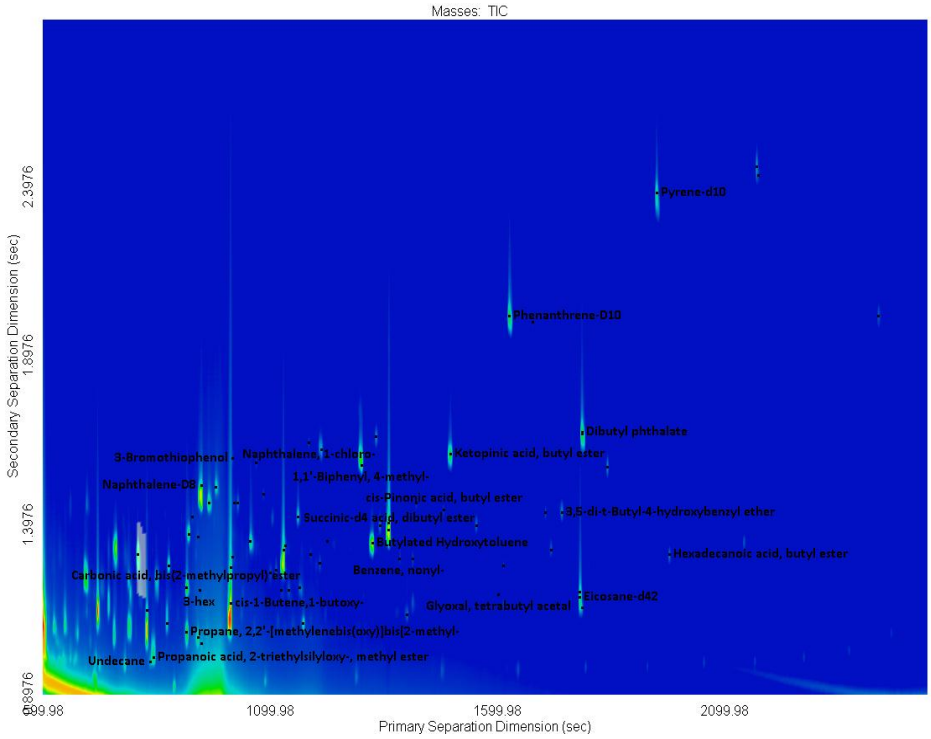

Figure H. Total ion chromatogram of the butylated no oxidant blank.

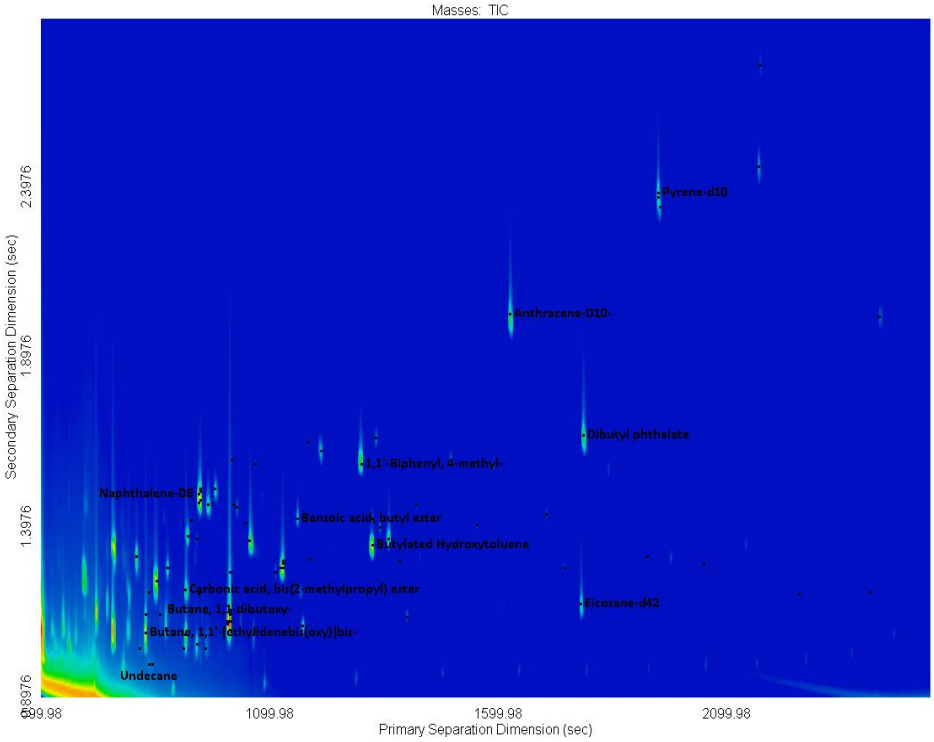

Figure I. Total ion chromatogram of butylated clean air blank.

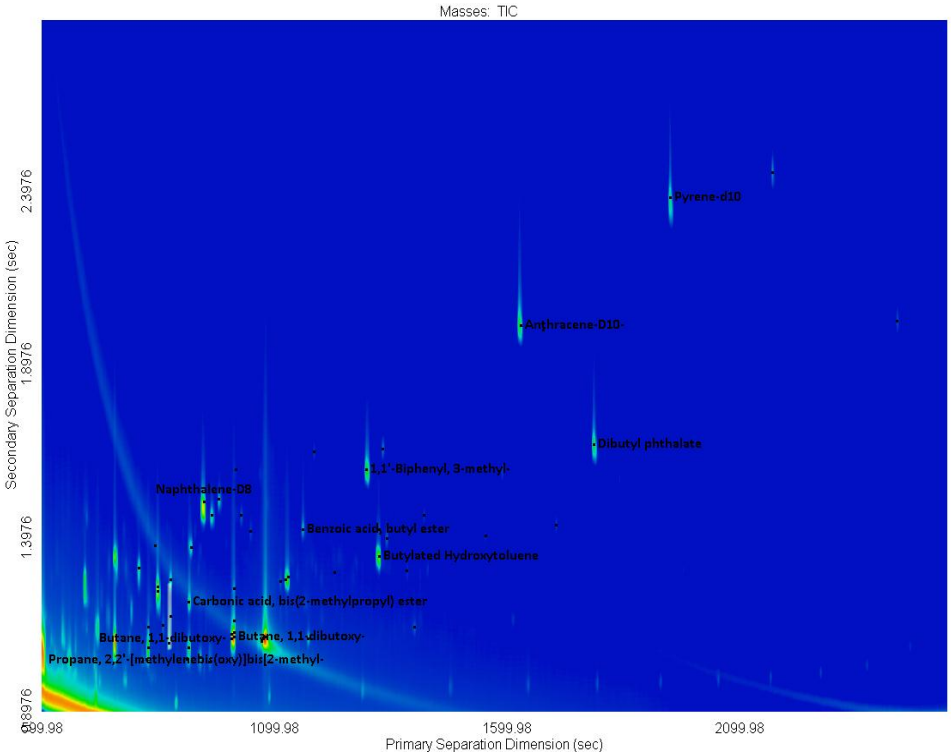

Figure J. Total ion chromatogram of butylated solvent blank.

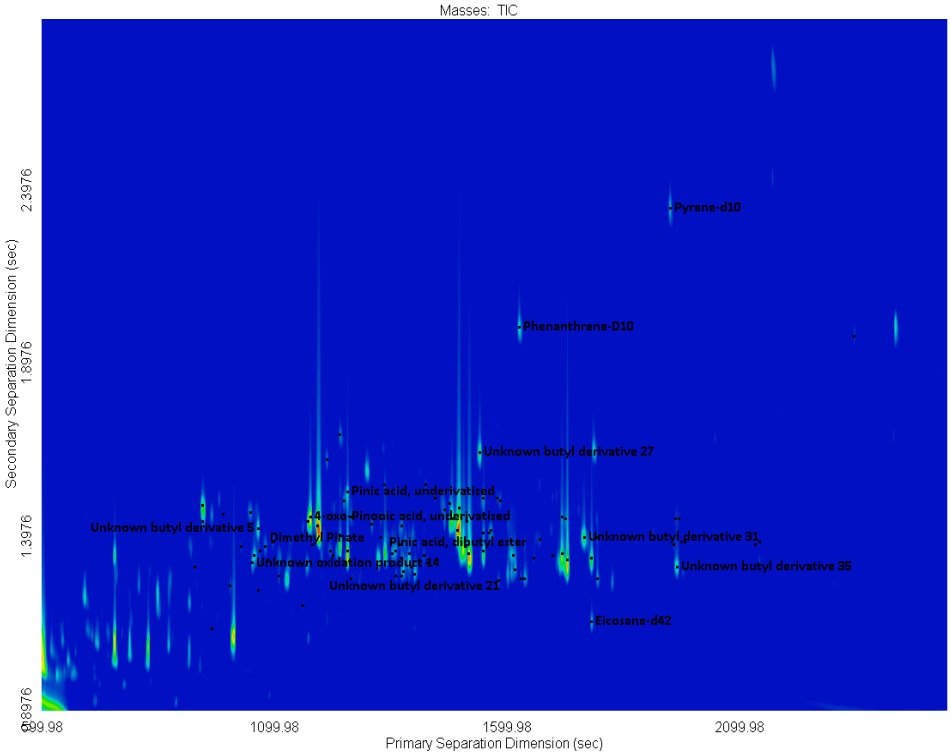

Figure K. Total ion chromatogram of butylated SOA sample 23-3.

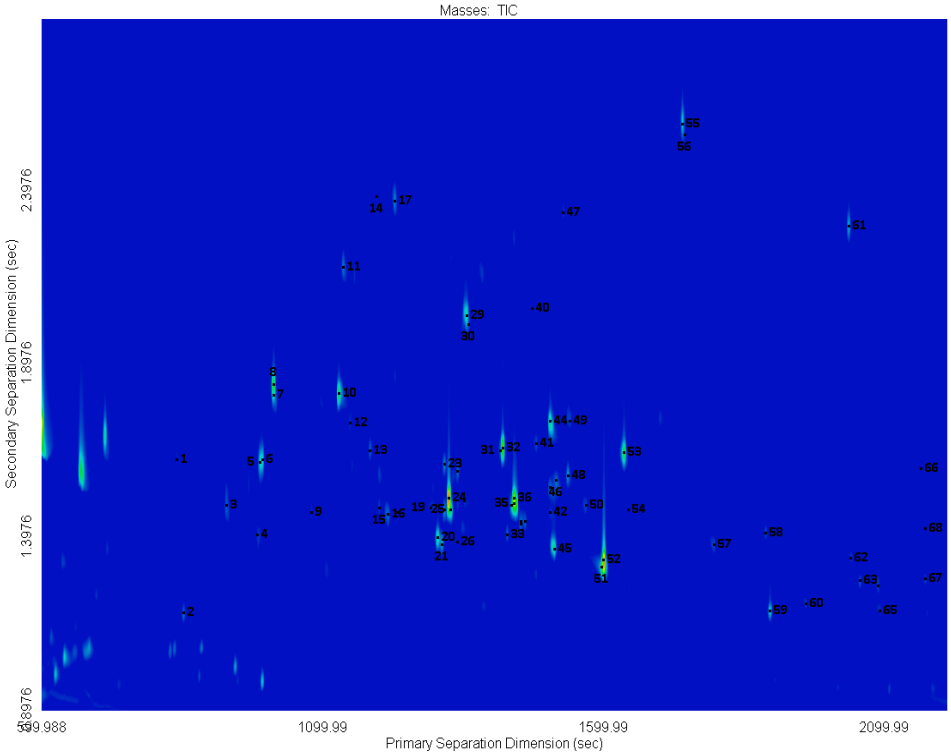

Figure L. Total ion chromatogram of trimethylsilylated sample 26-4. Similar slices were not combined.

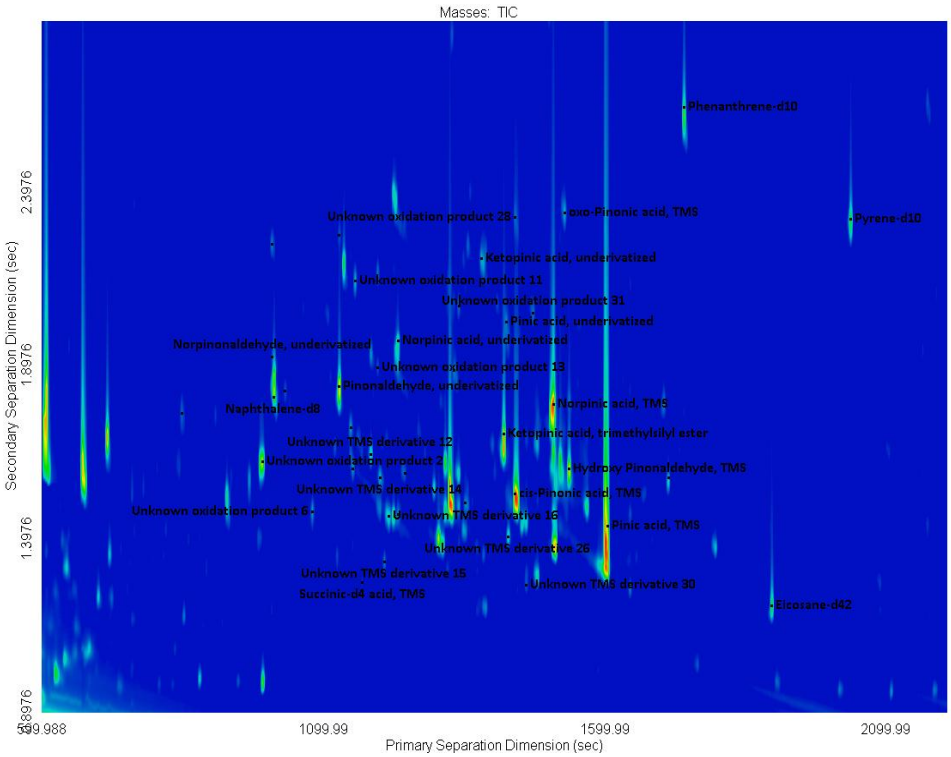

Figure M. Total ion chromatogram of trimethylsilylated SOA sample 26-3.

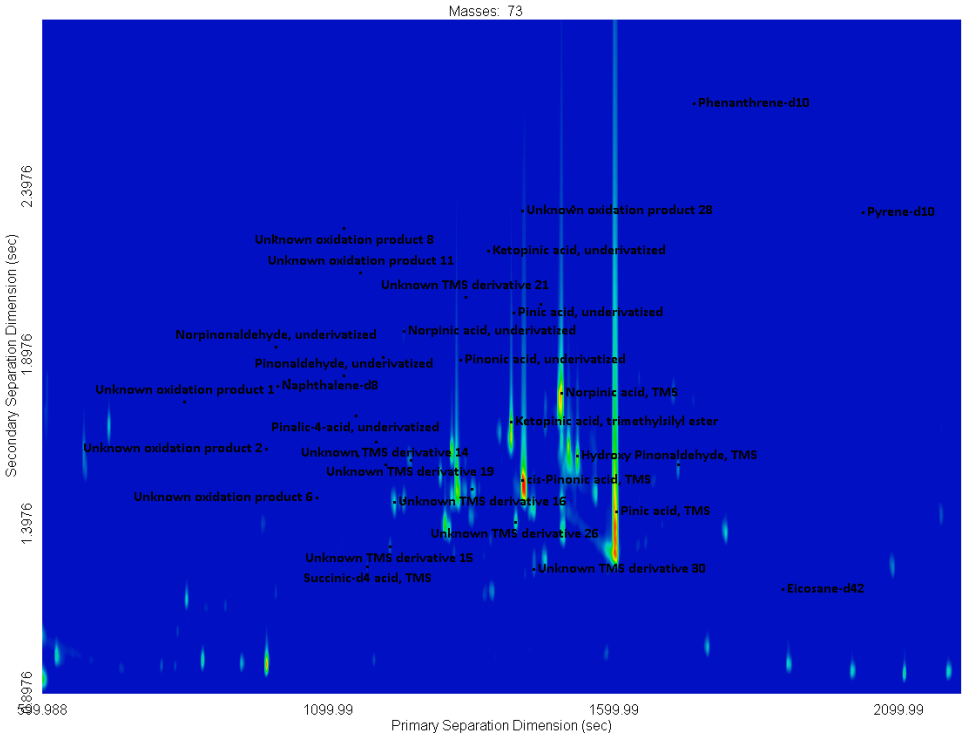

Figure N. Extracted ion chromatogram showing m/z 73 (trimethylsilylated compounds) of trimethysilylated SOA sample 26-3.

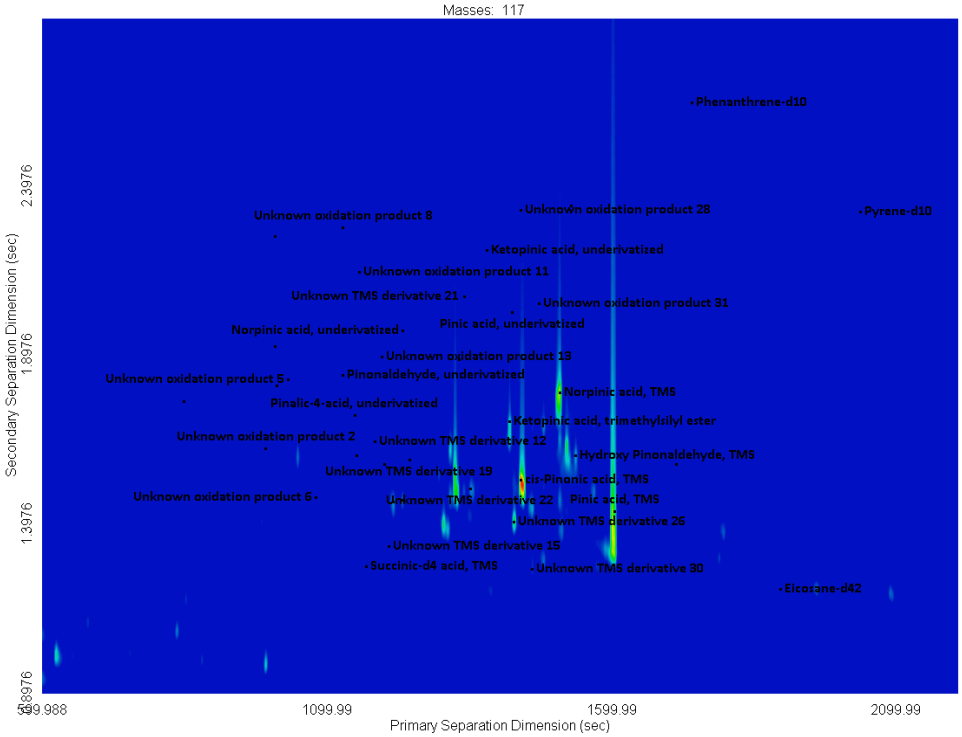

Figure O. Extracted ion chromatogram showing m/z 73 (TMS) of trimethysilylated SOA Sample 26-3.

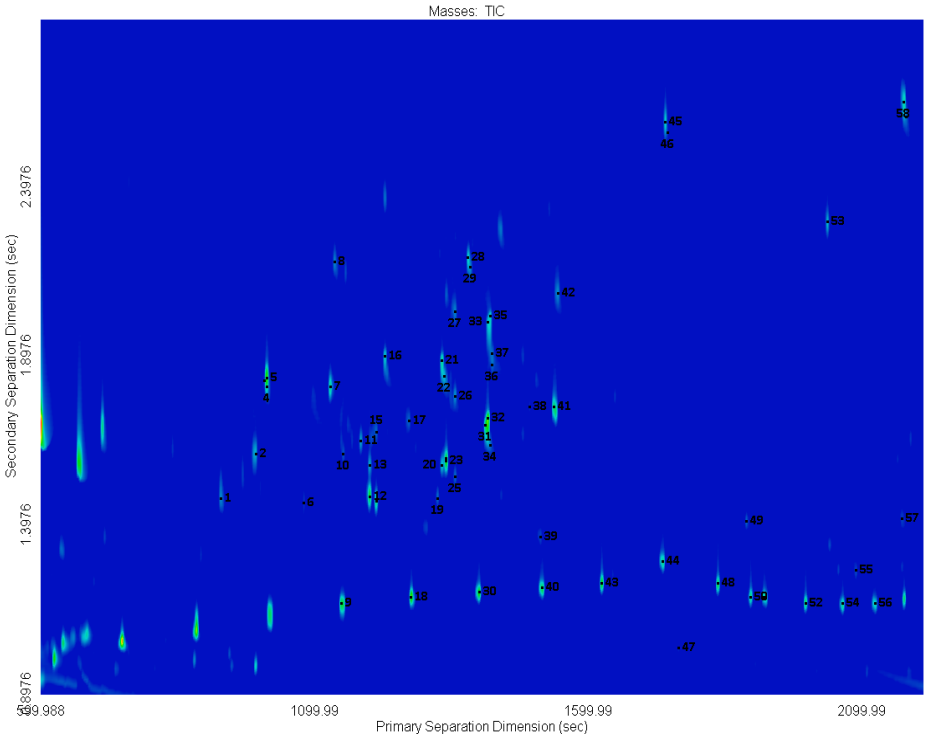

Figure P. Extracted ion chromatogram showing m/z 117 (trimethylsilylated acids) of trimethysilylated sample 26-3.

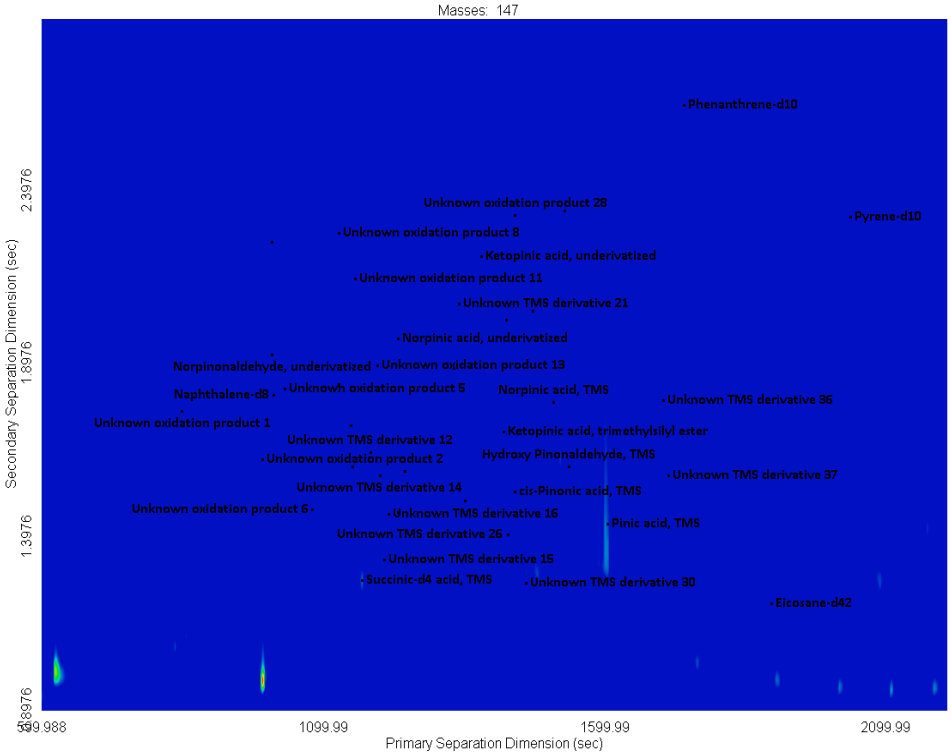

Figure Q. Extracted ion chromatogram showing m/z 147 (di-acids) of trimethysilylated sample 26-3.

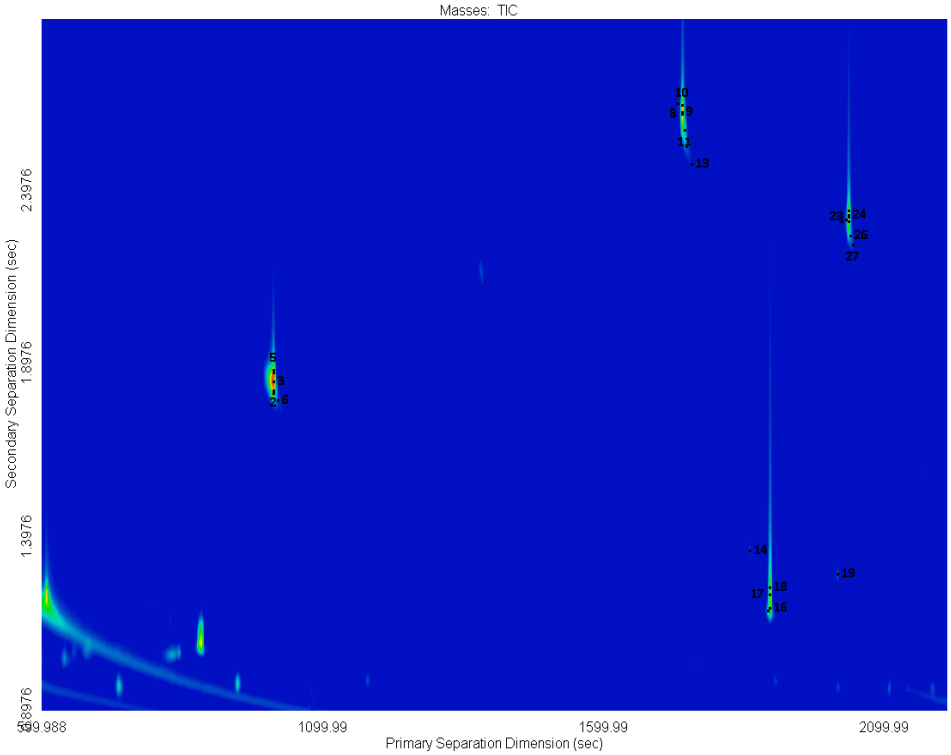

Figure R. Total ion chromatogram of underivatized travel blank. Similar slices were not combined.

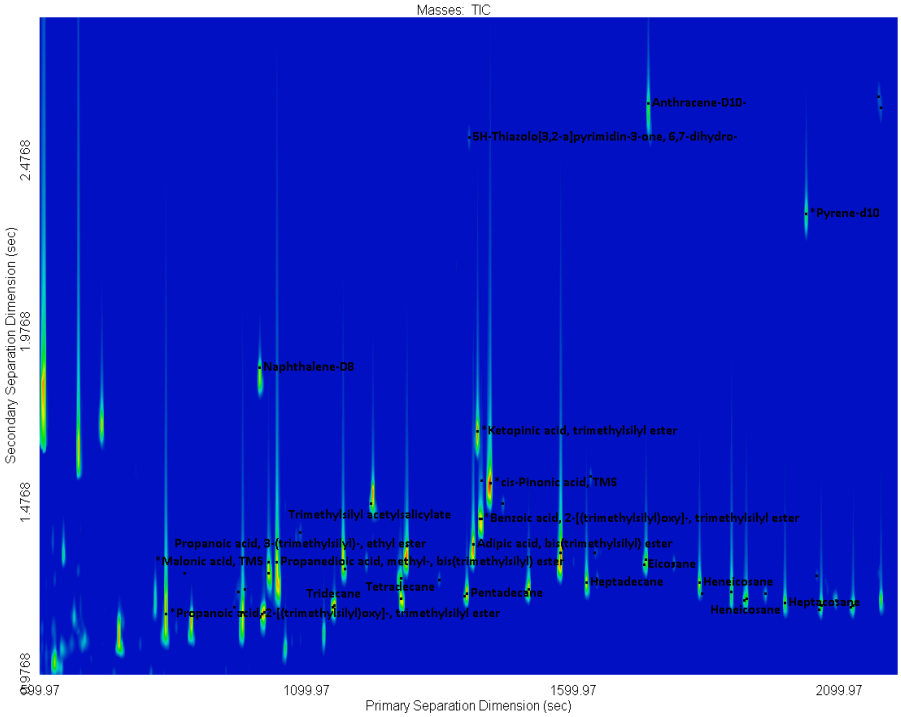

Figure S. Total ion chromatogram of trimethylsilylated and *n*-alkane standards at 10 ng/µL.

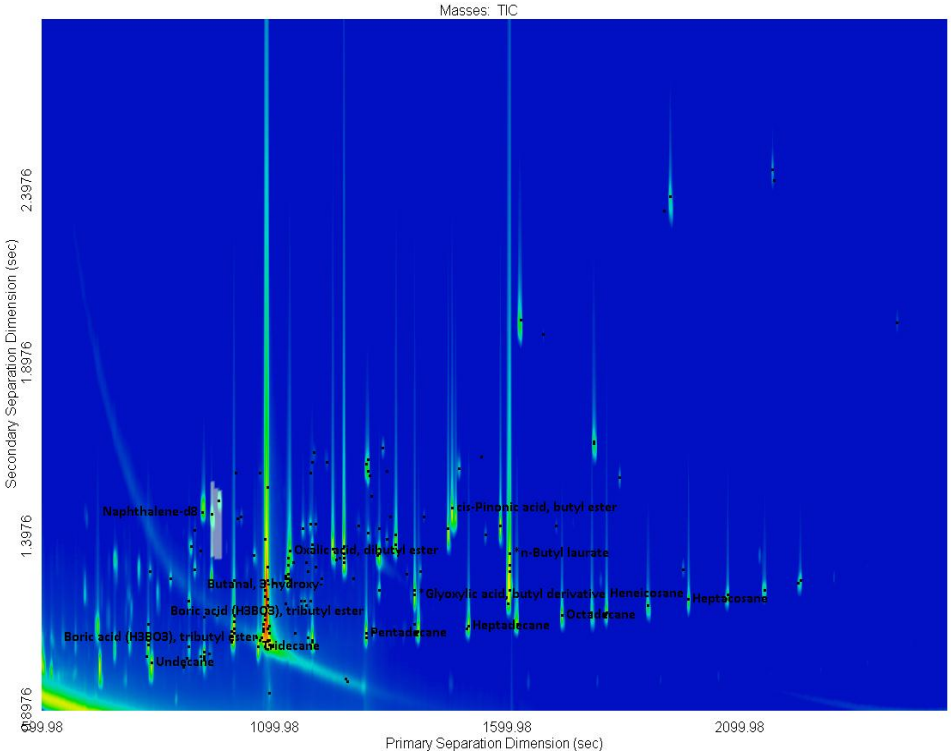

Figure T. Total ion chromatogram of butylated calibration curve standards and *n*-alkane standards at 10 ng/µL.

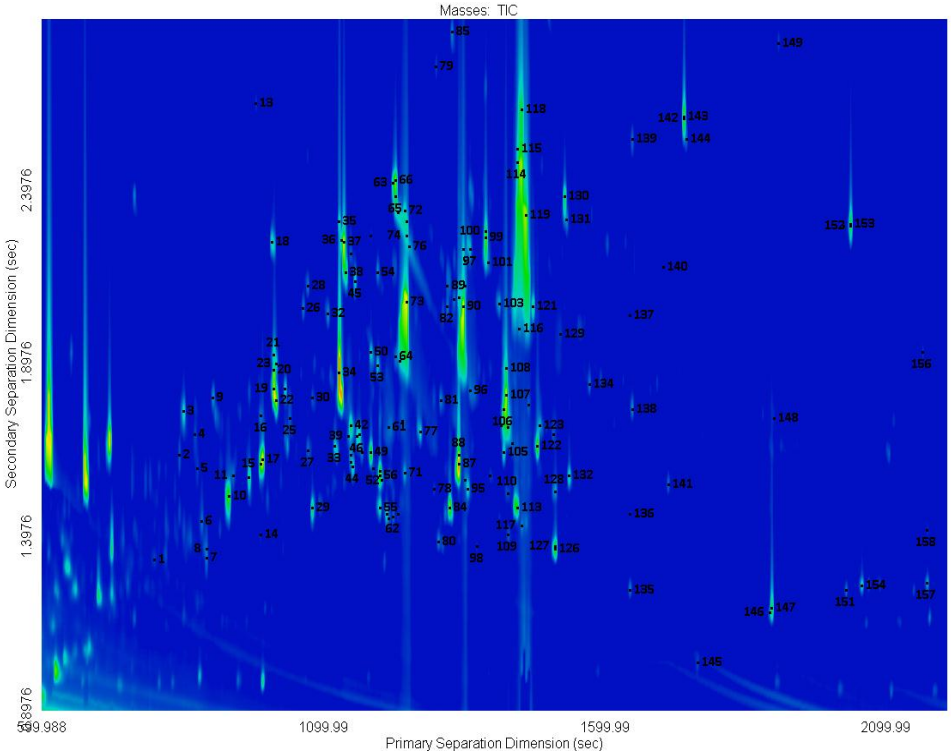

Figure U. Total ion chromatogram of trimethylsilylated SOA sample 23-3, injection 3.

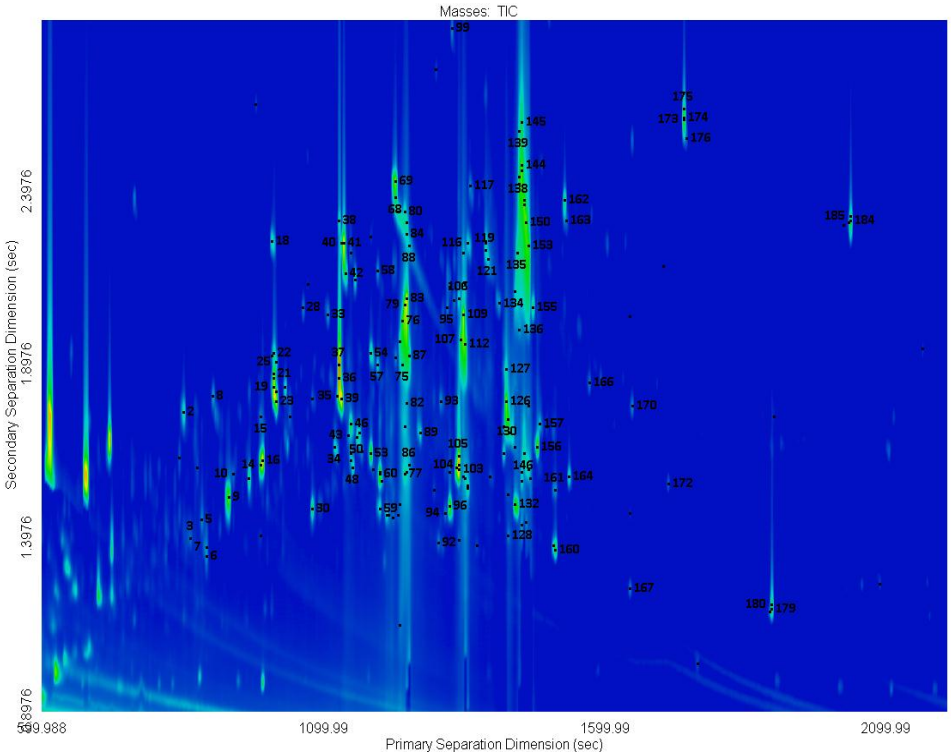

Figure V. Total ion chromatogram of trimethylsilylated SOA sample 23-3, injection 2.

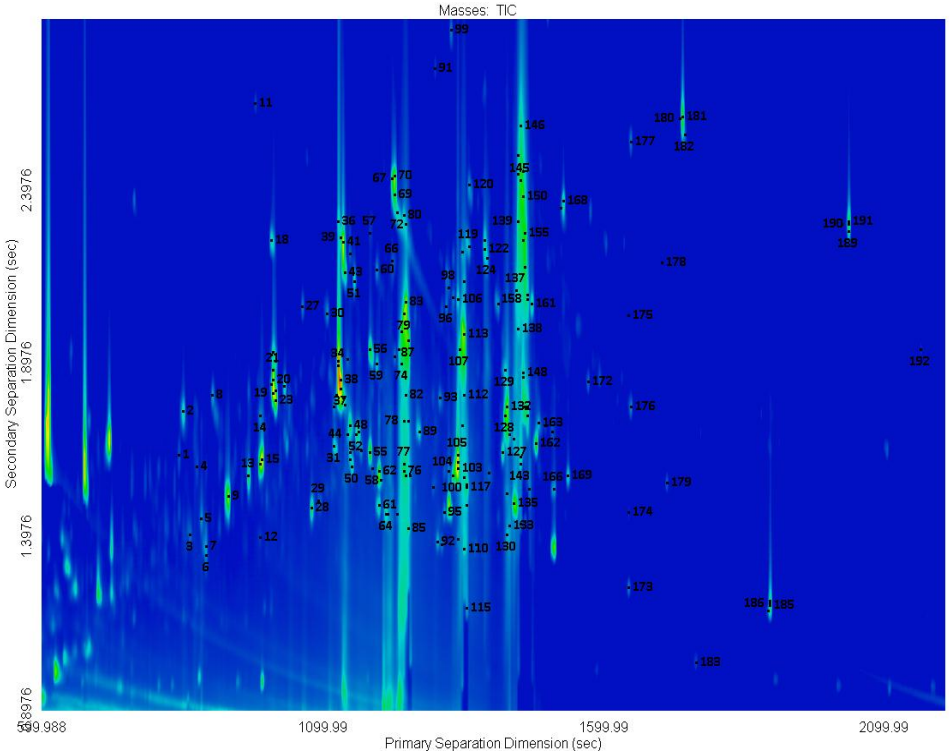

Figure W. Total ion chromatogram of trimethylsilylated SOA sample 23-3, injection 1.

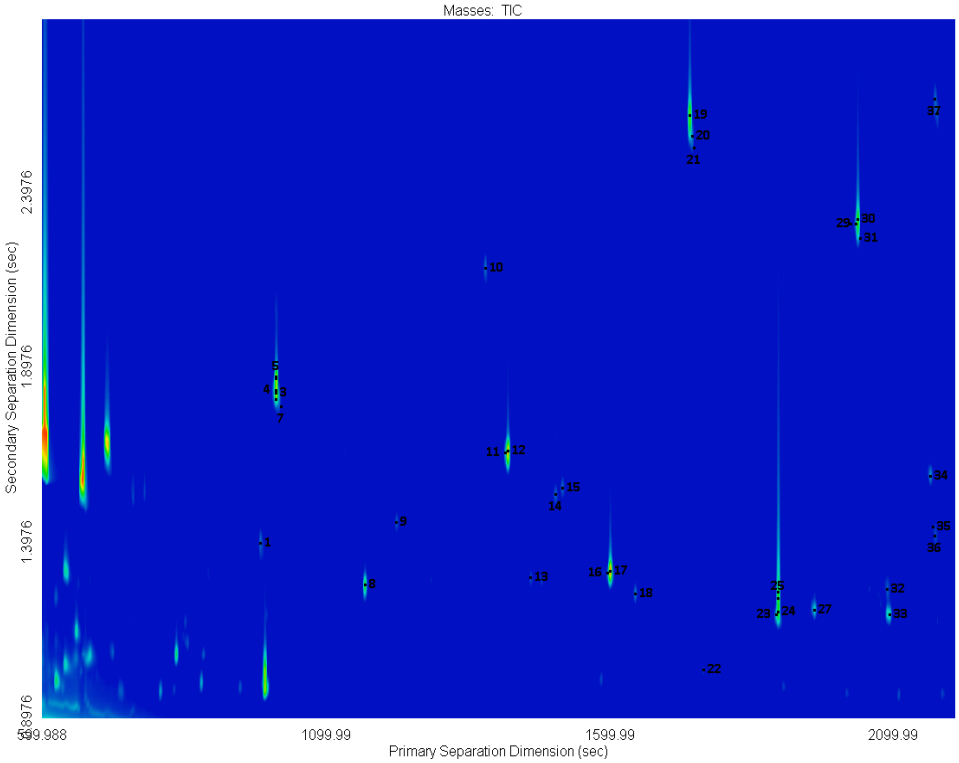

Figure X. Total ion chromatogram of trimethylsilylated travel blank (recovery included).

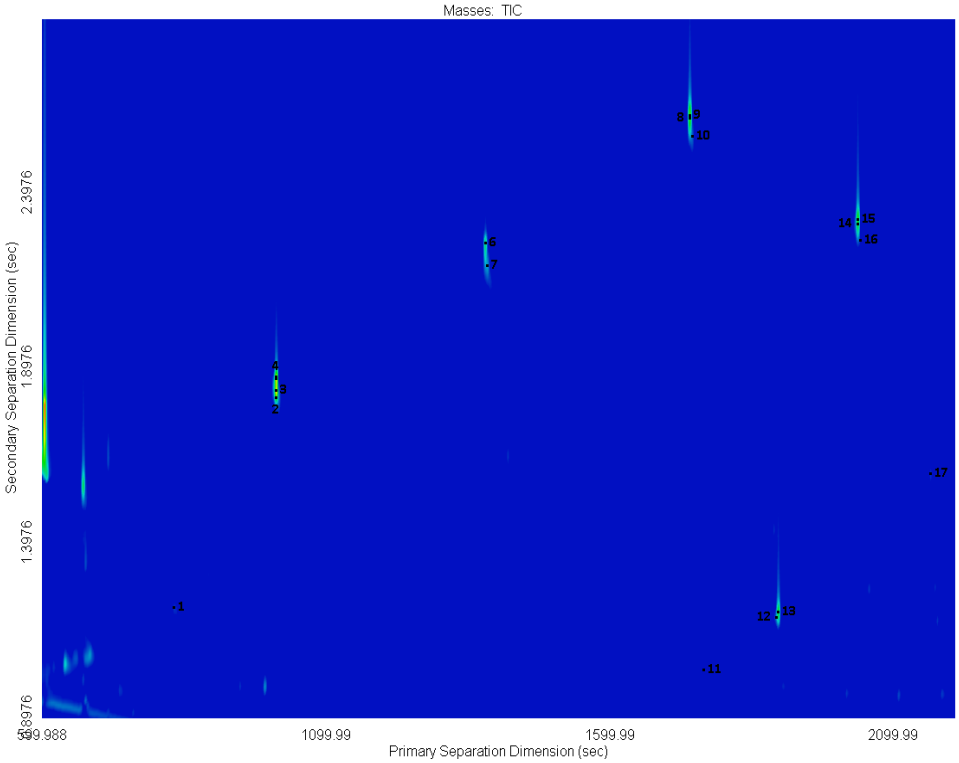

Figure Y. Total ion chromatogram of trimethylsilylated clean air blank.

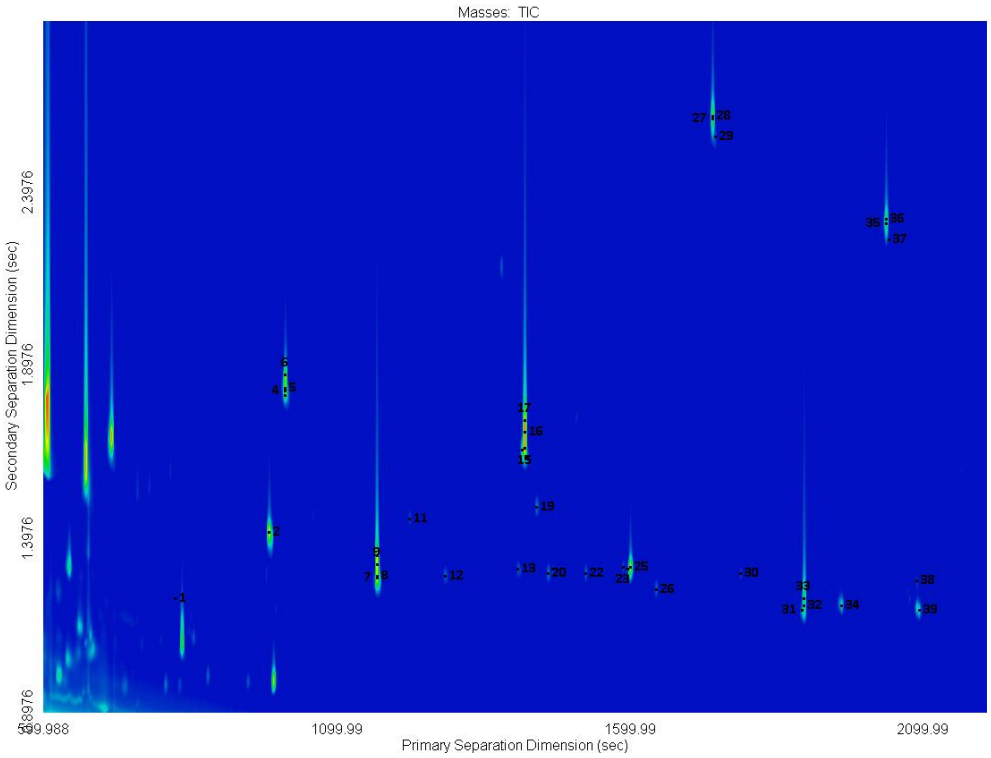

Figure Z. Total ion chromatogram of trimethylsilylated no oxidant blank (recovery standards included).

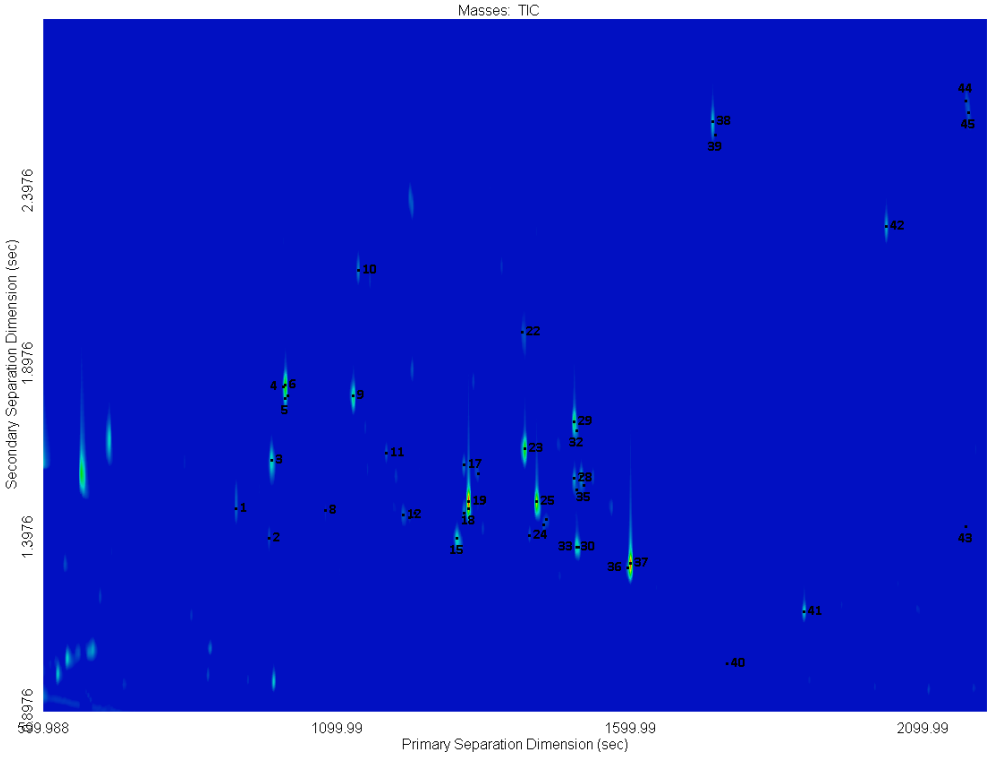

Figure AA. Total ion chromatogram of diluted trimethylsilylated SOA sample 26-3.

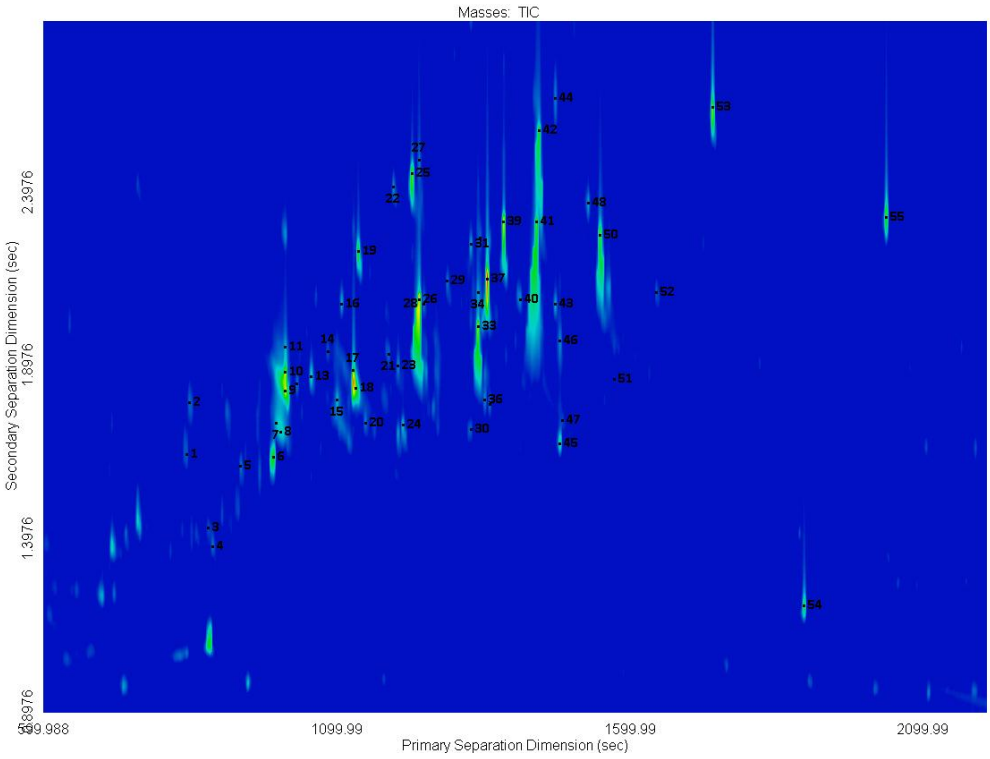

Figure BB. Total ion chromatogram of underivatized SOA sample 26-3.

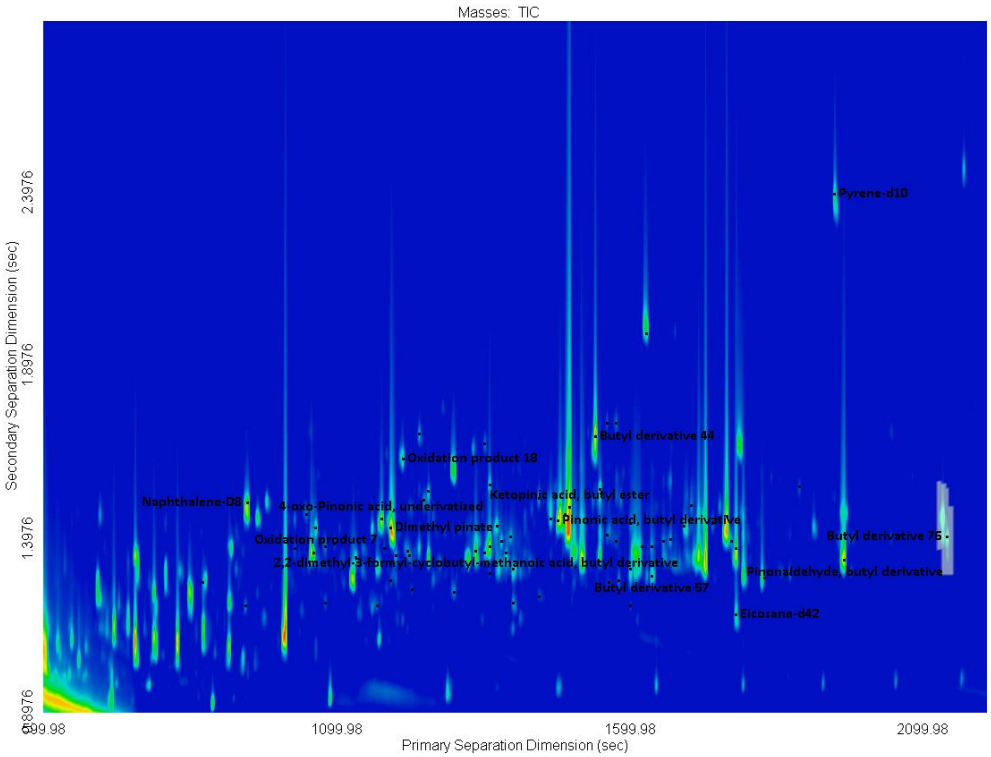

Figure CC. Total ion chromatogram of butylated SOA sample 26-3.

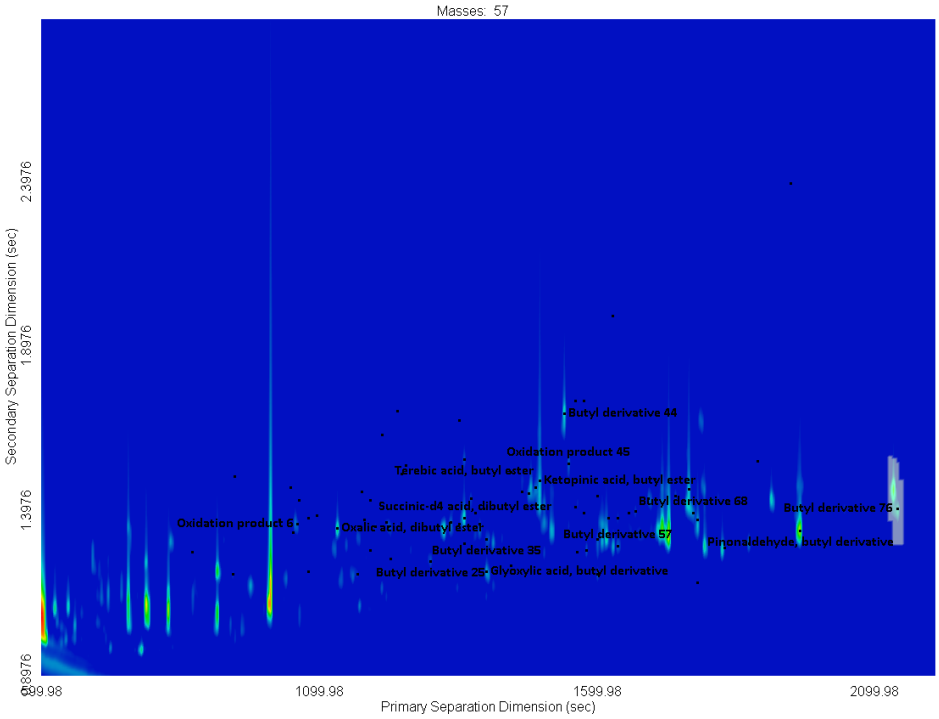

Figure DD. Extracted ion chromatogram showing m/z 57 (butyl derivatives) of butylated sample 26-3.

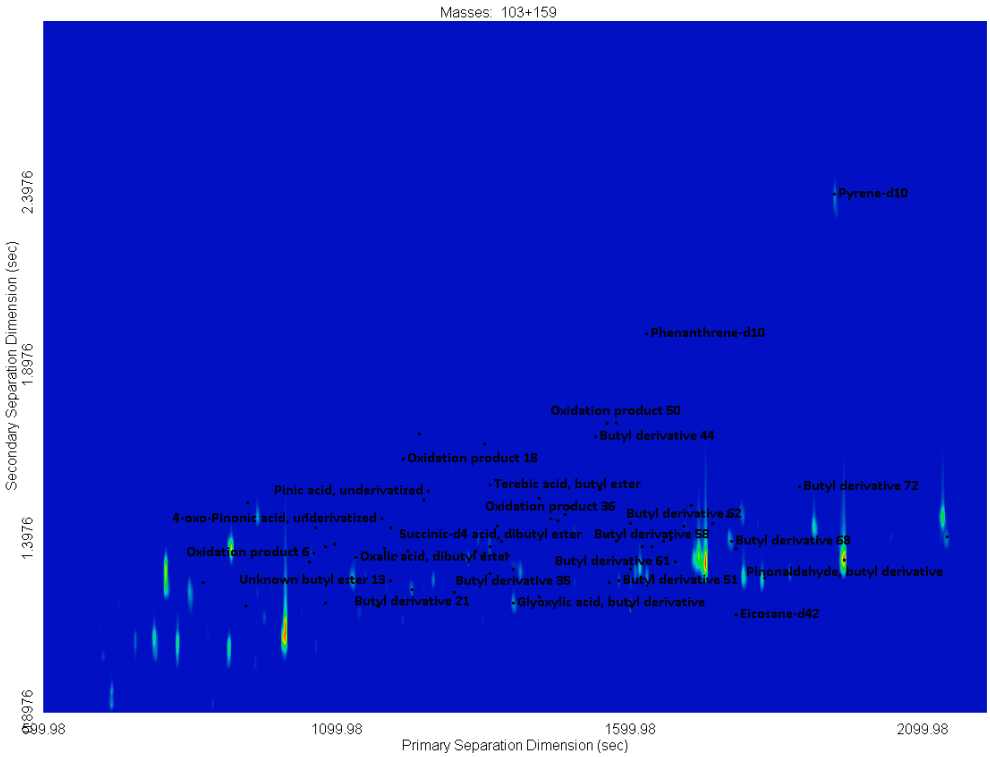

Figure EE. Extracted ion chromatogram showing m/z 103+159 (dibutyl acetals) of butylated sample 26-3.

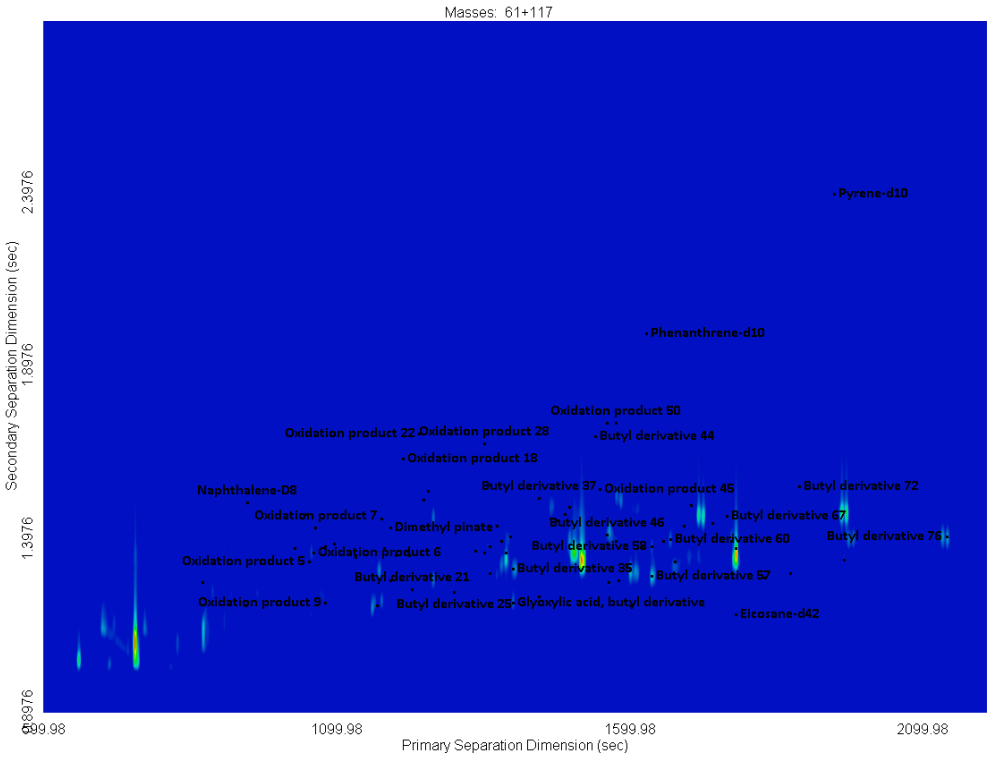

Figure FF. Extracted ion chromatogram showing m/z 61+117 (dibutyl ketals) of butylated sample 26-3.

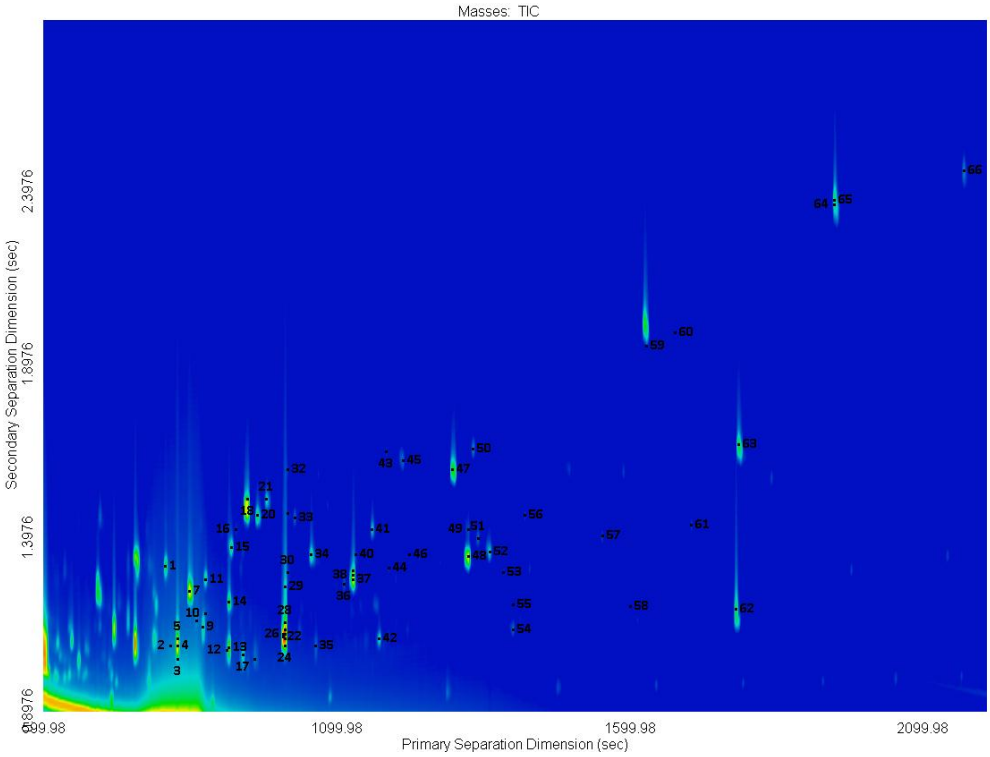

Figure GG. Total ion chromatogram of butylated travel blank.

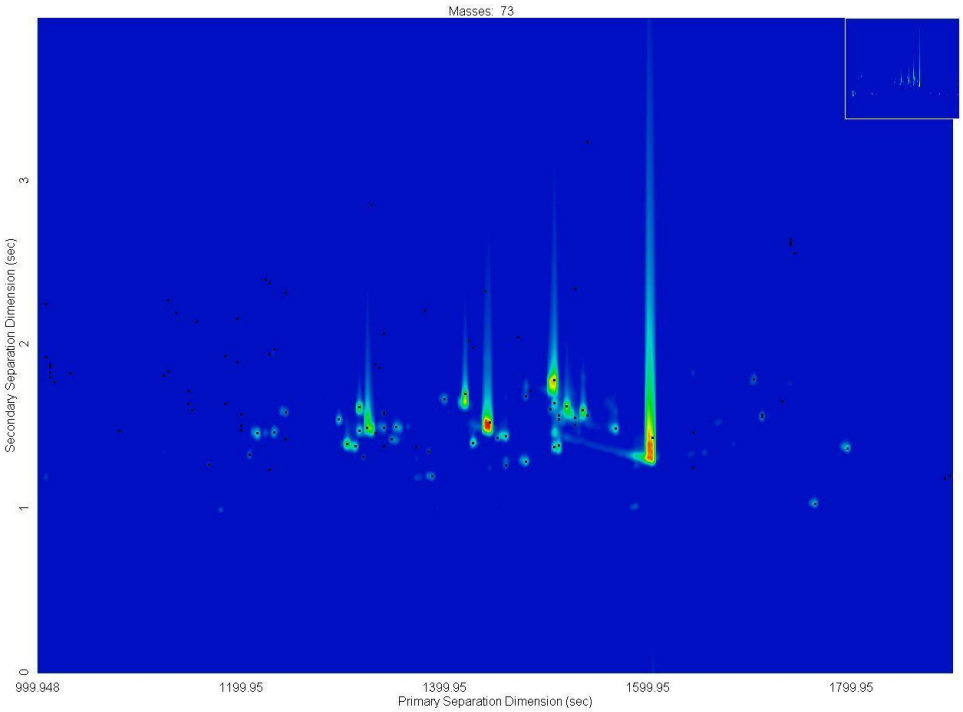

Figure HH. Extracted ion chromatogram of trimethylsilylated SOA sample 26-3 extract, showing abundances of m/z 73 (carboxylic acids and alcohols). No labels are included.

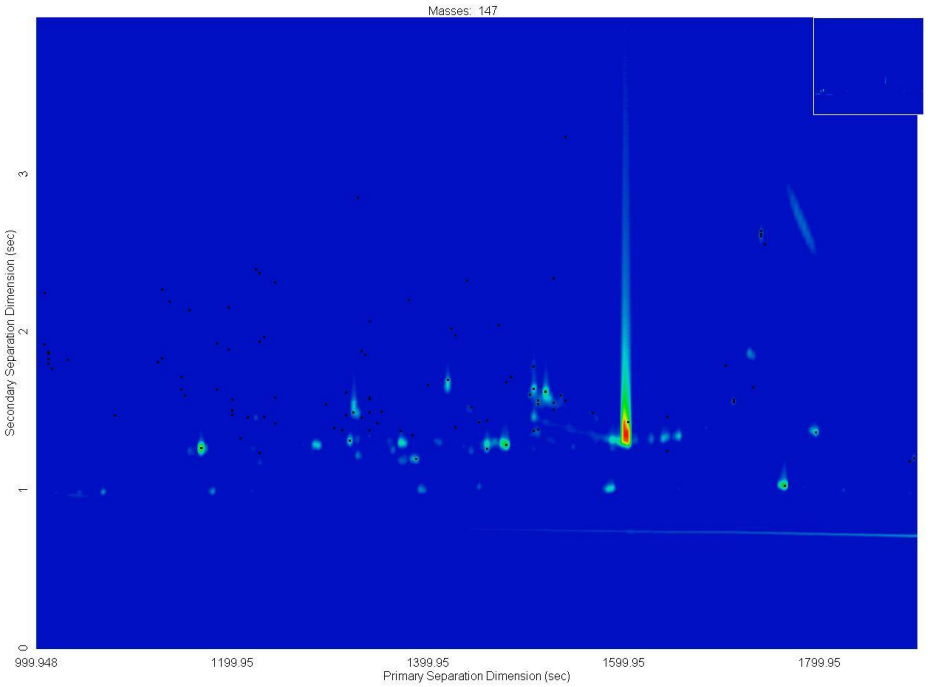

Figure II. Extracted ion chromatogram of trimethylsilylated SOA sample 26-3 extract, showing

abundances of m/z 147 (di-carboxylic acids, not including 2,2-dimethyl-cyclobutyl backbone compounds; fragment with m/z 147 within peak at ~1600 s primary retention time does not correspond to di-acid). No labels are included.

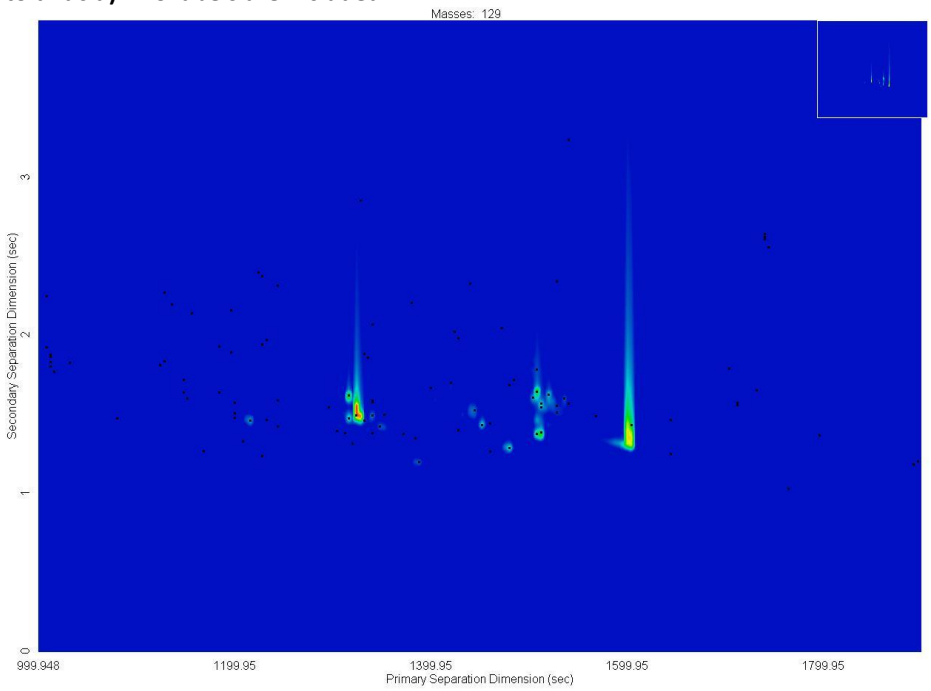

Figure JJ. Extracted ion chromatogram of trimethylsilylated SOA sample 26-3 extract, showing abundances of m/z 129 (likely trimethylsilylated carboxylic acids). No labels are included.

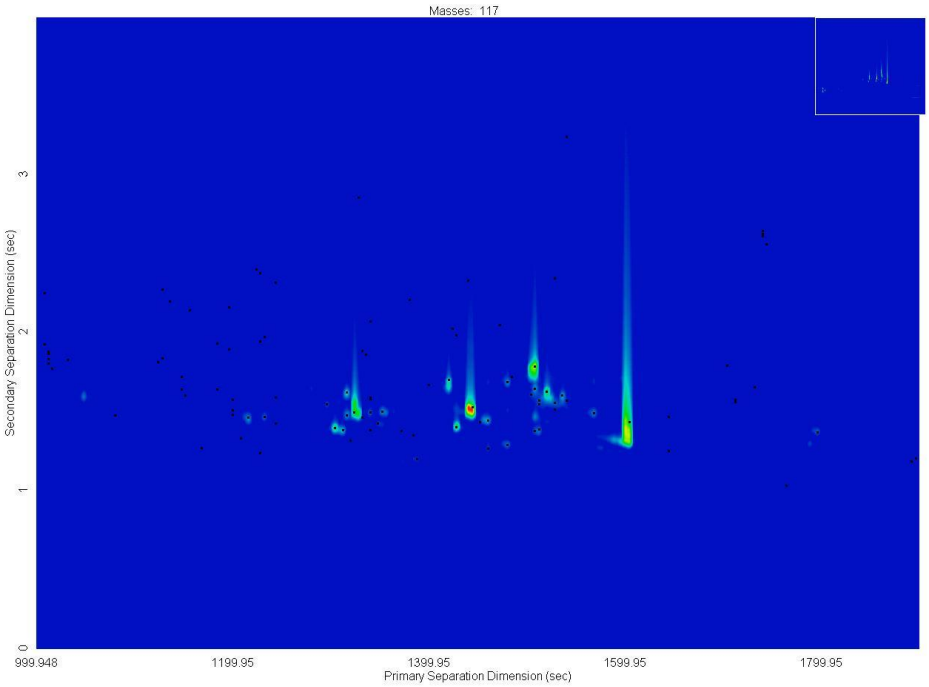

Figure KK.Extracted ion chromatogram of trimethylsilylated SOA sample 26-3 extract, showing abundances of m/z 117 (trimethylsiylated carboxylic acids). No labels are included.

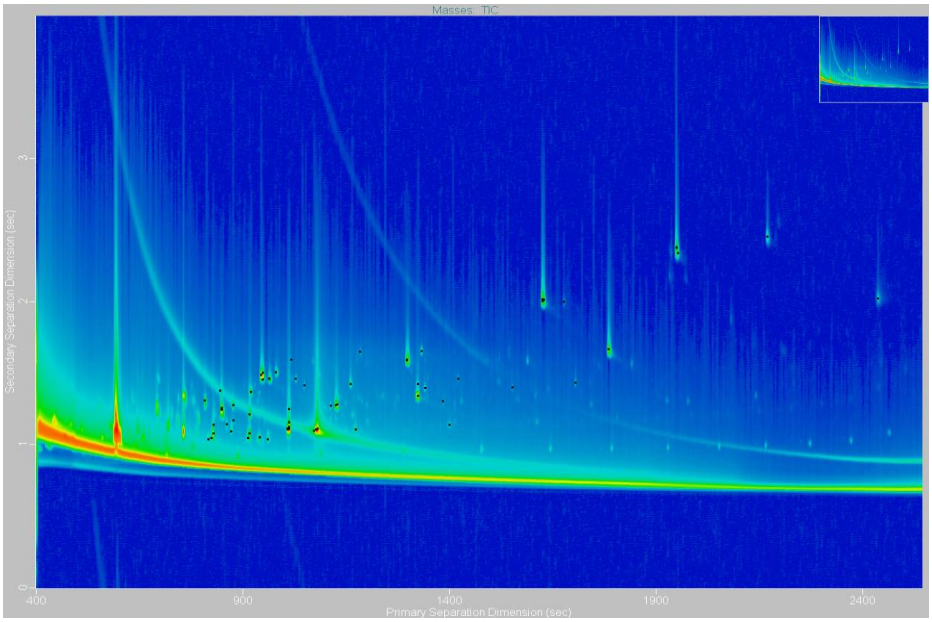

Figure LL. Full range chromatogram of travel blank, butylated. Large solvent front and peak at approximately 1100 seconds are attributable to butanol.

APPENDIX D: Values Used in the Effective Carbon Number Method for Derivatization Efficiency Approximation

Table W. Contributions from prior measurements of flame ionization detector responses to functional groups using the Effective Carbon Number correction scheme (Scanlon & WIllis, 1985; Docherty & Ziemann, 2001; see literature cited) for non-reduced carbon atoms. Values were used to find ECN_{calc} for each external calibration standard.

Group or Atom	ECN_{calc} Contribution
Trimethylsilyl carbon group (3 C, Si)	3.0
Aliphatic or aromatic carbon atom	1.0
Doubly bound carbon atom	0.95
Triply bound carbon atom	1.30
Neutral carbonyl	0
Carboxylic acid	0
Deuterated aliphatic or aromatic carbon atom	1.0
Ether group	-1.0
Primary alcohol group	-0.5
Secondary alcohol group	-0.75
Tertiary alcohol group	-0.25

Table X. Contributions of derivatization groups to ECNcalc values calculated from known "active" carbon atom contributions to flame ionization detector responses. The carbon number *n* used should be for the pre-derivatization compound; for example, for dibutyl adipate, ECN_{calc}=6+6.

Derivative Structure	ECN_{calc} Contribution
Butyl ester	*n*+3
Butyl di-ester	*n*+6
Di-butyl acetal	*n*+7
Tetra-butyl acetal	*n*+14
Butyl hydroxy-ester	*n*+2.5
Butyl keto-ester	*n*+2
Butyl dibutoxy-ester	*n*+10
Trimethylsilyl ester	*n*+2
Trimethylsilyl di-ester	***n*+4**
Trimethylsilyl ether	***n*+2.5**
***bis*(Trimethylsilyloxy)-trimethylsilyl ether**	***n*+4.5**
Trimethylsilyl keto-ester	***n*+1**

Table Y. Theoretical effective carbon numbers (ECNcalc) for the calibration standards used in the calculation of derivatization efficiency. Standards that were not derivatized using the specified reagent are indicated by '—'.

Calibration Standard	ECN_{calc} Butyl Derivative	MW_i Butyl Derivative (a.m.u.)	ECN_{calc} Trimethylsilyl Derivative	MW_i Trimethylsilyl Derivative
Adipic acid	12	258.1	10	290.5
Glutaric acid	11	244.1	9	276.5
Glyoxal	16	318.5	---	---
Glyoxylic acid	12	260.0	---	---
2-hydroxy-3-methyl-Butyric acid	7.5	174.1	9.5	262.5
Ketopinic acid	12	238.3	11	254.4
Lactic acid	5.5	146.1	7.5	234.4
Lauric acid	15	256.4	14	272.5
Malonic acid	9	216.1	7	248.5
methyl-Malonic acid	10	230.3	8	262.4
Oxalic acid	8	202.0	6	234.4
***cis*-Pinonic acid**	12	240.3	11	290.5
Salicylic acid	9.5	194.2	11.5	282.5
Succinic-d_4 acid	10	234.3	8	266.5

Table G. Response factors of calibration and reference standards used in the calculation of derivatization efficiency. Standard deviations between replicate analyses (listed horizontally) and standards (listed vertically) were low, showing that the mass response of the GCxGC-FID was replicable. Calculated using phenanthrene-d_{10} as a reference standard.

	GCxGC-FID Response Factor						
	Replicate 1	**Replicate 2**	**Replicate 3**	**Replicate 4**	**Replicate 5**	**Average**	**Std. Deviation**
Decane	3.093176682	3.054991152	3.545652754	3.466309481	3.621436843	3.356313382	0.263758885
Undecane	3.150524773	3.087076891	3.699295033	3.702169396	3.596148563	3.447042931	0.303501109
Dodecane	3.109743783	3.033508462	3.603000272	3.449420769	3.633597457	3.365854149	0.27881639
Tridecane	3.133172193	2.403085247	3.643315013	3.52191375	3.693609781	3.279019197	0.536685707
Tetradecane	3.09724849	3.073045637	3.663791999	3.415535507	3.735530731	3.397030473	0.308594388
Pentadecane	3.149419882	3.034783624	3.635662835	3.491173612	3.696499719	3.401507934	0.294925291
Hexadecane	3.051406137	4.039048214	3.558720803	3.388262934	3.676387048	3.542765027	0.3639062
Average	3.112098849	3.103648461	3.621348387	3.490683636	3.664744306		
Standard Deviation	0.035546285	0.479409739	0.055607662	0.103389032	0.049225555		
Lactic acid	0.267739936	0.205122521	0.264654851	0.264654851	0.120429107	0.224520253	0.063837199
2-hydroxy-3-methyl-Butyric acid	0.216994482	0.27417926	0.236726803	0.236726803	0.125193275	0.217964125	0.055838133
Malonic acid	0.008622532	0.005108868	0.037129956	0.037129956	0.041028156	0.025803894	0.017405609
methyl-Malonic acid	0.038406089	0.052967659	0.097487708	0.097487708	0.200992362	0.097468305	0.063611878
Succinic-d_4 acid	0.038915756	0.167985302	0.125124192	0.125124192	0.23044407	0.137518702	0.069987725
Glutaric acid	0.027301924	0.10037073	0.116784571	0.116784571	0.227129838	0.117674327	0.071499437
Adipic acid	0.068772865	0.155375153	0.170049846	0.170049846	0.285359658	0.169921474	0.077085413
Salicylic acid	0.106863117	0.261305566	0.163243769	0.163243769	0.481195339	0.235170312	0.14834163
Ketopinic acid	0.329079812	0.360805261	0.343489872	0.343489872	0.462238872	0.367820738	0.053964901
***cis*-Pinonic acid**	0.587830787	0.662277655	0.588033663	0.588033663	0.758591905	0.636953535	0.075227249
Dodecanoic acid	0.362682004	0.170672791	0.139518217	0.139518217	0.115575987	0.185593443	0.100909962
Average	0.186655391	0.219651888	0.207476677	0.207476677	0.277107143		
Standard Deviation	0.184625059	0.178325946	0.152166475	0.152166475	0.21159903		

Table Z. Tabulated response of the authentic standard dibutyl adipate (Dibutyl Adipate A. Std.), for comparison to the response of butylated adipic acid (measured at 0.5 ng/μL). The calculated average concentration of butylated adipic acid was within two standard deviations of the value introduced, 1 ng μL^{-1} injected. The uncertainty associated with the mass of dibutyl adipate, A. Std., was low. The average butyl DE_i of adipic acid measured using this method was 84%, and using the ECN method was 51-55%.

	Rep. 1	Rep. 2	Rep. 3	Average	Standard Deviation	RSD (%)
Area Phenanthrene-d_{10}	372319	619550	725839			
Area Dibutyl Adipate A. Std.	1977465	4036002	1695793			
Mass Dibutyl Adipate A. Std.	0.868	0.708	0.987	0.854	0.14	16.4
Area Phenanthrene-d_{10}	281477					
Area Butylated Adipic Acid	25845					
Mass Butylated Adipic Acid	0.717					

Table I. Measured effective carbon numbers (ECNi) of n-alkane reference standards used in the calculation of derivatization efficiency. A comparison between replicate analyses (listed horizontally) shows that <10% RSD was observed. Values were tabulated from five replicate BSTFA derivatized calibration standard solutions used in the calculation of derivatization efficiency, using phenanthrene-d10 as a reference

			ECN_i						
	ECN_{ref}	MW_{ref} (a.m.u.)	Replicate 1	Replicate 2	Replicate 3	Replicate 4	Replicate 5	Average	RSD (%)
Decane	10	142.3	11.1	11.3	12.9	12.6	13.2	12.2	7.86
Undecane	11	156	12.3	12.6	14.8	14.8	14.4	13.8	8.8
Dodecane	12	170.3	13.2	13.5	15.7	15	15.8	14.6	8.28
Tridecane	13	184.4	14.7	14.7	15.7	16.6	17.4	15.9	7.31
Tetradecane	14	198.4	15.7	15.7	18.5	17.3	18.9	17.2	8.89
Pentadecane	15	212.4	17	17	19.7	18.9	20	18.5	7.65
Hexadecane	16	226.4	17.1	17.6	20.5	19.5	21.2	19.2	9.31

Table J. Measured effective carbon numbers (ECN_i) of n-alkane reference standards used in the calculation of derivatization efficiency. A comparison between replicate analyses (listed horizontally) shows that <10% RSD was observed. Values were tabulated from five replicate BSTFA derivatized calibration standard solutions used in the calculation of derivatization efficiency, using phenanthrene-d_{10} as a reference

			ECN_i						
	ECN_{ref}	MW_{ref} (a.m.u.)	Replicate 1	Replicate 2	Replicate 3	Replicate 4	Replicate 5	Average	RSD (%)
Decane	10	142.3	11.1	11.3	12.9	12.6	13.2	12.2	7.86
Undecane	11	156	12.3	12.6	14.8	14.8	14.4	13.8	8.8
Dodecane	12	170.3	13.2	13.5	15.7	15	15.8	14.6	8.28
Tridecane	13	184.4	14.7	14.7	15.7	16.6	17.4	15.9	7.31
Tetradecane	14	198.4	15.7	15.7	18.5	17.3	18.9	17.2	8.89
Pentadecane	15	212.4	17	17	19.7	18.9	20	18.5	7.65
Hexadecane	16	226.4	17.1	17.6	20.5	19.5	21.2	19.2	9.31

Table K. External calibration of the method of GC×GC-TOF-MS based on the response of quantitation ions of each butyl derivative (as well as the recovery standard, eicosane-d_{42}).. Least squares equations were approximated using ChromaTOF Version 4.41 optimized for Pegasus®, response factor (RF) values were calculated manually, and average, standard deviation, and correlation coefficient (r^2) values were calculated using Microsoft Excel.

	Least Squares Equation	Average RF	Std. Dev. RF	RSD RF (%)	Correl. Coeff., r^2
Oxalic acid, dibutyl ester	y= +0.00586x - 0.00837	0.00742	0.00152	20.4	0.957
Malonic acid, dibutyl ester	y= +0.335x - 0.464	0.583	0.0552	9.47	0.968
Methyl-malonic acid, dibutyl ester	y= +0.402x - 0.333	1.03	0.202	19.7	0.985
Salicylic acid, butyl ester	y= +0.00200x + 0.0238	0.0115	0.00158	13.7	0.581
Succinic-d_4 acid, dibutyl ester	y= +0.0219x + 1.10	0.792	0.0963	12.2	0.0985
Glyoxylic acid, butyl derivative	y= +0.0665x - 0.163	0.0431	0.00994	231	0.932
Glutaric acid, dibutyl ester	y= +0.0288x - 0.0269	0.626	0.0414	6.62	0.977
cis-Pinonic acid, butyl ester	y= +0.0288x - 0.0269	0.287	0.0249	8.7	0.987
Ketopinic acid, butyl ester	y= +0.00656x - 0.00005	0.0152	0.00215	14.1	0.979
Adipic acid, dibutyl ester	y= +0.0286x - 0.0282	0.0603	0.014	23.3	0.992
Glyoxal, butyl derivative	y= +0.150x - 0.0834	0.363	0.0821	22.6	0.993
Dodecanoic acid, butyl ester	y= +0.0346x - 0.0363	0.0599	0.0156	26	0.994
Eicosane-d_{42}	y= +0.0587x - 0.0734	0.103	0.0132	12.8	0.985

Table L. External calibration of the method of GC×GC-TOF-MS based on the response of quantitation ions of each trimethylsilyl derivative (as well as the recovery standard, eicosane-d_{42}). Least squares equations were approximated using ChromaTOF Version 4.41 optimized for Pegasus®, response factor (RF) values were calculated manually, and average, standard deviation, and correlation coefficient (r^2) values were calculated using Microsoft Excel.

Name	Least Squares Equation	Average RF	Std. Dev. RF	RSD. RF (%)	Correl. Coeff., r^2
Lactic acid, TMS	y= +0.344x + 0.193	0.483	0.0283	5.86	0.993
2-Hydroxy-3-methyl-butyric acid, TMS	y= +0.324x + 0.0983	1.12	0.377	33.7	0.96
Malonic acid, TMS	y= +0.0979x - 0.00892	0.344	0.164	47.7	0.732
Methyl-malonic acid, TMS	y= +0.0975x - 0.00539	0.829	0.185	22.3	0.993
Succinic-d_4 acid, TMS	y= +0.117x + 0.0258	0.496	0.154	31.1	0.972
Glutaric acid, TMS	y= +0.0809x + 0.0315	0.265	0.045	16.9	0.997
Adipic acid, TMS	y= +0.0399x + 0.0385	0.262	0.0405	15.5	0.998
Ketopinic acid, TMS	y= +0.0187x + 0.0121	0.0686	0.0077	11.2	0.999
Salicylic acid, TMS	y= +0.0553x + 0.0622	0.424	0.285	67.3	0.969
cis-Pinonic acid, TMS	y= +0.464x + 0.0918	1.49	0.528	35.4	0.957
Dodecanoic acid, TMS	y= +0.115x + 0.138	0.612	0.137	22.3	0.969
Eicosane-d_{42}	y= +0.0652x + 0.0168	0.167	0.0581	34.7	0.905

Table AA. External calibration of the method of GC×GC/TOF-MS based on the total ion signal of each trimethylsilyl derivative (as well as the recovery standard, eicosane-d_{42}). Least squares equations were approximated using ChromaTOF Version 4.41 optimized for Pegasus®, response factor (RF) values were calculated manually, and average, standard deviation, and correlation coefficient (r^2) values were calculated using Microsoft Excel.

Name	Average RF	Std. Dev. RF	RSD RF (%)	Correlation Coefficient, r^2
Lactic acid, TMS	3.32	0.515	15.6	0.995
2-Hydroxy-3-methyl-butyric acid, TMS	5.44	3.17	58.2	0.977
Malonic acid, TMS	3.39	1.69	49.7	0.951
Methyl-malonic acid, TMS	7.48	1.88	25.2	0.997
Succinic-d_4 acid, TMS	4.17	1.00	24.1	0.997
Glutaric acid, TMS	4.93	2.87	58.3	0.985
Adipic acid, TMS	4.08	4.41	108	0.907
Ketopinic acid, TMS	2.96	1.94	65.4	0.970
Salicylic acid, TMS	3.05	2.22	72.6	0.980
cis-Pinonic acid, TMS	5.38	3.21	59.8	0.960
Dodecanoic acid, TMS	4.59	3.47	75.7	0.954
Eicosane-d_{42}	2.58	1.68	65.2	0.873

Table BB. External calibration of the method of GC×GC/TOF-MS based on the total ion signal of each butyl derivative (as well as the recovery standard, eicosane-d_{42}). Least squares equations were approximated using ChromaTOF Version 4.41 optimized for Pegasus®, response factor (RF) values were calculated manually, and average, standard deviation, and correlation coefficient (r^2) values were calculated using Microsoft Excel.

Name	Average RF	Std. Dev. RF	RSD RF (%)	Correl. Coeff., r^2
cis-Pinonic acid, butyl ester	5.09	2.49	48.9	0.999
Eicosane-d_{42}	3.23	2.07	64.1	0.968
Oxalic acid, dibutyl ester	3.25	1.46	44.9	0.989
Glutaric acid, dibutyl ester	1.45	0.867	59.9	0.993
Glyoxal, butyl derivative	12.7	2.16	17.0	0.995
Glyoxylic acid, butyl derivative	1.75	0.867	49.5	0.941
Adipic acid, dibutyl ester	2.33	2.92	125	0.992
Ketopinic acid, butyl ester	1.47	0.501	34.1	1.00
Dodecanoic acid, butyl ester	8.16	3.17	38.8	0.999
Malonic acid, dibutyl ester	7.18	2.82	39.2	0.970
Methyl-malonic acid, dibutyl ester	16.2	10.2	62.9	0.987
Salicylic acid, butyl ester	0.0368	0.0213	57.8	0.999
Succinic-d_4 acid, dibutyl ester	7.93	3.50	44.1	0.983

Table O. Precision of butyl external calibration standards, internal standards (naphthalene-d_8, phenanthrene-d_{10}, and pyrene-d_{10}), and recovery standards (succinic-d_4 acid, ketopinic acid, eicosane-d_{42}. Relative standard deviations (RSDs, %) of the primary retention time (^1t_R) and secondary retention time (^2t_R) are <5% in all cases; RSDs of the responses for the internal standards as given by the peak area were <40% (the concentration of the calibration standards was varied throughout the standard solutions examined here).

Name	Avg. ^1t_R (se	Std. Dev. ^1t_R	RSD ^1t	Avg. ^2t_R	Std. Dev. ^2t_R	RSD ^2t_R (%)	Avg. Area	Std. Dev. Are	RSD Area (%)
Oxalic acid	1131.93	0	0	1.36	0.02	1.43			
Malonic ac	1223.92	0	0	1.36	0.02	1.46			
Methyl-mal	1248.72	1.79	0.14	1.33	0.03	1.96			
Salicylic ac	1279.91	0	0	1.43	0.01	0.4			
Ketopinic a	1494.29	2.19	0.15	1.6	0	0.23			
Succinic-d_4	1359.9	0	0	1.39	0.04	3.09			
Glyoxylic a	1402.3	5.36	0.38	1.26	0.05	3.6			
Glutaric ac	1471.89	0	0	1.4	0.03	1.82			
cis-Pinonic	1479.89	0	0	1.46	0.02	1.58			
Adipic acid	1583.88	0	0	1.42	0.02	1.59			
Glyoxal, bu	1600.68	1.79	0.11	1.23	0.02	1.81			
Dodecanoic	1604.68	1.79	0.11	1.31	0.06	4.3			
Eicosane-d	1779.86	0	0	1.16	0.01	1.07			
Naphthaler	946.34	2.19	0.23	1.51	0.01	0.56	344576270	28655864	8.32
Phenanthre	1625.48	2.19	0.13	2.01	0.01	0.69	272094118	49140854	18.06
Pyrene-d_{10}	1947.85	0.01	0	2.38	0	0.17	86838874	34352025	39.56

Table P. Precision of trimethylsilyl external calibration standards, internal standards (naphthalene-d_8, phenanthrene-d_{10}, and pyrene-d_{10}), and recovery standards (succinic-d_4 acid, ketopinic acid, eicosane-d_{42}. Relative standard deviations (RSDs, %) of the primary retention time (^1t_R) and secondary retention time (^2t_R) are <5% in all cases; RSDs of the responses for the internal standards as given by the peak area were <40% (the concentration of the calibration standards was varied throughout the standard solutions examined here).

Name	Avg. ^1t_R (sec)	Std. Dev. ^1t_R	RSD ^1t_R (%)	Avg. ^2t_R (min)	Std. Dev. ^2t_R	RSD ^2t_R (%)	Avg. Area	Std. Dev. Area	RSD Area (%)
Lactic acid, TMS	835.95	0	0	1.17	0.07	5.99			
2-Hydroxy-3-methyl-butyric acid, TMS	979.93	0	0	1.15	0.05	4.33			
Malonic acid, TMS	1028.93	2	0.19	1.28	0.02	1.81			
Methyl-malonic acid, TMS	1044.93	2	0.19	1.33	0.14	10.27			
Glutaric acid, TMS	1257.9	57.36	4.56	1.32	0.03	2.02			
Adipic acid, TMS	1409.89	2.31	0.16	1.34	0.03	2.22			
Ketopinic acid, TMS	1410.89	18	1.28	1.83	0.01	0.64			
Salicylic acid, TMS	1423.89	0	0	1.42	0.01	0.95			
cis-Pinonic acid, TMS	1440.89	2	0.14	1.52	0.02	1.1			
Dodecanoic acid, TMS	1575.87	0	0	1.3	0.03	1.93			
Succinic-d_4 acid, TMS	1168.91	1.79	0.15	1.31	0	0.21			
Eicosane-d_{42}	1895.84	0.01	0	1.21	0.1	8.59			
Naphthalene-d_8	1011.93	1.79	0.18	1.88	0.03	1.55	201949783	39189209	19.4
Phenthanthrene-d_{10}	1739.86	0	0	2.64	0.03	1.05	160919241	22342620	13.9
Pyrene-d_{10}	2035.83	1.79	0.09	2.33	0.03	1.29	98435207	11208473	11.4

APPENDIX E: Mass Spectra of α-Pinene Ozonolysis Products

Table CC. Butylated α-pinene ozonolysis product mass spectra from GCxGC TOF-MS analysis. Identifications are tentatively made by comparison to available spectra of previously identified products as well as predictions of fragments in previously identified products. Some authentic standards were available: oxalic acid, malonic acid, methyl-malonic acid, and *cis*-pinonic acid, butyl derivatives. Ketopinic acid and succinic-d_4 acids, butyl derivatives, are standard compounds added to each filter in order to show that extraction occurred sufficiently. Naphthalene-d_8, phenanthrene-d_{10}, and pyrene-d_{10} are internal standards used for quantification; eicosane-d_{42} was used to adjust for extraction efficiencies from the samples below 80%. Compounds with characteristic ions sufficient to allow tentative functional group identifications are marked as such; some mass spectra did not contain sufficiently characteristic ions for any identification. Only some molecular ions were present; for those that are obvious, the value of the molecular weight is listed ("Deriv. M.W." is the derivatized molecular weight; "Un. M.W." is the underivatized molecular weight of each compound).

Peak	Name	^1t_R (sec)	^2t_R (sec)	Butylated Spectrum
2	Naphthalene-d_8	947.9	1.51	
3	Oxidation Product Possible M.W. 184 Methylene Carboxylic acid	1027.9	1.37	Peak True - sample "BuOH SOA 26-3:1", peak 5, at 1027.94 , 1.373 sec , sec 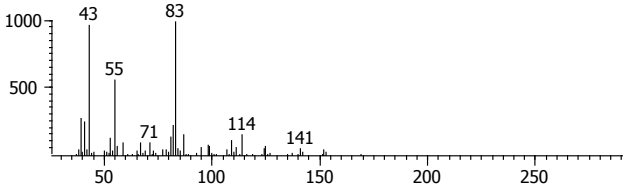 Library Hit - similarity 685, "4-Pentenoic acid, 2,4-dimethyl-, methyl ester" 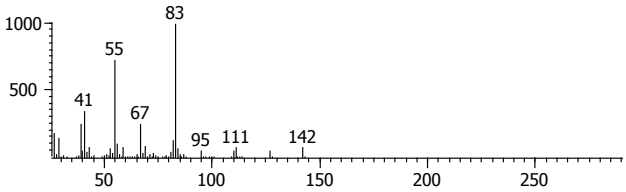
4	Pinonaldehyde M.W. 168 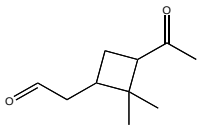	1047.9	1.47	Peak True - sample "BuOH SOA 26-3:1", peak 6, at 1047.94 , 1.472 sec , sec 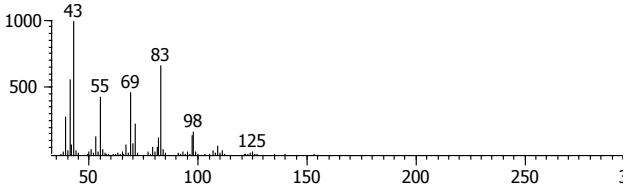 Library Hit - similarity 768, "3-Methylpenta-1,4-diene-3-ol" 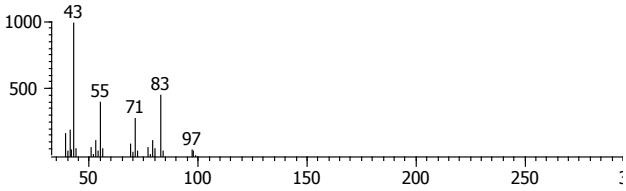

Peak	Name	$^{1}t_R$ (sec)	$^{2}t_R$ (sec)	Butylated Spectrum
5	Oxidation product Possible M.W. 202 Ring opening product with possible aldehyde	1051.9	1.33	Peak True - sample "BuOH SOA 26-3:1", peak 7, at 1051.93 , 1.333 sec , sec 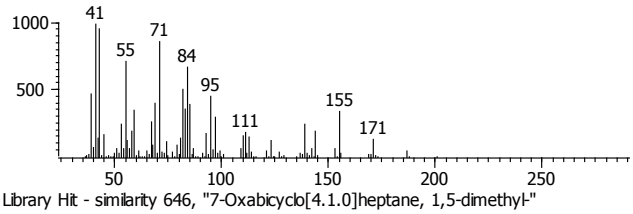 Library Hit - similarity 646, "7-Oxabicyclo[4.1.0]heptane, 1,5-dimethyl-" 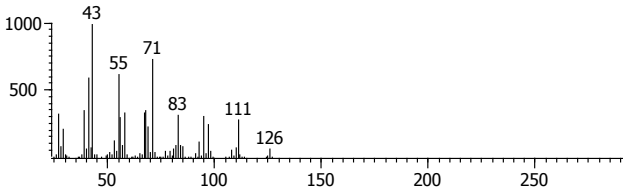
6	Oxidation product	1059.9	1.36	Peak True - sample "BuOH SOA 26-3:1", peak 9, at 1059.93 , 1.360 sec , sec 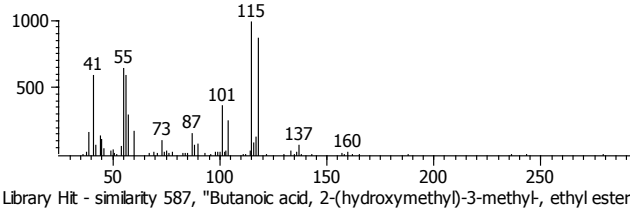 Library Hit - similarity 587, "Butanoic acid, 2-(hydroxymethyl)-3-methyl-, ethyl ester 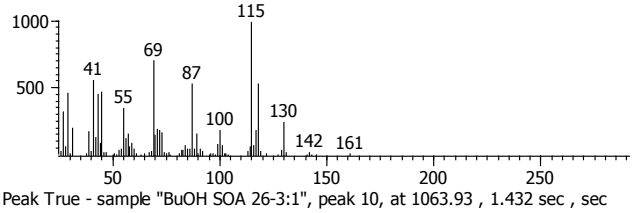
7	Oxidation product 7 Carboxylic acid	1063.9	1.43	Peak True - sample "BuOH SOA 26-3:1", peak 10, at 1063.93 , 1.432 sec , sec 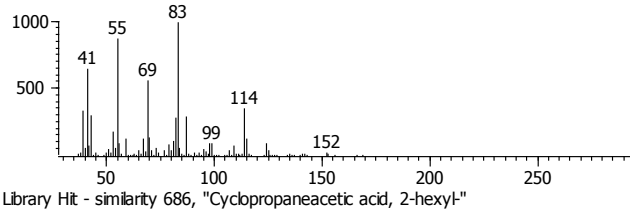 Library Hit - similarity 686, "Cyclopropaneacetic acid, 2-hexyl-" 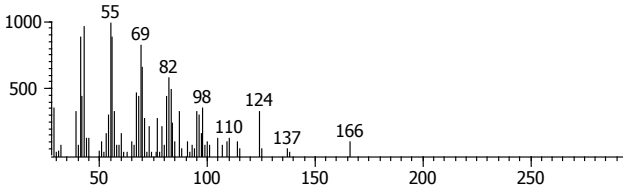

Peak	Name	$^{1}t_R$ (sec)	$^{2}t_R$ (sec)	Butylated Spectrum
8	Pinalic-4-acid M.W. 170 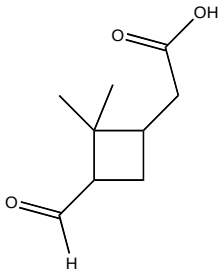	1079.9	1.38	Peak True - sample "BuOH SOA 26-3:1", peak 13, at 1079.93 , 1.379 sec , sec 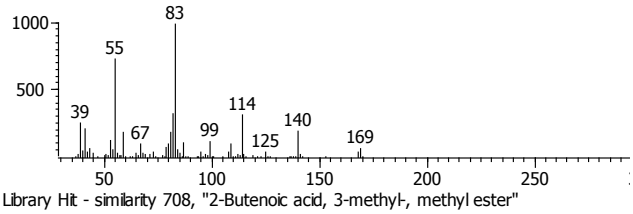 Library Hit - similarity 708, "2-Butenoic acid, 3-methyl-, methyl ester" 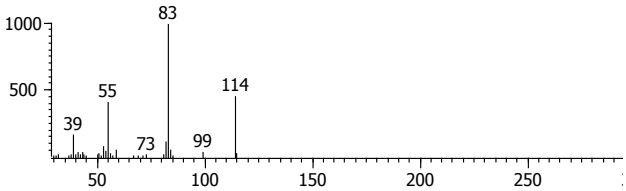
9	Oxidation product Carboxylic acid	1079.9	1.21	Peak True - sample "BuOH SOA 26-3:1", peak 12, at 1079.93 , 1.214 sec , sec 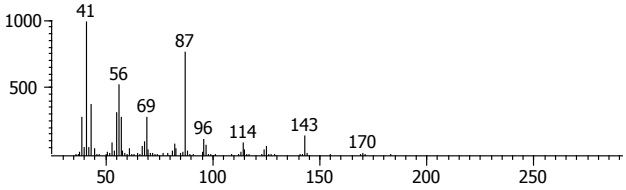 Library Hit - similarity 671, "2-Octenoic acid, methyl ester, (E)-" 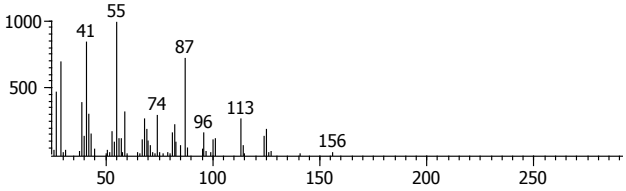
10	Oxidation product Carboxylic acid	1095.9	1.39	Peak True - sample "BuOH SOA 26-3:1", peak 14, at 1095.93 , 1.386 sec , sec 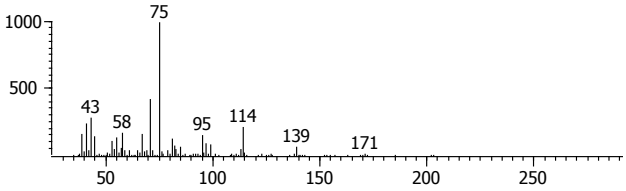 Library Hit - similarity 675, "Dodecane, 1,1-dimethoxy-" 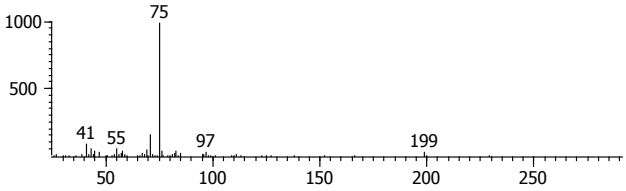

Peak	Name	$^{1}t_R$ (sec)	$^{2}t_R$ (sec)	Butylated Spectrum
11	Oxalic acid, dibutyl ester Deriv. M.W. 202 Un. M.W. 90 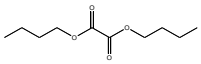	1131.9	1.35	Peak True - sample "BuOH SOA 26-3:1", peak 17, at 1131.93 , 1.346 sec , sec 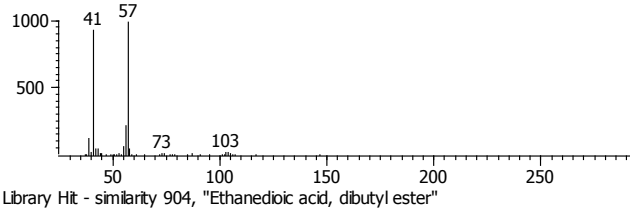 Library Hit - similarity 904, "Ethanedioic acid, dibutyl ester" 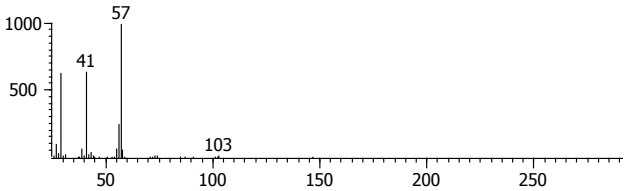
12	4-oxo-Pinonic acid M.W. 198 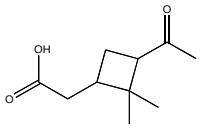	1175.9	1.46	Peak True - sample "BuOH SOA 26-3:1", peak 22, at 1175.92 , 1.459 sec , sec 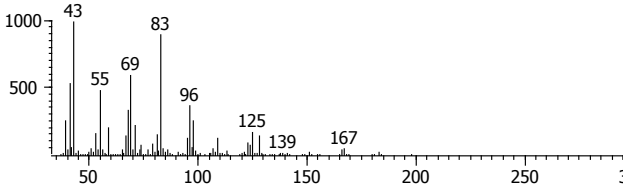 Library Hit - similarity 804, "cis-Pinonic acid, underivatized" 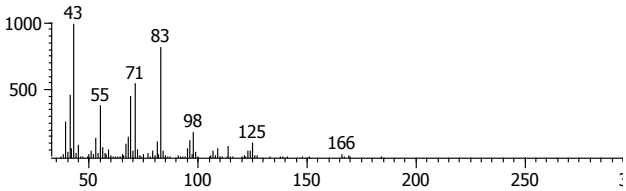
13	Oxidation product	1179.9	1.38	Peak True - sample "BuOH SOA 26-3:1", peak 24, at 1179.92 , 1.379 sec , sec 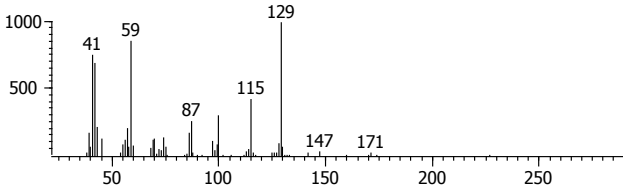 Library Hit - similarity 639, "Pentanedioic acid, ethyl methyl ester" 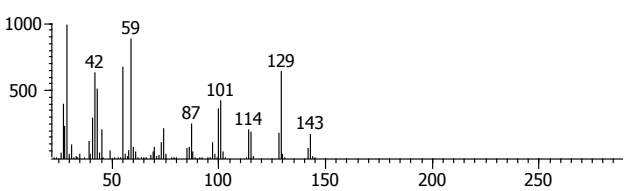

Peak	Name	$^{1}t_R$ (sec)	$^{2}t_R$ (sec)	Butylated Spectrum
15	Butyl ester Carboxylic acid	1191.9	1.28	Peak True - sample "BuOH SOA 26-3:1", peak 26, at 1191.92 , 1.280 sec , sec 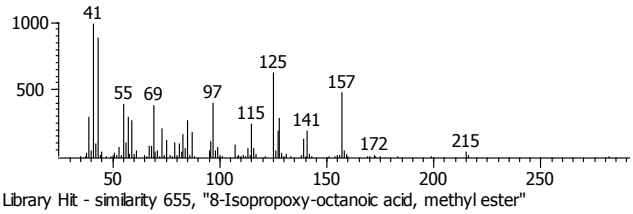 Library Hit - similarity 655, "8-Isopropoxy-octanoic acid, methyl ester" 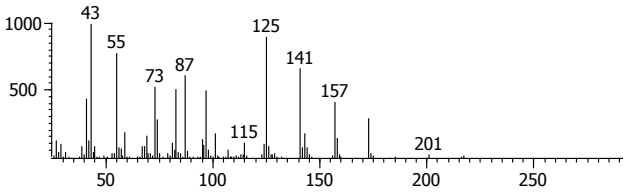
16	Dimethyl pinate M.W. 214	1191.9	1.43	Peak True - sample "Diluted BuOH SOA 23-3:1", peak 17, at 1195.92 , 1.403 sec , sec 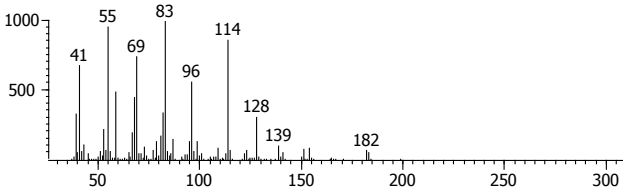 Library Hit - similarity 668, "2,6-Octadienoic acid, 3,7-dimethyl-, methyl ester" 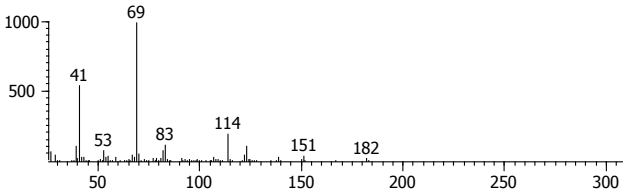
17	Oxidation product	1199.9	1.35	Peak True - sample "*BuOH SOA 26-3:1", peak 18, at 1199.92 , 1.353 sec , sec 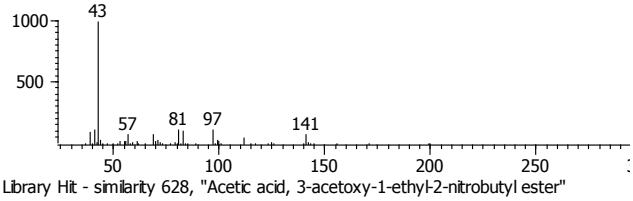 Library Hit - similarity 628, "Acetic acid, 3-acetoxy-1-ethyl-2-nitrobutyl ester" 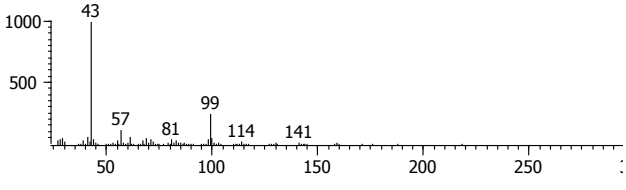

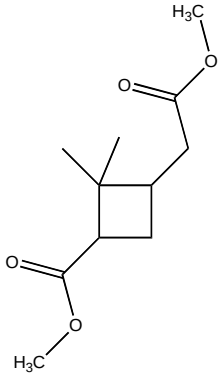

Peak	Name	$^{1}t_R$ (sec)	$^{2}t_R$ (sec)	Butylated Spectrum
18	Oxidation product M.W. 196 Ring-retaining	1211.9	1.63	Peak True - sample "BuOH Diluted SOA 23-3:1", peak 35, at 1211.92 , 1.624 sec , 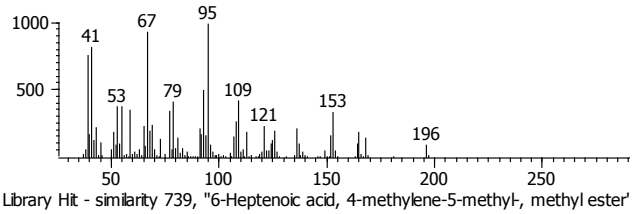 Library Hit - similarity 739, "6-Heptenoic acid, 4-methylene-5-methyl-, methyl ester" 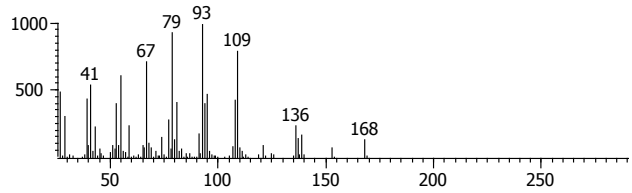
19	Butyl ester Carboxylic acid	1219.9	1.37	Peak True - sample "BuOH Diluted SOA 23-3:1", peak 36, at 1219.92 , 1.360 sec , 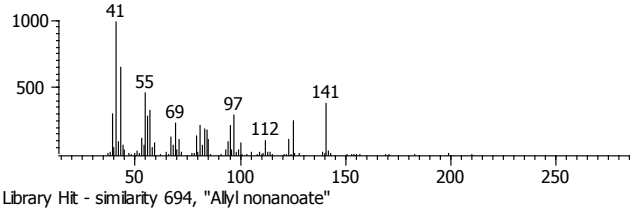 Library Hit - similarity 694, "Allyl nonanoate" 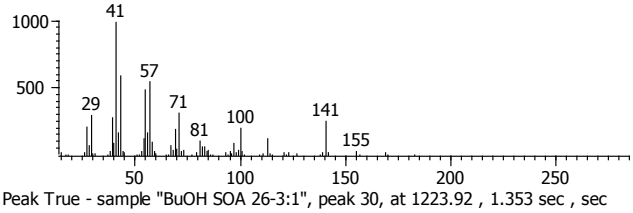
20	Malonic acid, dibutyl ester	1223.9	1.35	Peak True - sample "BuOH SOA 26-3:1", peak 30, at 1223.92 , 1.353 sec , sec 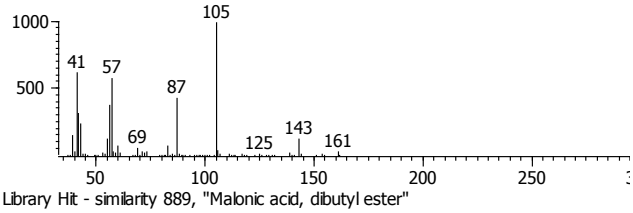 Library Hit - similarity 889, "Malonic acid, dibutyl ester" 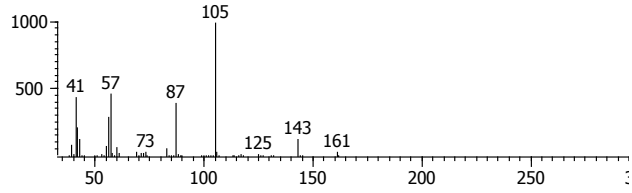

Peak	Name	$^{1}t_R$ (sec)	$^{2}t_R$ (sec)	Butylated Spectrum
21	Butyl derivative Aldehyde	1227.9	1.25	Peak True - sample "BuOH SOA 26-3:1", peak 31, at 1227.92 , 1.254 sec , sec 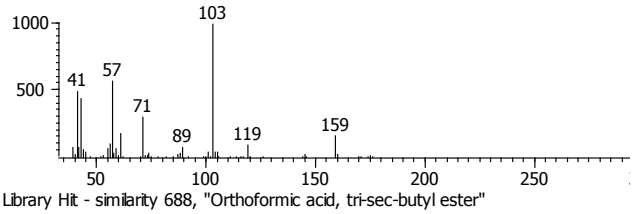 Library Hit - similarity 688, "Orthoformic acid, tri-sec-butyl ester" 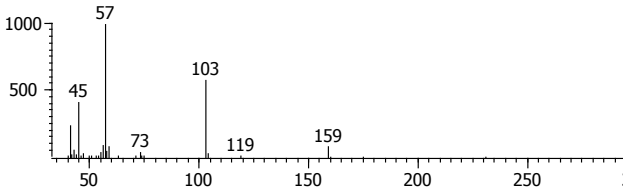
22	Butyl derivative Aldehyde	1239.9	1.70	Peak True - sample "BuOH SOA 26-3:1", peak 34, at 1239.92 , 1.703 sec , sec 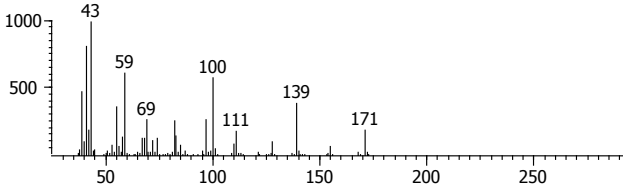 Library Hit - similarity 621, "1-(1-Hydroxy-1-methyl-ethyl)-cyclobutanecarboxylic acic 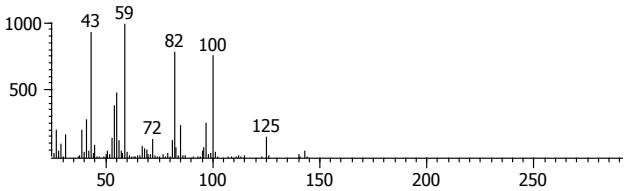
23	Oxidation product Carboxylic acid	1247.9	1.51	Peak True - sample "BuOH SOA 26-3:1", peak 35, at 1247.92 , 1.511 sec , sec 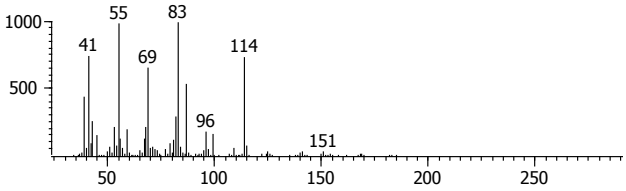 Library Hit - similarity 701, "2-Pentenoic acid, methyl ester, (E)-" 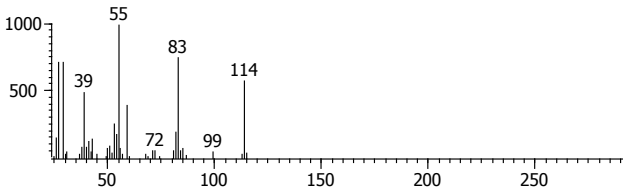

Peak	Name	$^{1}t_R$ (sec)	$^{2}t_R$ (sec)	Butylated Spectrum
24	Pinic acid M.W. 186 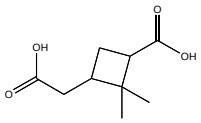	1255.9	1.54	Peak True - sample "BuOH SOA 26-3:1", peak 37, at 1255.91 , 1.538 sec , sec 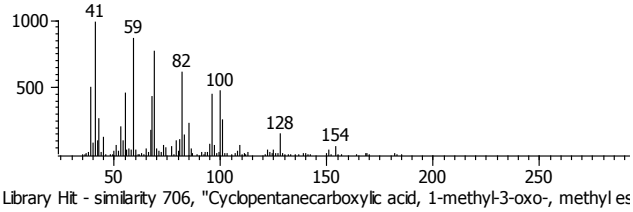 Library Hit - similarity 706, "Cyclopentanecarboxylic acid, 1-methyl-3-oxo-, methyl es 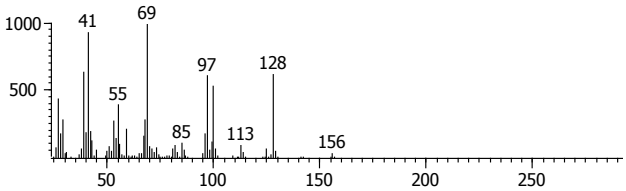
25	Butyl derivative Deriv. M.W. 236 Un. M.W. 180 Ring-retaining carboxylic acid	1299.9	1.25	Peak True - sample "BuOH SOA 26-3:1", peak 41, at 1299.91 , 1.247 sec , sec 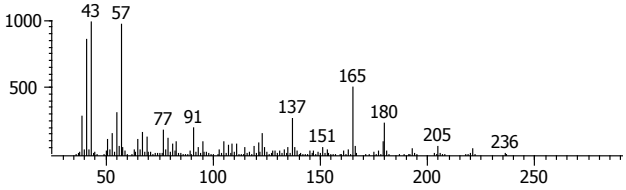 Library Hit - similarity 719, "4-(1-Hydroperoxy-2,2-dimethyl-6-methylene-cyclohexyl) 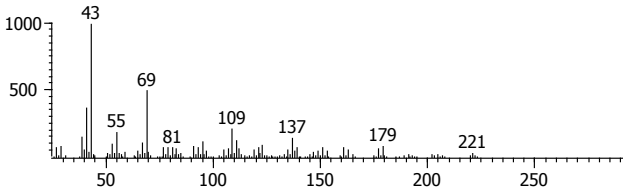
27	2,2-dimethyl-3-formyl-cyclobutyl-methanoic acid Deriv. M.W. 342 Un. M.W. 156 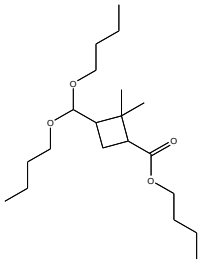	1335.9	1.36	Peak True - sample "BuOH SOA 26-3:1", peak 44, at 1335.91 , 1.360 sec , sec 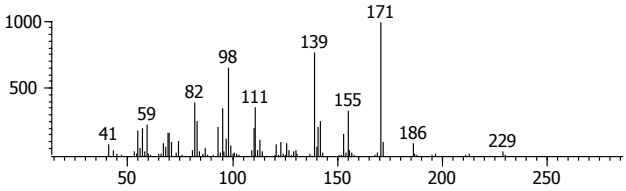 Library Hit - similarity 612, "Heptanedioic acid, 4-methyl-, dimethyl ester" 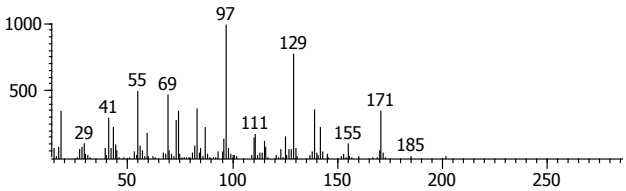

Peak	Name	$^{1}t_R$ (sec)	$^{2}t_R$ (sec)	Butylated Spectrum
28	Oxidation product M.W. 170 Isomer	1351.9	1.68	Peak True - sample "BuOH SOA 26-3:1", peak 47, at 1351.9 , 1.676 sec , sec 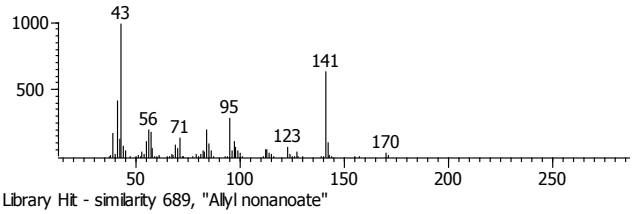 Library Hit - similarity 689, "Allyl nonanoate" 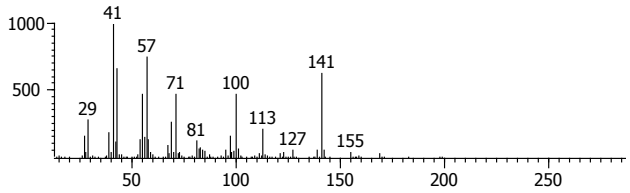
29	Succinic-*d4* acid	1359.9	1.38	
30	Butyl Derivative Deriv. M.W. 214 Un. M.W. 158	1359.9	1.56	Peak True - sample "BuOH SOA 26-3:1", peak 49, at 1359.9 , 1.558 sec , sec 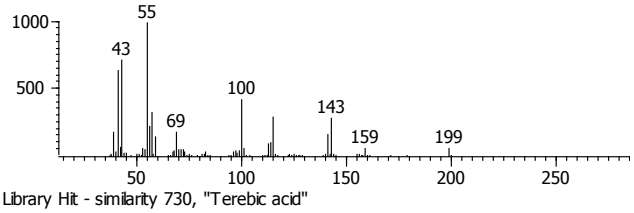 Library Hit - similarity 730, "Terebic acid" 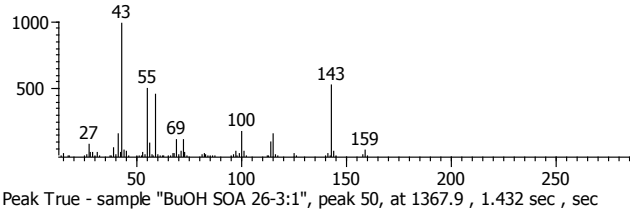
31	Pinalic-4-acid, butyl derivative Deriva M.W. 338 Un. M.W. 170 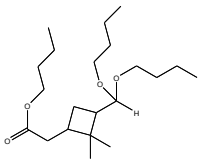	1367.9	1.43	Peak True - sample "BuOH SOA 26-3:1", peak 50, at 1367.9 , 1.432 sec , sec 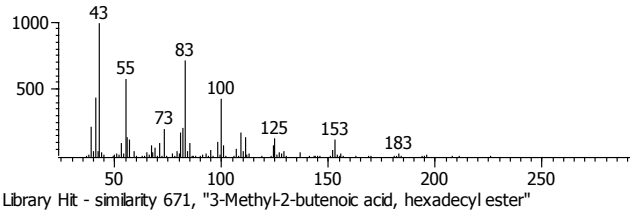 Library Hit - similarity 671, "3-Methyl-2-butenoic acid, hexadecyl ester" 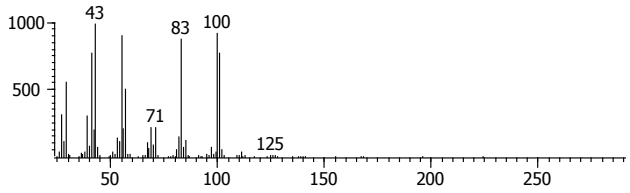

Peak	Name	$^{1}t_R$ (sec)	$^{2}t_R$ (sec)	Butylated Spectrum
32	Oxidation product Carboxylic acid	1379.9	1.39	Peak True - sample "BuOH SOA 26-3:1", peak 54, at 1379.9 , 1.393 s 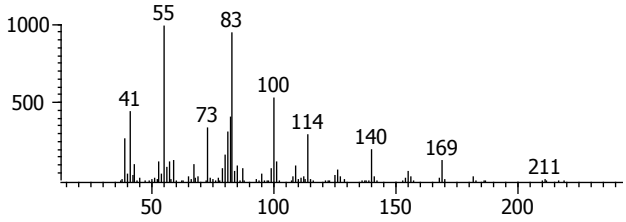 Library Hit - similarity 632, "2-Butenoic acid, 2-methyl-, 2-propenyl ester 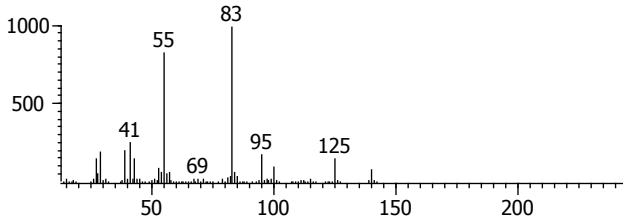
33	Butyl derivative Deriv. M.W. 242 Un. M.W. 130 Aldehyde	1387.9	1.36	Peak True - sample "BuOH SOA 26-3:1", peak 56, at 1387.9 , 1.360 sec , sec 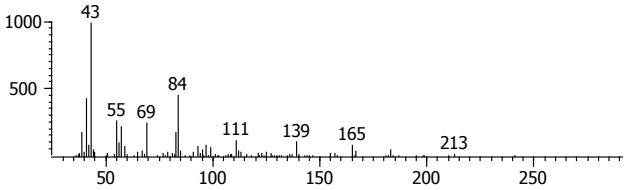 Library Hit - similarity 666, "2-Pentanone, 3-[(acetyloxy)methyl]-3,4-dimethyl-, (.+- 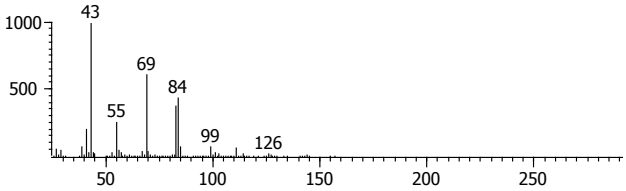
34	Butyl Derivative No identified functional groups	1395.9	1.41	Peak True - sample "BuOH Diluted SOA 23-3:1", peak 56, at 1395.9 , 1.406 sec , 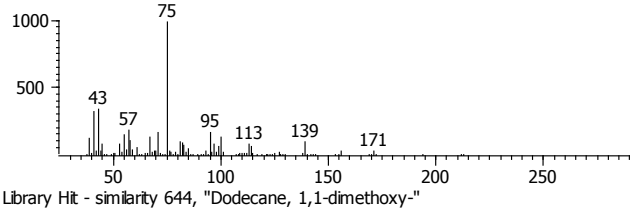 Library Hit - similarity 644, "Dodecane, 1,1-dimethoxy-" 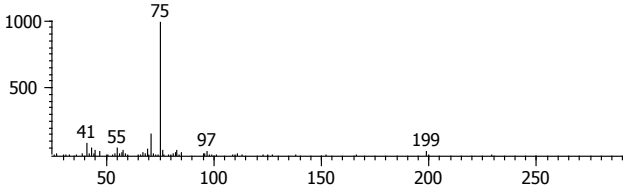

Peak	Name	$^{1}t_R$ (sec)	$^{2}t_R$ (sec)	Butylated Spectrum
35	Butyl Derivative Carboxylic acid, ketone	1399.9	1.31	Peak True - sample "BuOH SOA 26-3:1", peak 60, at 1399.9 , 1.313 sec , sec 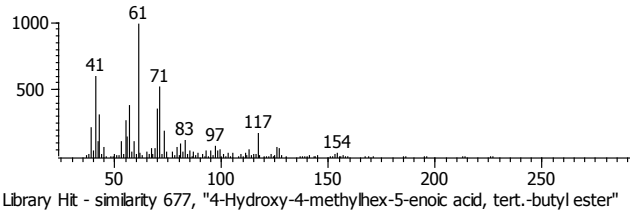 Library Hit - similarity 677, "4-Hydroxy-4-methylhex-5-enoic acid, tert.-butyl ester" 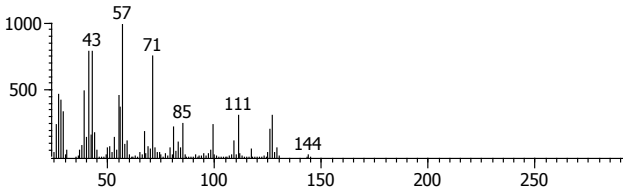
36	Glyoxylic acid, butyl derivative Deriv. M.W. Un. M.W.	1399.9	1.21	Peak True - sample "BuOH SOA 26-3:1", peak 58, at 1399.9 , 1.214 sec , sec 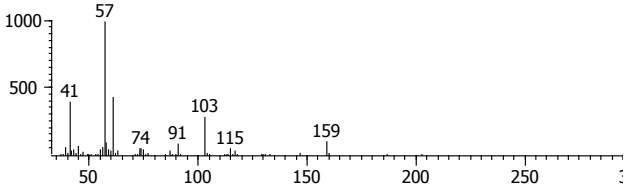 Library Hit - similarity 853, "Glyoxylic acid, butyl derivative" 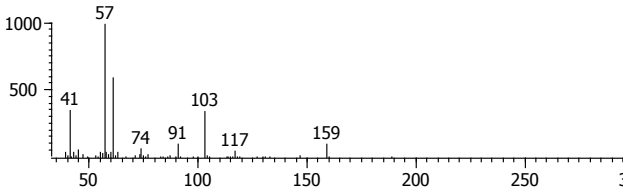
37	Butyl derivative Aldehyde	1443.9	1.52	Peak True - sample "BuOH SOA 26-3:1", peak 68, at 1443.9 , 1.518 sec , sec 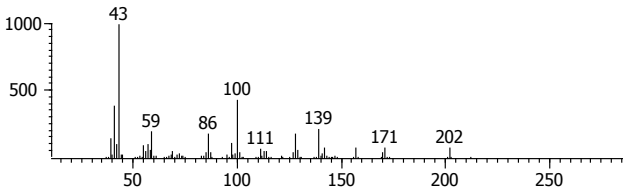 Library Hit - similarity 618, "1-Decanamine" 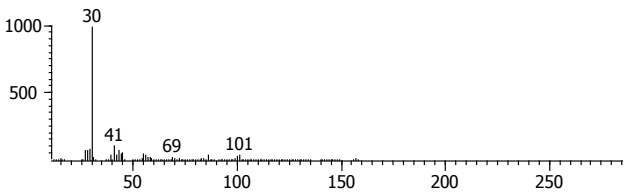

Peak	Name	$^{1}t_R$ (sec)	$^{2}t_R$ (sec)	Butylated Spectrum
38	Butyl derivative Deriv. M.W. 196 Un. M.W. 140 Carboxylic acid	1443.9	1.23	Peak True - sample "BuOH SOA 26-3:1", peak 67, at 1443.9 , 1.234 sec , sec 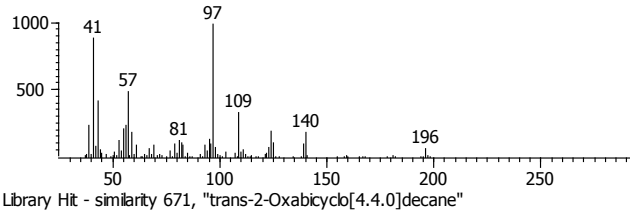 Library Hit - similarity 671, "trans-2-Oxabicyclo[4.4.0]decane" 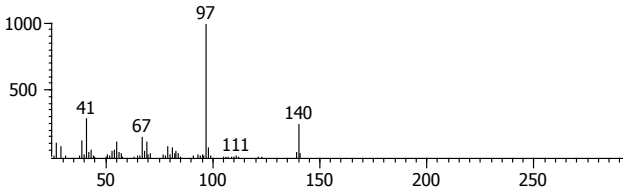
39	Oxidation product Deriv. M.W. 236 Un. M.W. 170 Carboxylic acid	1463.9	1.35	Peak True - sample "BuOH SOA 26-3:1", peak 69, at 1463.89 , 1.353 sec , sec 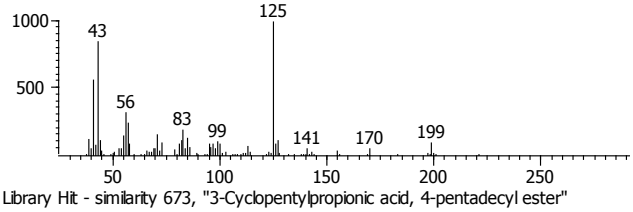 Library Hit - similarity 673, "3-Cyclopentylpropionic acid, 4-pentadecyl ester" 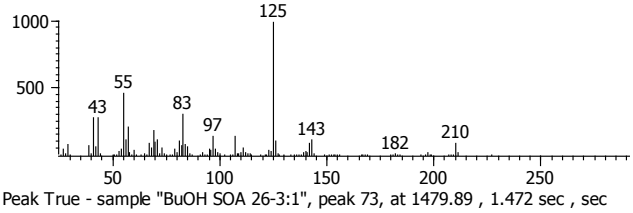
40	Pinonic acid, butyl ester Deriv. M.W. 240 Un. M.W. 184 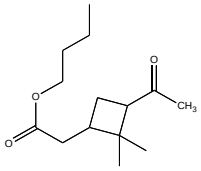	1479.9	1.47	Peak True - sample "BuOH SOA 26-3:1", peak 73, at 1479.89 , 1.472 sec , sec 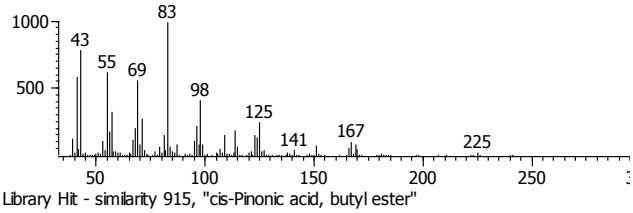 Library Hit - similarity 915, "cis-Pinonic acid, butyl ester" 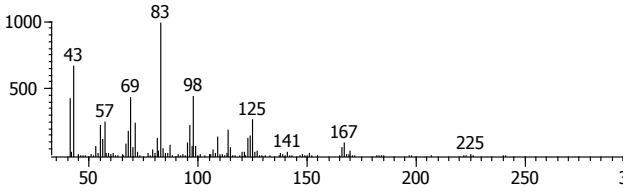

Peak	Name	$^{1}t_R$ (sec)	$^{2}t_R$ (sec)	Butylated Spectrum
41	Hydroxy pinonic acid, butyl ester Deriv. M.W. 256 Un. M.W. 200 e.g. 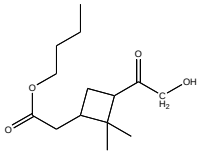	1487.9	1.47	Peak True - sample "BuOH SOA 26-3:1", peak 75, at 1487.89 , 1.472 sec , sec 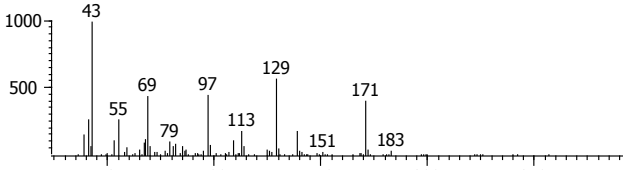 Library Hit - similarity 619, "3,5,9-Nonanetrione, 2,2-dimethyl-9-methoxy-" 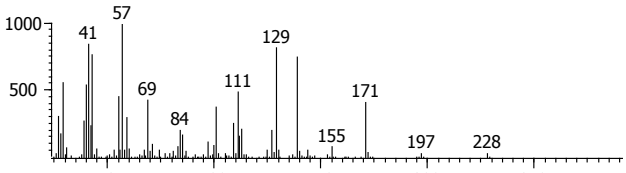
42	10-hydroxy-Pinonic acid M.W. 200 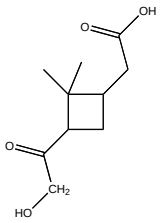	1495.9	1.47	Peak True - sample "Diluted BuOH SOA 23-3:1", peak 46, at 1495.89 , 1.426 sec , sec 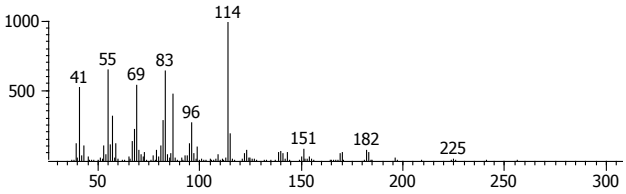 Library Hit - similarity 653, "2,6-Octadienoic acid, 3,7-dimethyl-, methyl ester" 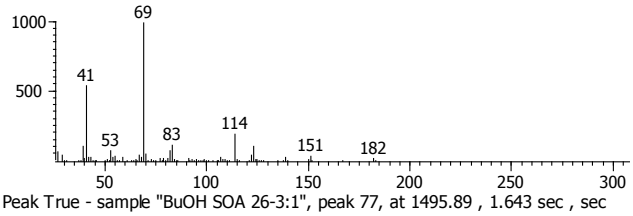
43	Ketopinic acid, butyl ester Deriv. M.W. 238 Un. M.W. 182 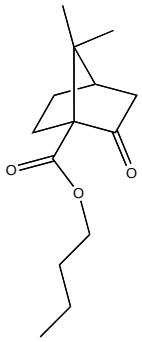	1495.9	1.64	Peak True - sample "BuOH SOA 26-3:1", peak 77, at 1495.89 , 1.643 sec , sec 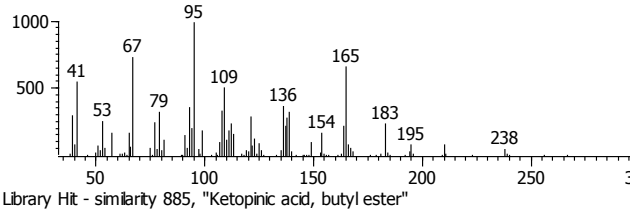 Library Hit - similarity 885, "Ketopinic acid, butyl ester" 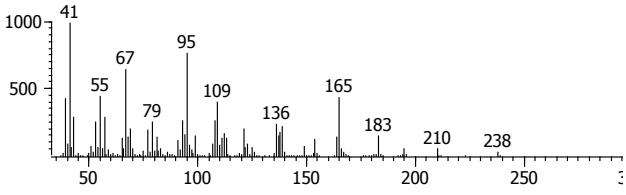

Peak	Name	$^{1}t_R$ (sec)	$^{2}t_R$ (sec)	Butylated Spectrum
44	Butyl derivative Aldehyde, carboxylic acid	1539.9	1.70	Peak True - sample "BuOH SOA 26-3:1", peak 84, at 1539.89 , 1.696 sec , sec 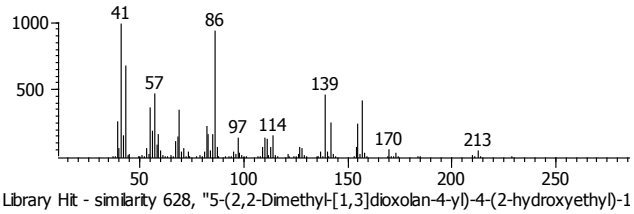 Library Hit - similarity 628, "5-(2,2-Dimethyl-[1,3]dioxolan-4-yl)-4-(2-hydroxyethyl)-1 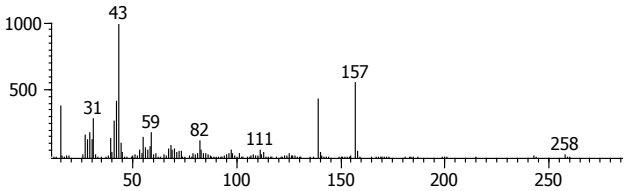
45	Oxidation product Deriv. M.W. 224 Un. M.W. 168 Carboxylic acid	1547.9	1.54	Peak True - sample "BuOH SOA 26-3:1", peak 86, at 1547.89 , 1.544 sec , sec 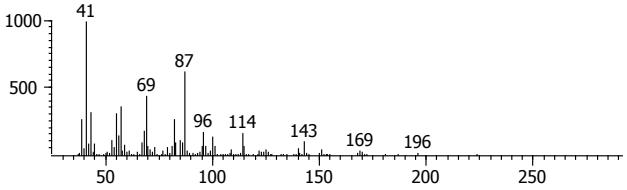 Library Hit - similarity 666, "2-Octenoic acid, methyl ester, (E)-" 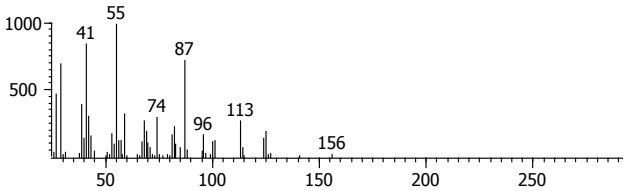
46	Butyl derivative Ketone, carboxylic acid	1559.9	1.41	Peak True - sample "BuOH SOA 26-3:1", peak 87, at 1559.88 , 1.412 sec , sec 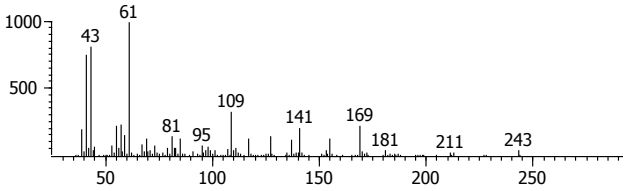 Library Hit - similarity 618, "1-(5-Methoxy-4,4-dimethyl-dihydro-furan-2-ylidene)-prop 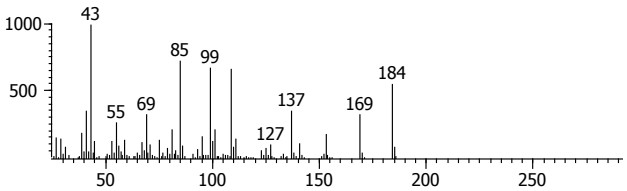

Peak	Name	$^{1}t_R$ (sec)	$^{2}t_R$ (sec)	Butylated Spectrum
47	Butyl derivative Ring-retaining aldehyde	1559.9	1.74	Peak True - sample "BuOH SOA 26-3:1", peak 88, at 1559.88 , 1.736 sec , sec 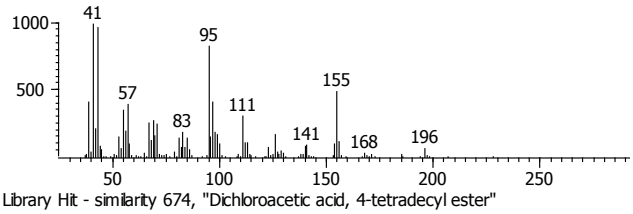 Library Hit - similarity 674, "Dichloroacetic acid, 4-tetradecyl ester" 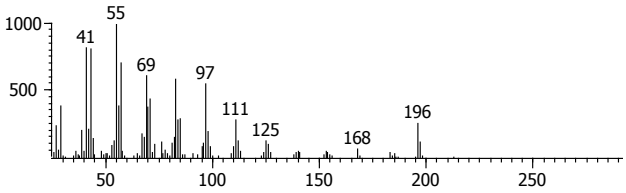
48	Butyl derivative	1563.9	1.27	Peak True - sample "BuOH SOA 26-3:1", peak 89, at 1563.88 , 1.274 sec , sec 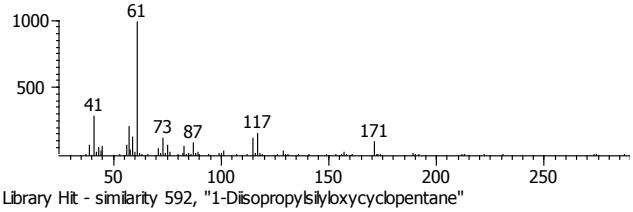 Library Hit - similarity 592, "1-Diisopropylsilyloxycyclopentane" 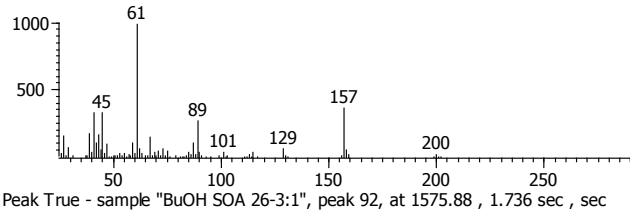
49	Butyl derivative Ring-retaining	1575.9	1.74	Peak True - sample "BuOH SOA 26-3:1", peak 92, at 1575.88 , 1.736 sec , sec 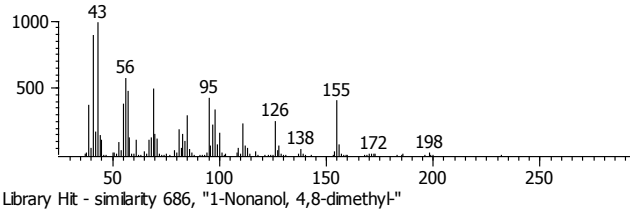 Library Hit - similarity 686, "1-Nonanol, 4,8-dimethyl-" 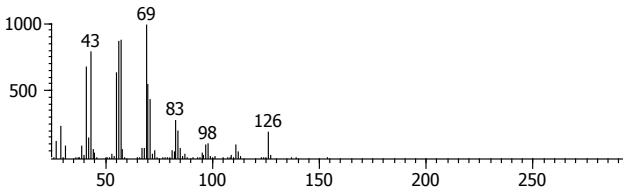

Peak	Name	$^{1}t_R$ (sec)	$^{2}t_R$ (sec)	Butylated Spectrum
50	Oxidation product Ketone	1575.9	1.39	Peak True - sample "BuOH SOA 26-3:1", peak 90, at 1575.88 , 1.393 sec , sec 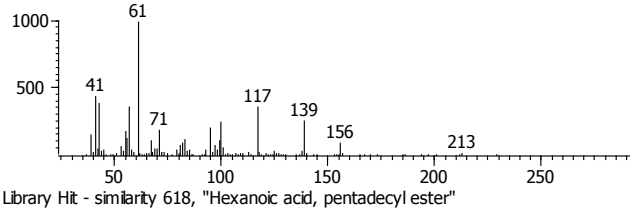 Library Hit - similarity 618, "Hexanoic acid, pentadecyl ester" 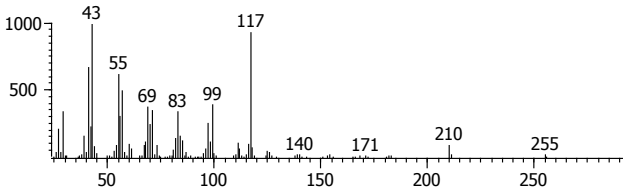
51	Butyl derivative Aldehyde	1579.9	1.28	Peak True - sample "BuOH SOA 26-3:1", peak 93, at 1579.88 , 1.280 sec , sec 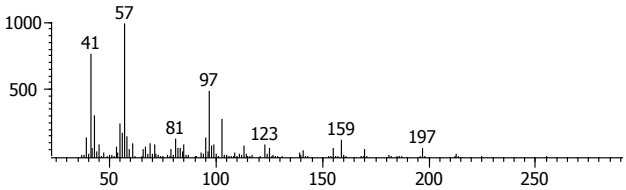 Library Hit - similarity 650, "Methoxyacetic acid, 3-tetradecyl ester" 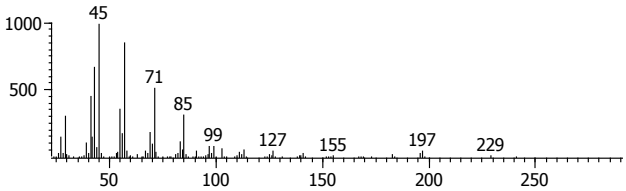
52	Butyl derivative Carboxylic acid	1599.9	1.31	Peak True - sample "BuOH SOA 26-3:1", peak 97, at 1599.88 , 1.313 sec , sec 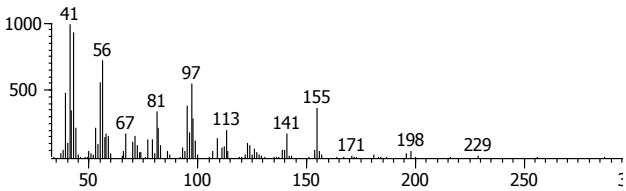 Library Hit - similarity 634, "2,2,6,6-Tetramethyl-4-acetoxyiminopiperidine-1-oxyl" 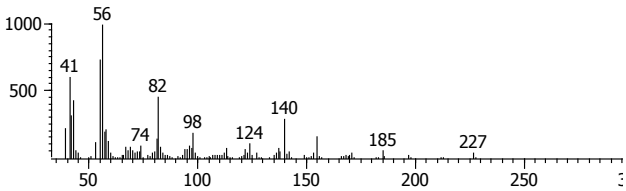

Peak	Name	$^{1}t_R$ (sec)	$^{2}t_R$ (sec)	Butylated Spectrum
53	Butyl derivative Carboxylic acid	1599.9	1.45	Peak True - sample "BuOH SOA 26-3:1", peak 98, at 1599.88 , 1.445 sec , sec 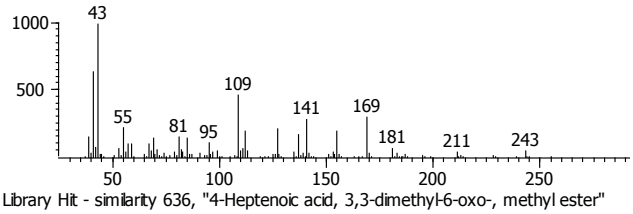 Library Hit - similarity 636, "4-Heptenoic acid, 3,3-dimethyl-6-oxo-, methyl ester" 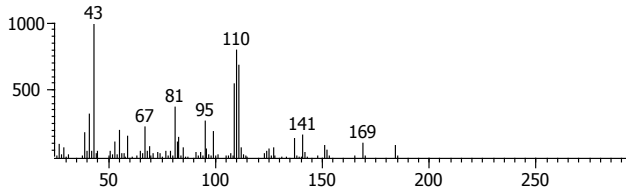
54	Glyoxal, tetrabutyl acetal Deriv. M.W. 318 Un. M.W. 58 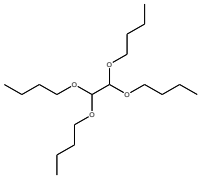	1599.9	1.21	Peak True - sample "BuOH SOA 26-3:1", peak 95, at 1599.88 , 1.208 sec , sec 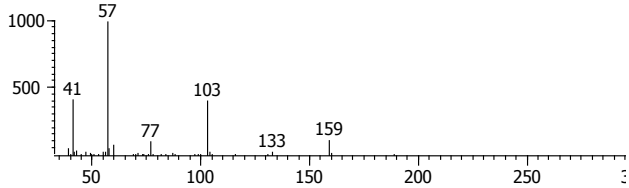 Library Hit - similarity 863, "Glyoxal, tetrabutyl acetal" 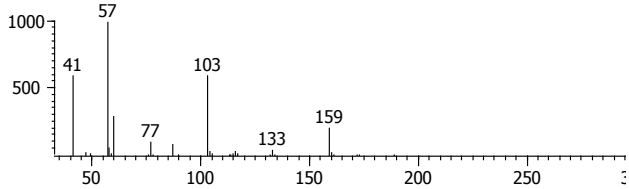
55	Butyl derivative Aldehyde	1619.9	1.38	Peak True - sample "BuOH SOA 26-3:1", peak 104, at 1619.88 , 1.379 sec , sec 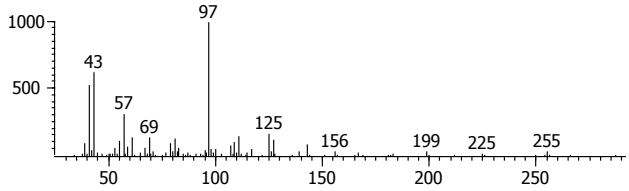 Library Hit - similarity 656, "2,2,3,3-Tetramethylcyclopropanecarboxylic acid, octyl e 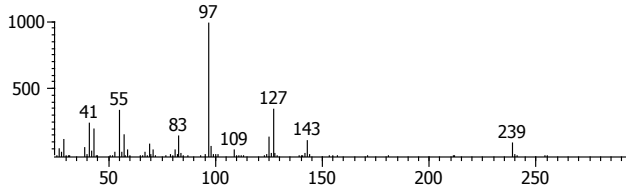
56	Phenanthrene-d_{10}	1623.9	2.03	

Peak	Name	$^{1}t_R$ (sec)	$^{2}t_R$ (sec)	Butylated Spectrum
57	Butyl derivative Ketone	1635.9	1.29	Peak True - sample "BuOH SOA 26-3:1", peak 106, at 1635.88 , 1.294 sec , sec 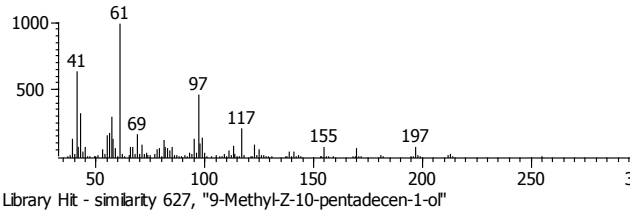 Library Hit - similarity 627, "9-Methyl-Z-10-pentadecen-1-ol" 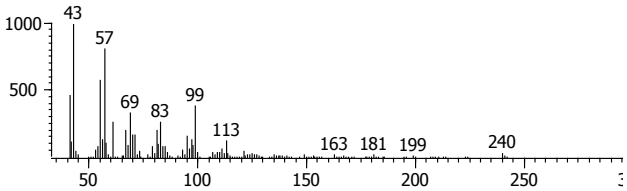
58	Butyl derivative Ketone	1635.9	1.38	Peak True - sample "BuOH SOA 26-3:1", peak 107, at 1635.88 , 1.379 sec , sec 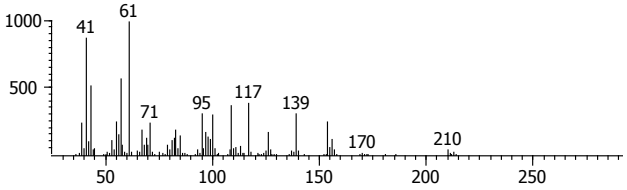 Library Hit - similarity 617, "Cyclohexanecarboxylic acid, 2-hydroxy-1,6-dimethyl-, [1 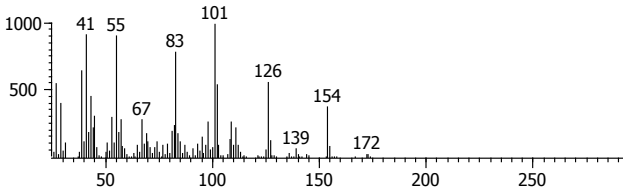
59	Norpinic acid, dibutyl ester Deriv. M.W. 284 Un. M.W. 172	1655.9	1.39	Peak True - sample "BuOH SOA 26-3:1", peak 109, at 1655.87 , 1.393 sec , sec 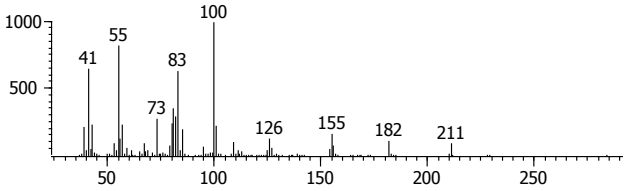 Library Hit - similarity 664, "3-Methyl-2-butenoic acid, pentadecyl ester" 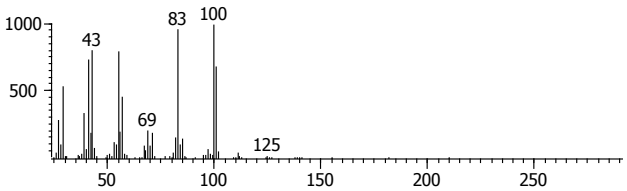

Peak	Name	$^{1}t_R$ (sec)	$^{2}t_R$ (sec)	Butylated Spectrum
60	Butyl derivative Ketone	1667.9	1.40	Peak True - sample "BuOH SOA 26-3:1", peak 110, at 1667.87 , 1.399 sec , sec 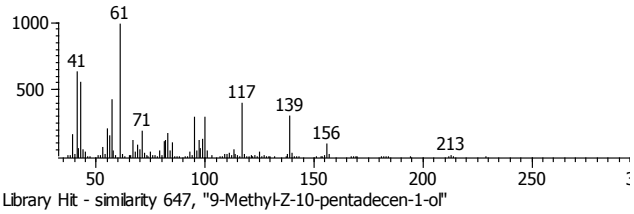 Library Hit - similarity 647, "9-Methyl-Z-10-pentadecen-1-ol" 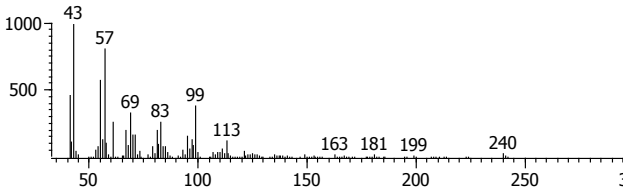
61	Butyl derivative No identified functional groups	1675.9	1.33	Peak True - sample "BuOH SOA 26-3:1", peak 112, at 1675.87 , 1.333 sec , sec 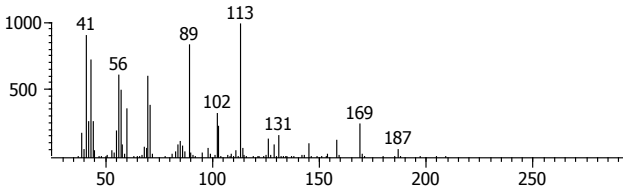 Library Hit - similarity 574, "Butanoic acid, heptyl ester" 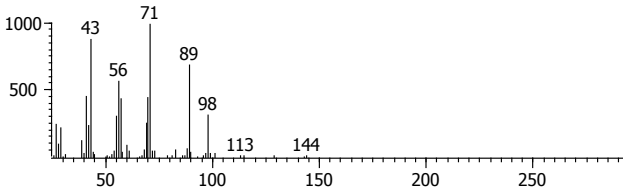
62	Butyl derivative No identified functional groups	1691.9	1.44	Peak True - sample "BuOH SOA 26-3:1", peak 113, at 1691.87 , 1.439 sec , sec 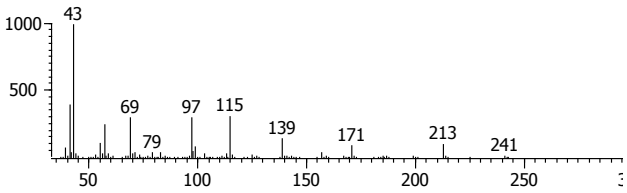 Library Hit - similarity 657, "1,2-Cyclohexanediol, 1-(1-methylethyl)-, cis-" 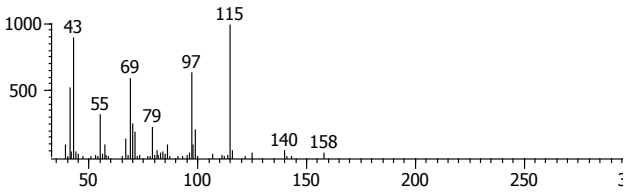

Peak	Name	$^{1}t_R$ (sec)	$^{2}t_R$ (sec)	Butylated Spectrum
63	Butyl derivative Deriv. M.W. 356 Un. M.W. 188 Carboxylic acid	1703.9	1.50	Peak True - sample "BuOH SOA 26-3:1", peak 115, at 1703.87 , 1.498 sec , sec 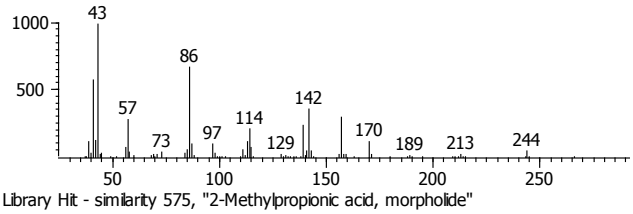 Library Hit - similarity 575, "2-Methylpropionic acid, morpholide" 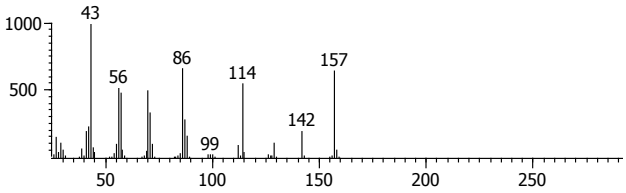
64	Norpinonaldehyde, butyl derivative M.W. 284 Un. M.W. 154 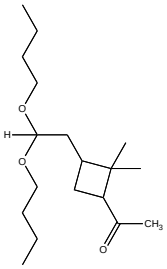	1739.9	1.45	Peak True - sample "BuOH SOA 26-3:1", peak 117, at 1715.87 , 1.366 sec , sec 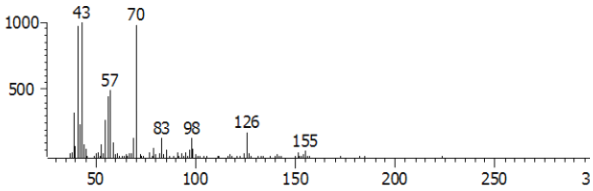 Library Hit - similarity 739, "2,4-Dimethyl-1-heptene" 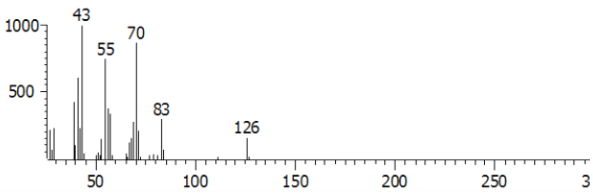
65	Norpinonaldehyde, butyl derivative (2)			Peak True - sample "BuOH SOA 26-3:1", peak 116, at 1715.87 , 1.353 sec , sec 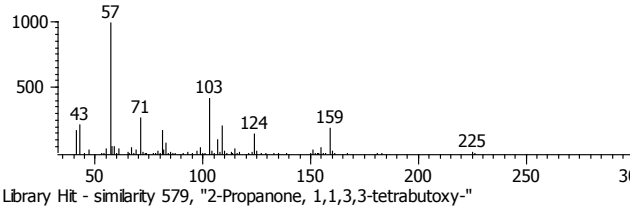 Library Hit - similarity 579, "2-Propanone, 1,1,3,3-tetrabutoxy-" 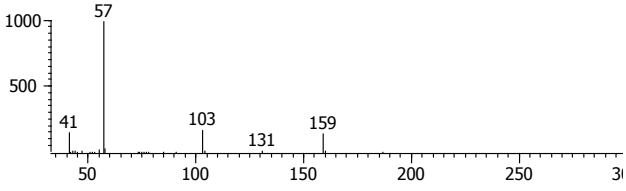

Peak	Name	$^{1}t_R$ (sec)	$^{2}t_R$ (sec)	Butylated Spectrum
67	Butyl derivative No identified functional groups	1763.9	1.47	Peak True - sample "BuOH SOA 26-3:1", peak 121, at 1763.86 , 1.465 sec , sec 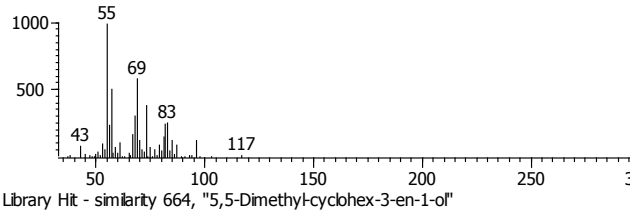 Library Hit - similarity 664, "5,5-Dimethyl-cyclohex-3-en-1-ol" 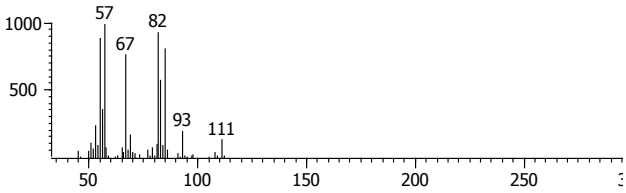
68	Butyl derivative Aldehyde, ketone	1771.9	1.39	Peak True - sample "Diluted BuOH SOA 23-3:1", peak 69, at 1771.86 , 1.406 sec , sec 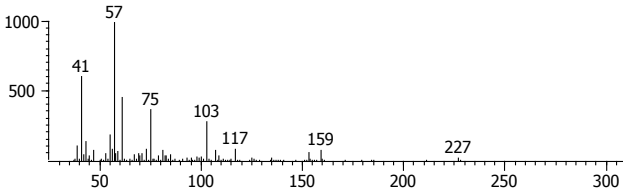 Library Hit - similarity 634, "6-Ethyl-3-di(tert-butyl)silyloxyoctane" 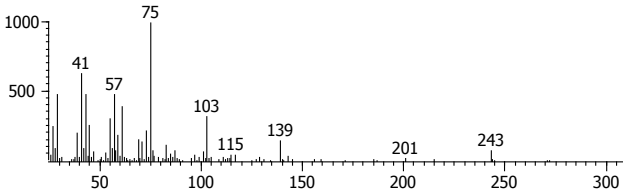
69	Eicosane-*d42*	1779.9	1.18	
70	Butyl derivative Ketone	1779.9	1.37	Peak True - sample "BuOH SOA 26-3:1", peak 125, at 1779.86 , 1.360 sec , sec 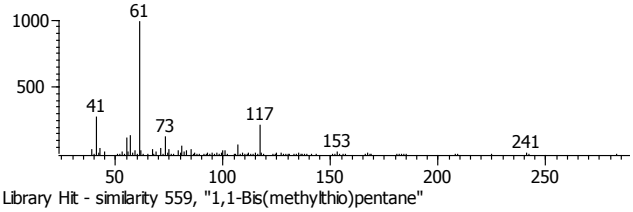 Library Hit - similarity 559, "1,1-Bis(methylthio)pentane" 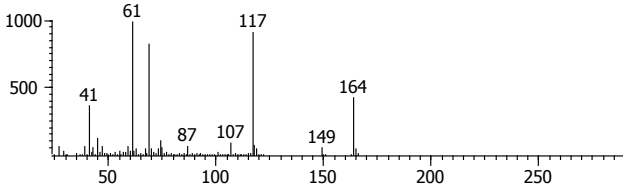

Peak	Name	$^{1}t_R$ (sec)	$^{2}t_R$ (sec)	Butylated Spectrum
71	Butyl derivative	1827.9	1.29	Peak True - sample "*BuOH SOA 26-3:1", peak 70, at 1827.86 , 1.287 sec , se 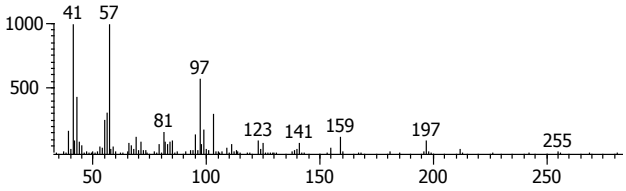 Library Hit - similarity 662, "2-Methyl-Z-4-tetradecene" 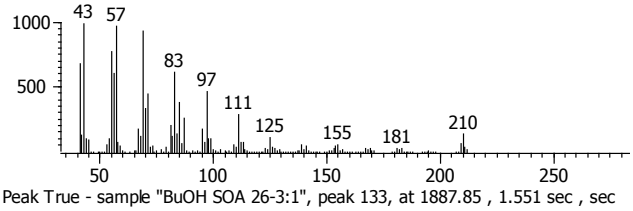
72	Butyl derivative Carboxylic acid	1887.9	1.55	Peak True - sample "BuOH SOA 26-3:1", peak 133, at 1887.85 , 1.551 sec , sec 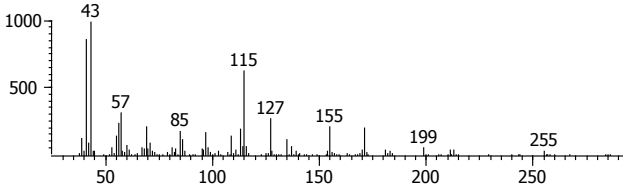 Library Hit - similarity 599, "5-Methyl(pentamethylene)silyloxytridecane" 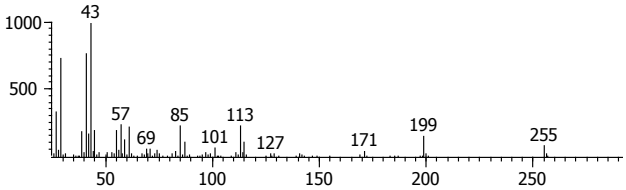
73	Pyrene-*d10*	1947.9	2.40	
74	Pinonaldehyde, dibutyl acetal Deriv. M.W. 298 Un. M.W. 168 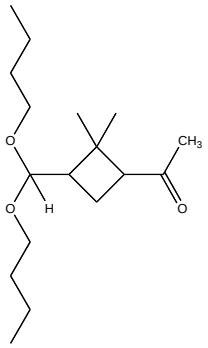 	1963.8	1.35	Peak True - sample "BuOH SOA 26-3:1", peak 137, at 1963.84 , 1.346 sec , sec 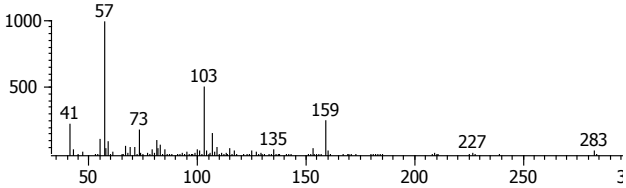 Library Hit - similarity 573, "2-Propanone, 1,1,3,3-tetrabutoxy-" 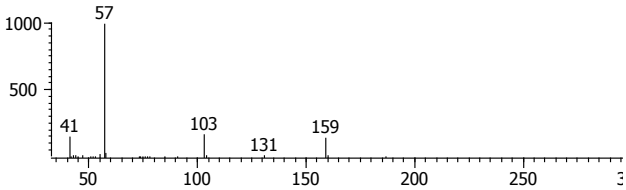

Peak	Name	$^{1}t_R$ (sec)	$^{2}t_R$ (sec)	Butylated Spectrum
75	Pinonaldehyde, dibutyl acetal (2)			Peak True - sample "BuOH SOA 26-3:1", peak 138, at 1963.84 , 1.366 sec , sec 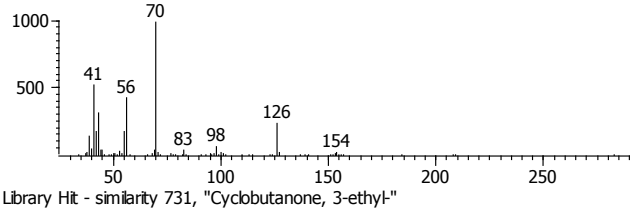 Library Hit - similarity 731, "Cyclobutanone, 3-ethyl-" 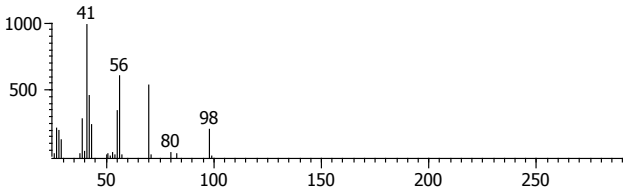
76	Butyl derivative Ketone	2139.9	1.39	Peak True - sample "BuOH Diluted SOA 23-3:1", peak 108, at 2139.83 , 1.386 sec 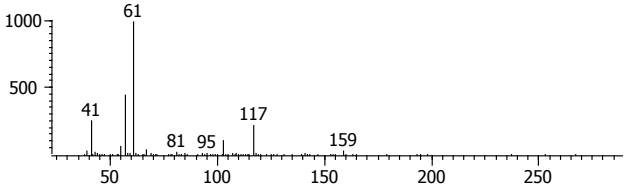 Library Hit - similarity 667, "Ethanethiol, 2-(diethylboryloxy)-" 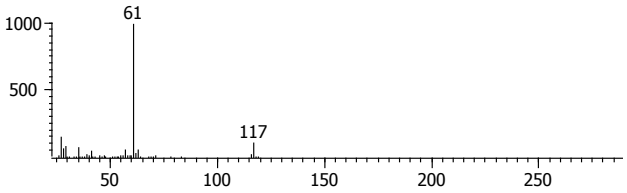

Table DD. Trimethylsilylated α-pinene ozonolysis product mass spectra from GCxGC TOF-MS analysis. Identifications are tentatively made by comparison to available spectra of previously identified products as well as predictions of fragments in previously identified products. One authentic standards of an identified compound was available: *cis*-pinonic acid. Ketopinic acid and succinic-d_4 acids are standard compounds added to each filter in order to show that extraction occurred sufficiently. Naphthalene-d_8, phenanthrene-d_{10}, and pyrene-d_{10} are internal standards used for quantification; eicosane-d_{42} was used to adjust for extraction efficiencies from the samples below 80%. Compounds with characteristic ions sufficient to allow tentative functional group identifications are marked as such; some mass spectra did not contain sufficiently characteristic ions for any identification. Only some molecular ions were present; for those that are obvious, the value of the molecular weight is listed ("Deriv. M.W." is the derivatized molecular weight; "Un. M.W." is the underivatized molecular weight of each compound).

Peak	Name	^1t_R (sec)	^2t_R (sec)	Trimethylsilylated Spectrum
1	Unknown oxidation product M.W. 128 $C_7H_{12}O_2$ e.g. 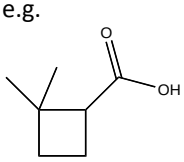	848.0	1.76	Peak True - sample "*TMS SOA 26-3:1", peak 1, at 847.964 , 1.762 sec , sec 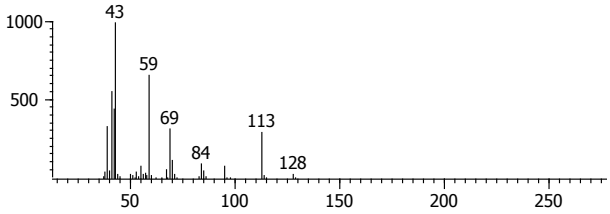 Library Hit - similarity 722, "Furan, tetrahydro-2,2,5,5-tetramethyl-" 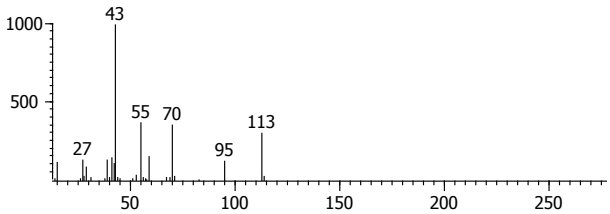
2	Unknown oxidation product Carboxylic acid	992.0	1.62	Peak True - sample "*TMS SOA 26-3:1", peak 2, at 991.949 , 1.624 sec , sec 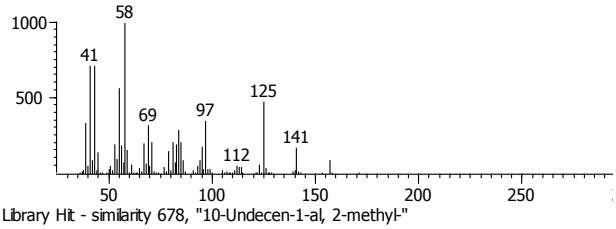 Library Hit - similarity 678, "10-Undecen-1-al, 2-methyl-" 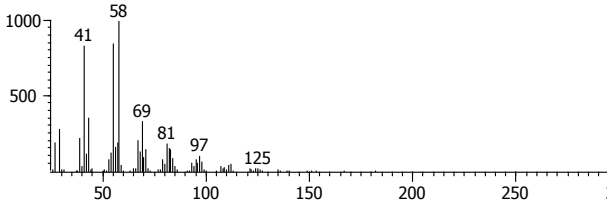

Peak	Name	$^{1}t_R$ (sec)	$^{2}t_R$ (sec)	Trimethylsilylated Spectrum
3	Norpinonaldehyde, underivatized M.W. 154 Aldehyde 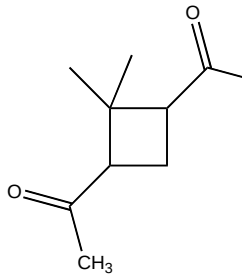	1008.0	1.93	Peak True - sample "*TMS SOA 26-3:1", peak 3, at 1007.95 , 1.927 sec , sec 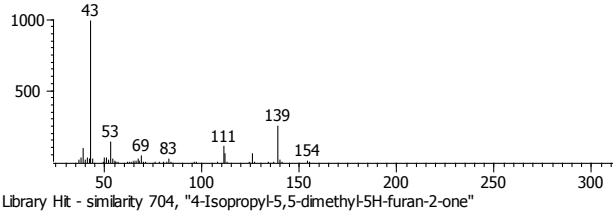 Library Hit - similarity 704, "4-Isopropyl-5,5-dimethyl-5H-furan-2-one" 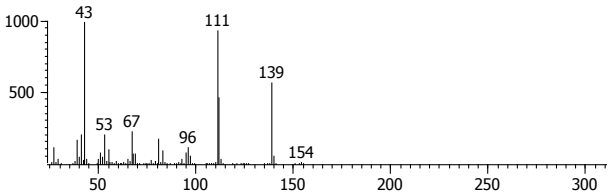
4	*Naphthalene-d8	1016.0	1.78	
5	Unknown oxidation product M.W. 140	1032.0	1.83	Peak True - sample "*TMS SOA 26-3:1", peak 6, at 1031.95 , 1.828 sec , sec 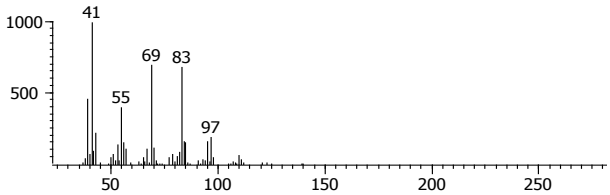 Library Hit - similarity 790, "Bicyclo[3.1.1]heptan-3-one, 2,6,6-trimethyl-, (1à,2á, 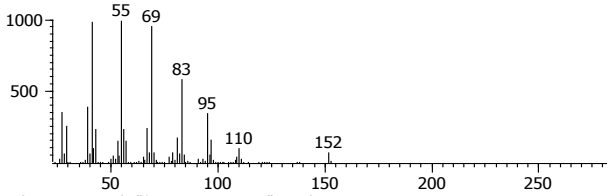
6	Unknown oxidation product	1080.0	1.48	Peak True - sample "*TMS SOA 26-3:1", peak 7, at 1079.94 , 1.478 sec , sec 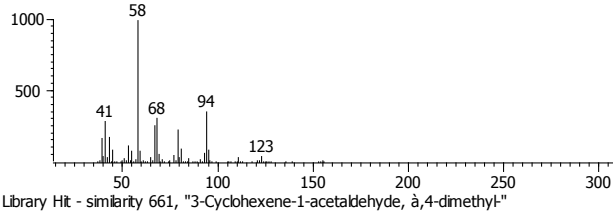 Library Hit - similarity 661, "3-Cyclohexene-1-acetaldehyde, à,4-dimethyl-" 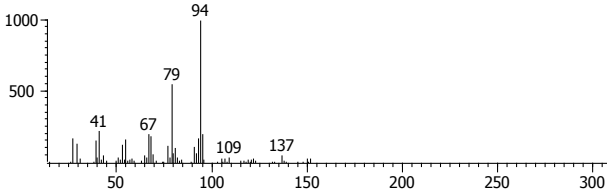

Peak	Name	$^{1}t_R$ (sec)	$^{2}t_R$ (sec)	Trimethylsilylated Spectrum
7	Pinonaldehyde, underivatized M.W. 168 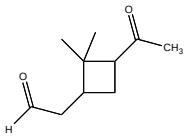	1127.94	1.841	Peak True - sample "*TMS SOA 26-3:1", peak 8, at 1127.94 , 1.841 sec , sec 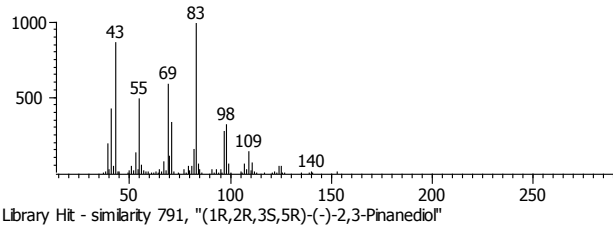 Library Hit - similarity 791, "(1R,2R,3S,5R)-(-)-2,3-Pinanediol" 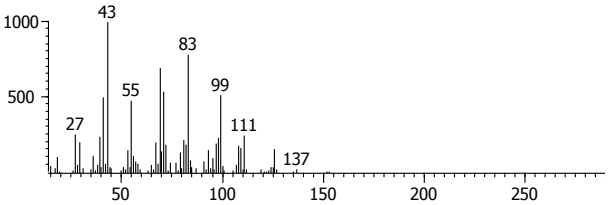
8	Unknown oxidation product M.W. 140	1127.94	2.277	Peak True - sample "*TMS SOA 26-3:1", peak 9, at 1127.94 , 2.277 sec , 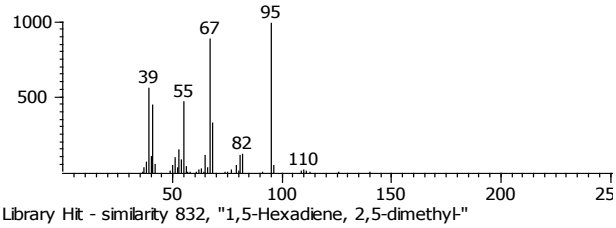 Library Hit - similarity 832, "1,5-Hexadiene, 2,5-dimethyl-" 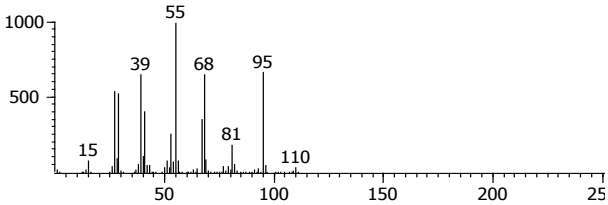
9	Pinalic-4- acid, underivatized M.W. 170 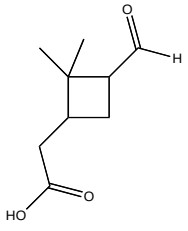	1147.93	1.723	Peak True - sample "*TMS SOA 26-3:1", peak 10, at 1147.93 , 1.723 sec , sec 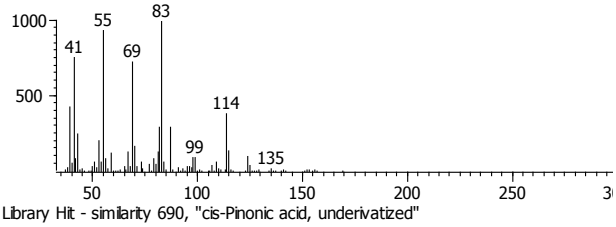 Library Hit - similarity 690, "cis-Pinonic acid, underivatized" 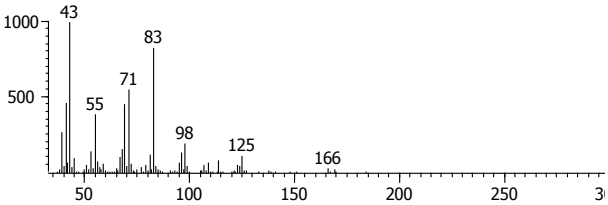

Peak	Name	$^{1}t_R$ (sec)	$^{2}t_R$ (sec)	Trimethylsilylated Spectrum
10	Unknown TMS derivative Deriv. M.W. 210 Un. M.W. 138	1151.93	1.604	Peak True - sample "*TMS SOA 26-3:1", peak 11, at 1151.93 , 1.604 sec , sec 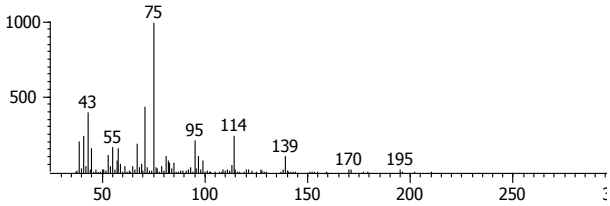 Library Hit - similarity 651, "Octanoic acid, 6,6-dimethoxy-, methyl ester" 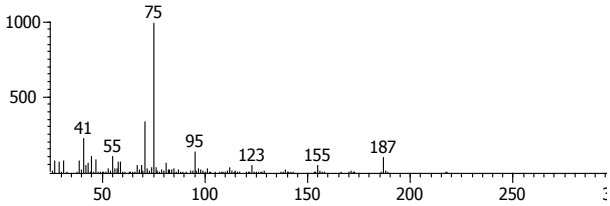
11	Unknown oxidation product M.W. 198 Methylene carboxylic acid	1155.93	2.145	Peak True - sample "*TMS SOA 26-3:1", peak 12, at 1155.93 , 2.145 sec , sec 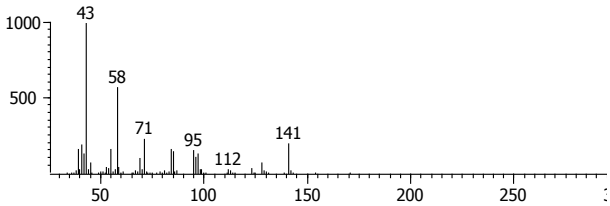 Library Hit - similarity 664, "2,11-Dodecanedione" 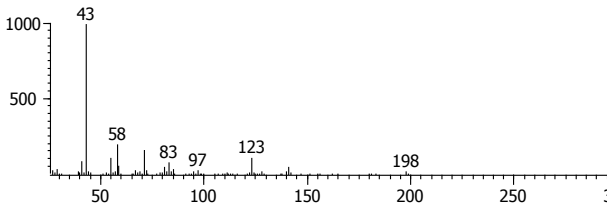
---	*Succinic-d4 acid, TMS	1167.93	1.274	
12	Unknown TMS derivative Deriv. M.W. 202 Un. M.W. 130 Carboxylic acid	1183.93	1.643	Peak True - sample "*TMS SOA 26-3:1", peak 14, at 1183.93 , 1.643 sec , sec 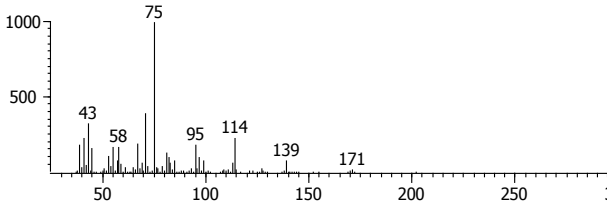 Library Hit - similarity 661, "Dodecane, 1,1-dimethoxy-" 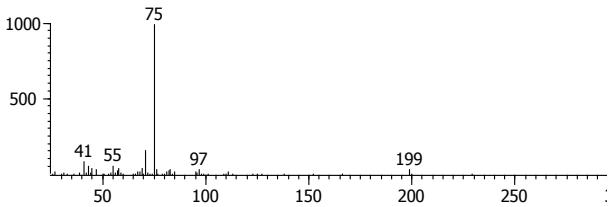

Peak	Name	$^{1}t_R$ (sec)	$^{2}t_R$ (sec)	Trimethylsilylated Spectrum
13	Unknown oxidation product No identified functional groups	1195.93	1.894	Peak True - sample "*TMS SOA 26-3:1", peak 15, at 1195.93 , 1.894 sec , sec 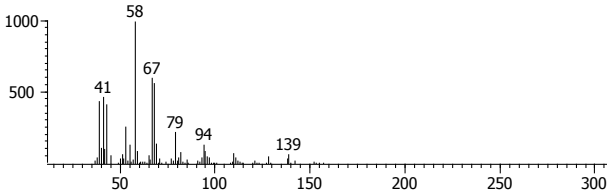 Library Hit - similarity 662, "Cyclohexanone, 2-[(dimethylamino)methyl]-" 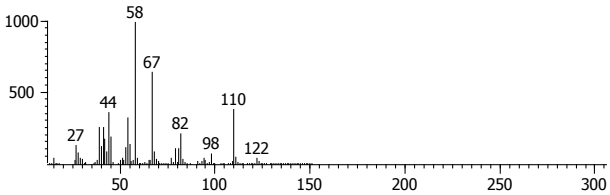
14	Unknown oxidation product Aldehyde	1199.93	1.577	Peak True - sample "*TMS SOA 26-3:1", peak 16, at 1199.93 , 1.577 sec , sec 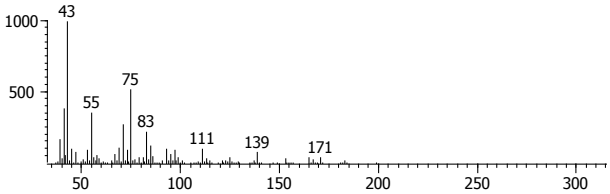 Library Hit - similarity 672, "Octan-2-one, 3,6-dimethyl-" 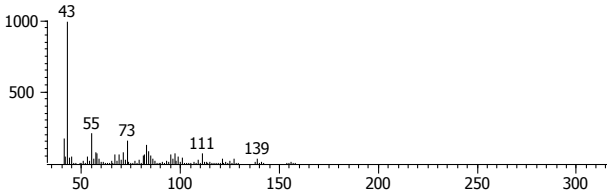
15	Unknown TMS derivative Carboxylic acid	1207.93	1.333	Peak True - sample "*TMS SOA 26-3:1", peak 17, at 1207.93 , 1.333 sec , sec 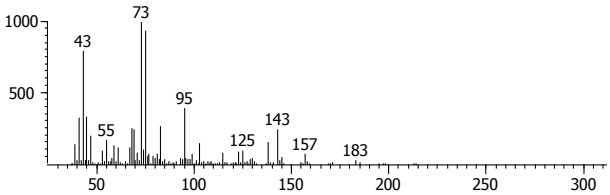 Library Hit - similarity 660, "Ether, 5,7-dimethyl-6-octyl-(trimethylsilyl)-" 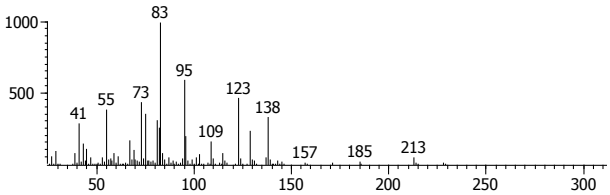

Peak	Name	$^{1}t_R$ (sec)	$^{2}t_R$ (sec)	Trimethylsilylated Spectrum
16	Unknown TMS derivative Alcohol or carboxylic acid	1215.93	1.465	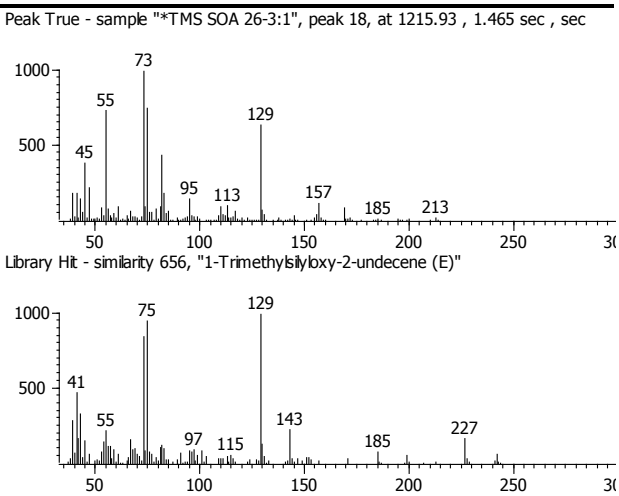
17	Norpinic acid, underivatized M.W. 186	1231.93	1.973	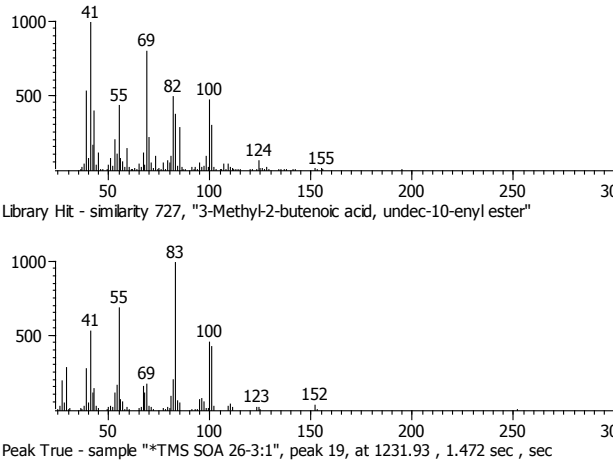
18	Unknown TMS derivative Carboxylic acid	1231.93	1.472	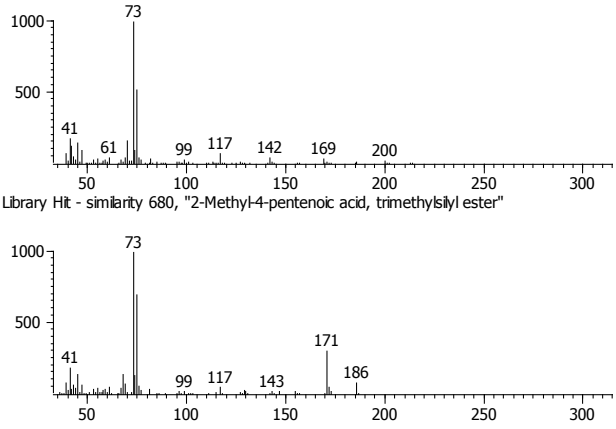

Peak	Name	$^{1}t_R$ (sec)	$^{2}t_R$ (sec)	Trimethylsilylated Spectrum
19	Unknown TMS derivative Deriv. M.W. 214 Un. M.W. Aldehyde, carboxylic acid, or ketone	1243.9	1.59	Peak True - sample "*TMS SOA 26-3:1", peak 21, at 1243.92 , 1.591 sec , sec 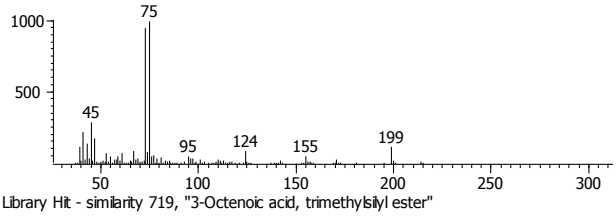 Library Hit - similarity 719, "3-Octenoic acid, trimethylsilyl ester" 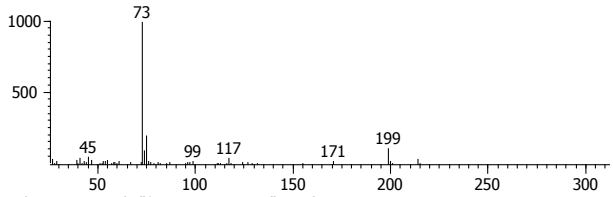
20	Pinonic acid, underivatized Un. M.W. 184 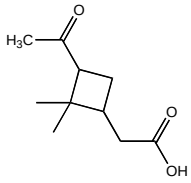	1331.9	1.89	Peak True - sample "*TMS SOA 26-3:1", peak 22, at 1331.92 , 1.888 sec , sec 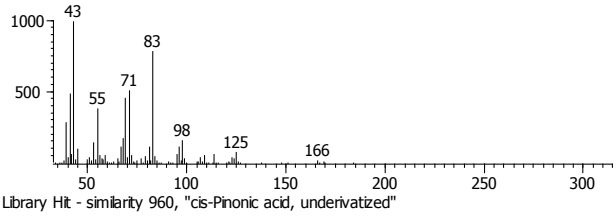 Library Hit - similarity 960, "cis-Pinonic acid, underivatized" 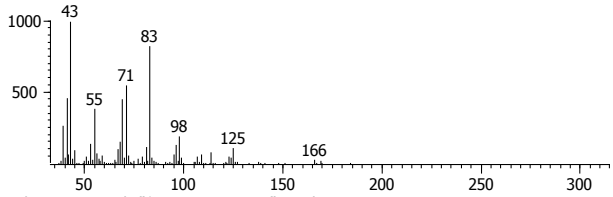
21	Unknown oxidation product Ring opening or di-acid with aldehyde	1339.9	2.07	Peak True - sample "*TMS SOA 26-3:1", peak 23, at 1339.91 , 2.072 sec , sec 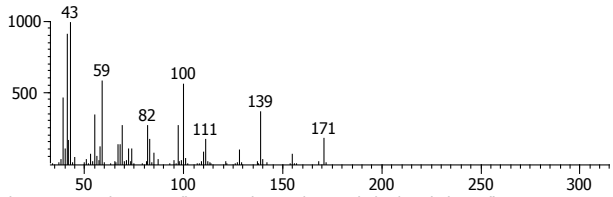 Library Hit - similarity 614, "Heptanedioic acid, 3-methyl-, dimethyl ester" 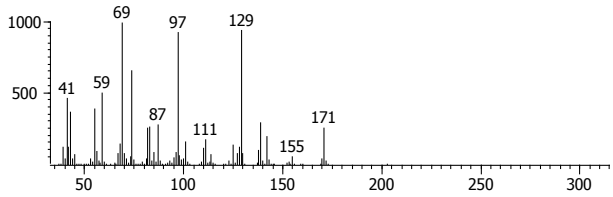

Peak	Name	$^{1}t_R$ (sec)	$^{2}t_R$ (sec)	Trimethylsilylated Spectrum
22	Unknown TMS derivative Carboxylic acid	1351.9	1.51	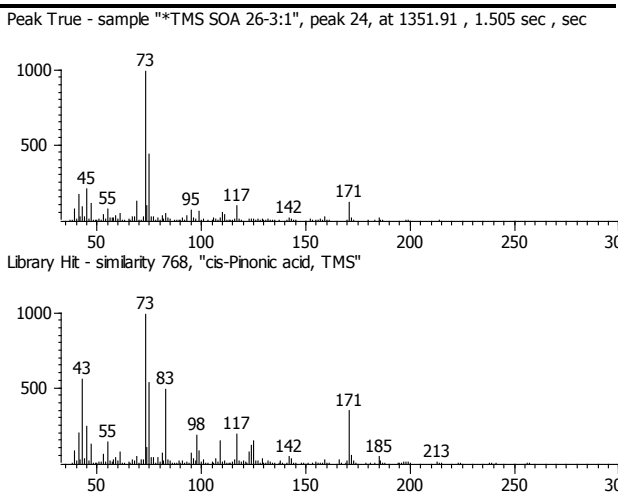
23	Standard: Ketopinic acid, underivatized	1379.9	2.21	
24	Standard: Ketopinic acid, trimethylsilyl ester	1419.9	1.70	
25	Pinic acid, underivatized M.W. 186 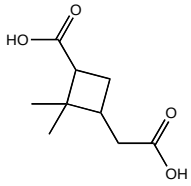	1423.91	2.026	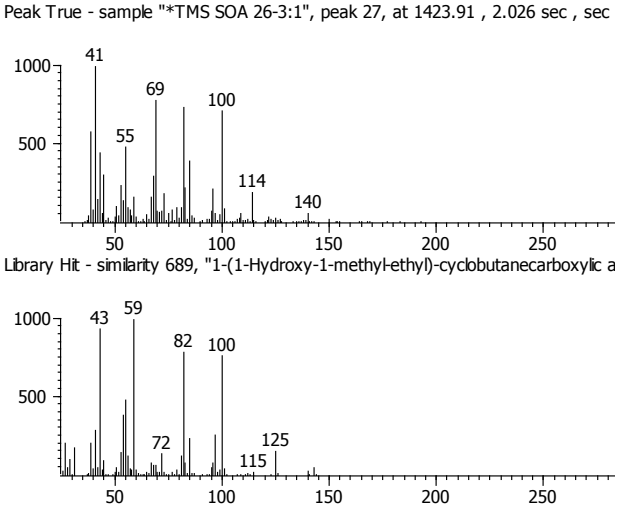

Peak	Name	$^{1}t_R$ (sec)	$^{2}t_R$ (sec)	Trimethylsilylated Spectrum
26	Unknown TMS derivative Carboxylic acid	1427.9	1.41	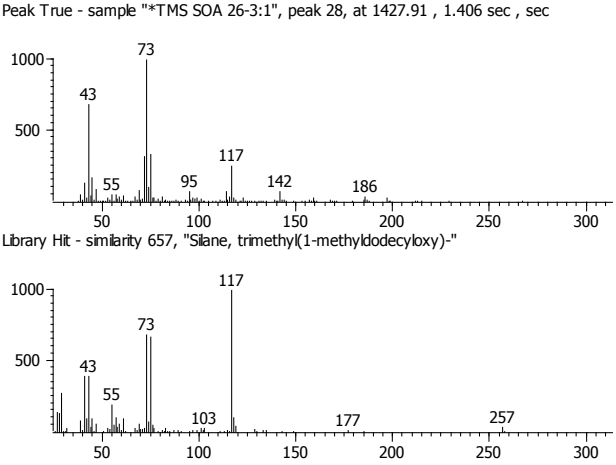
27	Pinonic acid, TMS derivative Deriv. M.W. 256 Un. M.W. 184 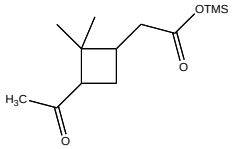	1439.9	1.53	
28	Unknown oxidation product M.W. 154 Aldehyde	1439.9	2.33	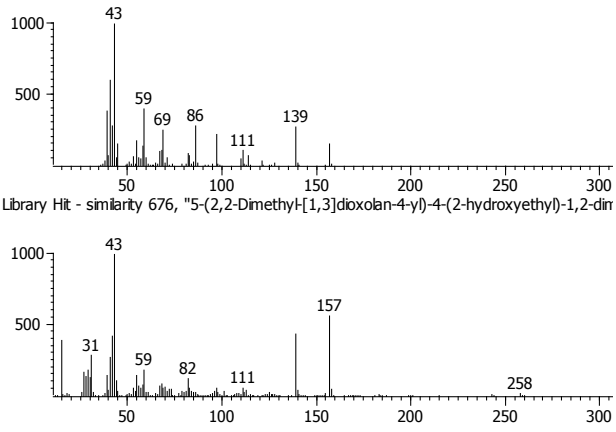

Peak	Name	$^{1}t_R$ (sec)	$^{2}t_R$ (sec)	Trimethylsilylated Spectrum
30	Unknown TMS derivative Deriv. M.W. 318 Un. M.W. 174 Carboxylic acid	1459.9	1.27	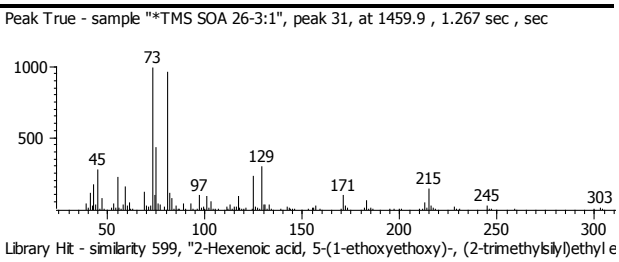
31	Unknown oxidation product Alcohol, carboxylic acid, or ketone	1471.9	2.05	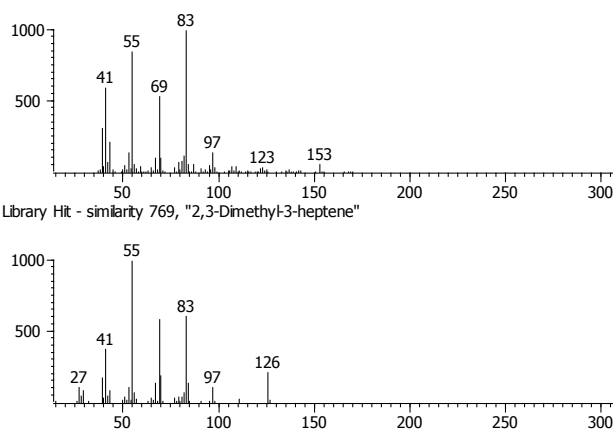
32	Norpinic acid, TMS ester Deriv. M.W. 316 Un. M.W. 172	1507.9	1.79	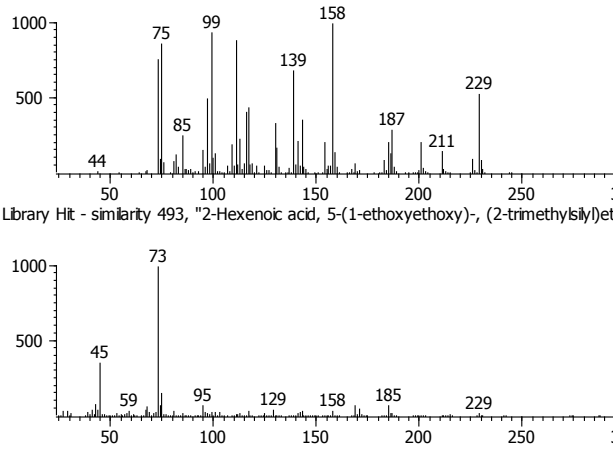

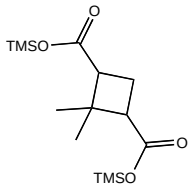

Peak	Name	$^{1}t_R$ (sec)	$^{2}t_R$ (sec)	Trimethylsilylated Spectrum
33	Oxo-Pinonic acid, TMS ester M.W. 198 e.g. 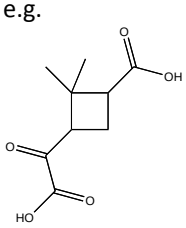	1527.9	2.34	Peak True - sample "*TMS SOA 26-3:1", peak 34, at 1527.9 , 2.343 sec , sec 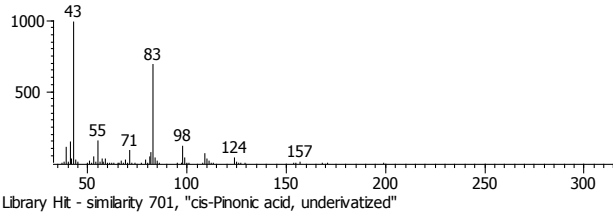 Library Hit - similarity 701, "cis-Pinonic acid, underivatized" 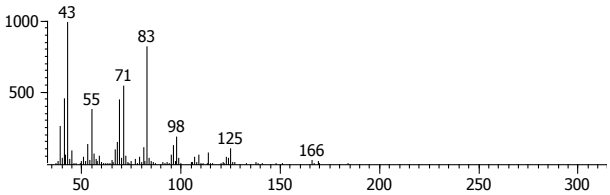
34	Hydroxy pinonaldehyde, TMS Deriv. M.W. 256 Un. M.W. 184 e.g. 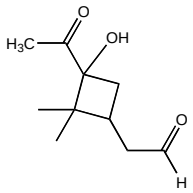	1535.9	1.60	Peak True - sample "*TMS SOA 26-3:1", peak 35, at 1535.89 , 1.604 sec , sec 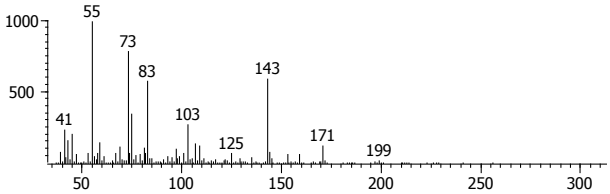 Library Hit - similarity 655, "cis-Pinonic acid, TMS" 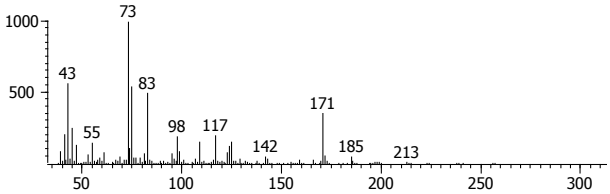
35	Pinic acid, TMS di-ester Deriv. M.W. 330 Un. M.W. 186 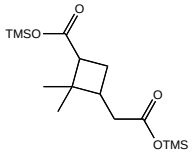	1603.9	1.44	Peak True - sample "*TMS SOA 26-3:1", peak 35, at 1535.89 , 1.604 sec , sec 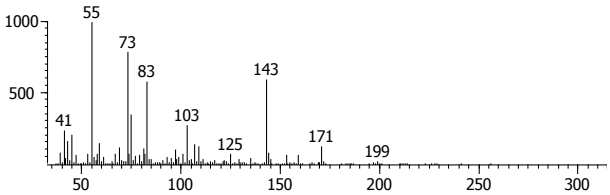 Library Hit - similarity 655, "cis-Pinonic acid, TMS" 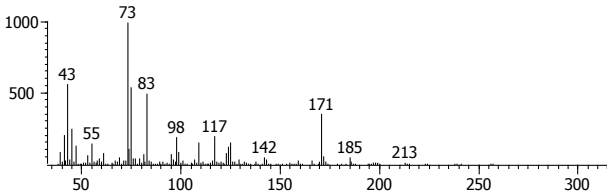

Peak	Name	^1t_R (sec)	^2t_R (sec)	Trimethylsilylated Spectrum
36	Unknown TMS derivative Carboxylic acid	1703.9	1.80	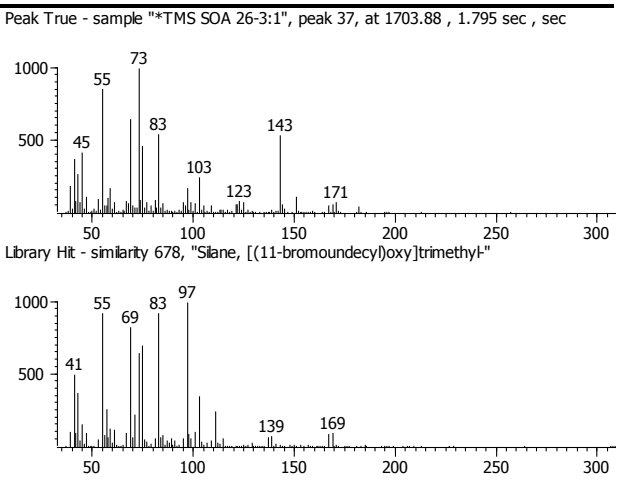
37	Unknown TMS derivative Carboxylic acid	1711.9	1.58	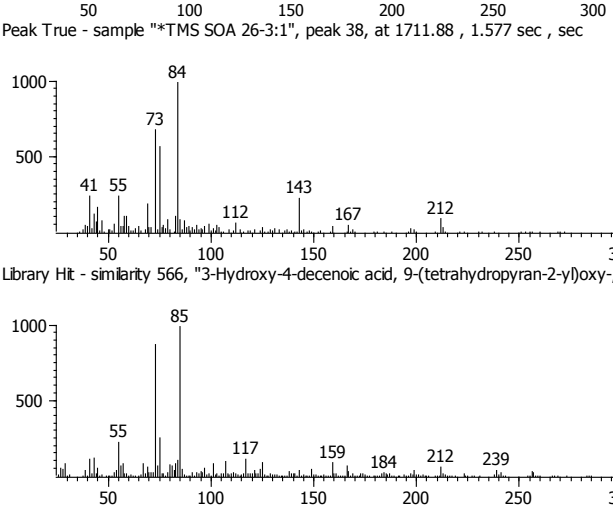
38	Standard: Phenanthrene-d_{10}	1739.9	2.65	
39	Standard: Eicosane-d_{42}	1895.9	1.21	
40	Standard: Pyrene-d_{10}	2035.8	2.32	

Table EE. Mass spectra of underivatized α-pinene ozonolysis products collected on a GCxGC TOF-MS. Each spectrum is tabulated according to retention times (primary in seconds, ^1t_R, and secondary in minutes, ^2t_R). The peak area of each component is also given to show the relative amount of each component in the sample (assuming similar sensitivities of the method to each component). All tentative identifications were made based on comparison to any available library and published spectra, as well as the predicted fragmentation pathways of previously identified α-pinene oxidation products.

Peak	Name	^1t_R (sec)	^2t_R (sec)	Underivatized Spectrum

Peak	Name	$^{1}t_R$ (sec)	$^{2}t_R$ (sec)	Underivatized Spectrum
1	Tentative Identification: None Underivatized Molecular weight: Unidentified Probable functional groups: Unidentified	836.0	1.43	Peak True - sample "Underiva SOA 23-3:1", peak 1, at 835.965 , 1.426 sec , sec 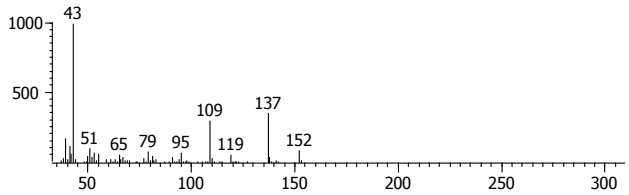 Library Hit - similarity 722, "Ethanone, 1-(1,4-dimethyl-3-cyclohexen-1-yl)-" 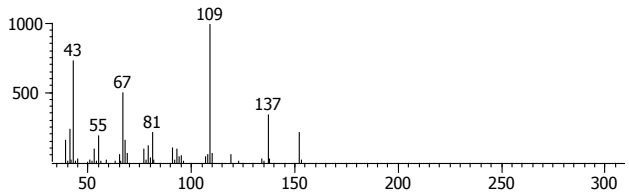
2	Tentative Identification: None Underivatized Molecular weight: Unidentified Probable functional groups: Unidentified	840.0	1.68	Peak True - sample "Underiva SOA 23-3:1", peak 2, at 839.964 , 1.676 sec , sec 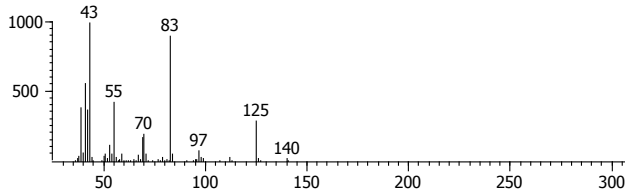 Library Hit - similarity 715, "2-Propanamine, N,N'-1,2-ethanediylidenebis-" 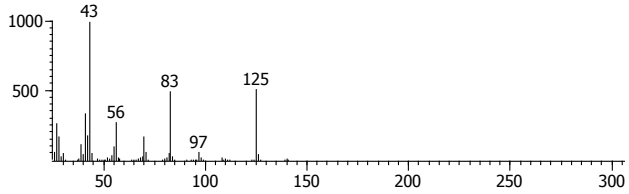
3	Tentative Identification: None Underivatized Molecular weight: Unidentified Probable functional groups: Unidentified	848.0	1.79	Peak True - sample "Underiva SOA 23-3:1", peak 3, at 847.964 , 1.789 sec , sec 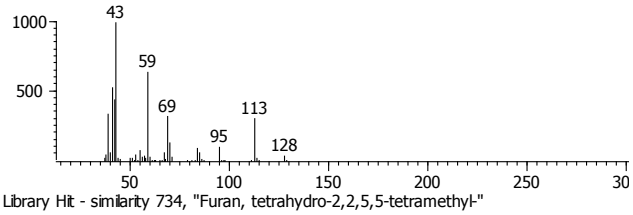 Library Hit - similarity 734, "Furan, tetrahydro-2,2,5,5-tetramethyl-" 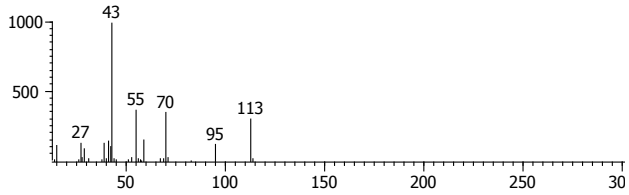

Peak	Name	$^{1}t_R$ (sec)	$^{2}t_R$ (sec)	Underivatized Spectrum
4	Tentative Identification: None Underivatized molecular weight: Unidentified Probable functional groups: Unidentified	860.0	1.42	Peak True - sample "Underiva SOA 23-3:1", peak 4, at 859.962 , 1.419 sec , sec 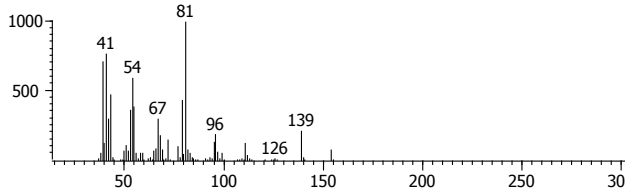 Library Hit - similarity 769, "2-Heptyne" 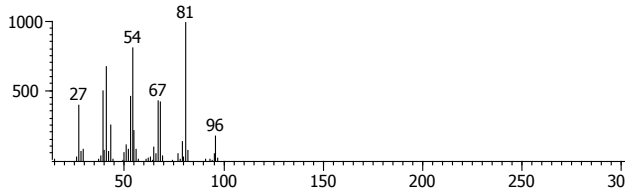
5	Tentative Identification: None Underivatized molecular weight: Unidentified Probable functional groups: Unidentified	884.0	1.43	Peak True - sample "Underiva SOA 23-3:1", peak 5, at 883.96 , 1.432 sec , sec 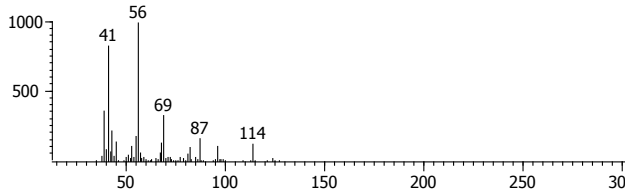 Library Hit - similarity 716, "Propane, 2-cyclopropyl-" 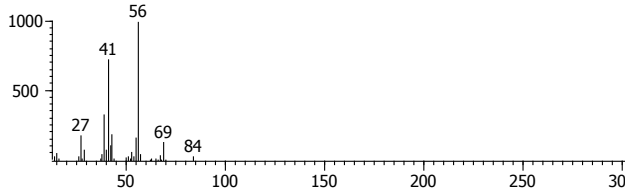
6	Tentative Identification: None Underivatized molecular weight: Unidentified Probable functional groups: Unidentified	888.0	1.42	Peak True - sample "Underiva SOA 23-3:1", peak 6, at 887.96 , 1.419 sec , sec 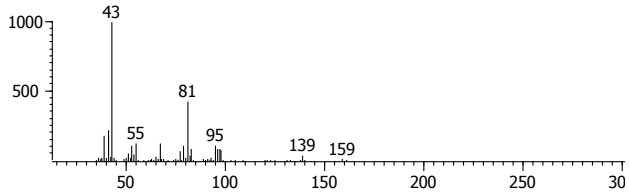 Library Hit - similarity 714, "1-Tetradecyne" 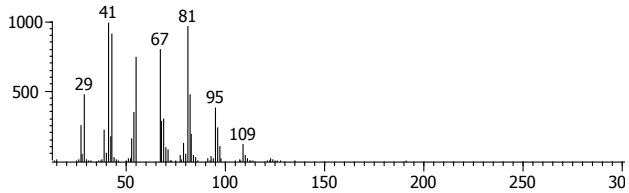

Peak	Name	$^{1}t_R$ (sec)	$^{2}t_R$ (sec)	Underivatized Spectrum
7	Tentative Identification: None Underivatized molecular weight: Unidentified Probable functional groups: Unidentified	904.0	1.48	Peak True - sample "Underiva SOA 23-3:1", peak 7, at 903.958 , 1.478 sec , sec 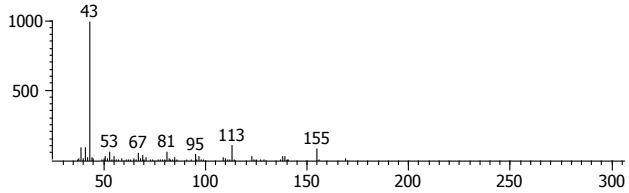 Library Hit - similarity 628, "1,6-Octadien-4-ol, 4,7-dimethyl-" 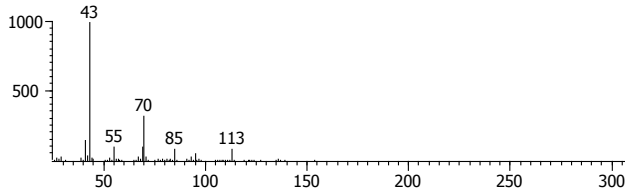
8	Tentative Identification: None Underivatized molecular weight: Unidentified Probable functional groups: Unidentified	928.0	1.53	Peak True - sample "Underiva SOA 23-3:1", peak 8, at 927.956 , 1.525 sec , sec 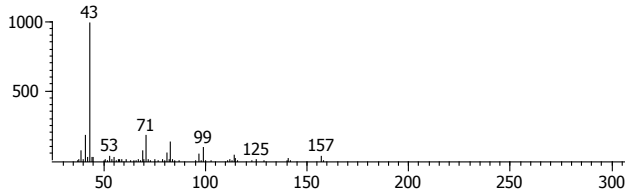 Library Hit - similarity 667, "4-Hexen-3-ol, 2-methyl-" 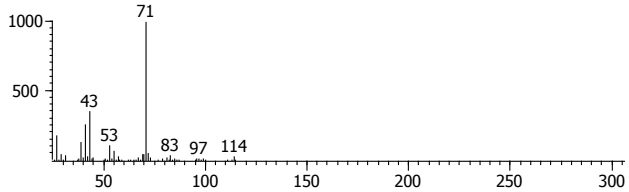
9	Tentative Identification: None Underivatized molecular weight: Unidentified Probable functional groups: Unidentified	936.0	1.60	Peak True - sample "Underiva SOA 23-3:1", peak 9, at 935.955 , 1.604 sec , sec 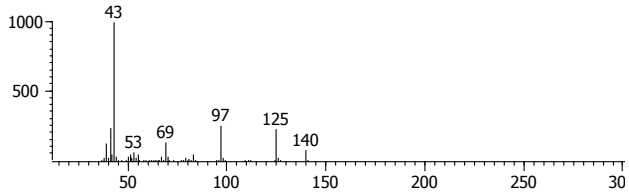 Library Hit - similarity 747, "3-Methylene-2,6-heptanedione" 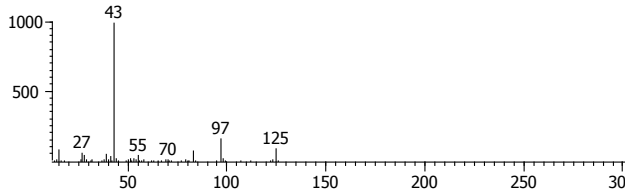

Peak	Name	$^{1}t_R$ (sec)	$^{2}t_R$ (sec)	Underivatized Spectrum
10	Tentative Identification: None Underivatized molecular weight: Unidentified Probable functional groups: Unidentified	968.0	1.58	Peak True - sample "Underiva SOA 23-3:1", peak 10, at 967.952 , 1.577 sec , sec 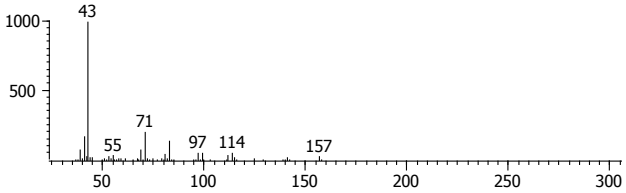 Library Hit - similarity 664, "1,5-Dimethyl-6-oxa-bicyclo[3.1.0]hexane" 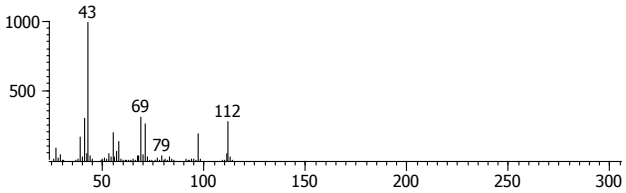
11	Tentative Identification: None Underivatized molecular weight: Unidentified Probable functional groups: Unidentified	992.0	1.63	Peak True - sample "Underiva SOA 23-3:1", peak 11, at 991.949 , 1.630 sec , sec 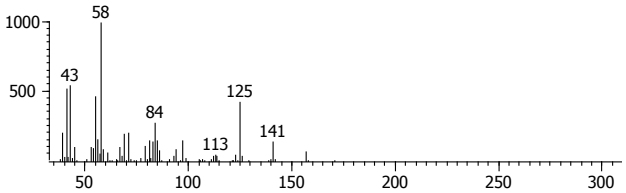 Library Hit - similarity 621, "3-Nonen-2-one" 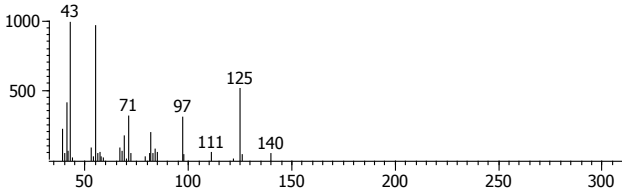
12	Tentative Identification: None Underivatized molecular weight: Unidentified Probable functional groups: Unidentified	996.0	1.74	Peak True - sample "Underiva SOA 23-3:1", peak 12, at 995.949 , 1.736 sec , sec 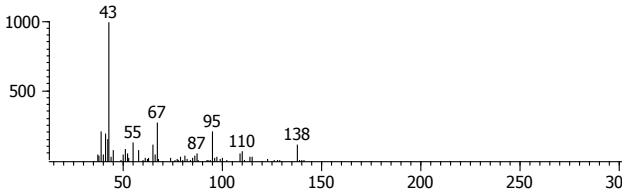 Library Hit - similarity 686, "5-Methyl-5-hexen-3-yn-2-ol" 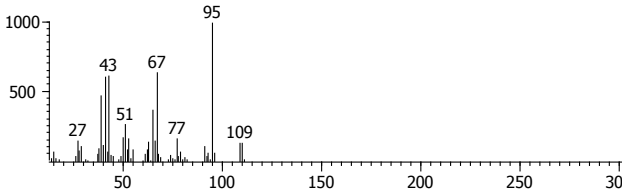

Peak	Name	$^{1}t_R$ (sec)	$^{2}t_R$ (sec)	Underivatized Spectrum
13	Tentative Identification: None Underivatized molecular weight: Unidentified Probable functional groups: Unidentified	1004.0	1.71	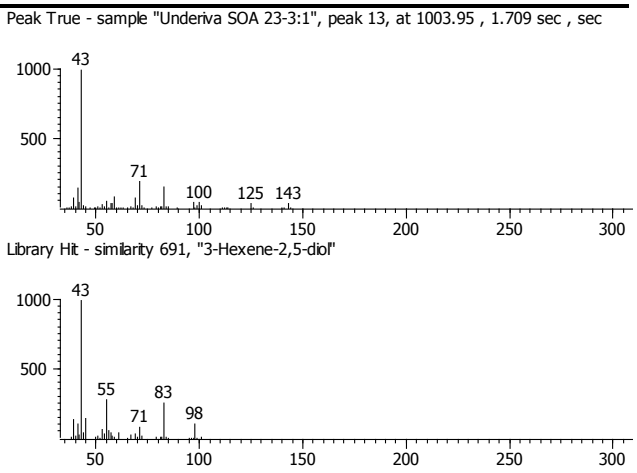
	Naphthalene-*d8*	1012.0	2.27	
14	Tentative Identification: None Underivatized molecular weight: Unidentified Probable functional groups: Aldehyde	1012.0	1.95	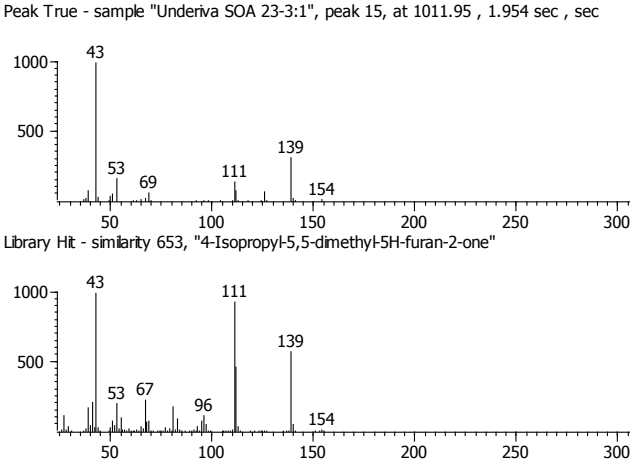
15	Tentative Identification: None Underivatized molecular weight: Unidentified Probable functional groups: Unidentified	1012.0	1.88	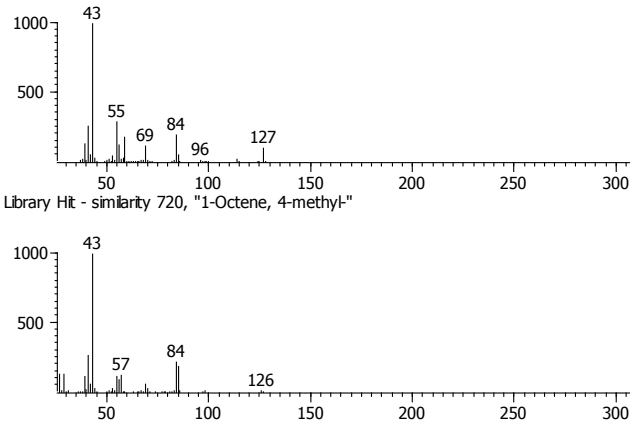

Peak	Name	$^{1}t_R$ (sec)	$^{2}t_R$ (sec)	Underivatized Spectrum
16	Tentative Identification: None Underivatized molecular weight: Unidentified Probable functional groups: Aldehyde, carboxylic acid, or ketone	1032.0	1.84	Peak True - sample "Underiva SOA 23-3:1", peak 18, at 1031.95 , 1.841 sec , sec 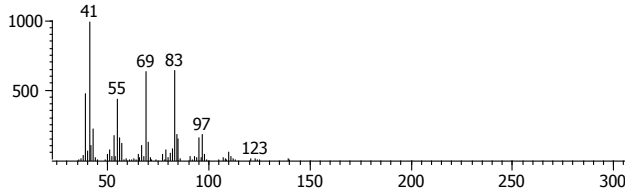 Library Hit - similarity 785, "Bicyclo[3.1.1]heptan-3-one, 2,6,6-trimethyl-, (1à,2á,5à)-" 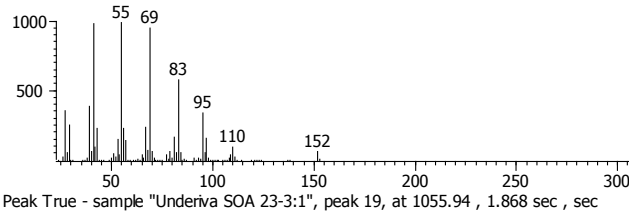
17	Tentative Identification: None Underivatized molecular weight: Unidentified Probable functional groups: Unidentified	1056.0	1.87	Peak True - sample "Underiva SOA 23-3:1", peak 19, at 1055.94 , 1.868 sec , sec 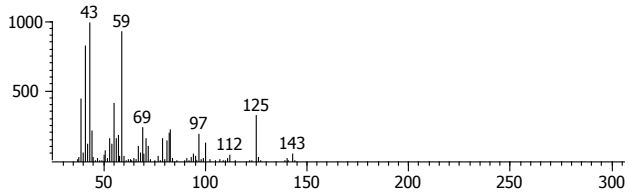 Library Hit - similarity 713, "1-(1-Hydroxy-1-methyl-ethyl)-cyclobutanecarboxylic acid" 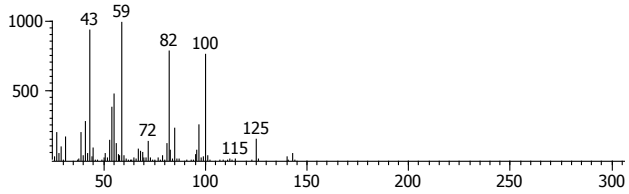
18	Tentative Identification: None Underivatized molecular weight: Unidentified Probable functional groups: Unidentified	1083.9	1.92	Peak True - sample "Underiva SOA 23-3:1", peak 20, at 1083.94 , 1.921 sec , sec 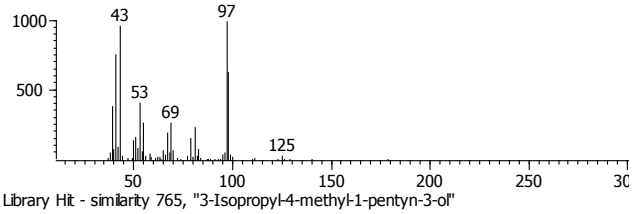 Library Hit - similarity 765, "3-Isopropyl-4-methyl-1-pentyn-3-ol" 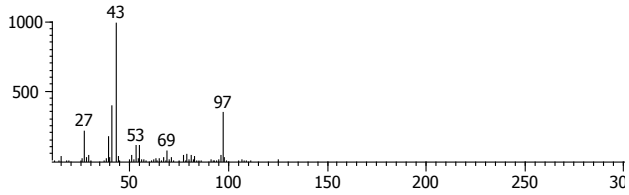

Peak	Name	$^{1}t_R$ (sec)	$^{2}t_R$ (sec)	Underivatized Spectrum
19	Tentative Identification: None Underivatized molecular weight: Unidentified Probable functional groups: Mono-acid	1099.9	1.80	Peak True - sample "Underiva SOA 23-3:1", peak 21, at 1099.94 , 1.802 sec , sec 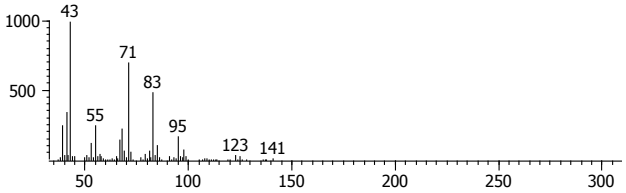 Library Hit - similarity 768, "cis-Pinonic acid, underivatized" 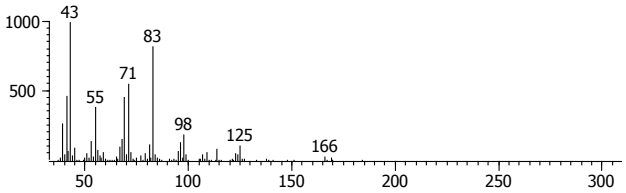
20	Tentative Identification: None Underivatized molecular weight: Unidentified Probable functional groups: Unidentified	1107.9	1.73	Peak True - sample "Underiva SOA 23-3:1", peak 22, at 1107.94 , 1.729 sec , sec 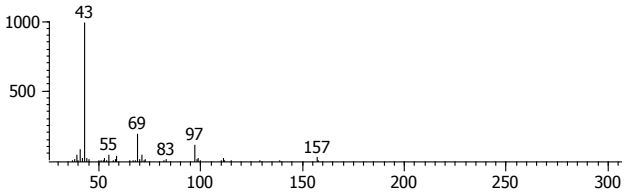 Library Hit - similarity 737, "5-Hexen-2-one, 5-methyl-" 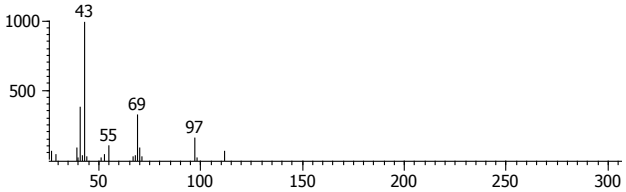
21	Tentative Identification: 2,2-dimethyl-3-formyl-cyclobutyl-methanoic acid Underivatized molecular weight: 156 Probable functional groups: Aldehyde, carboxylic acid	1107.9	2.07	Peak True - sample "Underiva SOA 23-3:1", peak 23, at 1107.94 , 2.072 sec , sec 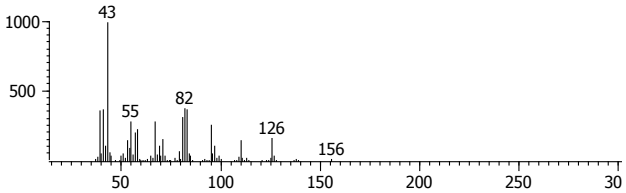 Library Hit - similarity 757, "Cyclohexanol, 2,4-dimethyl-" 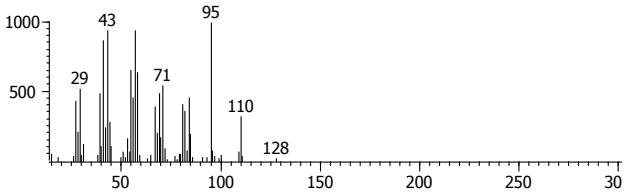

Peak	Name	$^{1}t_R$ (sec)	$^{2}t_R$ (sec)	Underivatized Spectrum
22	Tentative Identification: None Underivatized molecular weight: Unidentified Probable functional groups: Unidentified	1111.9	1.62	Peak True - sample "Underiva SOA 23-3:1", peak 24, at 1111.94 , 1.624 sec , sec 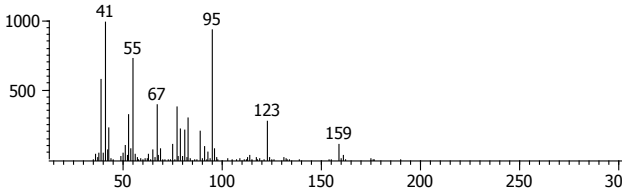 Library Hit - similarity 714, "Bicyclo[2.2.1]heptane-2,3-dione, 1,7,7-trimethyl-, (1R)-" 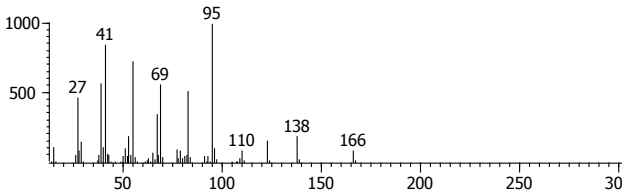
23	Tentative Identification: None Underivatized molecular weight: Unidentified Probable functional groups: Unidentified	1115.9	1.87	Peak True - sample "Underiva SOA 23-3:1", peak 25, at 1115.94 , 1.868 sec , sec 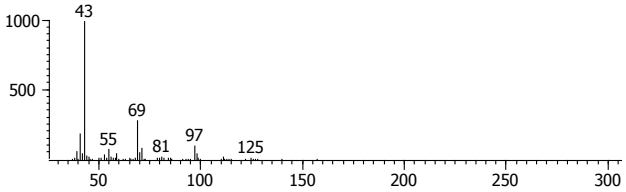 Library Hit - similarity 752, "5-Hexen-2-one, 5-methyl-" 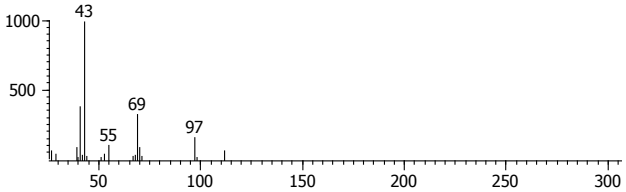
24	Tentative Identification: Pinalic-4-acid Underivatized molecular weight: 170 Probable functional groups:Aldehyde, carboxylic acid	1119.9	1.68	Peak True - sample "Underiva SOA 23-3:1", peak 26, at 1119.94 , 1.676 sec , sec 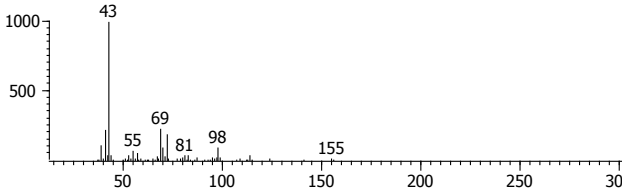 Library Hit - similarity 693, "2-Hexanone, 3,4-dimethyl-" 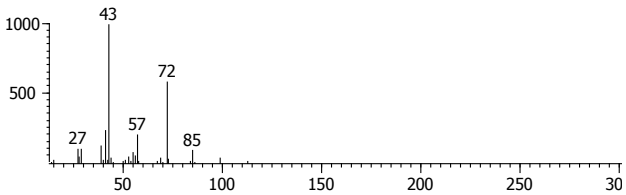

Peak	Name	$^{1}t_R$ (sec)	$^{2}t_R$ (sec)	Underivatized Spectrum
25	Tentative Identification: Pinonaldehyde Underivatized molecular weight: 168 Probable functional groups: Aldehyde, ketone	1127.9	2.31	Peak True - sample "Underiva SOA 23-3:1", peak 28, at 1127.94 , 1.894 sec , sec 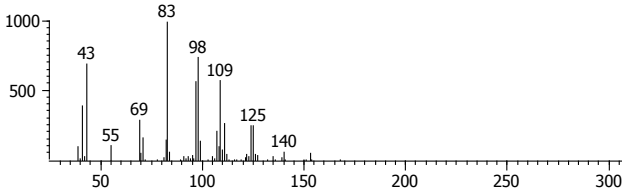 Library Hit - similarity 633, "8-Oxabicyclo[5.1.0]oct-5-en-2-ol, 1,4,4-trimethyl-" 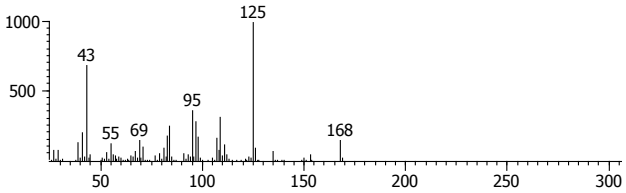
26	Tentative Identification: None Underivatized molecular weight: Unidentified Probable functional groups: Unidentified	1127.9	1.89	Peak True - sample "Underiva SOA 23-3:1", peak 29, at 1127.94 , 2.310 sec , sec 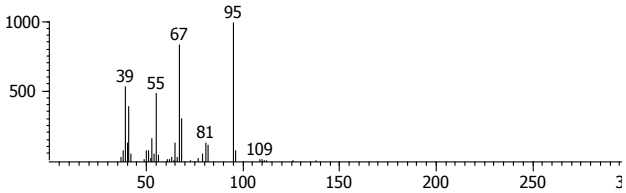 Library Hit - similarity 823, "1,5-Hexadiene, 2,5-dimethyl-" 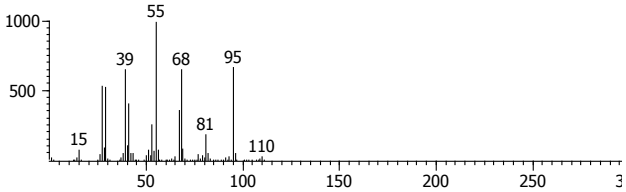
27	Tentative Identification: Pinic acid Underivatized molecular weight: Unidentified Probable functional groups: Carboxylic acid (2)	1131.9	1.90	Peak True - sample "Underiva SOA 23-3:1", peak 30, at 1131.94 , 1.901 sec , sec 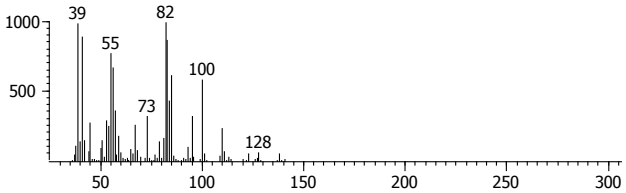 Library Hit - similarity 688, "3-Cyclobut-1-enyl-3-hydroxy-2-methyl-propionic acid" 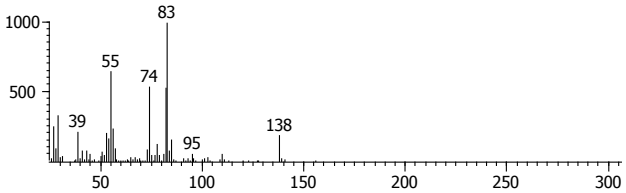

Peak	Name	$^{1}t_R$ (sec)	$^{2}t_R$ (sec)	Underivatized Spectrum
28	Tentative Identification: None Underivatized molecular weight: Unidentified Probable functional groups: Unidentified	1131.9	2.26	Peak True - sample "Underiva SOA 23-3:1", peak 31, at 1131.94 , 2.264 sec , sec 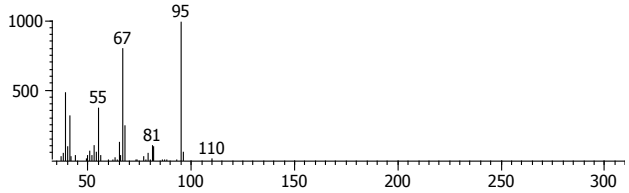 Library Hit - similarity 804, "Bicyclo[3.1.0]hexane, 1,5-dimethyl-" 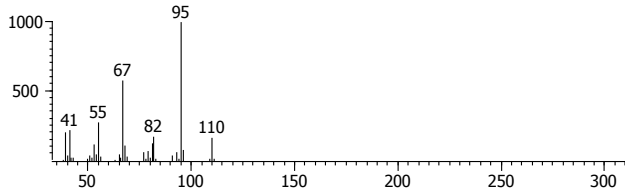
29	Tentative Identification: None Underivatized molecular weight: Unidentified Probable functional groups: Unidentified	1135.9	1.88	Peak True - sample "Underiva SOA 23-3:1", peak 32, at 1135.93 , 1.881 sec , sec 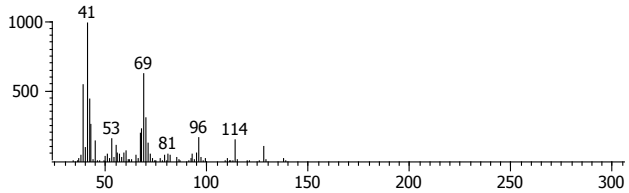 Library Hit - similarity 747, "1,2-Dimethylcyclopropanecarboxylic acid" 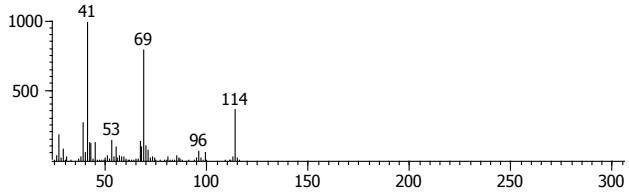
30	Tentative Identification: None Underivatized molecular weight: Unidentified Probable functional groups: Unidentified	1135.9	2.24	Peak True - sample "Underiva SOA 23-3:1", peak 33, at 1135.93 , 2.237 sec , sec 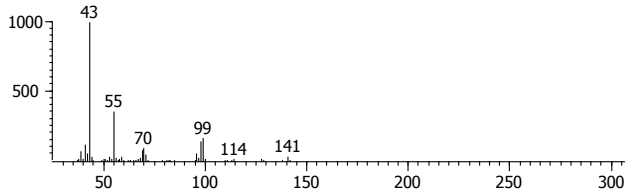 Library Hit - similarity 716, "3-Pentenoic acid, 4-methyl-" 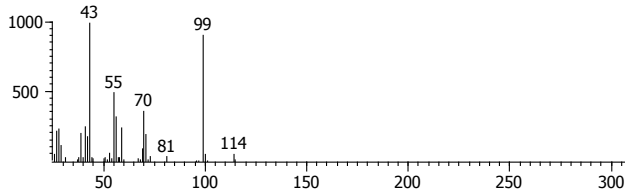

Peak	Name	$^{1}t_R$ (sec)	$^{2}t_R$ (sec)	Underivatized Spectrum
31	Tentative Identification: None Underivatized molecular weight: Unidentified Probable functional groups: Unidentified	1139.9	1.80	Peak True - sample "Underiva SOA 23-3:1", peak 34, at 1139.93 , 1.795 sec , sec 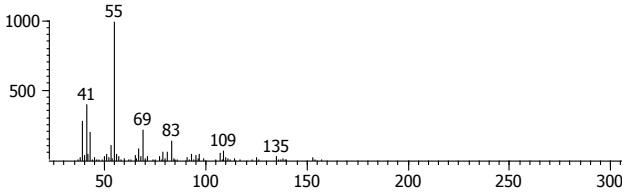 Library Hit - similarity 715, "Bicyclo[3.1.1]heptan-3-one, 2,6,6-trimethyl-, (1à,2á,5à)-" 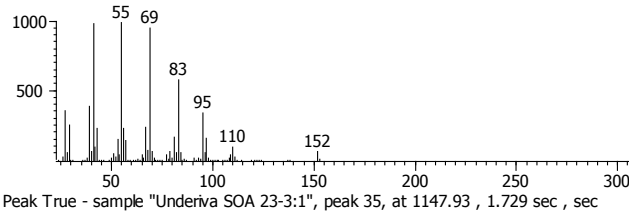
32	Tentative Identification: None Underivatized molecular weight: 168 Probable functional groups: Carboxylic acid	1147.9	1.73	Peak True - sample "Underiva SOA 23-3:1", peak 35, at 1147.93 , 1.729 sec , sec 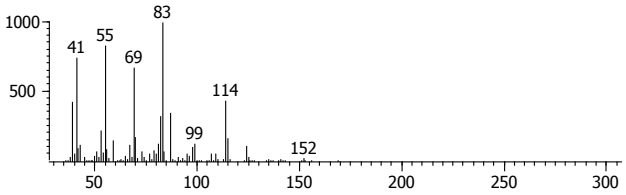 Library Hit - similarity 674, "Cyclopropaneacetic acid, 2-hexyl-" 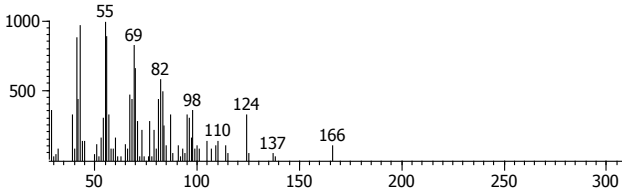
33	Tentative Identification: None Underivatized molecular weight: 154 Probable functional groups: Carboxylic acid (2)	1211.9	2.11	Peak True - sample "Underiva SOA 23-3:1", peak 38, at 1211.93 , 2.006 sec , sec 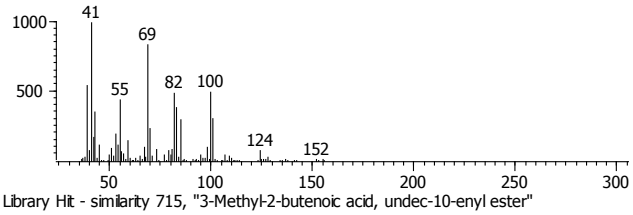 Library Hit - similarity 715, "3-Methyl-2-butenoic acid, undec-10-enyl ester" 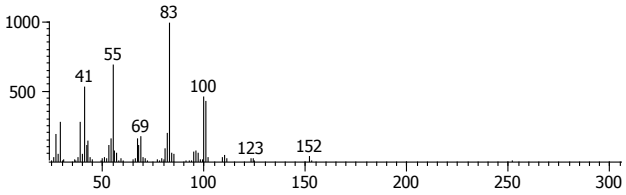

Peak	Name	$^{1}t_R$ (sec)	$^{2}t_R$ (sec)	Underivatized Spectrum
34	Tentative Identification: None Underivatized molecular weight: Unidentified Probable functional groups: Unidentified	1227.9	2.42	Peak True - sample "Underiva SOA 23-3:1", peak 41, at 1227.93 , 2.422 sec , sec 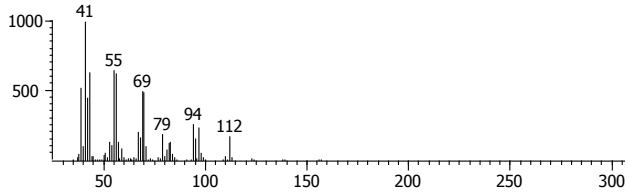 Library Hit - similarity 771, "2-Octene" 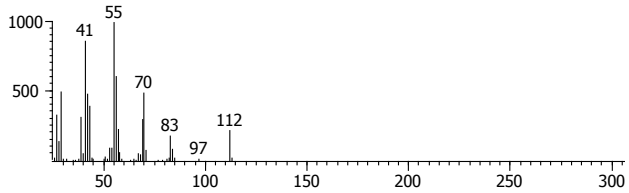
35	Tentative Identification: None Underivatized molecular weight: Unidentified Probable functional groups: Unidentified	1227.9	2.48	Peak True - sample "Underiva SOA 23-3:1", peak 42, at 1227.93 , 2.482 sec , sec 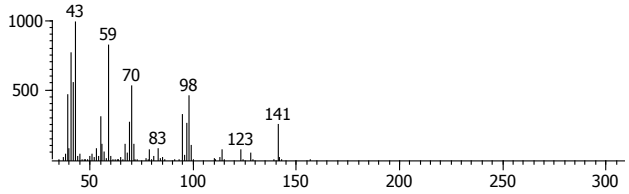 Library Hit - similarity 669, "7-Octen-2-ol, 2,6-dimethyl-" 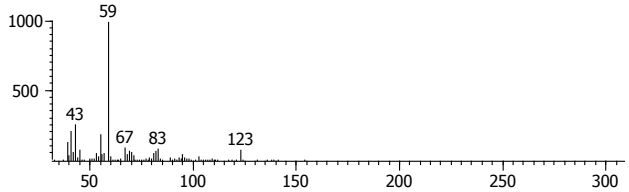
36	Tentative Identification: None Underivatized molecular weight: Unidentified Probable functional groups: Unidentified	1235.9	1.89	Peak True - sample "Underiva SOA 23-3:1", peak 43, at 1235.92 , 1.888 sec , sec 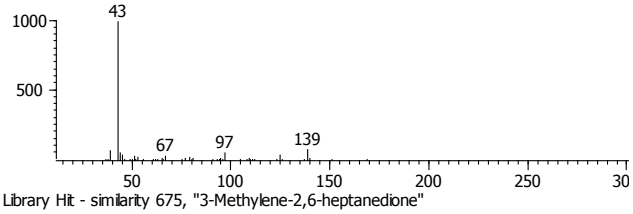 Library Hit - similarity 675, "3-Methylene-2,6-heptanedione" 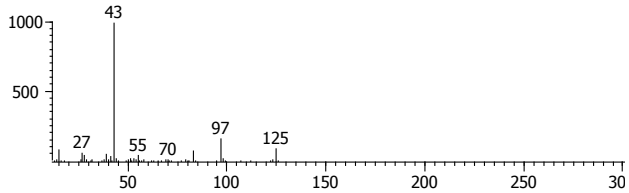

Peak	Name	$^{1}t_R$ (sec)	$^{2}t_R$ (sec)	Underivatized Spectrum
37	Tentative Identification: None Underivatized molecular weight: 154 Probable functional groups: Carboxylic acid (2)	1247.9	2.12	Peak True - sample "Underiva SOA 23-3:1", peak 44, at 1247.92 , 2.119 sec , sec 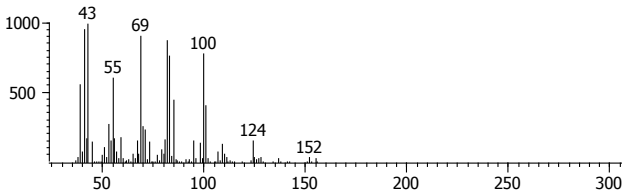 Library Hit - similarity 737, "3-Methyl-2-butenoic acid, hexadecyl ester" 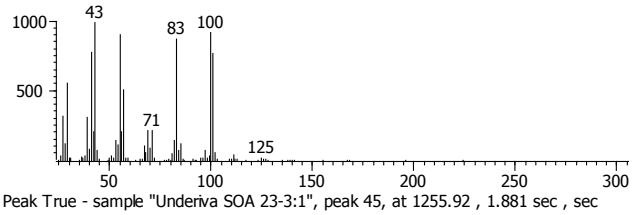
38	Tentative Identification: None Underivatized molecular weight: Unidentified Probable functional groups: Unidentified	1255.9	1.88	Peak True - sample "Underiva SOA 23-3:1", peak 45, at 1255.92 , 1.881 sec , sec 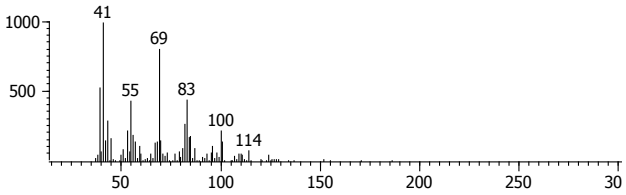 Library Hit - similarity 719, "Undecylenic Acid" 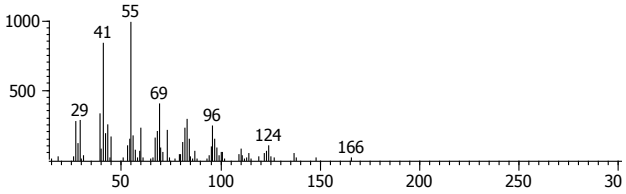
39	Tentative Identification: None Underivatized molecular weight: Unidentified Probable functional groups: Unidentified	1291.9	2.13	Peak True - sample "Underiva SOA 23-3:1", peak 46, at 1291.92 , 2.125 sec , sec 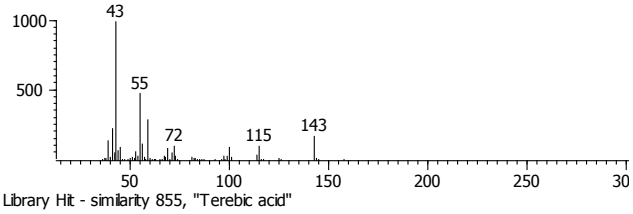 Library Hit - similarity 855, "Terebic acid" 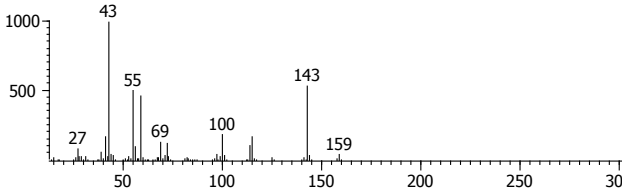

Peak	Name	$^{1}t_R$ (sec)	$^{2}t_R$ (sec)	Underivatized Spectrum
40	Tentative Identification: *cis*-Pinonic acid Molecular weight: 184 Underivatized molecular weight: 184 Probable functional groups: Carboxylic acid, ketone	1315.9	1.91	Peak True - sample "Underiva SOA 23-3:1", peak 47, at 1315.92 , 1.907 sec , sec 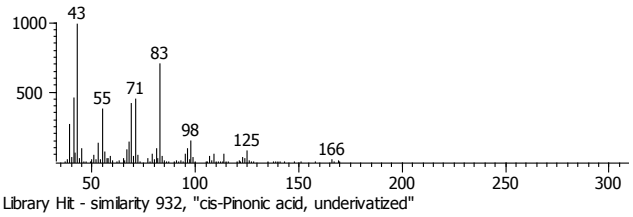 Library Hit - similarity 932, "cis-Pinonic acid, underivatized" 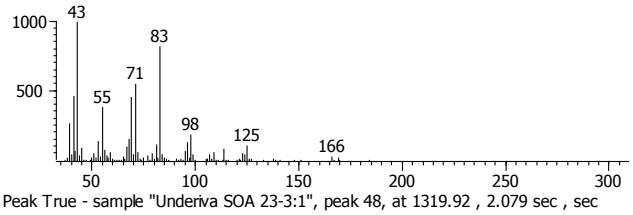
41	Tentative Identification: None Molecular weight: 170 Underivatized molecular weight: 170 Probable functional groups: Aldehyde	1319.9	2.08	Peak True - sample "Underiva SOA 23-3:1", peak 48, at 1319.92 , 2.079 sec , sec 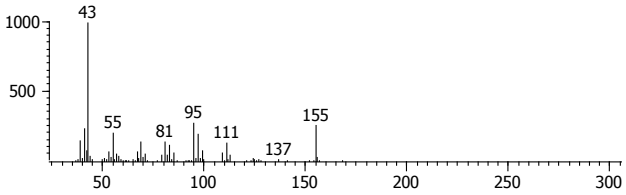 Library Hit - similarity 685, "4-Hexenoic acid, 2-acetyl-2-methyl-, ethyl ester, (E)-" 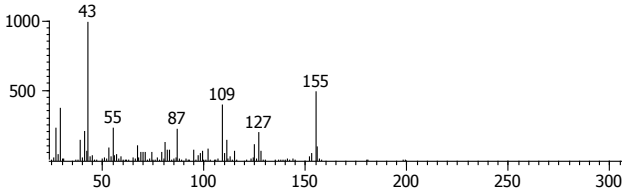
42	Tentative Identification: None Molecular weight: 140 Underivatized molecular weight: 140 Probable functional groups: Carboxylic acid	1327.9	1.74	Peak True - sample "Underiva SOA 23-3:1", peak 50, at 1327.92 , 1.736 sec , sec 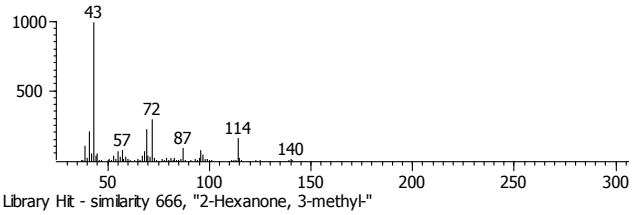 Library Hit - similarity 666, "2-Hexanone, 3-methyl-" 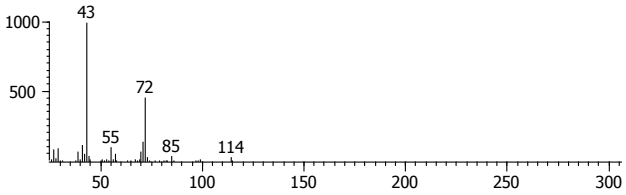

Peak	Name	$^{1}t_R$ (sec)	$^{2}t_R$ (sec)	Underivatized Spectrum
43	Tentative Identification: None Molecular weight: Unidentified Underivatized molecular weight: Unidentified Probable functional groups: Unidentified	1327.9	2.90	Peak True - sample "Underiva SOA 23-3:1", peak 52, at 1327.92 , 2.897 sec , sec 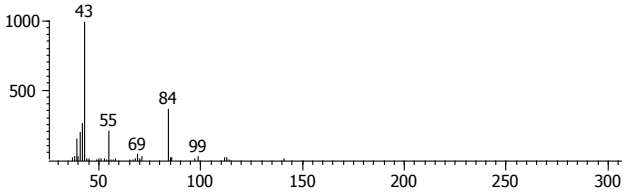 Library Hit - similarity 730, "3-Buten-2-one, 3-methyl-" 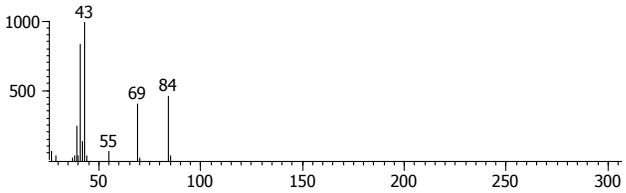
44	Tentative Identification: None Molecular weight: Unidentified Underivatized molecular weight: Unidentified Probable functional groups: Unidentified	1327.9	2.25	Peak True - sample "Underiva SOA 23-3:1", peak 51, at 1327.92 , 2.251 sec , sec 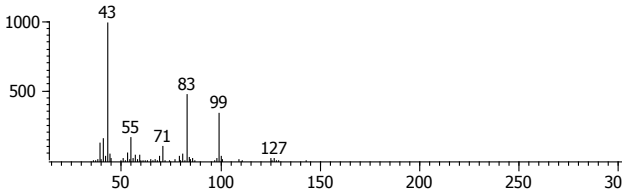 Library Hit - similarity 710, "Pentanoic acid, 4-methyl-, 1-buten-1-yl ester" 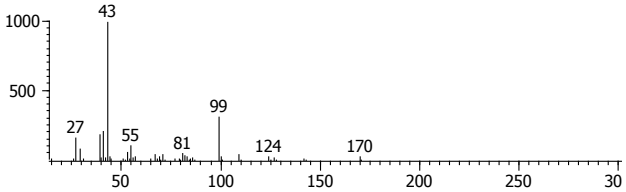
45	Tentative Identification: Pinic acid Underivatized molecular weight: 186 Probable functional groups: Carboxylic acid (2)	1335.9	1.92	Peak True - sample "Underiva SOA 23-3:1", peak 53, at 1335.91 , 1.921 sec , sec 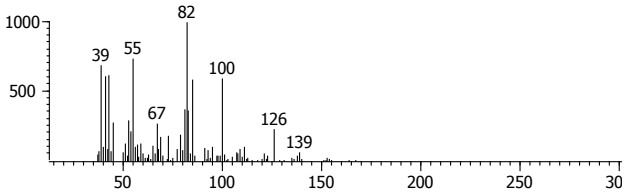 Library Hit - similarity 728, "(+-)-1-Isopropylcyclopropane-trnas-1,trans-2-dicarboxylic ac 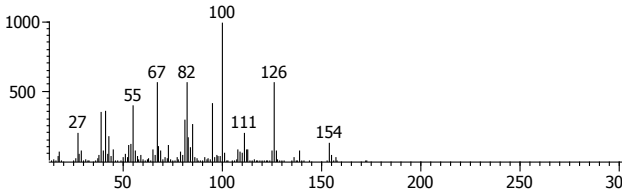

Peak	Name	$^{1}t_R$ (sec)	$^{2}t_R$ (sec)	Underivatized Spectrum
46	Tentative Identification: None Underivatized molecular weight: Unidentified Probable functional groups: Unidentified	1339.9	1.59	Peak True - sample "Underiva SOA 23-3:1", peak 55, at 1339.91 , 2.185 sec , sec 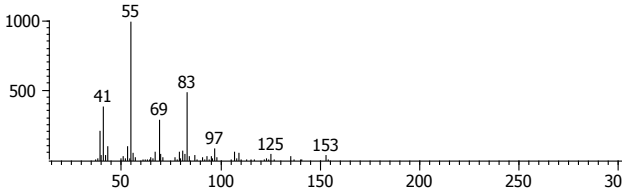 Library Hit - similarity 747, "2-Pentene, 4,4-dimethyl-, (E)-" 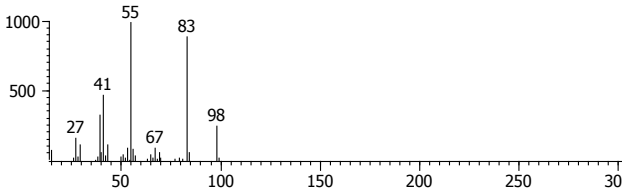
47	Tentative Identification: *cis*-Pinonic acid, underivatized Underivatized molecular weight: 184 Probable functional groups: Unidentified	1343.9	2.10	Peak True - sample "Underiva SOA 23-3:1", peak 56, at 1343.91 , 2.046 sec , sec 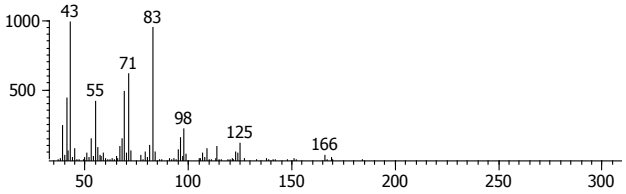 Library Hit - similarity 961, "cis-Pinonic acid, underivatized" 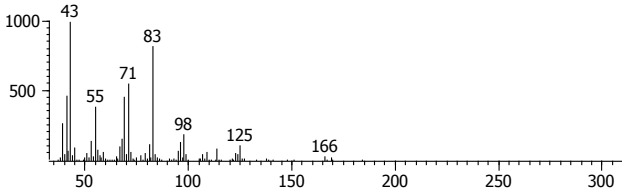
48	Tentative Identification: None Underivatized molecular weight: Unidentified Probable functional groups: Aldehyde, carboxylic acid	1343.9	2.05	Peak True - sample "Underiva SOA 23-3:1", peak 57, at 1343.91 , 2.099 sec , sec 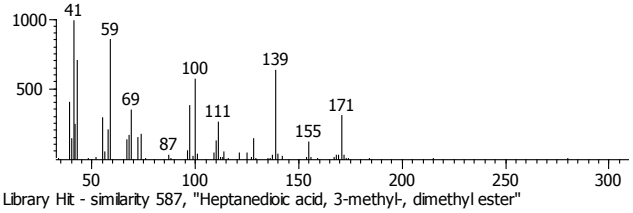 Library Hit - similarity 587, "Heptanedioic acid, 3-methyl-, dimethyl ester" 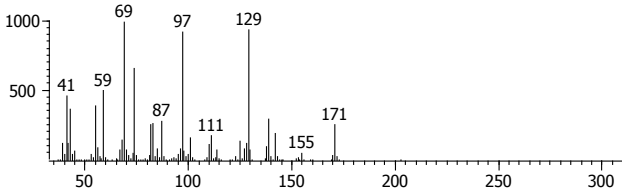

Peak	Name	$^{1}t_R$ (sec)	$^{2}t_R$ (sec)	Underivatized Spectrum
49	Tentative Identification: None Underivatized molecular weight: Unidentified Probable functional groups: Alcohol, carboxylic acid, or ketone	1351.9	1.83	Peak True - sample "Underiva SOA 23-3:1", peak 58, at 1351.91 , 1.828 sec , sec 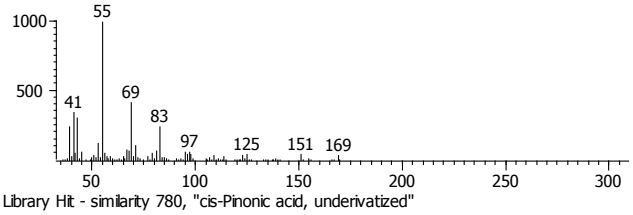 Library Hit - similarity 780, "cis-Pinonic acid, underivatized" 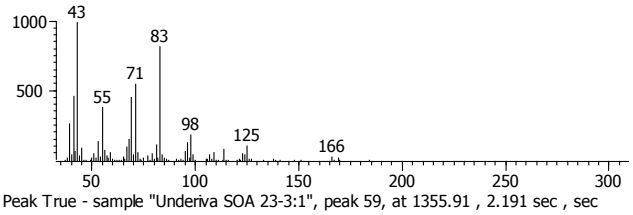
50	Tentative Identification: Pinonaldehyde Underivatized molecular weight: 158 Probable functional groups: Unidentified	1355.9	2.19	Peak True - sample "Underiva SOA 23-3:1", peak 59, at 1355.91 , 2.191 sec , sec 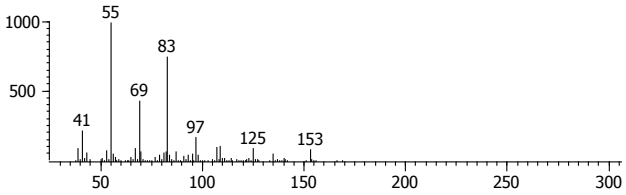 Library Hit - similarity 742, "3-Octene, 2,2-dimethyl-" 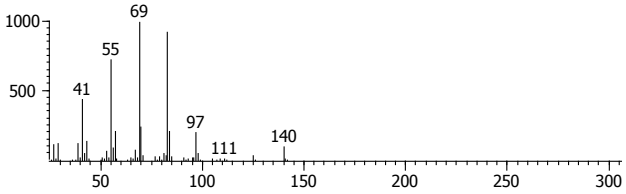
51	Tentative Identification: None Underivatized molecular weight: Unidentified Probable functional groups: Unidentified	1359.9	2.30	Peak True - sample "Underiva SOA 23-3:1", peak 60, at 1359.91 , 2.297 sec , sec 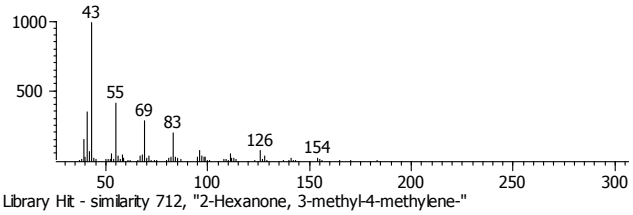 Library Hit - similarity 712, "2-Hexanone, 3-methyl-4-methylene-" 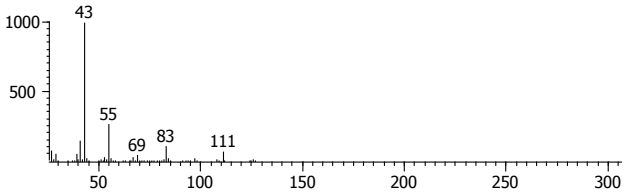

Peak	Name	$^{1}t_R$ (sec)	$^{2}t_R$ (sec)	Underivatized Spectrum
52	Identification: Ketopinic acid, underivatized Underivatized molecular weight: 182 Probable functional groups: Carboxylic acid, ketone	1387.9	2.24	Peak True - sample "Underiva SOA 23-3:1", peak 61, at 1387.91 , 2.237 sec , sec 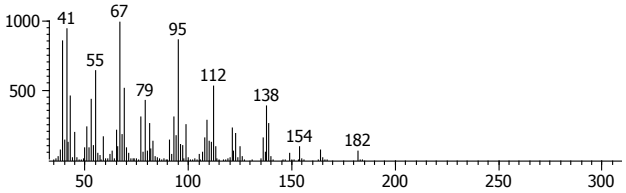 Library Hit - similarity 932, "Bicyclo[2,2,1]heptane-1-carboxylic acid, 7,7,0dimethyl-2-oxo 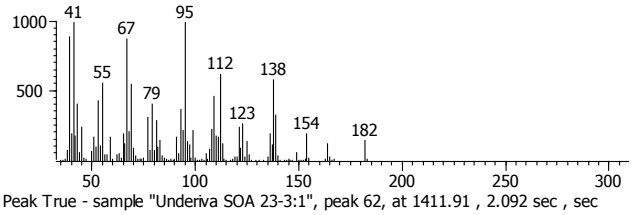
53	Tentative Identification: None Underivatized molecular weight: Unidentified Probable functional groups: Unidentified	1411.9	2.09	Peak True - sample "Underiva SOA 23-3:1", peak 62, at 1411.91 , 2.092 sec , sec 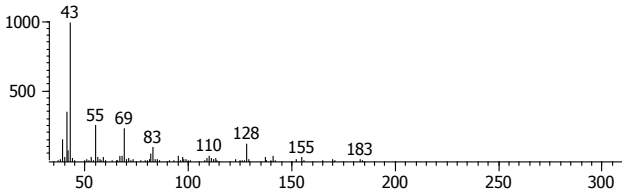 Library Hit - similarity 659, "2-Trifluoroacetoxytridecane" 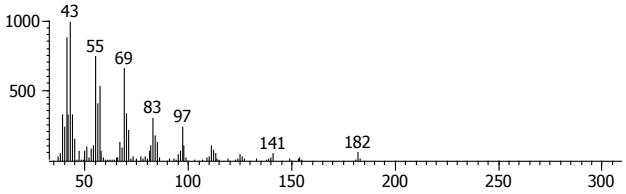
54	Tentative Identification: None Underivatized molecular weight: Unidentified Probable functional groups: Alcohol, carboxylic acid, or ketone	1447.9	2.01	4 Peak True - sample "Underiva SOA 23-3:1", peak 63, at 1447.9 , 2.013 sec , sec 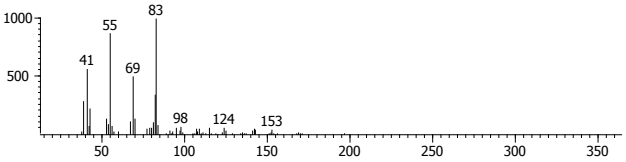 Library Hit - similarity 741, "2-Hexene, 4,4,5-trimethyl-" 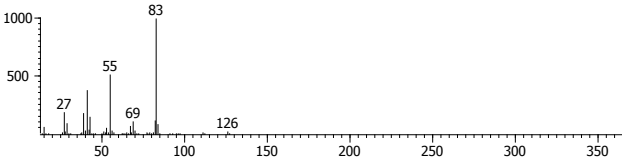

Peak	Name	$^{1}t_R$ (sec)	$^{2}t_R$ (sec)	Underivatized Spectrum
55	Tentative Identification: None Underivatized molecular weight: Unidentified Probable functional groups: Aldehyde	1447.9	2.63	Peak True - sample "Underiva SOA 23-3:1", peak 64, at 1447.9 , 2.627 sec , sec 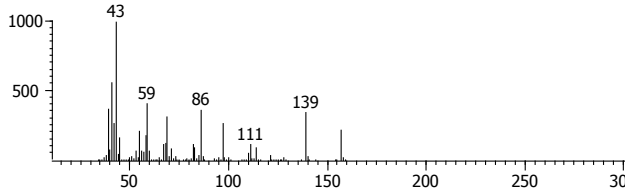 Library Hit - similarity 675, "5-(2,2-Dimethyl-[1,3]dioxolan-4-yl)-4-(2-hydroxyethyl)-1,2-d 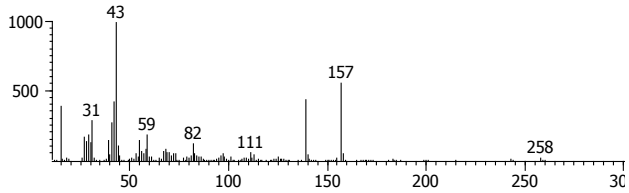
56	Tentative Identification: Pinic acid Underivatized molecular weight: 186 Probable functional groups: Carboxylic acid (2)	1455.9	2.30	Peak True - sample "Underiva SOA 23-3:1", peak 65, at 1455.9 , 2.297 sec , sec 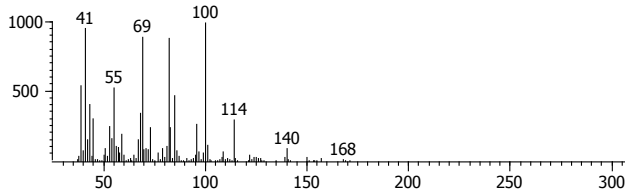 Library Hit - similarity 700, "1-(1-Hydroxy-1-methyl-ethyl)-cyclobutanecarboxylic acid" 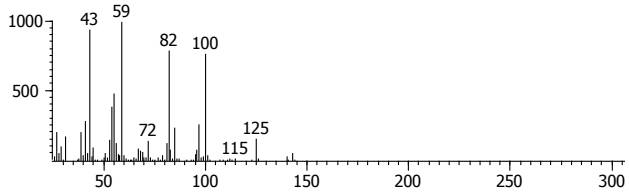
57	Tentative Identification: None Underivatized molecular weight: Unidentified Probable functional groups: Unidentified	1471.9	2.74	Peak True - sample "Underiva SOA 23-3:1", peak 66, at 1471.9 , 2.079 sec , sec 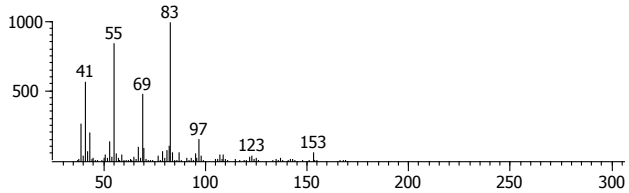 Library Hit - similarity 769, "3-Octene, 2,2-dimethyl-" 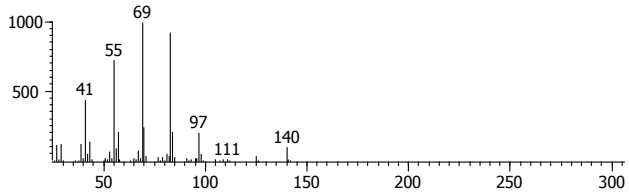

Peak	Name	$^{1}t_R$ (sec)	$^{2}t_R$ (sec)	Underivatized Spectrum
58	Tentative Identification: None Underivatized molecular weight: Unidentified Probable functional groups: Unidentified	1471.9	2.08	Peak True - sample "Underiva SOA 23-3:1", peak 67, at 1471.9 , 2.739 sec , sec 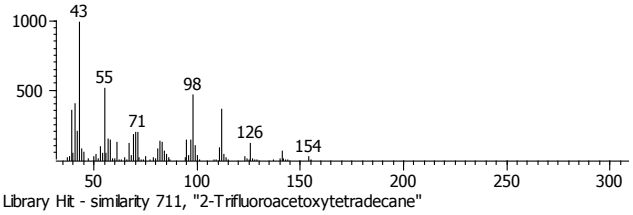 Library Hit - similarity 711, "2-Trifluoroacetoxytetradecane" 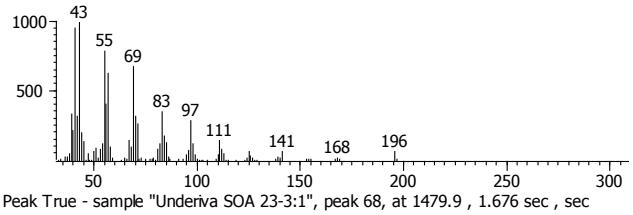
59	Tentative Identification: Hydroxy pinonaldehyde Underivatized molecular weight: 184 Probable functional groups: Alcohol, aldehyde, and ketone	1479.9	1.68	Peak True - sample "Underiva SOA 23-3:1", peak 68, at 1479.9 , 1.676 sec , sec 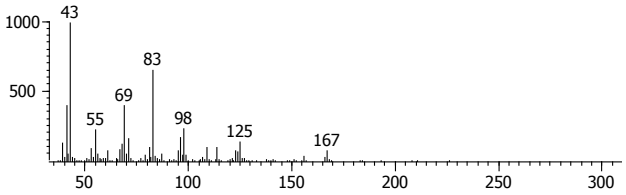 Library Hit - similarity 890, "cis-Pinonic acid, butyl ester" 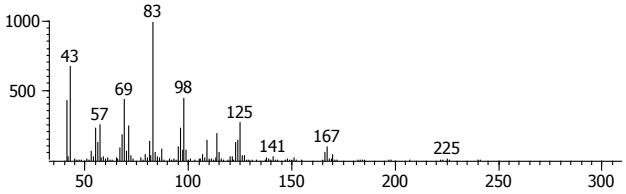
60	Tentative Identification: None Underivatized molecular weight: Unidentified Probable functional groups: Unidentified	1483.9	1.96	Peak True - sample "Underiva SOA 23-3:1", peak 69, at 1483.9 , 1.960 sec , sec 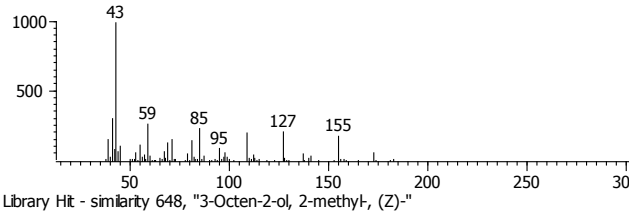 Library Hit - similarity 648, "3-Octen-2-ol, 2-methyl-, (Z)-" 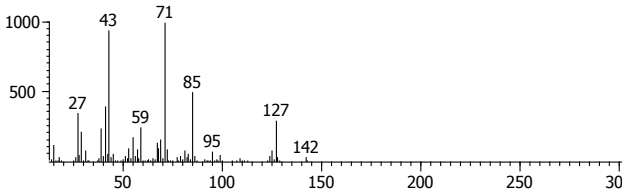

Peak	Name	$^{1}t_R$ (sec)	$^{2}t_R$ (sec)	Underivatized Spectrum
61	Tentative Identification: None Underivatized molecular weight: Unidentified Probable functional groups: Unidentified	1527.9	2.38	Peak True - sample "Underiva SOA 23-3:1", peak 70, at 1527.9 , 2.376 sec , sec 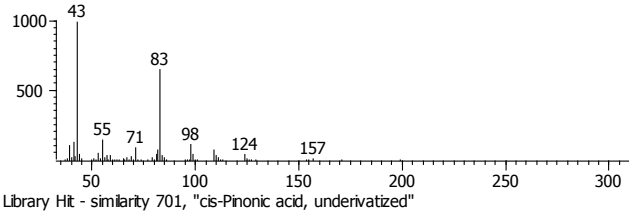 Library Hit - similarity 701, "cis-Pinonic acid, underivatized" 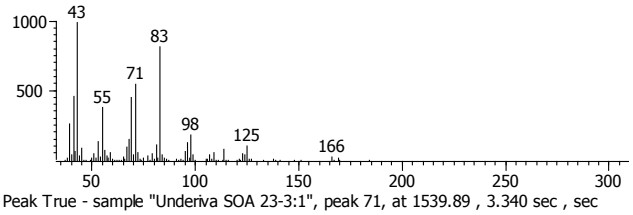
62	Tentative Identification: None Underivatized molecular weight: Unidentified Probable functional groups: Unidentified	1539.9	3.34	Peak True - sample "Underiva SOA 23-3:1", peak 71, at 1539.89 , 3.340 sec , sec 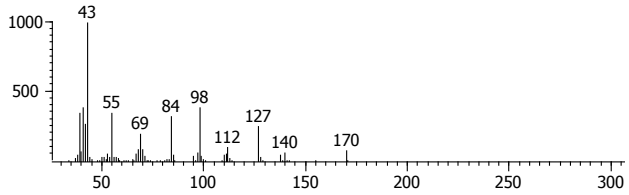 Library Hit - similarity 696, "1-Butanamine, 2-methyl-N-(2-methylbutylidene)-" 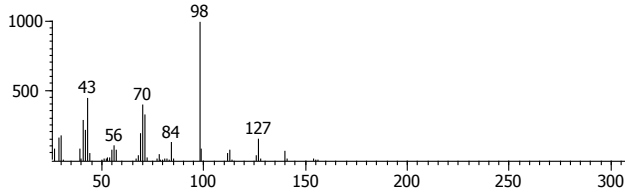
63	Tentative Identification: None Underivatized molecular weight: Unidentified Probable functional groups: Unidentified	1555.9	2.37	Peak True - sample "Underiva SOA 23-3:1", peak 73, at 1555.89 , 2.369 sec , sec 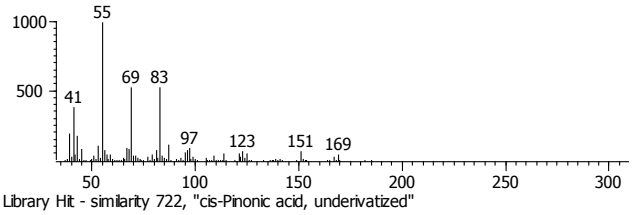 Library Hit - similarity 722, "cis-Pinonic acid, underivatized" 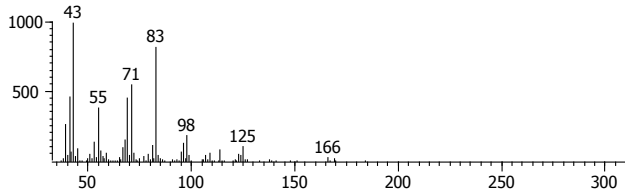

Peak	Name	$^{1}t_R$ (sec)	$^{2}t_R$ (sec)	Underivatized Spectrum
64	Tentative Identification: None Underivatized molecular weight: Unidentified Probable functional groups: Unidentified	1647.9	2.12	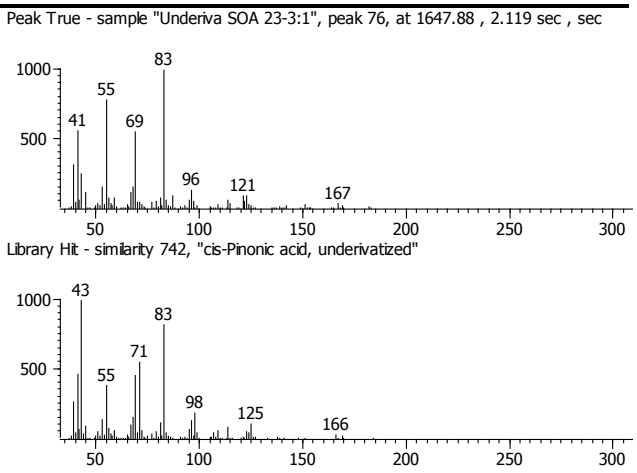
	Phenanthrene-*d10*	1739.9	2.66	
	Eicosane-*d42*	1895.9	1.20	
	Pyrene-*d10*	2035.8	2.33	

APPENDIX F: Study of Oxidation Products of Anthropogenic, Aromatic Hydrocarbons

In order to increase the identified OPM mass in urban air, the oxidation products of anthropogenic, aromatic compounds such as toluene and the xylenes are studied. No compounds could be determined with certainty to be contained in the samples, however, including hydrocarbons or oxidation products. Despite the inconclusive results of this study, the examination of anthropogenic, aromatic hydrocarbon oxidation products using the comprehensive analytical technique of GCxGC TOF-MS and derivatization is potentially interesting, and should be considered as a possible future study.

The published oxidation products of these compounds have included only a few carboxylic acids, which would account for the lack of derivatives in the sample. Forstner, *et al.* (1997) identified 9.2 ± 4.6% of the total *m*-xylene oxidation product particulate mass as carboxylic acid-containing (only *m*-toluic acid was identified, among 20 compounds), while Yu, *et al.* (1997) reported no carboxylic acids (using derivatization by PFBHA for neutral carbonyls).

Bulk analyses of these products using an aerosol mass spectrometer (AMS) show, in contrast, that a relatively large fraction should be contributed by carboxylic acids. This is shown in Figure X, where the fragment m/z 44, which indicates the loss of CO_2^+ and is positively correlated to carboxylic acids (Sato, *et al.,* 2010), makes up more than 20% of the total organic mass in oxidation reactions of toluene.

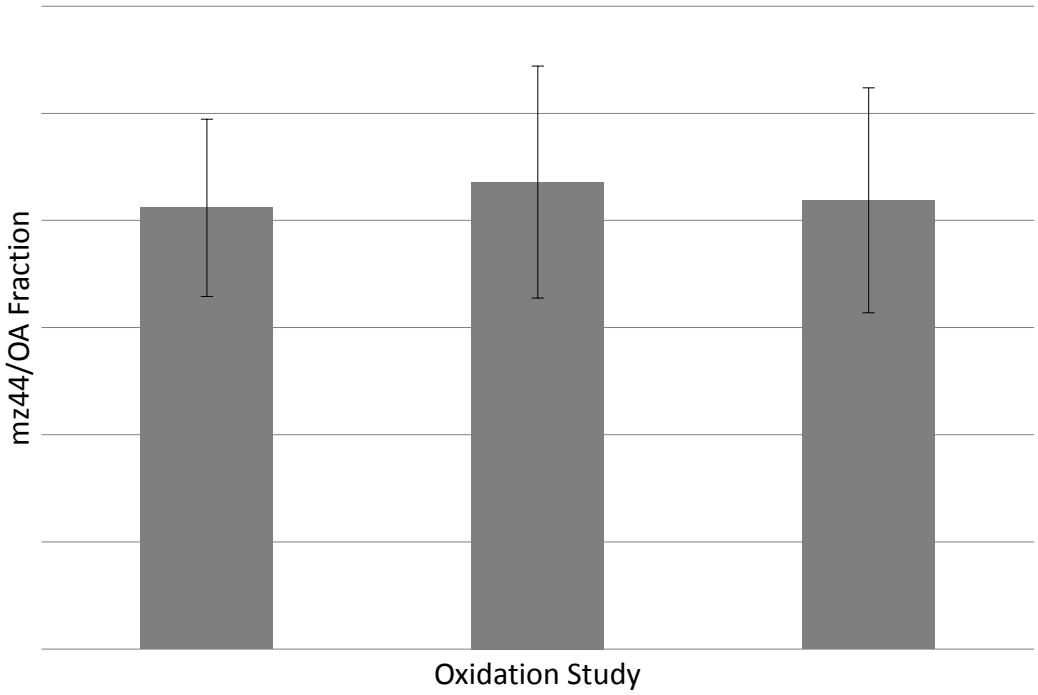

Figure MM. Comparison of three aerosol mass spectrometer data sets collected during the oxidation of *meta*-xylene. The three averaged values (with error bars of two standard deviations) show that the fraction of the fragment m/z 44 (correlated with the presence of carboxylic acid groups) is greater than 0.2, indicating that carboxylic acids may be up to one fifth of the total oxidation product organic mass.

The fraction of the fragment m/z 44 in the total organic mass (mz44/OA) is shown in Figure MM, averaged over the reaction time after first particle formation. A relatively constant value of the mz44/OA over that time period is shown by the standard deviation (the error bar represents twice the standard deviation for each study), which is approximately 25% of the values of mz44/OA.

Through the use of derivatization to target carboxylic and neutral carbonyls in toluene oxidation particulate matter, the number of carboxylic-containing compounds was increased from one (benzoic acid) to four (also including salicylic acid, 3-nitrobenzoic

acid, and 2-hydroxy-4-nitrobenzoic acid), although all were noted to be minor or trace constituents (Jang & Kamens, 2001). There is potential, therefore, for a further increase in the number of identified oxidation products for anthropogenic, aromatic compounds via the comprehensive derivatization/GCxGC TOF-MS method used in the present study. Compounds identified in previous studies to be in the particle-phase oxidation products of anthropogenic, aromatic hydrocarbons are tabulated in Table FF.

Table FF. Previously published oxidation products of several anthropogenic, aromatic hydrocarbons. Products of toluene oxidation found in concentrations greater than 5% of the total organic mass, or tabulated as a "major" product in the particle phase are listed as "major". Carboxylic acid containing oxidation products are underlined. Note that only one oxidation product was recorded in the particle phase during the oxidation of benzene. The precursor *1,2,4*-trimethyl-benzene was not examined in the present study, but is included because a relatively large number of oxidation products have been reported. (Sources: Forstner, *et al.,* 1997, Jang & Kamens, 2001, Kleindienst, *et al.,* 2007, Rea, *et al.,* 2001, Yu, *et al.,* 1997.)

Oxidation Product	**Toluene**	***m*-Xylene**	***1,2,4*-Trimethyl-Benzene**	***2,4*-Xylenol**
1,4-dioxo-2-Butene	x			
2-acetyl-5-methyl-Furan		x	x	
2-Furaldehyde	x			
2-hydroxy-Benzaldehyde (o, m, p)	x			
2-hydroxy-Benzoic acid (o, m, p)	x			
2-methyl-1,4-Benzoquinone	x			
2-methyl-2-Butendial (isomers)	major			
2-methyl-2,4-Hexanedienedial	x			
2-methyl-Butanedial		x	x	
2,3-Butanedione			x	
2,3-dihydroxy-4-oxo-Pentanoic acid	x			
2,3-dioxo-Butanal	x			
2,3,5-trimethyl-1,4-Benzoquinone			x	
2,4-dimethyl-Benzaldehyde			x	
2,4-dimethyl-Phenol		x	x	
2,5-dimethyl-Benzaldehyde			x	
2,5-dimethyl-Phenol			x	
2,5-Furandione	major	x	x	
2,6-dimethyl-1,4-Benzoquinone		x		x
2,6-dimethyl-Phenol				
3-acetyl-2,5-dimethyl-Furan			x	
3-ethyl-2,5-Furandione				
3-Hexene-2,5-dione			x	
3-hydroxy-Benzaldehyde	x			
3-methyl-2,5-Furandione	major	x	x	
3-methyl-2,5-Hexanedione			x	
3-methyl-2(*5H*)-Furanone	x	x		
3-methyl-Benzyl alcohol		x		
3,4-dimethyl-Benzaldehyde			x	
3,4-dimethyl-Benzoic acid			x	
3,4-dimethyl-Furandione		x	x	
3,4,5-trimethyl-2(*3H*)-Furanone			x	
3,4/4,5-dimethyl-2(*3H*)-Furanone			x	
3,5-dimethyl-2(*3H*)-Furanone		x		
3,5-dimethyl-(*2H*)-Pyran-2-one		x		
4-methyl-Benzaldehyde	x	x		

Oxidation Product	Toluene	*m*-Xylene	*1,2,4*-Trimethyl-Benzene	*2,4*-Xylenol
4-methyl-Phthalic acid			x	
4-oxo-2-Pentenal	major	x		x
5-ethyl-2-Furaldehyde				
5-ethyl-2(*3H*)-Furanone				
5-methyl-2-Furancarboxaldehyde	x		x	
5-methyl-2(*3H*)-Furanone	x	x	x	
5-methyl-6-oxo-2,4-Hexadienal	x			
5-methyl-Furfural		x		
6-hydroxy-2-methyl-1,4,5-trioxo-2-Cyclohexene (isomers)	x			
6-oxo-2,4-Heptadienal	x			
Acetophenone				
2-ethyl-1,4-Benzoquinone				
2-methyl-Benzoquinone (isomers)	major			
Dimethylbenzoquinone (isomers)		x	x	
Methyl Benzoquinone isomers (mono-derivative)	x			
methyl-*p*-Benzoquinone	x	x		
Trimethylbenzoquinone (isomers)			x	
Benzaldehyde	major			
Benzoic acid	major			
Benzoquinone (mono-derivative, underivatized)	x			
Benzyl alcohol	x			
Butanedial	x	x		
C_3 Hydroxy dicarbonyl	x			
C_4 Epoxy dicarbonyl or C_4 trione	x			
C_4 Hydroxy dicarbonyl (monoderivative)	x	x	x	
C_4 Saturated dicarbonyl or C_3 trione	x			
C_5 Epoxy dicarbonyl or C_5 trione	x			
C_5 Hydroxy carbonyl or mono-derivative of C4 hydroxy dicarbonyl	x			
C_6 Di-unsaturated carbonyl or furfural/methyl furfural or acetyl furan	x			
C_6 Unsaturated hydroxy epoxy cyclic carbonyl	x			
C_7 Unsaturated epoxy dicarbonyl/methylglyoxal	x			
cis-2-methyl-4-oxo-2-Pentanal		x		
Di-unsaturated 1,6-dicarbonyl (C7, C8)	x	x		
dihydro-2,5-Furandione	major			

Oxidation Product	Toluene	*m*-Xylene	*1,2,4*-Trimethyl-Benzene	*2,4*-Xylenol
dihydro-5-methyl-2(3H)-Furanone				
Glycolaldehyde	x	x	x	
Glyoxal	major	x	x	
Hydroxyacetone	x	x	x	
m-Cresol	x			
m-Tolualdehyde	x	x		
m-Toluic acid		x		
Methyl furfural or acetyl furan	x			
methyl-2-Furaldehydes (isomers)	x			
methyl-Cyclohexene tricarbonyls (isomers)	major			
Methylglyoxal	major	x	x	
o-Cresol	x			
p-Cresol	x			
p-Tolualdehyde	x	x		
Phenol				
Propanedial	x			
sec-Phenethyl alcohol				
trans-2-methyl-4-oxo-2-Pentanal		x	x	
Tri-oxo-pentane	x			

Despite the tentative identification of many compounds in the particle phase, the estimated fraction in the particle phase is low (based upon the high mass loading of the *m*-xylene oxidation study presented here). This disparity indicates that some of these compounds may have been byproducts of sample preparation or impurities. The values of the estimated fraction of some of these compounds in the particle phase are given in GG.

Table GG. Estimated phases in high mass loading of high percent yield or repeatedly published oxidation products of anthropogenic, aromatic hydrocarbons. Fraction in the particle phase, f_i, was estimated using M=117 ug/m^3, from the *m*-xylene oxidation study presented here. Vapor pressures, $P°_{L,i}$, sub-cooled if necessary, are predicted by EPA EPI Suite MPBPWIN, collected from previous studies using the ChemSpider database, or estimated using SIMPOL, Pankow & Asher 2008). Pinonic acid, naphthalene, and toluene are also listed, as common compounds, for comparison to the oxidation products tabulated. *They were not identified as oxidation products.*

Oxidation Product	$P°_{L,i}$ Liquid Vapor Pressure (mm Hg)	f_i Fraction in the Particle Phase	Estimated Phase
2-hydroxy-3-methyl-Benzaldehyde	0.00753	0.00290	Gas
2-hydroxy-Benzaldehyde (*o, m, p*)	0.329	6.66×10^{-5}	Gas
2-hydroxy-Benzoic acid (*o, m, p*)	0.0017	0.0127	Particle
2-methyl-1,4-Benzoquinone	0.0889	0.000246	Gas
2,3,5-trimethyl-1,4-Benzoquinone	0.0187	0.00117	Gas
2,4-dimethyl-Benzaldehyde	0.679	3.23×10^{-5}	Gas
2,4-dimethyl-Phenol	0.102	0.000215	Gas
2,5-dimethyl-1,4-Benzoquinone	0.0402	0.000545	Gas
2,6-dimethyl-1,4-Benzoquinone	0.0402	0.000542	Gas
Benzaldehyde	1.01	4.66×10^{-6}	Gas
Benzoic acid	0.00643	0.000700	Gas
Benzoquinone (mono-derivative, underivatized)	0.710	3.07×10^{-5}	Gas
m-Cresol	0.207	0.000105	Gas
m-Tolualdehyde	1.78	1.22×10^{-5}	Gas
p-Tolualdehyde	0.250	8.72×10^{-5}	Gas
Phenol	0.503	4.34×10^{-5}	Gas
2-acetyl-5-methyl-Furan	1.82	2.57×10^{-6}	Gas
2-Furaldehyde	2.21	4.86×10^{-5}	Gas
2,5-Furandione	0.471	0.000227	Gas
3-methyl-2,5-Furandione	0.183	0.000119	Gas
2-methyl-2-Butendial (and isomers)	17.9	5.99×10^{-6}	Gas
2-methyl-2,4-Hexanedienedial	0671	0.000160	Gas
2,5-Hexanedione	0.688	3.17×10^{-5}	Gas
3-Hexene-2,5-dione	2.17	1.00×10^{-5}	Gas
4-oxo-2-Pentenal	1340	7.98×10^{-8}	Gas
Glyoxal	255	1.09×10^{-6}	Gas
Methylglyoxal	0.159	0.000674	Gas
Pinonic acid	*0.00230*	*0.0446*	*Particle*
Napthalene	*0.299*	*0.000931*	*Gas*
Toluene	*28.4*	*7.68E-07*	*Gas*

Compounds shown in Table X with $P°_{L,i}$ below 0.006 mm Hg were predicted to be less than 1% by mass in the particle phase (based upon a high mass loading of 117 μg m^3

measured in the study done here), which is true for nearly all of these major or repeatedly published anthropogenic, aromatic oxidation products. This shows that while organic mass is collected during oxidation studies of these precursors, many of the compounds reported to account for a large percentage of the identified mass may only account for a small mass in actuality, and that the probability of other compounds in the particle phase is high. Because carboxylic acid groups lower the vapor pressure of a given hydrocarbon structure by a large amount ($10^{6.4}$ mm Hg at 20°C using the SIMPOL.1 prediction algorithm, Pankow & Ahser, 2008), and given their anticipated presence in oxidative paticulate matter by bulk analyses, carboxylic acids are likely to make up a significant fraction of the total OPM from anthropogenic, aromatic hydrocarbon oxidations.

No compounds could be determined with certainty to be present in the samples analyzed in this study because several potential analytes were discovered in calibration standard solution chromatograms. Further analyses of the reagents and solvents revealed that the reagent BSTFA used in the analyses of anthropogenic, aromatic hydrocarbon oxidation products contained a series of carboxylic acids.

APPENDIX G: Plots of Thermal Optical Method Determination of Total Organic Carbon on α-Pinene Ozonolysis Filter Samples

Sample ID: Sucrose 35.04ug

Analysis Date/Time 7/7/2011 2:28:23 PM
Instrument: Inst #269-68 Mode: Transmittance
Organic C = 36.90 +-1.94 ug/sq cm
Carbonate C = 0.00 +- ug/sq cm
Elemental C = 0.00 +-0.10 ug/sq cm
Total C = 36.90 +-2.04 ug/sq cm
EC/TC ratio = 0.000
FID: FID1: OK FID2: OK DL = 10
Punch Area, sq cm = 1
Calibration Constant = 22.485
Calibration area Used = 354194.0
Laser correction factor = 0.98
Split time Used = 698 seconds Split time Calculated = 698 seconds
Pk1 = 20.10 Pk2 = 5.52 Pk3 = 7.12 PK4 = 3.23
EC1 = 0.10 EC2 = 0.38 EC3 = 0.16 PyC = 0.94

FID1 FID2 Laser Transmission Temperature Absorbance FID GRAPHIC SCALE= 10

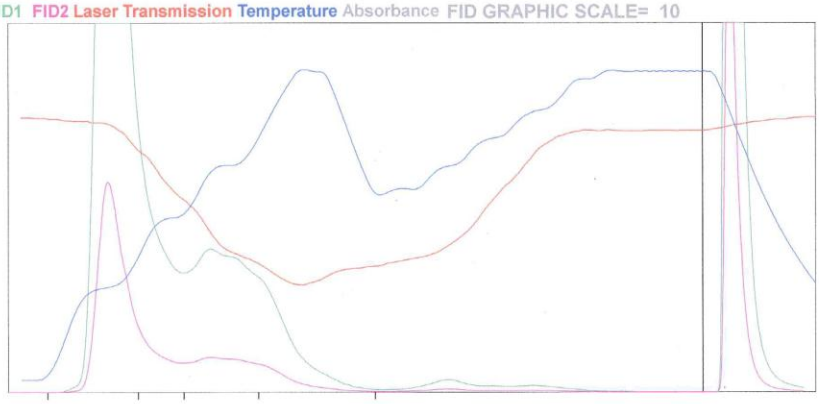

Inital absorbance = 0.001 Absorbance at StartPyrolize = 0.758
Absorbtion Coefficient of original elemental C =2000000000.0
Absorbance plotted from 0 to 6

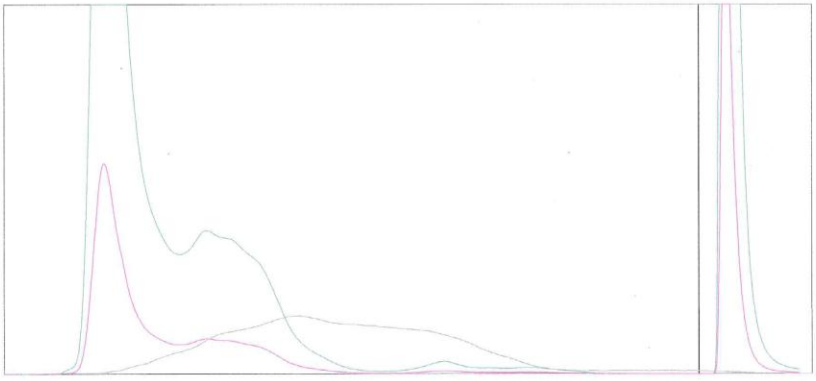

OC/EC Analysis Program (c) Sunset Laboratory, Inc. Analyst - BRC

Sample ID: BLANK (no collection)

Analysis Date/Time 7/7/2011 3:17:39 PM
Instrument: Inst #269-68 Mode: Transmittance
Organic C = 0.57 +-0.13 ug/sq cm
Carbonate C = 0.00 +- ug/sq cm
Elemental C = 0.00 +-0.10 ug/sq cm
Total C = 0.57 +-0.23 ug/sq cm
EC/TC ratio = 0.000
FID: FID1: OK FID2: OK DL = 10
Punch Area, sq cm = 1.5
Calibration Constant = 22.485
Calibration area Used = 354450.0
Laser correction factor = 0.97
Split time Used = 691 seconds Split time Calculated = 691 seconds
Pk1 = 0.41 Pk2 = 0.10 Pk3 = 0.03 PK4 = 0.01
EC1 = 0.00 EC2 = 0.01 EC3 = 0.01 PyC = 0.02

FID1 FID2 Laser Transmission Temperature Absorbance FID GRAPHIC SCALE= 10

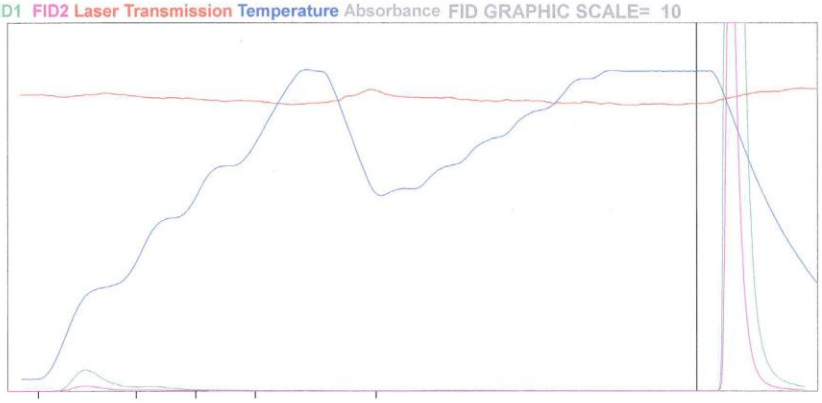

Inital absorbance = 0.014 Absorbance at StartPyrolize = 0.020
Absorbtion Coefficient of original elemental C =2000000000.0
Absorbance plotted from 0 to 6

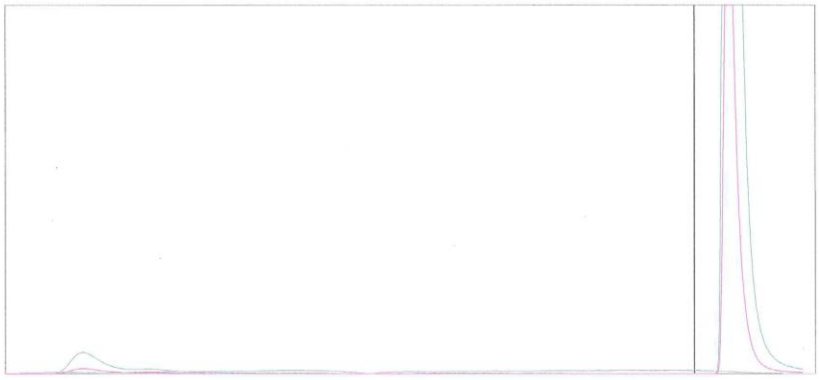

OC/EC Analysis Program (c) Sunset Laboratory, Inc. Analyst - BRC

aP

Sample ID: 062311-2 (aP+prop)

Analysis Date/Time 7/7/2011 4:01:31 PM
Instrument: Inst #269-68 Mode: Transmittance
Organic C = 0.89 +-0.14 ug/sq cm
Carbonate C = 0.00 +- ug/sq cm
Elemental C = 0.00 +-0.10 ug/sq cm
Total C = 0.89 +-0.24 ug/sq cm
EC/TC ratio = 0.000
FID: FID1: OK FID2: OK DL = 10
Punch Area, sq cm = 1.5
Calibration Constant = 22.485
Calibration area Used = 350070.0
Laser correction factor = 0.98
Split time Used = 709 seconds Split time Calculated = 709 seconds
Pk1 = 0.52 Pk2 = 0.23 Pk3 = 0.10 PK4 = 0.04
EC1 = 0.00 EC2 = 0.01 EC3 = 0.00 PyC = 0.01

FID1 FID2 Laser Transmission Temperature Absorbance FID GRAPHIC SCALE= 10

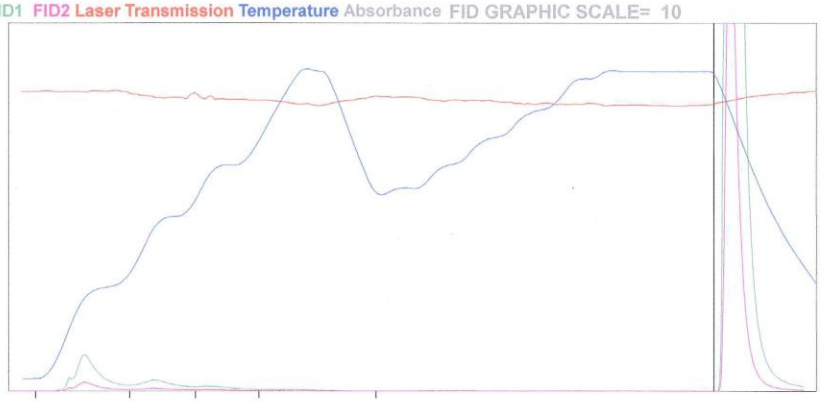

Inital absorbance = 0.000 Absorbance at StartPyrolize = 0.022
Absorbtion Coefficient of original elemental C = -961.1
Absorbance plotted from 0 to 6

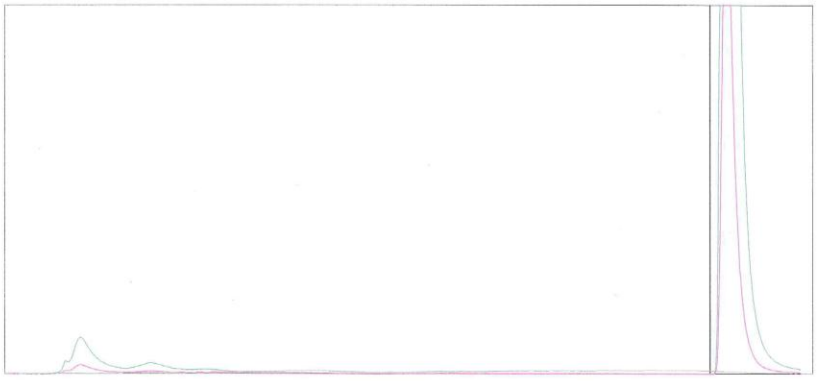

OC/EC Analysis Program (c) Sunset Laboratory, Inc. Analyst - BRC

Sample ID: 062311-1 (clean air)

Analysis Date/Time 7/7/2011 3:38:12 PM
Instrument: Inst #269-68 Mode: Transmittance
Organic C = 0.97 +-0.15 ug/sq cm
Carbonate C = 0.00 +- ug/sq cm
Elemental C = 0.00 +-0.10 ug/sq cm
Total C = 0.97 +-0.25 ug/sq cm
EC/TC ratio = 0.000
FID: FID1: OK FID2: OK DL = 10
Punch Area, sq cm = 1.5
Calibration Constant = 22.485
Calibration area Used = 357102.0
Laser correction factor = 0.98
Split time Used = 710 seconds Split time Calculated = 710 seconds
Pk1 = 0.38 Pk2 = 0.29 Pk3 = 0.14 PK4 = 0.09
EC1 = 0.03 EC2 = 0.02 EC3 = 0.01 PyC = 0.08

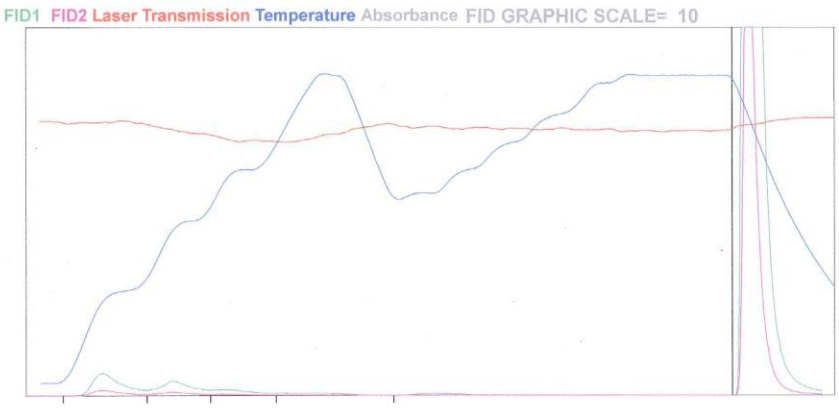

Inital absorbance = 0.010 Absorbance at StartPyrolize = 0.033
Absorbtion Coefficient of original elemental C = -22917.9
Absorbance plotted from 0 to 6

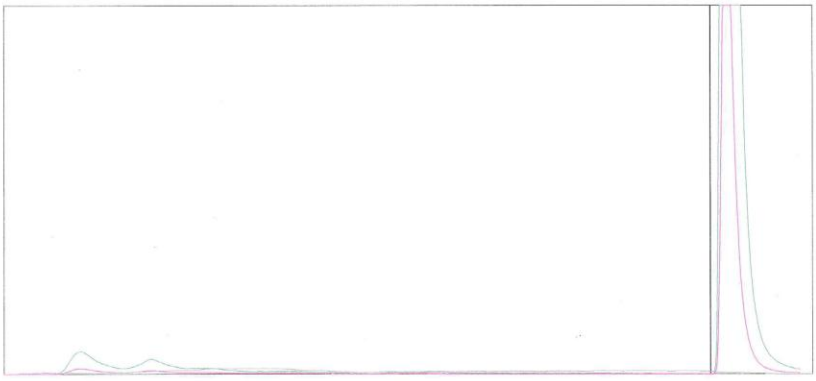

OC/EC Analysis Program (c) Sunset Laboratory, Inc. Analyst - BRC

Sample ID: 062611-3 (SOA)

Analysis Date/Time 7/7/2011 5:44:28 PM
Instrument: Inst #269-68 Mode: Transmittance
Organic C = 38.28 +-2.01 ug/sq cm
Carbonate C = 0.00 +- ug/sq cm
Elemental C = 0.00 +-0.10 ug/sq cm
Total C = 38.28 +-2.11 ug/sq cm
EC/TC ratio = 0.000
FID: FID1: OK FID2: OK DL = 10
Punch Area, sq cm = 1.5
Calibration Constant = 22.485
Calibration area Used = 354214.0
Laser correction factor = 0.98
Split time Used = 709 seconds Split time Calculated = 709 seconds
Pk1 = 16.40 Pk2 = 8.83 Pk3 = 5.78 PK4 = 6.09
EC1 = 0.25 EC2 = 0.32 EC3 = 0.15 PyC = 1.18

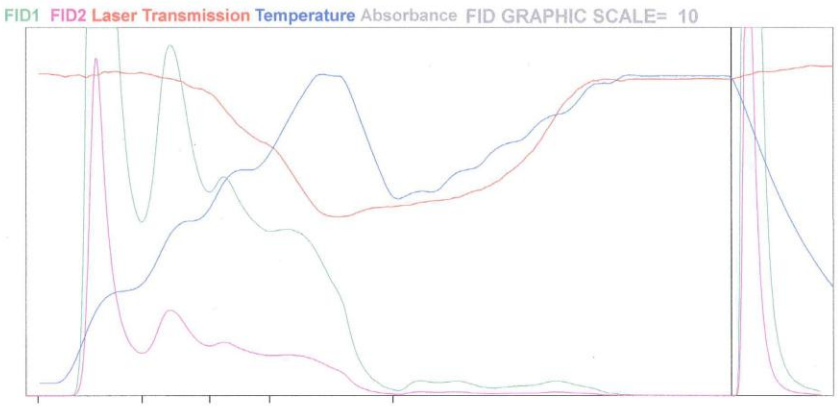

Inital absorbance = 0.016 Absorbance at StartPyrolize = 0.548
Absorbtion Coefficient of original elemental C = -37812.7
Absorbance plotted from 0 to 6

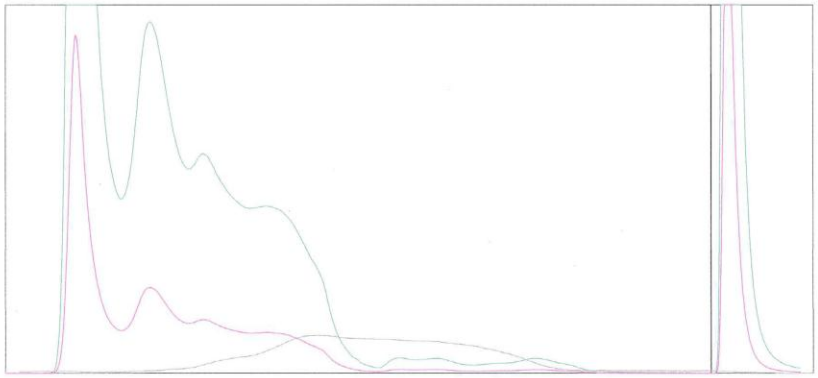

OC/EC Analysis Program (c) Sunset Laboratory, Inc. Analyst - BRC

Sample ID: 062611-4 (SOA)

Analysis Date/Time 7/7/2011 6:10:28 PM
Instrument: Inst #269-68 Mode: Transmittance
Organic C = 50.35 +-2.62 ug/sq cm
Carbonate C = 0.00 +- ug/sq cm
Elemental C = 0.00 +-0.10 ug/sq cm
Total C = 50.35 +-2.72 ug/sq cm
EC/TC ratio = 0.000
FID: FID1: OK FID2: OK DL = 10
Punch Area, sq cm = 1.5
Calibration Constant = 22.485
Calibration area Used = 351664.0
Laser correction factor = 0.98
Split time Used = 690 seconds Split time Calculated = 690 seconds
Pk1 = 20.85 Pk2 = 12.56 Pk3 = 6.95 PK4 = 6.86
EC1 = 1.70 EC2 = 0.51 EC3 = 0.27 PyC = 3.14

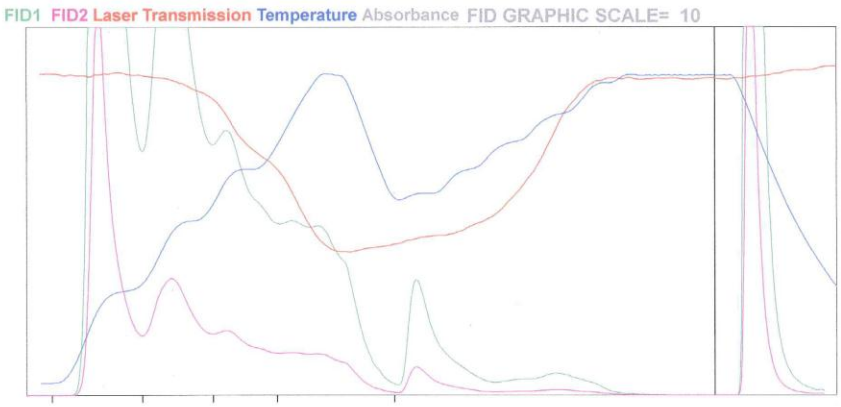

Inital absorbance = 0.018 Absorbance at StartPyrolize = 0.754
Absorbtion Coefficient of original elemental C = -14362.8
Absorbance plotted from 0 to 6

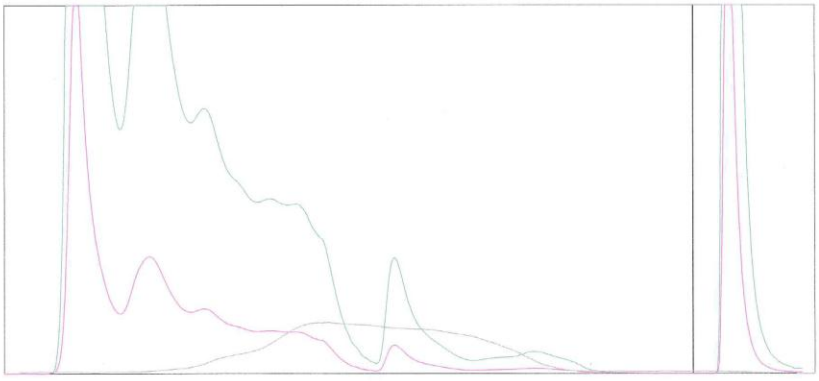

OC/EC Analysis Program (c) Sunset Laboratory, Inc. Analyst - BRC

αP

Sample ID: 062311-3 (aP + SOA)

Analysis Date/Time 7/7/2011 4:26:55 PM
Instrument: Inst #269-68 Mode: Transmittance
Organic C = 105.21 +-5.36 ug/sq cm
Carbonate C = 0.00 +- ug/sq cm
Elemental C = 0.00 +-0.10 ug/sq cm
Total C = 105.21 +-5.46 ug/sq cm
EC/TC ratio = 0.000
FID: FID1 OFFSCALE!!! FID2: OK DL = 10
Punch Area, sq cm = 1.5
Calibration Constant = 22.485
Calibration area Used = 85910.0
Laser correction factor = 0.98
Split time Used = 709 seconds Split time Calculated = 709 seconds
Pk1 = 51.55 Pk2 = 24.41 Pk3 = 10.55 PK4 = 12.29
EC1 = 4.06 EC2 = 0.88 EC3 = 0.41 PyC = 6.41

FID1 FID2 Laser Transmission Temperature Absorbance FID GRAPHIC SCALE= 10

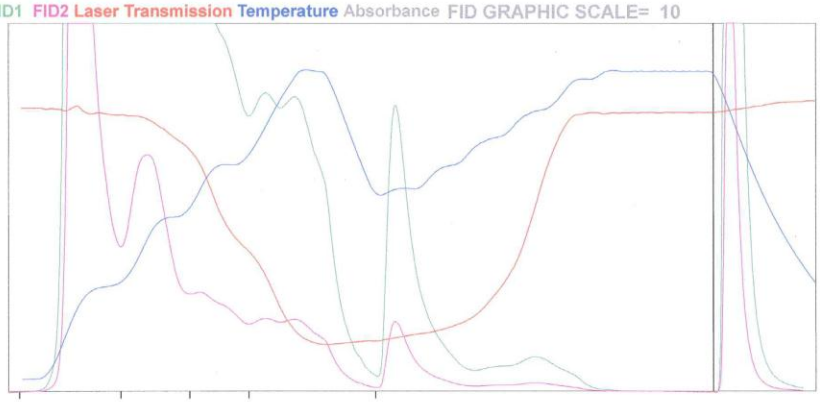

Inital absorbance = 0.019 Absorbance at StartPyrolize = 1.719
Absorbtion Coefficient of original elemental C = -10991.7
Absorbance plotted from 0 to 6

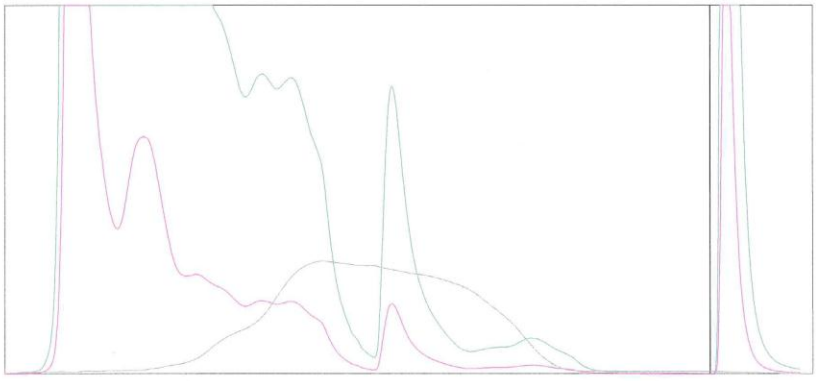

OC/EC Analysis Program (c) Sunset Laboratory, Inc. Analyst - BRC

Sample ID: 062611-1 (clean)

Analysis Date/Time 7/7/2011 4:50:27 PM
Instrument: Inst #269-68 Mode: Transmittance
Organic C = 1.34 +-0.17 ug/sq cm
Carbonate C = 0.00 +- ug/sq cm
Elemental C = 0.00 +-0.10 ug/sq cm
Total C = 1.34 +-0.27 ug/sq cm
EC/TC ratio = 0.000
FID: FID1: OK FID2: OK DL = 10
Punch Area, sq cm = 1.5
Calibration Constant = 22.485
Calibration area Used = 353361.0
Laser correction factor = 0.97
Split time Used = 697 seconds Split time Calculated = 697 seconds
Pk1 = 0.52 Pk2 = 0.32 Pk3 = 0.36 PK4 = 0.09
EC1 = 0.01 EC2 = 0.01 EC3 = 0.01 PyC = 0.06

FID1 FID2 Laser Transmission Temperature Absorbance FID GRAPHIC SCALE= 10

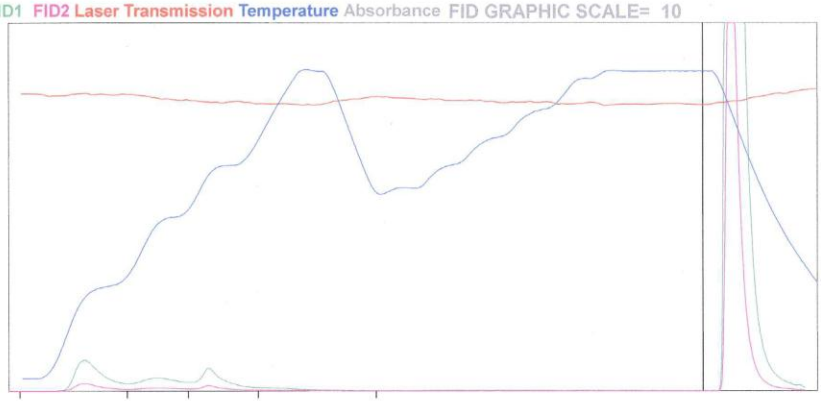

Inital absorbance = 0.013 Absorbance at StartPyrolize = 0.027
Absorbtion Coefficient of original elemental C = 10550.0
Absorbance plotted from 0 to 6

OC/EC Analysis Program (c) Sunset Laboratory, Inc. Analyst - BRC

aP

Sample ID: 062611-2 (aP + 1-prop)

Analysis Date/Time 7/7/2011 5:23:00 PM
Instrument: Inst #269-68 Mode: Transmittance
Organic C = 1.59 +-0.18 ug/sq cm
Carbonate C = 0.00 +- ug/sq cm
Elemental C = 0.00 +-0.10 ug/sq cm
Total C = 1.59 +-0.28 ug/sq cm
EC/TC ratio = 0.000
FID: FID1: OK FID2: OK DL = 10
Punch Area, sq cm = 1.5
Calibration Constant = 22.485
Calibration area Used = 353898.0
Laser correction factor = 0.98
Split time Used = 710 seconds Split time Calculated = 710 seconds
Pk1 = 0.80 Pk2 = 0.44 Pk3 = 0.23 PK4 = 0.08
EC1 = 0.00 EC2 = 0.02 EC3 = 0.01 PyC = 0.03

FID1 FID2 Laser Transmission Temperature Absorbance FID GRAPHIC SCALE= 10

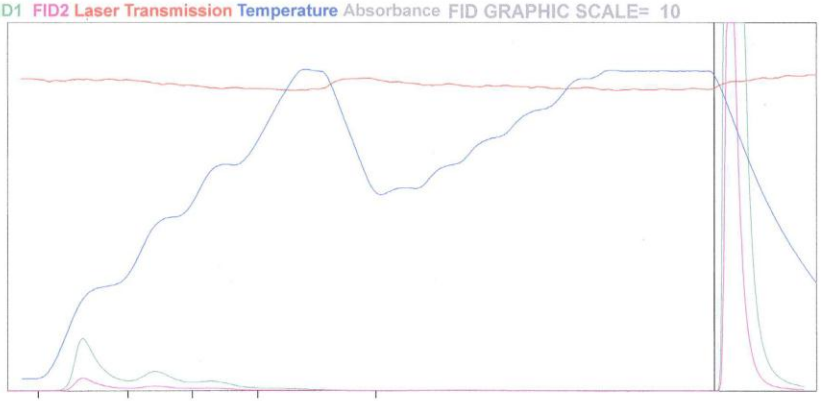

Inital absorbance = 0.012 Absorbance at StartPyrolize = 0.023
Absorbtion Coefficient of original elemental C =2000000000.0
Absorbance plotted from 0 to 6

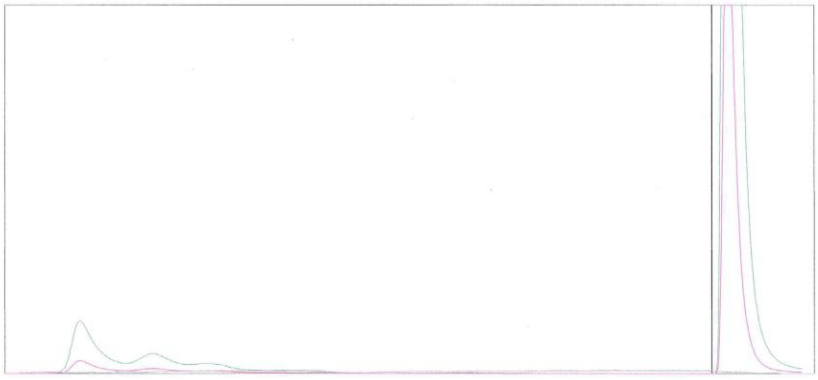

OC/EC Analysis Program (c) Sunset Laboratory, Inc. Analyst - BRC

APPENDIX H: Compared Efficacy of Data Processing Methods

The processing of GC×GC data is intensive, and the analysis of highly complex samples can lead to uncertain compound identifications and quantification. The primary drawbacks of GC×GC/TOF-MS data processing are: a) interpretation of a large number of peaks in a chromatogram that are sometimes challenging to differentiate as separate peaks or modulated "slices" of primary dimension tailing peaks, and b) interpretation of time of flight and sometimes incorrectly separated ("deconvoluted") mass spectra. Although subtraction of a method blank from the sample chromatogram might be helpful in eliminating some peaks corresponding to byproducts and background, significant variation can be observed in the background signals.

For chromatograms of samples containing homologous series of compounds such as hydrocarbons, retention time patterns in the first and second dimensions can be recognized so that compounds not identified easily by a mass spectral library match can be identified by retention time trends. Added derivatization groups decrease peak tailing and may allow the retention time of a compound to be more accurate as the peak shape becomes sharper. Visually and mathematically represented retention time trends have been recognized for both derivatized compounds with similar structures and using GC×GC. The series of di-acid derivatives in the calibration standards (C_3—C_6 di-acids) could be usually recognized as a homologous series (referred to as "band separation") in chromatograms, but was not recognizable mathematically. No patterns could be recognized visually or mathematically in the analyzed SOA samples (Section 3.3.f). The

results of the study using derivatization and GC×GC for the identification of anthropogenic, aromatic hydrocarbon oxidation[6] were used to explore the efficacy of the method in terms of its relative ease of data processing.

The use of extracted ions can be particularly helpful for derivatized samples in which high abundance diagnostic ions are present in the mass spectra (for example, the mass 73, corresponding to the loss of the trimethylsilyl group after BSTFA derivatization). Table 3.11 outlines several of these diagnostic ions particular to both derivatization reagent systems used this study. Derivatization diagnostic ions are normally viewed as extracted ion chromatograms, but can also be marked using ChromaTOF™ Script written to access spectra. The output can be displayed within the application both graphically and .as delimited text classifications (Figure **3.6**).

[6] The results of the study of OPM collected from anthropogenic, aromatic hydrocarbon oxidations showed few possible oxidation products and high responses for carboxylic acids that were also found in blank chromatograms. Therefore, the results of the study were not presented this document.

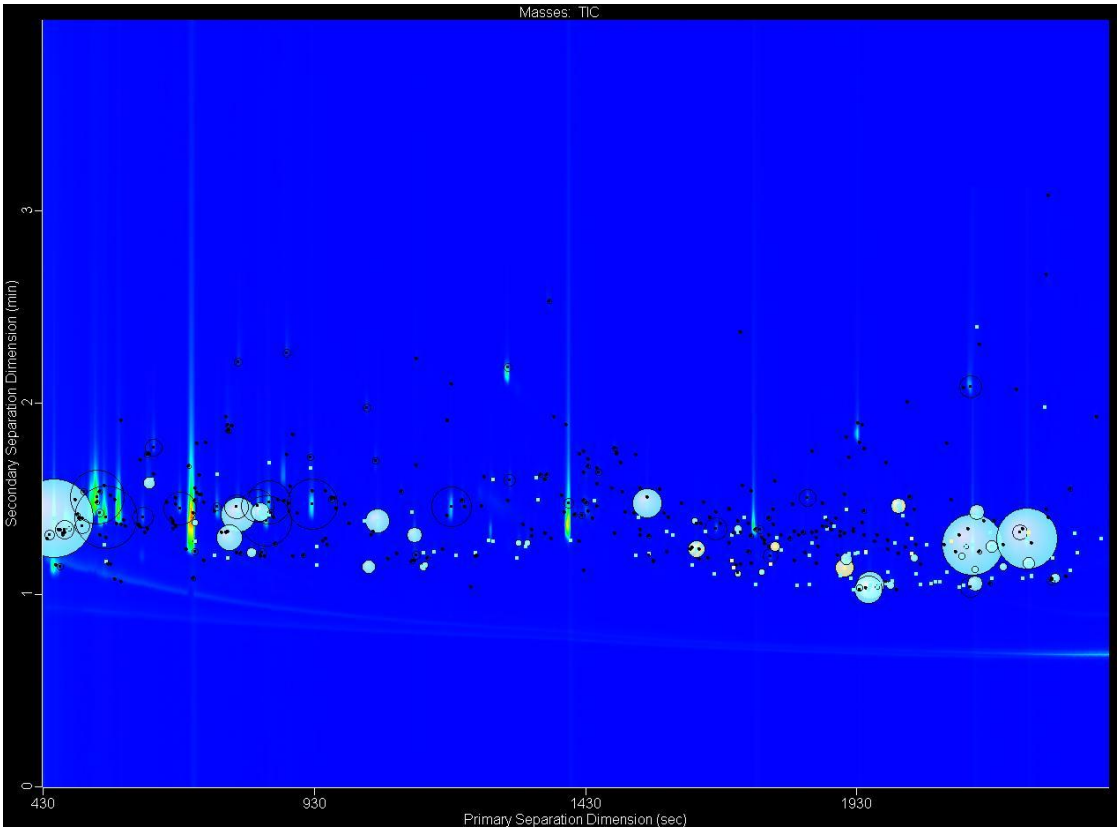

Figure NN. GC×GC total ion chromatogram of butylated m-xylene oxidation extract, with blue bubbles showing results of script for all butylated compounds, and yellow bubbles showing results for butylated aldehydes and ketones. Many of the classifications of peaks are not in agreement with the results of the spectral data processing, probably due to the classification of reagent byproducts and other compounds containing the scripted characteristic ions, which are not uncommon in spectra.

The use of these scripts to show analyte peaks has been previously explored (Vogt, 2007; Welthagen, 2003), but has not been published to our knowledge for use with derivatization. Several scripts were written in the study of anthropogenic aromatic oxidation products to show diagnostic ions of butylated and trimethylsilylated analytes. The scripts were applied to "Classifications", which allowed the results to be shown on each chromatogram. The number of peaks identified as derivatives by the script was compared to the results of a more traditional, spectral based data processing method. A

comparison was also made for particular functionalities derivatized by each reagent system used: carboxylic acids including hydroxy-acids by BSTFA and aldehydes, acidic ketones, and carboxylic acids including oxo-acids by BF_3/*n*-butanol. For butylated derivatives, the use of the script was effective in identifying dibutyl acetals and dibutyl ketals. More butyl derivatives were identified using the script than with the spectral data processing method (125 script, 97 spectral) (Table HH), although some peaks could have been misidentified. This problem is likely to be greater for butyl derivatives because of the use of the common ions m/z 41 and 57 in the script.

Table HH. Comparison of script and spectral methods of data processing for butyl derivatives (total 458 peaks in chromatogram). "Agreement" denotes the number of compounds positively identified using both methods of data processing. "Unknown agreement" denotes the number of compounds classified as "unknown" derivatives by the spectral method, and as derivatives by the script method.

	Spectral Method	Script Method	Agreement
Identified as derivatives	97	125	42
Unknown peaks with diagnostic ions (103, 159, 117, 61)	33	22	11
Unknown peaks with general diagnostic ions (57)	19	-	10
Misidentified as butyl by script	-	83	-

Agreement was low between the two methods of data processing: only 34% all derivatives and 33% aldehydes and ketones were identified using both methods. The script algorithm here did not sufficiently filter underivatized compounds in the sample; therefore, the script method would be most effective for the initial identification of potential dibutyl acetals and dibutyl ketals. Further refining of the script to include retention time limitations or characteristic loss ions (such as $[M-55]^+$) may allow for more accurate results.

The use of spectral data processing allowed ~24% more trimethylsilyl derivatives and 29% more derivatives of carboxylic acids to be identified (Table II).

Table II. Comparison of script and spectral methods of data processing for TMS derivatives (a total of 177 peaks were in the chromatogram). While the script method did not show improvement in positive identification of TMS or TMS acid compounds, only eight compounds were "misidentified" by the method.

	Spectral Method	**Script Method**	**Agreement**
Iidentified as derivatives	66	50	14
Unknown peaks with diagnostic ions (117, 147)	21	15	17
Unknown peaks with general diagnostic ions (73)	53	-	7
Misidentified as TMS by script	-	8	-

Agreement was low between data processing methods for all trimethylsilylated compounds, but more than half of the carboxylic acid derivatives were identified using both the script and spectral methods. Additionally, only eight of 50 script-identified TMS peaks were "misidentified" by comparison to the spectral method results. While the TMS diagnostic ions are uncommon in other spectra and prominent in the derivative spectra, the script did not provide a complete chromatographic analysis, and trimethyilsilylated compounds should only be surveyed by script.

APPENDIX I: Contamination Study

During the qualitative analysis of anthropogenic aromatic hydrocarbon oxidation products, a series of carboxylic acids was found to be present in both the sample and "blank" chromatograms with varying estimated concentrations. These compounds were eliminated as potential target compounds, limiting the results of the study. Their identities were noted when analyzing data from oxidized α-pinene samples, and background concentrations of these compounds measured were tabulated alongside the concentration identified within sample chromatograms. Only a few of these contaminating compounds were identified in the background of the samples. Contaminating compounds in α-pinene ozonolysis samples that were not tabulated because they had been previously noted as background and were not found in the samples in high concentrations included: decanoic acid, undecanoic acid, tetradecanoic acid octanoic acid, nonanoic acid, hexadecanoic acid, and butyl hexadecanoate. Most of these compounds were identified using both derivatization methods (butylation and TMS).

In order to reduce the likelihood of this occurring in the quantitative analysis of α–pinene oxidation products, a series of tests was conducted in order to show the source of the contamination. Contamination of the derivatization reagent BSTFA was shown through multiple derivatizations with differing solvents and contrasting results of an alternate derivatization reagent. The carboxylic acid compounds in the contaminated derivatization reagent and oxidation samples are listed in **Error! Reference source not**

found.. Identification of the sources of all contaminants and therefore an exhaustive list of the compounds could not be made.

Table JJ. Compounds tentatively identified in the oxidation studies of anthropogenic aromatic hydrocarbons and in the source of the contaminated reagent BSTFA were tabulated after testing to locate the source of the contamination using a 1D-GC (labeled 1D-GC, TMS) and during data processing of the *m*-xylene oxidation products (labeled GC×GC, butyl or TMS). The approximate retention times were calculated from analyses made using the system parameters indicated in Section 2.4.b. Mass spectral similarities are based on the results of a library search of the NIST and Wiley libraries.

Compound	Mass Spectral Similarity	Primary Retention Time (min)	Instrument, Derivatization Method
Lactic acid	94%	15.83	GC×GC, Butyl
2-methyl-Propanoic acid	95%	14.03	GC×GC, Butyl
2-methyl-Propanoic acid	81%	12.13	GC×GC, TMS
2-Oxo-malonic acid	57%	34.83	GC×GC, Butyl
2-Oxo-propanoic acid	81%	29.50	GC×GC, Butyl
2-Propenoic acid	88%	12.10	GC×GC, Butyl
2,2-dimethyl-Propanoic acid	71%	31.23	GC×GC, Butyl
3-methyl-Butanoic acid	74%	10.80	GC×GC, TMS
3-oxo-Propionic acid	79%	30.70	GC×GC, Butyl
4-oxo-Butanoic acid	74%	31.90	GC×GC, Butyl
4-oxo-Pentanoic acid,	88%	23.23	GC×GC, Butyl
Acetic Acid	72%	9.57	GC×GC, Butyl
Adipic acid	72%	27.01	1D-GC, TMS
Adipic acid	67%	31.63	GC×GC, Butyl
Benzoic acid	90%	19.71	1D-GC, TMS
Benzoic acid	80%	26.10	GC×GC, Butyl
Butanoic acid	93%	15.43	GC×GC, Butyl
Decanedioic acid	81%	35.56	GC×GC, Butyl
Decanoic acid	83%	25.54	1D-GC, TMS
Dodecanoic acid	91%	29.00	GC×GC, TMS
Glutaric acid	68%	30.36	GC×GC, Butyl
Hexadecanoic acid	91%	35.70	GC×GC, Butyl
Hexadecanoic acid	94%	34.40	GC×GC, TMS
Hexanoic acid	82%	21.43	GC×GC, Butyl
Itaconoic acid	74%	29.56	GC×GC, Butyl
Lactic acid	90%	14.45	1D-GC, TMS
Dodecanoic acid	86%	31.83	GC×GC, Butyl
methyl-Malonic acid	89%	27.16	GC×GC, Butyl
Myristic acid	86%	33.90	GC×GC, Butyl

Compound	Mass Spectral Similarity	Primary Retention Time (min)	Instrument, Derivatization Method
Nonanoic acid	91%	22.95	1D-GC, TMS
Octadecanoic acid	82%	37.36	GC×GC, Butyl
Octadecanoic acid	92%	35.47	GC×GC, TMS
Octanoic acid	90%	20.29	1D-GC, TMS
Oxalic acid	93%	25.70	GC×GC, Butyl
Pentanoic acid	80%	18.50	GC×GC, Butyl
Phthalic acid	93%	33.76	GC×GC, Butyl
Propanoic acid	73%	12.50	GC×GC, Butyl
Succinic acid	91%	21.82	1D-GC, TMS
Tetradecanoic acid	87%	31.53	GC×GC, TMS
trans-9-Octadecanoic acid	74%	36.00	GC×GC, TMS